Cell

The Chara genome: secondary complexity and implications for plant terrestrialization

--Manuscript Draft--

Manuscript Number:	CELL-D-17-02529R4
Full Title:	The Chara genome: secondary complexity and implications for plant terrestrialization
Article Type:	Research Article
Keywords:	plant evolution; charophyte; phytohormones; transcriptional regulation; Phragmoplastophyta; Chara; streptophyte; Reactive oxygen species; phragmoplast
Corresponding Author:	Stefan A Rensing, Ph.D. University of Marburg Marburg, GERMANY
First Author:	Tomoaki Nishiyama
Order of Authors:	Tomoaki Nishiyama
	Hidetoshi Sakayama
	Jan de Vries
	Henrik Buschmann
	Denis Saint-Marcoux
	Kristian K Ullrich
	Fabian B Haas
	Lisa Vanderstraeten
	Dirk Becker
	Daniel Lang
	Stanislav Vosolsobe
	Stephane Rombauts
	Per KI Wilhelmsson
	Philipp Janitza
	Ramona Kern
	Alexander Heyl
	Florian Rümpler
	Luz Irina A. Calderón Villalobos
	John M Clay
	Roman Skokan
	Atsushi Toyoda
	Yutaka Suzuki
	Hiroshi Kagoshima
	Elio Schijlen
	Navindra Tajeshwar
	Bruno Catarino
	Alexander J Hetherington
	Assia Saltykova

	Clemence Bonnot
	Holger Breuninger
	Aikaterini Symeonidi
	Guru V Radhakrishnan
	Filip Van Nieuwerburgh
	Dieter Deforce
	Caren Chang
	Kenneth G Karol
	Rainer Hedrich
	Peter Ulvskov
	Gernot Glöckner
	Charles F Delwiche
	Jan Petrasek
	Yves Van de Peer
	Jiri Friml
	Mary Beilby
	Liam Dolan
	Yuji Kohara
	Sumio Sugano
	Asao Fujiyama
	Pierre-Marc Delaux
	Marcel Quint
	Günter Theissen
	Martin Hagemann
	Jesper Harholt
	Christophe Dunand
	Sabine Zachgo
	Jane Langdale
	Florian Maumus
	Dominique Van Der Straeten
	Sven Gould
	Stefan A Rensing, Ph.D.
Abstract:	Land plants evolved from charophytic algae, among which Charophyceae possess the most complex body plans. We present the genome of Chara braunii; comparison of the genome to those of land plants identified evolutionary novelties for plant terrestrialization and land plant heritage genes. C. braunii employs unique xylan synthases for cell wall biosynthesis, a phragmoplast (cell separation) mechanism similar to that of land plants, and many phytohormones. C. braunii plastids are controlled via land plant-like retrograde signaling, and transcriptional regulation is more elaborate than in other algae. The morphological complexity of this organism may result from expanded gene families, with three cases of particular note: genes effecting tolerance to reactive oxygen species (ROS), LysM receptor-like kinases, and transcription factors (TFs). Transcriptomic analysis of sexual reproductive structures reveals intricate control by TFs, activity of the ROS gene network, and the ancestral

	use of plant-like storage and stress protection proteins in the zygote.
Opposed Reviewers:	John Bowman john.bowman@sci.monash.edu.au Conflict of interest (Marchantia paper)
Suggested Reviewers:	David Domozych ddomoz@skidmore.edu Expert on charophytes
	Linda Graham lkgraham@wisc.edu Expert on charophytes
	James Leebens-Mack jleebensmack@uga.edu Expert on plant phylogenomics / plant genome evolution

The *Chara* genome: secondary complexity and implications for plant terrestrialization

Tomoaki Nishiyama[1,*], Hidetoshi Sakayama[2,*], Jan de Vries[4,5], Henrik Buschmann[3], Denis Saint-Marcoux[6,7], Kristian K. Ullrich[8,40], Fabian B. Haas[8], Lisa Vanderstraeten[9], Dirk Becker[10], Daniel Lang[38], Stanislav Vosolsobě[17], Stephane Rombauts[11], Per K.I. Wilhelmsson[8], Philipp Janitza[12], Ramona Kern[13], Alexander Heyl[14], Florian Rümpler[15], Luz Irina A. Calderón Villalobos[30], John M. Clay[16], Roman Skokan[17], Atsushi Toyoda[18], Yutaka Suzuki[19], Hiroshi Kagoshima[20], Elio Schijlen[39], Navindra Tajeshwar[14], Bruno Catarino[6], Alexander J Hetherington[6], Assia Saltykova[11,21,22], Clemence Bonnot[6,36], Holger Breuninger[6,23], Aikaterini Symeonidi[8], Guru V. Radhakrishnan[24], Filip Van Nieuwerburgh[37], Dieter Deforce[37], Caren Chang[16], Kenneth G. Karol[25], Rainer Hedrich[10], Peter Ulvskov[26], Gernot Glöckner[27], Charles F. Delwiche[16], Jan Petrášek[17], Yves Van de Peer[11,28], Jiri Friml[29], Mary Beilby[31], Liam Dolan[6], Yuji Kohara[20], Sumio Sugano[19], Asao Fujiyama[18], Pierre-Marc Delaux[32], Marcel Quint[12,30], Günter Theißen[15], Martin Hagemann[13], Jesper Harholt[33], Christophe Dunand[32], Sabine Zachgo[3], Jane Langdale[6], Florian Maumus[34], Dominique Van Der Straeten[9], Sven B. Gould[4], Stefan A. Rensing[8,35,*,+]

[1] Advanced Science Research Center, Kanazawa University, Kanazawa 920-0934, Japan

[2] Graduate School of Science, Kobe University, Kobe 657-8501, Japan

[3] Botany Department, School of Biology and Chemistry, Osnabrück University, 49076 Osnabrück, Germany.

[4] Institute for Molecular Evolution, Heinrich Heine University, 40225 Düsseldorf, Germany

[5] Department of Biochemistry and Molecular Biology, Dalhousie University, Halifax, Nova Scotia B3H 4R2, Canada

[6] Department of Plant Sciences, University of Oxford, Oxford, OX1 3RB, United Kingdom

[7] Université de Lyon, UJM-Saint-Étienne, CNRS, BVpam FRE3727, 42023 Saint-Étienne, France

[8] Plant Cell Biology, Faculty of Biology, University of Marburg, 35043 Marburg, Germany

[9] Laboratory of Functional Plant Biology, Department of Biology, Gent University, 9000 Gent, Belgium

[10] Molecular Plant Physiology & Biophysics, University of Wuerzburg, 97082 Wuerzburg, Germany

[11] Department of Plant Biotechnology and Bioinformatics, Gent University and VIB Center for Plant Systems Biology, 9052 Gent, Belgium

[12] Institute of Agricultural and Nutritional Sciences, Martin-Luther-University Halle-Wittenberg, 06120 Halle (Saale), Germany

[13] Plant Physiology, University Rostock, 18051 Rostock, Germany

[14] Department of Biology, Adelphi University, Garden City, NY 11530, USA

[15] Department of Genetics, Friedrich Schiller University Jena, 07743 Jena, Germany

[16] CBMG, University of Maryland, College Park, MD 20742, USA

[17] Department of Experimental Plant Biology, Faculty of Science, Charles University, 128 44 Prague 2, Czech Republic

[18] Comparative Genomics Laboratory and Advanced Genomics Center, National Institute of Genetics, Shizuoka 411-8540, Japan

[19] Department of Computational Biology and Medical Sciences, University of Tokyo, Kashiwa, Chiba 277-8562, Japan

[20] Genome Biology Laboratory, National Institute of Genetics, Shizuoka 411-8540, Japan

[21] Platform Biotechnology and Molecular Biology, Scientific Institute of Public Health (WIV-ISP), Brussels, Belgium

[22] Department of Information Technology, Gent University, IMinds, 9052 Gent, Belgium

[23] ZMBP, Entwicklungsgenetik, 72076 Tübingen, Germany

[24] Department of Cell and Developmental Biology, John Innes Centre, Norwich NR4 7UH, United Kingdom

[25] Lewis B. and Dorothy Cullman Program for Molecular Systematics, The New York Botanical Garden, Bronx, NY 10458, USA

[26] Department of Plant and Environmental Sciences, University of Copenhagen, DK-1871 Frederiksberg C, Denmark

[27] Biochemistry I, Medical Faculty, University of Cologne, 50931 Cologne, Germany

[28] Department of Biochemistry, Genetics and Microbiology, University of Pretoria, Pretoria, 0028, South Africa

[29] Institute of Science and Technology, 3400 Klosterneuburg, Austria

[30] Department of Molecular Signal Processing, Leibniz Institute of Plant Biochemistry, 06120 Halle (Saale), Germany

[31] School of Physics, University of NSW, Sydney, Kensington, 2052, NSW, Australia

[32] Laboratoire de Recherche en Sciences Végétales, Université de Toulouse, CNRS, UPS, Auzeville, BP42617, 31326 Castanet Tolosan, France

[33] Carlsberg Research Laboratory, 1799 Copenhagen V, Denmark

[34] URGI, INRA, Université Paris-Saclay, 78026 Versailles, France

[35] BIOSS Centre for Biological Signalling Studies, Unigersity Freiburg, Germany

[36] Present address: Labex ARBRE, UMR 1136 INRA-Université de Lorraine (IAM), INRA-Grand Est-Nancy, Champenoux, France

[37] Laboratory of Pharmaceutical Biotechnology, Gent University, 9000, Gent, Belgium

[38] PGSB, Helmholtz Center Munich, 85764 Neuherberg, Germany

[39] Wageningen University, B.U. Bioscience, 6700 AA Wageningen, The Netherlands

[40] Present address: Max Planck Institute for Evolutionary Biology, 24306, Ploen, Germany.

+ Lead contact: Stefan A. Rensing

* Authors for correspondence:

tomoakin@staff.kanazawa-u.ac.jp

hsak@port.kobe-u.ac.jp

stefan.rensing@biologie.uni-marburg.de

Summary

Land plants evolved from charophytic algae, among which Charophyceae possess the most complex body plans. We present the genome of *Chara braunii*; comparison of the genome to those of land plants identified evolutionary novelties for plant terrestrialization and land plant heritage genes. *C. braunii* employs unique xylan synthases for cell wall biosynthesis, a phragmoplast (cell separation) mechanism similar to that of land plants, and many phytohormones. *C. braunii* plastids are controlled *via* land plant-like retrograde signaling, and transcriptional regulation is more elaborate than in other algae. The morphological complexity of this organism may result from expanded gene families, with three cases of particular note: genes effecting tolerance to reactive oxygen species (ROS), LysM receptor-like kinases, and transcription factors (TFs). Transcriptomic analysis of sexual reproductive structures reveals intricate control by TFs, activity of the ROS gene network, and the ancestral use of plant-like storage and stress protection proteins in the zygote.

Keywords: plant evolution, charophyte, phytohormones, transcriptional regulation, Phragmoplastophyta, Chara, streptophyte, reactive oxygen species, phragmoplast

Introduction

A pivotal event in the emergence of plant life was the mid-Paleozoic adaptation to land. While several algal lineages evolved to occupy terrestrial environments, only one represents the land plant ancestor; its terrestrialization event was fostered by a range of evolutionary novelties. The specific complement of traits that allowed a particular algal lineage to give rise to land plants and dominate the terrestrial environment remains under active study. Similarity of critical plant developmental, sensory, and regulatory pathways to homologous pathways in charophyte green algae has been demonstrated in several recent studies, emphasizing the close relationship among these lineages (reviewed in (Rensing, 2018)).

Charophytic algae are the closest living relatives of land plants (embryophytes), with both groups collectively referred to as streptophytes (Fig. 1). The Charophyceae, Coleochaetophyceae, and Zygnematophyceae together with the land plants represent the clade Phragmoplastophyta (Lecointre and Le Guyader, 2006), united by the presence of the phragmoplast (Pickett-Heaps, 1975), an array of microtubules perpendicular to the cell division plane that functions in the formation of the nascent cell wall. The Klebsormidiophyceae, Chlorokybophyceae, and Mesostigmatophyceae share fewer traits with land plants (Fig. 1). While Charophyceae were hypothesized to be most closely related to land plants on the basis of similar body plans (Pringsheim, 1862), recent studies indicated that the Zygnematophyceae are the land plant sister group (Wickett et al., 2014).

Extant Zygnematophyceae have simple body plans that seem to reflect secondary loss of morphological complexity. In contrast, the earlier diverging Charophyceae are morphologically more complex than all other charophytic algae: the haploid thallus body plan encompasses a shoot-like axis consisting of nodes with whorls, internodes, a simplex apical meristem, plus multicellular rhizoids (Fig. 2). Cells of the internode are large and complex, featuring endo- and ectoplasma, multiple plastids and nuclei, and communicate *via* electrical signals. The morphology of extant charophytic groups thus infers mosaic evolution and suggests that the genomes of Charophyceae, not Zygnematophyceae, will likely reveal the suite of traits that facilitated terrestrialization (Delwiche, 2016).

Here we present the genome sequence of the charophycean alga *Chara braunii*, one of the most morphologically complex extant Charophyta, shedding light on early embryophyte diversification and the colonization of land by plants.

Results and Discussion

The *Chara braunii* genome: assembly, annotation and comparison

C. braunii features a haplontic life cycle (Fig. 2), the draft sequence reported here represents a haploid genome. 1.75 Gbp of nuclear scaffold data were obtained, of which 1.43 Gbp were assembled into contigs, corresponding to ~74% of the *C. braunii* genome. RNA-seq of vegetative and reproductive stages was used together with full-length cDNA sequences to annotate the genome. 23,546 putative protein coding gene models were identified, of which 53% are supported by RNA-seq data (Table S4). At least 94% of several conserved core gene sets are encoded by the genome, indicating its suitability for genomic and comparative analyses (STAR Methods).

The observed chromosome number n=14 (Fig. S1) corresponds to the base chromosome number of *Chara* species. Indeed, synonymous substitution distance (Ks)-based analysis of *C. braunii* paralogs revealed no evidence of whole genome duplication (WGD) events (Fig. S3) and thus paralog acquisition and retention is probably due to small-scale duplications. Repetitive elements (Table S1F, S1G) collectively contribute approximately 1.1 Gbp (61%, or 75% if gaps are excluded). Unlike in most plants and green algae, there are no Copia-type long terminal repeat (LTR) retrotransposons (RT) detectable. We discovered a family of repeats with putative GIY-YIG homing endonuclease and reverse transcriptase domains, which are hallmarks of Penelope RTs and group II introns that are uncommon in plant genomes.

The density of LTR elements in the genome is intermediate between compact genomes like those of *Arabidopsis thaliana* or *Klebsormidium nitens*, and other large genomes such as maize and barley (Fig. 3). *C. braunii* introns are an order of magnitude longer than in any of the other genomes investigated here (Table S1L), although intron boundaries appear to be conserved. The high intron length coincides with a low number of introns per gene (3.82), similar to the value for the barley genome (3.89, Table S1L); intron length and number show negative correlation (r = -0.42). Repetitive elements represent 39% of the intron space (Fig. 3, Mendeley archive) which is strikingly enriched with Penelope-like elements and depleted of other types of repeats including Class 2 transposable elements (Helitrons and DNA transposons), suggesting differential integration bias and/or retention in introns as compared to intergenic space (Table S1L).

Evolutionary novelties enabling terrestrialization and land plant heritage genes (LPHG)

The lineage harboring *C. braunii* diverged from land plants 550–750 Ma (Morris et al., 2018). By identifying features that are shared between the *C. braunii* genome and extant land plants, putative ancestral traits can be identified that have been retained over several hundred Ma. Here we refer to the genes underlying these traits as land plant heritage genes (LPHG) and similarly deduce evolutionary novelties.

Cell division and cell wall

C. braunii, like land plants, performs cytokinesis by assembling a cell plate using a phragmoplast microtubule array while *K. nitens* divides by an evolutionarily older cleavage (Fig. 1). Phragmoplast-mediated cell division is assumed to have enabled filament branching through a shift in the plane of cell division (Buschmann and Zachgo, 2016). Land plants also evolved another microtubule array, the preprophase band (PPB), which functions in phragmoplast and cell plate guidance. Focusing on genes for phragmoplast and PPB function, a list of 221 *A. thaliana* cytokinesis genes was compiled (Table S1C). Sequence comparisons showed that the genomes of *A. thaliana*, *P. patens*, *C. braunii* and *K. nitens* have a highly similar complement of cytokinesis-related genes while the unicellular chlorophyte *Chlamydomonas reinhardtii* is divergent. Interestingly, the *C. braunii* genome lacks the *TANGLED1* gene. In land plants, microtubule-associated TANGLED1 localizes to PPBs and is required for phragmoplast guidance (Walker et al., 2007). Since TANGLED1 homologs are found in several bryophytes, but none in any algae, this gene likely played an important role in PPB evolution (Fig. 1). To gain further insight into the evolution of the phragmoplast, we determined how many paralogs each of the cytokinesis genes has in *C. braunii* as compared to *K. nitens*. In this way we identified possible phragmoplast signature genes (Table S1C). Among others, we detected expansion of cyclins as well as EXOCYST and SNARE complex members (Table S1C, Data S1Q-S). The expansion of phragmoplast-related gene families in *C. braunii* / the Phragmoplastophyta, but not in Chlorophyta, *K. nitens* or *M. viride*, suggests their sub- and neofunctionalization to enable phragmoplast function.

Like land plant cell walls, those of *C. braunii* consist of cellulose embedded within a pectin and hemicellulose matrix (Sorensen et al., 2011), its synthesis is orchestrated by a repertoire of glycosyltransferases much like in land plants (Table S1H), with the exception of an apparently unique mechanism for xylan synthesis. The GT47 xylan synthase XYS1 has been identified in *K. nitens*, as well as IRX9 and IRX14 from GT43 (Data S1A), implicated in xylan biosynthesis despite no apparent requirement for being an active enzyme (Ren et al., 2014). Orthologs to neither XYS1 nor IRX9/14 could be identified in *C. braunii*, however, a deep branching, highly diverged form of GT43 was identified as the most likely *C. braunii* xylan synthase, providing the first hint that GT43 sequences are enzymatically involved in synthesizing xylan.

Phytohormones

Phytohormones enable the integration of environmental stimuli with developmental programs. As such, they are a key feature of land plants, with some apparently having origins in algae (Hori et al., 2014; Ju et al., 2015; Wang et al., 2015). Potential orthologs of phytohormone pathway genes were defined across *K. nitens*, *C. braunii*, *P. patens* and *A. thaliana* (Table 1, Fig. 4, Table S1J).

Auxin (AUX)

AUX is one of the major regulators of plant growth and development. Biosynthesis of AUX (Hori et al., 2014) as well as transcriptional and physiological response to high concentrations have been shown in *K. nitens* (Ohtaka et al., 2017). In contrast to *K. nitens,* genes enconding biosynthetic enzymes of the TAA and YUCCA families are absent from *C. braunii* (Table 1). In *C. australis* IAA, serotonin and melatonin accumulate in a synchronized manner during the day/night cycle (Beilby et al., 2015). As the tryptamine IAA biosynthetic pathway intersects with the serotonin/melatonin pathway (Tivendale et al., 2014), *Chara* may synthesize and metabolize AUX *via* a different route than land plants.

Homologous genes for both *PIN*s and *ABCBs* are present in the *C. braunii* genome (Table 1, Table S1K), supporting previous data on polar AUX transport (PAT) in *K. nitens* (Hori et al., 2014) and Charales (Boot et al., 2012). Homologous sequences for AUX1/LAX-like influx carriers as well as the intracellular PIN-like (PILS) transporters, however, are absent from the *C. braunii* genome (Table 1), suggesting that AUX transport and homeostasis display an evolutionary history different from other streptophytes.

The land plant-type AUX signaling cascade, consisting of SCF$^{TIR1/AFB}$ and Aux/IAA co-receptors and ARF TFs, was suggested to be absent in *K. nitens* (Hori et al., 2014; Ohtaka et al., 2017). *K. nitens* encodes an Aux/IAA domain containing protein (Wang et al., 2015) that features an additional B3 domain, is not induced by IAA (Ohtaka et al., 2017) and thus not classified as canonical Aux/IAA (Table 1). In addition to all components of the ubiquitin-proteasome system (Table S1I), *C. braunii* features a single *ARF* (Data S1E) with land plant-like domain composition (Flores-Sandoval et al., 2018), and two Aux/IAA-like sequences (Table 1, Data S1F) clustering with the *A. thaliana* non-canonical IAA33 (lacking a TOPLESS interacting motif and degron for AUX-dependent SCF$^{TIR1/AFB}$-Aux/IAA interactions.

C. braunii also encodes several F-box proteins (FBPs) with sequence similarity to land plant phytohormone co-receptors (Data S1P). None of the TIR1/AFB-like FBPs cluster with the land plant AUX co-receptor gene family (Data S1G). Our structural modeling, however, reveals that the *C. braunii* sequences adopt a solenoid-fold architecture resembling TIR1 (Tan et al., 2007). Ligand binding modeling supported the potential ability to form an AUX binding pocket (Data S1P). The existence of only degron-less *C. braunii* Aux/IAAs, however, prompts to postulate that a land plant-like TIR1/AFB-Aux/IAA co-receptor pair is most likely not functional in *C. braunii*.

Consequently, while obvious candidates for canonical land plant AUX biosynthesis genes are lacking, there is a partial candidate gene set of the major land plant AUX signaling and PAT pathways in *C. braunii*. In conclusion, AUX biosynthesis, transport, and some form of signaling were already present in the last common ancestor of *C. braunii* and *K. nitens*, but AUX signaling *via* ARFs was apparently gained in the common ancestor of Phragmoplastophyta, as was ARF repression by Aux/IAAs (Table S1Q, Fig. 4).

Cytokinin (CK)

The CK signaling pathway consists of four protein families: the receptor, the histidine-containing phosphotransfer protein, and the type A and B response regulators (RRA and RRB) (Heyl et al., 2013). The *C. braunii* genome encodes members of the first three, but no RRBs (Table 1, Fig. 4). This is contrast to their presence in all chlorophytes and charophytes analysed (Hori et al., 2014; Wang et al., 2015). Several RR domains closely related to RRBs were found, but none contained the Myb domain essential for RRB function (Table S1J). Given the complexity of the *C. braunii* genome, it is possible that not all genes were correctly or completely predicted, but neither genome nor transcriptome data (Data S1H) provide evidence for RRB genes. Their loss suggests either the rewiring of CK signaling or substitution of RRB function by other genes.

Ethylene (ETH)

The *C. braunii* genome possesses one or more potential homologs of all of the core components associated with ETH signaling (Table 1, Fig. 4 and Table S1J). *Chara* exhibits ETH-binding activity (Wang et al., 2006), and *C. braunii* encodes several ETH receptor homologs. Notably, *C. braunii* possesses a full-length homolog of *EIN2*, a central regulator in ETH signaling. This is in contrast to both the *K. nitens* genome, which lacks *EIN2* (Hori et al., 2014), and the *Spirogyra pratensis* transcriptome, which shows only a partial *EIN2* sequence (Ju et al., 2015). Except for *EIN2*, *S. pratensis* possesses an ETH signaling pathway that is functionally conserved with the pathway known in land plants (Ju et al., 2015). These findings indicate that the land plant-like ETH signaling pathway was established in the common ancestor of the Phragmoplastophyta, after its divergence from the lineage leading to *Klebsormidium*.

Abscisic acid (ABA)

Orthologs of the core ABA signaling components are present in bryophytes and it has been suggested that all ABA biosynthesis/signaling components were gained in the common ancestor of Charophyta (Ju et al., 2015; Wang et al., 2015), with the exception of PYR/PYL receptors that were probably gained in the common ancestor of Zygnematophyceae and land plants (de Vries et al., 2018). The *C. braunii* genome does not contain homologs of the co-receptors ABI/HAB, nor the PYR/RCAR family of receptors (Park et al., 2009), but possesses homologs of genes encoding enzymes that act early in the ABA synthesis pathway (from carotenoid synthesis to violaxanthin; Table 1, Fig. 4 and Table S1J). Given that the presence of ABA has been confirmed in *C. braunii* (Hackenberg and Pandey, 2014), it is likely that the biosynthetic pathway differs from that found in land plants, with ABA possibly being synthesized directly from farnesyl pyrophosphate.

Strigolactones (SL)

Orthologs of all the core SL signaling components have been identified exclusively in the genomes of seed plants; however, D14-like receptor homologs are found encoded by bryophytes and charophytes (Bythell-Douglas et al., 2017; Wang et al., 2015). Two SL-related homologs were identified in *C. braunii*, one encoding beta-carotene isomerase D27, and one encoding the candidate SL/karrikin receptor D14-like (Table 1, Fig. 4 and Table S1J). Given the presence of SL in several Charales species, and the activity of the synthetic SL GR24 on *Chara corallina* rhizoid growth (Delaux et al., 2012), it is likely that SL synthesis and signaling differ in charophyceans and in seed plants (Bythell-Douglas et al., 2017). It has been suggested that D14-like proteins might act as (the) SL receptor(s) in this group.

In summary, although the phytohormones AUX and CK seem to be ancestral features of streptophytes, and SL and ABA of Phragmoplastophyta (Fig. 1), the respective biosynthesis and/or signaling pathways differ between seed plants and *C. braunii.* Some features of these four phytohormone networks, and of ETH signaling, first appeared in the Phragmoplastophyta as evident by their presence in *C. braunii*. Others were either not present in the ancestor or have since diverged.

Plastid evolution: photorespiration and retrograde signaling

Photorespiration, which recycles the 2-carbon compound formed when ribulose bisphosphate carboxylase/oxygenase reacts with oxygen instead of CO_2, is crucial to photosynthesis in an oxygen-rich atmosphere. The *C. braunii* genome encodes proteins necessary to carry out a plant-like photorespiratory cycle, including a plant-type glycolate oxidase (GOX) (Table S1M) with structural features preferring glycolate over lactate (Hackenberg et al., 2011). Plant-type GOX is also present in *K. nitens*, while *C. reinhardtii* uses a mitochondrial glycolate dehydrogenase for photorespiratory glycolate metabolism (Nakamura et al., 2005). Apparently, plant-like photorespiration was present in the common ancestor of Streptophyta, the pathway being a feature that might have aided terrestrialization.

The plastid to nucleus signaling network optimizes plastid function in land plants. All Chloroplastida (Fig. 1) share EXECUTOR-transduced singlet oxygen and a rudimentary tetrapyrrole-derived retrograde signaling, to which streptophytes recruited GUN2/3 (Fig. 5A). Our data show that *C. braunii,* but not *K. nitens*, encodes GUN1, at which multiple retrograde signals converge in land plants (reviewed by (Chan et al., 2016)). The only GUN1 candidate protein in *K. nitens* (kfl00096_0090) clustered with streptophyte algae- and bryophyte-specific PPRs, but not GUN1 (Data S1I). Hence, retrograde signaling featuring GUN1 might represent an evolutionary novelty of the Phragmoplastophyta (Fig. 1).

Plastid-encoded RNA-polymerase (PEP) is the ancestral and for most Archaeplastida the only PEP. In land plants, PEP activity is controlled through PEP-associated proteins (PAPs) (Pfalz and Pfannschmidt, 2013). We detected 5, 8, 10 and 11 PAP orthologs in *C. reinhardtii*, *K. nitens*, *C. braunii*, and *P. patens*, respectively. PAPs were thus already present in streptophyte algae (Fig. 5A) and underwent expansion in land plants. Most of the detected PAPs are predicted to be targeted to the chloroplast, the mitochondrion or both (Table S1N); dual-localization of PAPs to both organelles might be an ancient and conserved character state.

Transcriptional regulation

Within the Chloroplastida, morphological complexity correlates with the number of TF (acting in a sequence-specific manner, typically by binding to *cis*-regulatory elements) and transcriptional regulator (TR, acting on chromatin or *via* protein-protein interaction) genes (Lang et al., 2010). We identified 730 TF/TR genes in the *C. braunii* genome (Table S1Q), the complement of such proteins thus being larger than in *K. nitens* (627) or *C. reinhardtii* (542), coinciding with morphological complexity. *C. braunii* encodes several TFs that are not present in other algae, including *K. nitens*. Based on the available data, these families first appear in the Phragmoplastophyta, although they were previously thought to have been gained in the common ancestor of Coleochaetophyceae, Zygnematophyceae and land plants (Wilhelmsson et al., 2017). They include the single canonical ARF mentioned before, as well as TCP, HRT and

Zn cluster TFs (Fig. 1). The *C. braunii* genome encodes two TCP genes, which belong to TCP-P (class I) and TCP-C (class II). The two TCP subgroups are known to exert antagonistic functions in *A. thaliana* with regard to growth proliferation of organs and tissues (Nicolas and Cubas, 2016), implying that the appearance of two different TCP genes might have contributed to regulation of proliferation in the Phragmoplastophyta.

Two separate clades of MADS-box genes exist (Type I and II), with land plant Type II genes further subdivided into so called MIKC^{C} and MIKC*-type genes (Gramzow and Theißen, 2010). No Type I genes were identified in the *C. braunii* genome, but three Type II genes, of which only *CbMADS1* shows a canonical MIKC-type domain structure. Phylogeny reconstructions together with exon-intron structure analysis (Fig. 5B; Fig. S5, Data S1K) suggest that MIKC^{C} and MIKC*-type genes evolved from the duplication of an ancestral Type II gene followed by different exon duplications in both gene lineages. As such, *CbMADS1* may serve as a model for the ancestral MIKC-type gene that gave rise to MIKC^{C}- and MIKC*-type genes of land plants.

C. braunii encodes 11 bHLH TFs in 5 subfamilies. The Va(2) subfamily is present in chlorophytic and charophytic genomes and not present in land plants, suggesting that this subfamily was lost in the lineage leading to land plants (Table S1O, S1P). The *C. braunii* genome encodes 11 homeodomain (HD) TFs grouped into 9 subfamilies (Table S1O, S1P). Consistent with previous analyses (Catarino et al., 2016), *C. braunii* contains members of the KNOX, BEL, DDT and PINTOX subfamilies that are conserved in chlorophytes.

Zygotes and spores as analogs to seeds

Dormant haploid spores of mosses share features of regulation and coat biosynthesis with diploid seeds of flowering plants (Daku et al., 2016; Vesty et al., 2016). The diploid zygotes of *Chara* are dormant diaspores that presumably undergo meiosis and germinate upon suitable environmental cues (Delwiche and Cooper, 2015). Differential expression analysis shows that a number of transcripts related to seed storage proteins (cupin superfamily, oleosins) and to stress tolerance proteins found in seeds (e.g. late embryogenesis abundant), accumulate to high levels in zygotes (Fig. S4). These proteins probably enable the *C. braunii* zygotes to withstand harsh environmental conditions and represent a reservoir of nutrients to facilitate germination and growth. Homologs of these genes have apparently been adopted during land plant evolution to enable dormancy in other diaspores, namely spores and seeds.

Evolutionary novelties of the *Chara* lineage

Trihelix TFs

The number of TFs per family is lower in *C. braunii* than in land plants for most families, with the trihelix family being an exception: 302 members are encoded, while land plant genomes typically encode ca. 30 copies (Table S1Q). Trihelix TFs are involved in the regulation of development (e.g. embryogenesis, flower development), as well as responses to abiotic and biotic factors. Based on RNA-seq data, at least 28 of the *C. braunii* genes are expressed (Table S4, Fig. S4); 19 in vegetative tissue (of which 6 are expressed exclusively in vegetative tissue) and 22 in reproductive tissues (antheridia, oogonia, zygotes; Fig. S4). Phylogenetic analysis shows that the vast majority of *C. braunii* trihelix paralogs groups outside of the four clades previously defined (Kaplan-Levy et al., 2012) (Data S1J). Similar to secondary expansion of TF families in other lineages the expansion of trihelix TFs in *C. braunii* might be connected to the independent evolution of morphological complexity.

Phytohormones: PINs

There are six PIN AUX transporter proteins potentially encoded by the *C. braunii* genome (Table S1J). In land plants, the evolution of morphological complexity in the gametophytic generation, and later in the sporophytic generation, coincides with independent radiations within the *PIN* gene family (Bennett, 2015). Given its high morphological complexity, the same might have occurred in *C. braunii.*

Motor network

The evolution of land plants is accompanied by increased abundance of myosin and kinesin domain proteins. Because *K. nitens* has slightly more predicted kinesins than *C. braunii* (Table S1S), it appears that phragmoplast evolution did not depend on the neofunctionalization of kinesin paralogs. However, myosin motors use filamentous actin as tracks. The expansion of the actin family in *C. braunii* (*K. nitens* and *C. reinhardtii* encode 7 actin genes, whereas *C. braunii* has 16; Data S1T, U), with each gene encoding a slightly different protein, hints at varying functions among the cytoskeleton. Land plants have 9 actin genes (*Marchantia polymorpha*) to often 12 (*A. thaliana*, papaya, *Amborella trichocarpa*), and up to 34 in the polyploid maize, while transcriptomic data of other Charales suggests high numbers of underlying genes, e.g. 27 transcripts in *Nitella mirabilis*, 101 in *N. hyalina* (and 46 in the desmid *Penium margaritaceum*). The high numbers of actin genes detected in the amoebal protist *Naegleria gruberi* (86), and the slime mold *Dictyostelium discoideum* (39) (Joseph et al., 2008), can to a large part be explained by their involvement in cell movement. Thus, the additional actin genes of *Chara*, *Nitella* and *Penium* may serve the enhanced cytoplasmic streaming observed in these organisms.

Electrical excitability

Inspired by the work of (Hodgkin and Huxley, 1952) on the squid axon, the large internodal cells of *Chara* emerged as an excellent experimental system for electrophysiological studies on plant excitability - the "Green Axon" (Beilby, 2007). On a slower time scale (1000x), the internodal cells fire action potentials (APs) in response to such as depolarization, light, heat shock, injury or touch. The *C. braunii* genome encodes several putative Touch/Mechano-Sensitive (MS) channels: two members of the MscS-like (MSL) family, as well as an ortholog of the eukaryote specific Piezo-type channel. The negative resting potential (up to -250 mV) across the plasma membrane is generated by the P-type H^+-ATPases, encoded in the *C. braunii* genome (Table S1R). Ca^{2+} and Cl^- contribute to the depolarizing phase of the *Chara* AP, while K^+ efflux shapes the AP repolarization phase as in animals. No animal-like voltage-gated Na^+

or Ca^{2+} channels were identified, but a single ALMT-type anion channel gene is present in *C. braunii*. The anion channel in *Chara* is Ca^{2+}-activated and voltage sensitive, so an Anoctamin-like channel poses another possibility. A Shaker-type, voltage-gated K^+ channel in *C. braunii* genome probably mediates the depolarization-activated potassium efflux of the AP repolarization phase. The *C. braunii* habit of long internodal cells might require long distance electrical signaling (Beilby, 2015) enabled by its peculiar set of ion channels. The similarities or differences of *C. braunii* AP, as compared to flowering plants, are yet to be established.

Sensing of biotic interaction and microbiome

Land plants harbor a large number of LysM receptor-like kinases (RLK) involved in the perception of chitin-based signals produced by pathogenic and beneficial microorganisms. One member of this family has been described in charophytic algae suggesting either an inability to discriminate microorganisms or an alternative system to do so (Delaux et al., 2015). The *C. braunii* genome revealed the presence of seven LysM-RLKs (Fig. 5C; Data S1N) that expanded independently of land plant LysM-RLKs. This expansion may reflect an adaptation of *C. braunii* to an extended range of interacting microorganisms (co-cultured bacteria: Table S1T, S1U). This is noteworthy given that many have failed to axenically cultivate Charophyceae, raising the possibility that growth may be dependent on microbiotic commensalism or mutualism.

Sexual reproduction and the ROS network

To analyze reproductive mechanisms, transcriptomes of antheridia, oogonia and zygotes were generated (Fig. 5/6, Fig. S6, Table S2 & S3). For antheridia, the data demonstrate that cell motility is up-regulated as expected (Fig. 5D; Fig. S6A). Of 949 differentially expressed genes (DEGs) upregulated in antheridia, 49 encode proteins harboring dynein heavy chains. Dynein-mediated transport is employed in flagellate cells such as spermatozoids and was lost during land plant evolution, concomitant with the loss of motile cells (Rensing et al., 2008). 22 of 302 trihelix TFs are expressed in reproductive tissues. Of those, 9 are expressed in all three tissues, 5 specifically in antheridia, 7 in oogonia and antheridia, and 1 specifically in the zygote (Fig. S4B). This expression profile may suggest a possible role for these genes in sexual reproduction, in particular in antheridia. Transcripts of a HMG TR and a RWP-RK TF also specifically accumulated in antheridia. Members of these families were shown to be involved in mating in fungi (Barve et al., 2003) and gamete differentiation in *C. reinhardtii* (Lin and Goodenough, 2007), and the single RWP-RK TF in *M. polymorpha* keeps egg cells quiescent in the absence of fertilization (Rovekamp et al., 2016).

Zygote transcriptome profiles are characterized by transcription, microtubule-based movement and protein kinase activities (Fig. S6D), processes that might be hallmarks of the diploid zygote maturing and entering dormancy. 87 TFs/TRs are differentially expressed between zygotes and oogonia, among them families typically linked to the regulation of development (e.g. bHLH, HD, AP2/EREBP; Fig. S4C), supporting the hypothesis that transcription undergoes a switch after fertilization. One of the seven LysM RLKs (g44510) is strongly induced in zygotes. In line with potential commensalism mentioned above, this protein might detect the presence of beneficial microbes as a putative factor triggering meiosis and germination of the dormant zygote.

Of particular interest is the up-regulation of oxidation reduction processes in oogonia as compared to antheridia or zygotes (Fig. 5E; Fig. S6B/C). Like all living organisms, *C. braunii* needs to deal with constitutive production of reactive oxygen species (ROS) using the ROS gene network (Fig. S7, Table S1X). In contrast to land plants, aquatic plants have the option to let ROS diffuse into the water. *C. braunii* encodes all families responsible for ROS scavenging, but with lower gene copy number in comparison to land plants. In contrast, CC-type glutaredoxins (GRX) (ROXYs in *A. thaliana*), which exert crucial functions during angiosperm reproductive development (Gutsche et al., 2015), could not be detected (Table S1X). Among redox-associated genes (Table S1X) the class III peroxidases (Prx), thioredoxins and respiratory burst oxidase homologs expanded greatly during land plant evolution. However, only Prx expanded in *C. braunii* compared to *K. nitens* (Data S1O). With both peroxidative and hydroxylic catalytic cycles, these enzymes can regulate ROS and polymerize cell wall compounds (Francoz et al., 2015). Most of the *C. braunii* Prx are predicted to be secreted, as such, they may contribute to the formation of the strikingly elaborate reproductive structures, e.g. the thick zygote wall (Fig. 2).

7 out of 12 Prx are 2-8 fold higher expressed in oogonia than in antheridia or zygotes (Fig. 6). The higher expression of the ROS gene network could be related to the ROS homeostasis regulation necessary for an optimum fecundation. Flowering plant stigmas exhibit high levels of peroxidase activity when receptive to pollen (McInnis et al., 2006) and have been discussed to be involved in pollen-pistil interaction or pollen tube growth/penetration (Beltramo et al., 2012). For *A. thaliana* root and shoot apical meristems it was shown that stem cell-specific Prx fine tune the balance between superoxide anions ($O_{2.-}$) and hydrogen peroxide (H_2O_2) and thereby affect the switch between cell maintenance and differentiation (Zeng et al., 2017). Differential regulation of ROS levels by Prx might control sexual reproduction in *C. braunii*. Potentially, this mechanism arose in the common ancestor of Phragmoplastophyta and has been recruited from the gametophyte to the sporophyte during land plant evolution.

Conclusions

The *C. braunii* genome encodes more proteins than other algae, but less than most land plants. Both, specific gains / expansions and losses, can be attributed to the *Chara* lineage (Fig. 1). In absence of a WGD gene family expansions resulted from gene duplication and differential loss. Many of these events likely represent secondary gains in *Chara* complexity *via* sub- and neofunctionalization. We hypothesize that many gene family expansions detected in the *C. braunii* genome underpin its strikingly complex morphology.

Comparative genome analysis clearly reflects the phylogenetic placement of *C. braunii* as a close relative of land plants, with both striking similarities and important differences. It demonstrates the substantial insights into fundamental aspects of plant biology that can be gained by comparing diverse relatives. Molecular signatures across genomes reveal that AUX transport *via* PINs, trihelix TFs, MIKC-type MADS genes as well as photorespiration and diaspore storage proteins were present prior to the divergence of *K. nitens* (Fig. 1). Other features, such as the non-motile vegetative phase and filamentous growth, evolved later.

Hence, much of what was previously considered land plant-like features clearly evolved in the common ancestor of the Phragmoplastophyta (Fig. 1). These features include polyplastidy, branching, cellulose synthase rosettes, apical cell growth, several features of phytohormone networks, potential involvement of ROS in sexual reproduction and the phragmoplast. Some features evolved after the split of Charophyceae or Coleochaetophyceae such as GRAS TFs and the PPB-like isthmus band of microtubules. Life on land meant increased exposure to UV light. RNA editing repairs UV-B induced mutations in land plants (Maier et al., 2008). Editing evolved after the divergence of Charophyceae from the lineage leading to Zygnematophyceae and land plants (Cahoon et al., 2017). Key editing factors (PPR proteins) are much less abundant in *C. braunii* (57) than in the *Spirogyra* (379) or *P. patens* (100) genomes (Table S1Y). Other features, such as the multicellular sporophyte and embryogenesis, the synthesis of a complex cuticle and the ability to associate with arbuscular mycorrhizal fungi evolved at the base of the land plants, and further during land plant evolution (Fig. 1). Among the latter features are hallmarks of plants' adaptations to land. Yet, before any of these adaptations evolved, LPHGs enabled the first steps of terrestrialization. The key to their identification lies in comparative genomics studies using streptophyte algae, as exemplified here for *C. braunii*.

Acknowledgements

We thank K. Yamada, M. Göttig, M. Schallenberg-Rüdinger and F. Donges for technical assistance and S. Kato for kind assistance with strain isolation. Financial support was provided MEXT & JSPS KAKENHI (17020008 to YK, YS, SS, 20017013, 22128008, 24370095 to TN, 22770083, 24570100, 15K07185 to HS, 221S0002 to AT, AF, YS, SS); Hyogo Science and Technology Association grant to HS; DFG (GO1825/4-1 & CRC1208 to SBG, VR 132/1-1 to JdV, SFB 944 to HB and SZ, FOR964 to DB and RH, SFB 924 for DL); MEYS CR project LO1417 to SV, RS and JP; Carlsberg Foundation and the Villum Foundation's Young Investigator Programme to JH; LRSV laboratory (ANR-10-LABX-41) to PMD; Gent University to DVDS; Research Foundation Flanders (G.0317.17N to DVDS and PhD fellowship 1S17917N to LV); ERC Advanced Grants (EVO500 to LD, ETAP to JF and EDIP to JAL); Leibniz Association to MQ; NSF (DEB-1020660 and DEB-1036466 to KGK, MCB1714993 to CC, DEB 1036506 to CFD). Computation was partially performed at NIG and NIBB, Japan & High Performance and Cloud Computing University Tübingen, Baden-Württemberg bwHPC, Germany.

Authors' contributions

AF, AT, ES, HK, HS, JF, JAL, LD, MB, MQ, SAR, SR, SS, TN, YK, YS, YVP provided resources and materials.

AF, AiS, AT, SAR, SR, TN generated the draft genome.

AH, AiS, AsS, BC, CC, CD, CFD, DB, DL, DS-M, DVDS, FBH, FM, FR, GG, GT, GVR, HB, HS, JdV, JH, JMC, JP, KGK, KKU, LIACV, LV, MH, NT, PJ, PKIW, PMD, PU, RH, RK, RS, SAR, SG, SH, SR, SV, SZ, TN analyzed data.

JdV, JAL, LD, SAR, SG, TN wrote the paper.

All authors helped discuss the results and write the paper.

Declaration of Interests

The authors declare no competing interests.

References

Abouelhoda, M.I., Kurtz, S., and Ohlebusch, E. (2004). Replacing suffix trees with enhanced suffix arrays. Journal of Discrete Algorithms *2*, 53-86.

Alneberg, J., Bjarnason, B.S., de Bruijn, I., Schirmer, M., Quick, J., Ijaz, U.Z., Lahti, L., Loman, N.J., Andersson, A.F., and Quince, C. (2014). Binning metagenomic contigs by coverage and composition. Nat Methods *11*, 1144-1146.

Altschul, S.F., Madden, T.L., Schaffer, A.A., Zhang, J., Zhang, Z., Miller, W., and Lipman, D.J. (1997). Gapped BLAST and PSI-BLAST: a new generation of protein database search programs. Nucleic Acids Res *25*, 3389-3402.

Barve, M.P., Arie, T., Salimath, S.S., Muehlbauer, F.J., and Peever, T.L. (2003). Cloning and characterization of the mating type (MAT) locus from Ascochyta rabiei (teleomorph: Didymella rabiei) and a MAT phylogeny of legume-associated Ascochyta spp. Fungal Genet Biol *39*, 151-167.

Bauwe, H., Hagemann, M., and Fernie, A.R. (2010). Photorespiration: players, partners and origin. Trends Plant Sci *15*, 330-336.

Beilby, M.J. (2007). Action potential in charophytes. Int Rev Cytol *257*, 43-82.

Beilby, M.J. (2015). Salt tolerance at single cell level in giant-celled Characeae. Front Plant Sci *6*, 226.

Beilby, M.J., Turi, C.E., Baker, T.C., Tymm, F.J., and Murch, S.J. (2015). Circadian changes in endogenous concentrations of indole-3-acetic acid, melatonin, serotonin, abscisic acid and jasmonic acid in Characeae (Chara australis Brown). Plant Signal Behav *10*, e1082697.

Beltramo, C., Torello Marinoni, D., Perrone, I., and Botta, R. (2012). Isolation of a gene encoding for a class III peroxidase in female flower of Corylus avellana L. Mol Biol Rep *39*, 4997-5008.

Bennett, T. (2015). PIN proteins and the evolution of plant development. Trends Plant Sci *20*, 498-507.

Bolger, A.M., Lohse, M., and Usadel, B. (2014). Trimmomatic: a flexible trimmer for Illumina sequence data. Bioinformatics *30*, 2114-2120.

Boot, K.J., Libbenga, K.R., Hille, S.C., Offringa, R., and van Duijn, B. (2012). Polar auxin transport: an early invention. J Exp Bot *63*, 4213-4218.

Buschmann, H., and Zachgo, S. (2016). The Evolution of Cell Division: From Streptophyte Algae to Land Plants. Trends Plant Sci *21*, 872-883.

Bythell-Douglas, R., Rothfels, C.J., Stevenson, D.W.D., Graham, S.W., Wong, G.K., Nelson, D.C., and Bennett, T. (2017). Evolution of strigolactone receptors by gradual neo-functionalization of KAI2 paralogues. BMC Biol *15*, 52.

Cahoon, A.B., Nauss, J.A., Stanley, C.D., and Qureshi, A. (2017). Deep Transcriptome Sequencing of Two Green Algae, Chara vulgaris and Chlamydomonas reinhardtii, Provides No Evidence of Organellar RNA Editing. Genes (Basel) *8*.

Catarino, B., Hetherington, A.J., Emms, D.M., Kelly, S., and Dolan, L. (2016). The Stepwise Increase in the Number of Transcription Factor Families in the Precambrian Predated the Diversification of Plants On Land. Mol Biol Evol *33*, 2815-2819.

Chan, K.X., Phua, S.Y., Crisp, P., McQuinn, R., and Pogson, B.J. (2016). Learning the Languages of the Chloroplast: Retrograde Signaling and Beyond. Annu Rev Plant Biol *67*, 25-53.

Chin, C.S., Alexander, D.H., Marks, P., Klammer, A.A., Drake, J., Heiner, C., Clum, A., Copeland, A., Huddleston, J., Eichler, E.E*., et al.* (2013). Nonhybrid, finished microbial genome assemblies from long-read SMRT sequencing data. Nat Methods *10*, 563-569.

Daku, R.M., Rabbi, F., Buttigieg, J., Coulson, I.M., Horne, D., Martens, G., Ashton, N.W., and Suh, D.Y. (2016). PpASCL, the *Physcomitrella patens* Anther-Specific Chalcone Synthase-Like Enzyme Implicated in Sporopollenin Biosynthesis, Is Needed for Integrity of the Moss Spore Wall and Spore Viability. PLoS One *11*, e0146817.

Darriba, D., Taboada, G.L., Doallo, R., and Posada, D. (2011). ProtTest 3: fast selection of best-fit models of protein evolution. Bioinformatics *27*, 1164-1165.

de Vries, J., Curtis, B.A., Gould, S.B., and Archibald, J.M. (2018). Embryophyte stress signaling evolved in the algal progenitors of land plants. Proc Natl Acad Sci U S A.

Delaux, P.-M., Xie, X., Timme, R.E., Puech-Pages, V., Dunand, C., Lecompte, E., Delwiche, C.F., Yoneyama, K., Bécard, G., and Séjalon-Delmas, N. (2012). Origin of strigolactones in the green lineage. New Phytologist *195*, 857-871.

Delaux, P.M., Radhakrishnan, G.V., Jayaraman, D., Cheema, J., Malbreil, M., Volkening, J.D., Sekimoto, H., Nishiyama, T., Melkonian, M., Pokorny, L.*, et al.* (2015). Algal ancestor of land plants was preadapted for symbiosis. Proc Natl Acad Sci U S A *112*, 13390-13395.

Delcher, A.L., Kasif, S., Fleischmann, R.D., Peterson, J., White, O., and Salzberg, S.L. (1999). Alignment of whole genomes. Nucleic Acids Res *27*, 2369-2376.

Delwiche, C.F. (2016). The genomes of charophyte green algae. Adv Bot Res *78*, 255-270.

Delwiche, C.F., and Cooper, E.D. (2015). The Evolutionary Origin of a Terrestrial Flora. Current biology : CB *25*, R899-910.

Dierckxsens, N., Mardulyn, P., and Smits, G. (2017). NOVOPlasty: de novo assembly of organelle genomes from whole genome data. Nucleic Acids Res *45*, e18.

Duong, T., Cowling, A., Koch, I., and Wand, M.P. (2008). Feature significance for multivariate kernel density estimation. Computational Statistics & Data Analysis *52*, 4225-4242.

Edgar, R.C. (2004). MUSCLE: a multiple sequence alignment method with reduced time and space complexity. BMC Bioinformatics *5*, 113.

Flores-Sandoval, E., Eklund, D.M., Hong, S.F., Alvarez, J.P., Fisher, T.J., Lampugnani, E.R., Golz, J.F., Vazquez-Lobo, A., Dierschke, T., Lin, S.S.*, et al.* (2018). Class C ARFs evolved before the origin of land plants and antagonize differentiation and developmental transitions in Marchantia polymorpha. New Phytol *218*, 1612-1630.

Francoz, E., Ranocha, P., Nguyen-Kim, H., Jamet, E., Burlat, V., and Dunand, C. (2015). Roles of cell wall peroxidases in plant development. Phytochemistry *112*, 15-21.

Gao, X.H., Huang, X.Z., Xiao, S.L., and Fu, X.D. (2008). Evolutionarily conserved DELLA-mediated gibberellin signaling in plants. J Integr Plant Biol *50*, 825-834.

Garcia, M., Myouga, F., Takechi, K., Sato, H., Nabeshima, K., Nagata, N., Takio, S., Shinozaki, K., and Takano, H. (2008). An Arabidopsis homolog of the bacterial peptidoglycan synthesis enzyme MurE has an essential role in chloroplast development. Plant J *53*, 924-934.

Gnerre, S., Maccallum, I., Przybylski, D., Ribeiro, F.J., Burton, J.N., Walker, B.J., Sharpe, T., Hall, G., Shea, T.P., Sykes, S.*, et al.* (2011). High-quality draft assemblies of mammalian genomes from massively parallel sequence data. Proc Natl Acad Sci U S A *108*, 1513-1518.

Gramzow, L., and Theißen, G. (2010). A hitchhiker's guide to the MADS world of plants. Genome Biology *11*, 214.

Guindon, S., Dufayard, J.F., Lefort, V., Anisimova, M., Hordijk, W., and Gascuel, O. (2010). New algorithms and methods to estimate maximum-likelihood phylogenies: assessing the performance of PhyML 3.0. Syst Biol *59*, 307-321.

Gutsche, N., Thurow, C., Zachgo, S., and Gatz, C. (2015). Plant-specific CC-type glutaredoxins: functions in developmental processes and stress responses. Biol Chem *396*, 495-509.

Haas, B.J., Papanicolaou, A., Yassour, M., Grabherr, M., Blood, P.D., Bowden, J., Couger, M.B., Eccles, D., Li, B., Lieber, M.*, et al.* (2013). De novo transcript sequence reconstruction from RNA-seq using the Trinity platform for reference generation and analysis. Nature protocols *8*, 1494-1512.

Hackenberg, C., Kern, R., Huge, J., Stal, L.J., Tsuji, Y., Kopka, J., Shiraiwa, Y., Bauwe, H., and Hagemann, M. (2011). Cyanobacterial lactate oxidases serve as essential partners in N2 fixation and evolved into photorespiratory glycolate oxidases in plants. Plant Cell *23*, 2978-2990.

Hackenberg, D., and Pandey, S. (2014). Heterotrimeric G-proteins in green algae. An early innovation in the evolution of the plant lineage. Plant Signal Behav *9*, e28457.

Han, G.Z. (2017). Evolution of jasmonate biosynthesis and signaling mechanisms. J Exp Bot *68*, 1323-1331.

Heyl, A., Brault, M., Frugier, F., Kuderova, A., Lindner, A.C., Motyka, V., Rashotte, A.M., Schwartzenberg, K.V., Vankova, R., and Schaller, G.E. (2013). Nomenclature for members of the two-component signaling pathway of plants. Plant Physiol *161*, 1063-1065.

Hodgkin, A.L., and Huxley, A.F. (1952). A quantitative description of membrane current and its application to conduction and excitation in nerve. J Physiol *117*, 500-544.

Hori, K., Maruyama, F., Fujisawa, T., Togashi, T., Yamamoto, N., Seo, M., Sato, S., Yamada, T., Mori, H., Tajima, N*., et al.* (2014). *Klebsormidium flaccidum* genome reveals primary factors for plant terrestrial adaptation. Nature Communications *5*, 3978.

Huang, X., and Madan, A. (1999). CAP3: A DNA sequence assembly program. Genome Res *9*, 868-877.

Huelsenbeck, J.P., and Ronquist, F. (2001). MRBAYES: Bayesian inference of phylogenetic trees. Bioinformatics *17*, 754-755.

Huson, D.H., Beier, S., Flade, I., Gorska, A., El-Hadidi, M., Mitra, S., Ruscheweyh, H.J., and Tappu, R. (2016). MEGAN Community Edition - Interactive Exploration and Analysis of Large-Scale Microbiome Sequencing Data. PLoS Comput Biol *12*, e1004957.

Inupakutika, M.A., Sengupta, S., Devireddy, A.R., Azad, R.K., and Mittler, R. (2016). The evolution of reactive oxygen species metabolism. J Exp Bot *67*, 5933-5943.

Iseli, C., Jongeneel, C.V., and Bucher, P. (1999). ESTScan: a program for detecting, evaluating, and reconstructing potential coding regions in EST sequences. In Proc Int Conf Intell Syst Mol Biol (Menlo Park, CA, USA: American Association for Artificial Intelligence), pp. 138-148.

Joseph, J.M., Fey, P., Ramalingam, N., Liu, X.I., Rohlfs, M., Noegel, A.A., Muller-Taubenberger, A., Glockner, G., and Schleicher, M. (2008). The actinome of Dictyostelium discoideum in comparison to actins and actin-related proteins from other organisms. PLoS One *3*, e2654.

Jouffroy, O., Saha, S., Mueller, L., Quesneville, H., and Maumus, F. (2016). Comprehensive repeatome annotation reveals strong potential impact of repetitive elements on tomato ripening. BMC Genomics *17*, 624.

Ju, C., Van de Poel, B., Cooper, E.D., Thierer, J.H., Gibbons, T.R., Delwiche, C.F., and Chang, C. (2015). Conservation of ethylene as a plant hormone over 450 million years of evolution. Nat Plants *1*, 14004.

Kaplan-Levy, R.N., Brewer, P.B., Quon, T., and Smyth, D.R. (2012). The trihelix family of transcription factors--light, stress and development. Trends Plant Sci *17*, 163-171.

Katoh, K., and Standley, D.M. (2013). MAFFT Multiple Sequence Alignment Software Version 7: Improvements in Performance and Usability. Molecular Biology and Evolution *30*, 772-780.

Keller, O., Kollmar, M., Stanke, M., and Waack, S. (2011). A novel hybrid gene prediction method employing protein multiple sequence alignments. Bioinformatics *27*, 757-763.

Kelley, L.A., Mezulis, S., Yates, C.M., Wass, M.N., and Sternberg, M.J. (2015). The Phyre2 web portal for protein modeling, prediction and analysis. Nat Protoc *10*, 845-858.

Kent, W.J. (2002). BLAT--the BLAST-like alignment tool. Genome Res *12*, 656-664.

Kim, D., Pertea, G., Trapnell, C., Pimentel, H., Kelley, R., and Salzberg, S.L. (2013). TopHat2: accurate alignment of transcriptomes in the presence of insertions, deletions and gene fusions. Genome Biol *14*, R36.

Köster, J., and Rahmann, S. (2012). Snakemake--a scalable bioinformatics workflow engine. Bioinformatics *28*, 2520-2522.

Kwantes, M., Liebsch, D., and Verelst, W. (2012). How MIKC* MADS-box genes originated and evidence for their conserved function throughout the evolution of vascular plant gametophytes. Mol Biol Evol *29*, 293-302.

Lagesen, K., Hallin, P., Rodland, E.A., Staerfeldt, H.H., Rognes, T., and Ussery, D.W. (2007). RNAmmer: consistent and rapid annotation of ribosomal RNA genes. Nucleic Acids Res *35*, 3100-3108.

Lang, D., Ullrich, K.K., Murat, F., Fuchs, J., Jenkins, J., Haas, F.B., Piednoel, M., Gundlach, H., Van Bel, M., Meyberg, R.*, et al.* (2018). The Physcomitrella patens chromosome-scale assembly reveals moss genome structure and evolution. Plant J *93*, 515-533.

Lang, D., Weiche, B., Timmerhaus, G., Richardt, S., Riano-Pachon, D.M., Correa, L.G., Reski, R., Mueller-Roeber, B., and Rensing, S.A. (2010). Genome-wide phylogenetic comparative analysis of plant transcriptional regulation: a timeline of loss, gain, expansion, and correlation with complexity. Genome Biol Evol *2*, 488-503.

Lawrence, M., Huber, W., Pages, H., Aboyoun, P., Carlson, M., Gentleman, R., Morgan, M.T., and Carey, V.J. (2013). Software for computing and annotating genomic ranges. PLoS Comput Biol *9*, e1003118.

Lecointre, G., and Le Guyader, H. (2006). The Tree of Life: A Phylogenetic Classification (Harvard University Press).

Lee, E., Helt, G.A., Reese, J.T., Munoz-Torres, M.C., Childers, C.P., Buels, R.M., Stein, L., Holmes, I.H., Elsik, C.G., and Lewis, S.E. (2013). Web Apollo: a web-based genomic annotation editing platform. Genome Biol *14*, R93.

Leinonen, R., Sugawara, H., Shumway, M., and International Nucleotide Sequence Database, C. (2011). The sequence read archive. Nucleic Acids Res *39*, D19-21.

Li, B., and Dewey, C.N. (2011). RSEM: accurate transcript quantification from RNA-Seq data with or without a reference genome. BMC Bioinformatics *12*, 323.

Li, H., and Durbin, R. (2010). Fast and accurate long-read alignment with Burrows-Wheeler transform. Bioinformatics *26*, 589-595.

Lin, H., and Goodenough, U.W. (2007). Gametogenesis in the Chlamydomonas reinhardtii minus mating type is controlled by two genes, MID and MTD1. Genetics *176*, 913-925.

Love, M.I., Huber, W., and Anders, S. (2014). Moderated estimation of fold change and dispersion for RNA-seq data with DESeq2. Genome Biol *15*, 550.

Maier, U.G., Bozarth, A., Funk, H.T., Zauner, S., Rensing, S.A., Schmitz-Linneweber, C., Borner, T., and Tillich, M. (2008). Complex chloroplast RNA metabolism: just debugging the genetic programme? BMC Biol *6*, 36.

Marcais, G., and Kingsford, C. (2011). A fast, lock-free approach for efficient parallel counting of occurrences of k-mers. Bioinformatics *27*, 764-770.

McInnis, S.M., Desikan, R., Hancock, J.T., and Hiscock, S.J. (2006). Production of reactive oxygen species and reactive nitrogen species by angiosperm stigmas and pollen: potential signalling crosstalk? New Phytol *172*, 221-228.

Morris, J.L., Puttick, M.N., Clark, J.W., Edwards, D., Kenrick, P., Pressel, S., Wellman, C.H., Yang, Z., Schneider, H., and Donoghue, P.C.J. (2018). The timescale of early land plant evolution. Proc Natl Acad Sci U S A.

Nakamura, Y., Kanakagiri, S., Van, K., He, W., and Spalding, M.H. (2005). Disruption of the glycolate dehydrogenase gene in the high-CO2-requiring mutant HCR89 of *Chlamydomonas reinhardtii*. Canadian Journal of Botany *83*, 820-833.

Nguyen, L.T., Schmidt, H.A., von Haeseler, A., and Minh, B.Q. (2015). IQ-TREE: a fast and effective stochastic algorithm for estimating maximum-likelihood phylogenies. Mol Biol Evol *32*, 268-274.

Nicolas, M., and Cubas, P. (2016). TCP factors: new kids on the signaling block. Curr Opin Plant Biol *33*, 33-41.

Ohtaka, K., Hori, K., Kanno, Y., Seo, M., and Ohta, H. (2017). Primitive Auxin Response without TIR1 and Aux/IAA in the Charophyte Alga Klebsormidium nitens. Plant Physiol *174*, 1621-1632.

Park, S.Y., Fung, P., Nishimura, N., Jensen, D.R., Fujii, H., Zhao, Y., Lumba, S., Santiago, J., Rodrigues, A., Chow, T.F.*, et al.* (2009). Abscisic acid inhibits type 2C protein phosphatases via the PYR/PYL family of START proteins. Science *324*, 1068-1071.

Parra, G., Bradnam, K., and Korf, I. (2007). CEGMA: a pipeline to accurately annotate core genes in eukaryotic genomes. Bioinformatics *23*, 1061-1067.

Pfalz, J., and Pfannschmidt, T. (2013). Essential nucleoid proteins in early chloroplast development. Trends Plant Sci *18*, 186-194.

Pickett-Heaps, J.D. (1975). Green Algae: Structure. Reproduction and Evolution in Selected Genera (Sinauer).

Pringsheim, M. (1862). On the Pro-Embryos of the Charae. The Annals and Magazine of Natural History *59*, 321-326.

Pruesse, E., Peplies, J., and Glockner, F.O. (2012). SINA: accurate high-throughput multiple sequence alignment of ribosomal RNA genes. Bioinformatics *28*, 1823-1829.

Puranik, S., Acajjaoui, S., Conn, S., Costa, L., Conn, V., Vial, A., Marcellin, R., Melzer, R., Brown, E., Hart, D.*, et al.* (2014). Structural basis for the oligomerization of the MADS domain transcription factor SEPALLATA3 in Arabidopsis. Plant Cell *26*, 3603-3615.

Quinlan, A.R. (2014). BEDTools: The Swiss-Army Tool for Genome Feature Analysis. Curr Protoc Bioinformatics *47*, 11 12 11-34.

Ren, Y., Hansen, S.F., Ebert, B., Lau, J., and Scheller, H.V. (2014). Site-directed mutagenesis of IRX9, IRX9L and IRX14 proteins involved in xylan biosynthesis: glycosyltransferase activity is not required for IRX9 function in Arabidopsis. PLoS One *9*, e105014.

Rensing, S.A. (2018). Great moments in evolution: the conquest of land by plants. Curr Opin Plant Biol *42*, 49-54.

Rensing, S.A., Ick, J., Fawcett, J.A., Lang, D., Zimmer, A., Van de Peer, Y., and Reski, R. (2007). An ancient genome duplication contributed to the abundance of metabolic genes in the moss *Physcomitrella patens*. BMC Evol Biol *7*, 130.

Rensing, S.A., Lang, D., Zimmer, A.D., Terry, A., Salamov, A., Shapiro, H., Nishiyama, T., Perroud, P.-F., Lindquist, E.A., Kamisugi, Y*., et al.* (2008). The *Physcomitrella* genome reveals evolutionary insights into the conquest of land by plants. Science *319*, 64-69.

Ronquist, F., Teslenko, M., van der Mark, P., Ayres, D.L., Darling, A., Hohna, S., Larget, B., Liu, L., Suchard, M.A., and Huelsenbeck, J.P. (2012). MrBayes 3.2: Efficient Bayesian Phylogenetic Inference and Model Choice Across a Large Model Space. Syst Biol *61*, 539-542.

Rost, B. (1999). Twilight zone of protein sequence alignments. Protein Eng *12*, 85-94.

Rovekamp, M., Bowman, J.L., and Grossniklaus, U. (2016). *Marchantia* MpRKD Regulates the Gametophyte-Sporophyte Transition by Keeping Egg Cells Quiescent in the Absence of Fertilization. Curr Biol *26*, 1782-1789.

Saier, M.H., Jr., Reddy, V.S., Tsu, B.V., Ahmed, M.S., Li, C., and Moreno-Hagelsieb, G. (2016). The Transporter Classification Database (TCDB): recent advances. Nucleic Acids Res *44*, D372-379.

Sakayama, H., Kasai, F., Nozaki, H., Watanabe, M.M., Kawachi, M., Shigyo, M., Nishihiro, J., Washitani, I., Krienitz, L., and Ito, M. (2009). Taxonomic reexamination of *Chara globularis* (Charales, Charophyceae) from Japan based on oospore morphology and rbcL gene sequences, and the description of *C. leptospora* sp. nov. J Phycol *45*, 917-927.

Schwacke, R., Schneider, A., van der Graaff, E., Fischer, K., Catoni, E., Desimone, M., Frommer, W.B., Flugge, U.I., and Kunze, R. (2003). ARAMEMNON, a novel database for Arabidopsis integral membrane proteins. Plant Physiol *131*, 16-26.

Scrucca, L., Fop, M., Murphy, T.B., and Raftery, A.E. (2016). mclust 5: Clustering, Classification and Density Estimation Using Gaussian Finite Mixture Models. R J *8*, 289-317.

Simao, F.A., Waterhouse, R.M., Ioannidis, P., Kriventseva, E.V., and Zdobnov, E.M. (2015). BUSCO: assessing genome assembly and annotation completeness with single-copy orthologs. Bioinformatics *31*, 3210-3212.

Sorensen, I., Pettolino, F.A., Bacic, A., Ralph, J., Lu, F., O'Neill, M.A., Fei, Z., Rose, J.K., Domozych, D.S., and Willats, W.G. (2011). The charophycean green algae provide insights into the early origins of plant cell walls. Plant J *68*, 201-211.

Steinbiss, S., Willhoeft, U., Gremme, G., and Kurtz, S. (2009). Fine-grained annotation and classification of de novo predicted LTR retrotransposons. Nucleic Acids Res *37*, 7002-7013.

Tan, X., Calderon-Villalobos, L.I., Sharon, M., Zheng, C., Robinson, C.V., Estelle, M., and Zheng, N. (2007). Mechanism of auxin perception by the TIR1 ubiquitin ligase. Nature *446*, 640-645.

Theißen, G., Melzer, R., and Rümpler, F. (2016). MADS-domain transcription factors and the floral quartet model of flower development: linking plant development and evolution. Development *143*, 3259-3271.

Timme, R.E., Bachvaroff, T.R., and Delwiche, C.F. (2012). Broad phylogenomic sampling and the sister lineage of land plants. PLoS ONE *7*, e29696.

Tivendale, N.D., Ross, J.J., and Cohen, J.D. (2014). The shifting paradigms of auxin biosynthesis. Trends Plant Sci *19*, 44-51.

Trapnell, C., Williams, B.A., Pertea, G., Mortazavi, A., Kwan, G., van Baren, M.J., Salzberg, S.L., Wold, B.J., and Pachter, L. (2010). Transcript assembly and quantification by RNA-Seq reveals unannotated transcripts and isoform switching during cell differentiation. Nat Biotechnol *28*, 511-515.

Van Bel, M., Proost, S., Wischnitzki, E., Movahedi, S., Scheerlinck, C., Van de Peer, Y., and Vandepoele, K. (2012). Dissecting plant genomes with the PLAZA comparative genomics platform. Plant Physiol *158*, 590-600.

Vesty, E.F., Saidi, Y., Moody, L.A., Holloway, D., Whitbread, A., Needs, S., Choudhary, A., Burns, B., McLeod, D., Bradshaw, S.J*., et al.* (2016). The decision to germinate is regulated by divergent molecular networks in spores and seeds. New Phytol *211*, 952-966.

Vriet, C., Lemmens, K., Vandepoele, K., Reuzeau, C., and Russinova, E. (2015). Evolutionary trails of plant steroid genes. Trends Plant Sci *20*, 301-308.

Walker, K.L., Muller, S., Moss, D., Ehrhardt, D.W., and Smith, L.G. (2007). Arabidopsis TANGLED identifies the division plane throughout mitosis and cytokinesis. Curr Biol *17*, 1827-1836.

Wang, C., Liu, Y., Li, S.S., and Han, G.Z. (2015). Insights into the origin and evolution of the plant hormone signaling machinery. Plant Physiol *167*, 872-886.

Wang, W., Esch, J.J., Shiu, S.H., Agula, H., Binder, B.M., Chang, C., Patterson, S.E., and Bleecker, A.B. (2006). Identification of important regions for ethylene binding and signaling in the transmembrane domain of the ETR1 ethylene receptor of Arabidopsis. Plant Cell *18*, 3429-3442.

Wass, M.N., Kelley, L.A., and Sternberg, M.J. (2010). 3DLigandSite: predicting ligand-binding sites using similar structures. Nucleic Acids Res *38*, W469-473.

Wickett, N.J., Mirarab, S., Nguyen, N., Warnow, T., Carpenter, E., Matasci, N., Ayyampalayam, S., Barker, M.S., Burleigh, J.G., Gitzendanner, M.A*., et al.* (2014). Phylotranscriptomic analysis of the origin and early diversification of land plants. Proc Natl Acad Sci U S A *111*, E4859-4868.

Wilhelmsson, P.K.I., Muhlich, C., Ullrich, K.K., and Rensing, S.A. (2017). Comprehensive Genome-Wide Classification Reveals That Many Plant-Specific Transcription Factors Evolved in Streptophyte Algae. Genome Biol Evol *9*, 3384-3397.

Xiong, W., He, L., Lai, J., Dooner, H.K., and Du, C. (2014). HelitronScanner uncovers a large overlooked cache of Helitron transposons in many plant genomes. Proc Natl Acad Sci U S A *111*, 10263-10268.

Yang, Z. (2007). PAML 4: phylogenetic analysis by maximum likelihood. Mol Biol Evol *24*, 1586-1591.

Zeng, J., Dong, Z., Wu, H., Tian, Z., and Zhao, Z. (2017). Redox regulation of plant stem cell fate. EMBO J *36*, 2844-2855.

Figure titles and legends

Figure 1: Evolution of charophytic algae and land plant features

Cladogram symbolizing streptophytic evolution shows gain/expansion (green lines) and loss (red lines) of features; topology as in (Wickett et al., 2014) with phytohormone-related terms in blue and transcription factors (TF) and transcriptional regulators (TR) in brown. Expansions (and gains/losses) detected in the *Chara* lineage are shown by asterisk. See text for abbreviations. Modes of cytokinesis: a cleavage furrow with persistent telophase spindle as seen in *Klebsormidium*, and a phragmoplast seen in *Chara* that differs from that of land plants as the cell plate in *Chara* shows little centrifugal growth but is formed simultaneously across the cell's equator.

Figure 2: Life cycle and habit of *Chara braunii*

Meiosis occurs just prior to germination. At germination, a positively gravitropic rhizoid and a protonema that develops into the thallus are formed. The shoot-like thallus (phototropic and negatively gravitropic) comprises stem-like structures (axes) and whorls of branchlets (lateral organs appended to the main axes having adaxial-abaxial differentiation) at axial nodes. Growth of the axis/stem is axial from the terminal (apical) cell. Internodal cells, up to 5 cm long, are multinucleate. Internodal cells and branchlets are connected *via* specialized nodes or central cells connecting the internodes. Nodal cells can serve asexual propagation as they can form apical cells *de novo*. Female (oogonia) and male (antheridia) gametangia are borne on branchlet nodes of the monoicous thalli and generate female (egg cell) and male (sperm cell) gametes. The oogonial complex is comprised of egg cell and associated corona, jacket (five spiral tube cells), and basal cells. Sperm cells arise from filaments produced on the inner surfaces of antheridial shield cells. Upon fertilization the only diploid cell of the life cycle, the dormant zygote or oospore, is formed. Charasomes are plasmamembrane invaginations that allow carbon concentration *via* local acidification. Cells are connected by plasmodesmata. Actin-myosin based cytoplasmic streaming provides a fast transport mechanism. *C. braunii* is ecorticate, other species develop cortical cells (filaments with spine cells) from the nodes that cover the axis and branchlet internodal cells. LS: longitudinal section.

Figure 3: Gene and transposon length and density in selected plant and algal genomes.

Comparative box and whisker plots depicting distributions of feature lengths (A) and densities in 100 kbp windows (B). Organisms are ordered top-down by decreasing genome size; x-axes are logarithmic scale. Features are color-coded (legend on the right) and comprise predicted genes, helitrons, intact full-length long terminal repeat elements (flLTRE) and potentially fragmented copies (LTREs).

Figure 4: Overview of predicted presence of factors in phytohormone biosynthesis and signaling pathways of *C. braunii*.

Shown are biosynthesis enzymes (rectangles), receptors (pentagons), signal transduction components (hexagons), and TFs (ovals). Elements for which no orthologs were found (light green dashed boxes) and for which putative orthologs were identified (dark green boxes) (*cf.* Table 1, S10/11). Abbreviations as in Table 1.

Figure 5: Land plant heritage genes present in the *C. braunii* genome

(A) Growing repertoire of retrograde signaling components as well as PAPs along the streptophyte trajectory. Potential retrograde signaling orthologs are marked with colored dots (see species key). PEP-associated proteins (PAPs) are shown in the bottom inset. XRN2/XRN3 were not distinguished due to paralogy; faded dots mark the paralogy of *Chlamydomonas* FSD2 and the detection of *P. patens* PTAC7 ortholog with $E<10^{-4}$; mosses encode the cyanobacterial (i.e. non-PAP) version of MurE (Garcia et al., 2008), potentially applying for algal MurEs, too. (B) Bayesian inference phylogenetic tree of plant MADS-box genes. Posterior probabilities (≥0.6) of main branches are depicted next to the tree. Insert shows the exon-intron structures of representatives of MIKC^{C}-type genes together with the *Chara* MIKC-type genes. (C) Condensed ML tree of the LysM-RLK family. The Charales sequences form a single clade (blue branches) encompassing 7 *C. braunii* sequences. Duplication (red circle) leading to the LYK (orange) and LYR (green) subclades occurred at the base of the embryophytes. The moss and liverwort clades are clustered. (D, E) GO enrichment word clouds (biological process). Word clouds of genes down-regulated (D) or up-regulated (E) in oogonia as compared to antheridia. Font size correlates with significance; red terms are depleted, green terms enriched; top three terms each are shown. See also Fig. S5, S6, related to Table S2-S4.

Figure 6: Expression of the ROS gene network during sexual reproduction.

ROS-related gene abundance expressed in transcripts per million (TPM) was transformed to log scale and represented as heatmap in zygotes, oogonia and antheridia. Gene distance was calculated using the Euclidean method and genes were clustered using complete linkage. DEGs ($p < 0.01$) between zygotes and oogonia / oogonia and antheridia are depicted: green up arrow, log2(fold-change) > 0; red down arrow, log2(fold-change) < 0. The expanded family of class III peroxidases is shown in bold. See also Fig. S4, S6, S7, related to Table S2-S4.

Tables

Gene/ Gene family	*K. nitens*	*C. braunii*	*P. patens*	*A. thaliana*
AUX biosynthesis				
Tryptophan aminotransferase-related proteins (TAA/TAR)	1	0	6	5
YUCCA (YUC)	1	0	8	11
AUX signaling				
Transport inhibitor response 1/AUX signaling F-box (TIR1/AFB)	0	0	5	5
AUX response factor (ARF)	0	1	15	22
Indole-3-acetic acid inducible (Aux/IAA)	1/0[a]	2	4	29
AUX metabolism				
Gretchenhagen (GH)	4	1	2	20
AUX transport				
ATP-binding cassette B (ABCB)	7	5	10	22
AUX resistance 1 (AUX1/LAX)	1	0	9	4
PIN-formed 1 (PIN)	1	6	4	8
PIN-likes 1 (PILS)	3	0	3	7
CK Signaling				
CHASE domain containing histidine kinase (CHK)	6	2	11	3
Histidine-containing phosphotransfer proteins (HPT)	1	1	2	5
Response regulator type B (RRB)	1	0	5	11
Response regulator type A (RRA)	1	2	7	10
ETH biosynthesis				
1-aminocyclopropane-1-carboxylate synthase (ACS)	1	2	2	12
1-aminocyclopropane-1-carboxylate oxidase (ACO)	0	0	0	5
ETH signaling				
ETH response/ETH response sensor (ETR/ERS)	5	4	8	5
Constitutive triple response1 (CTR1)	1	2	1	1
ETH insensitive2 (EIN2)	0	1	2	1
ETH insensitive3 (EIN3)	1	4	2	6
EIN3 binding F-box protein (EBF1)	1	1	2	2

ABA biosynthesis				
Phytoene synthase1 (PSY1)	1	1	3	1
Phytoene desaturase (PDS)	2	1	2	1
Lutein deficient (LUT)	1	1	1	3
Zeaxanthin epoxidase (ZEP/ABA1)	1	1	1	1
9-Cis-epoxycarotenoid dioxygenase (NCED)	0	0	2	5
Abscisic aldehyde oxidase3 (AAO3)	1	0	2	1
ABA signaling				
Pyrabactin resistance (PYR)	0	0	4	14
Protein phosphatase 2C (PP2C - Group A)	1	0	2	9
SNF related kinase (SnRK)	1	1	4	5
CBL-interacting protein kinase (CIPK)	1	0	7	25
Calcium-dependent protein kinase (CPK)	1	2	30	34
SL synthesis				
Beta-carotene isomerase (D27)	2	1	1	1
Carotenoid cleavage dioxygenase (CCD7)	2	0	1	1
Carotenoid cleavage dioxygenase (CCD8)	2	0	1	1
SL signaling				
Alfa beta hydrolase (D14)	0	0	0	1
D14-like/ Karrikin insensitive2 (KAI2)	2	1	11	2
More axillary branching 2 (MAX2)	0	0	1	1

Table 1: Comparison of gene families operating in the biosynthesis and signaling networks of phytohormones.

A specific set of individual genes or gene families encoding steps in the phytohormone biosynthesis/signaling/metabolism/transport networks have been analysed in *K. nitens*, *C. braunii*, *P. patens* and *A. thaliana* (Table S1J).

a, kfl00094_0070 features Aux/IAA domains but also a B3 domain (see text for details).

Supplemental Figure Titles and Legends

Figure S1, related to STAR methods: Chromosomes in an antheridial filament of *C. braunii* (n=14, strain S276).

The chromosomes during cell division in young antheridial filaments of strain S276 were observed after Feulgen staining. The chromosome number n=14 was confirmed by counts made on chromosomes during metaphase or anaphase. Most Chara species have either n=14 or n=28 chromosomes, Nitella and the other genera have different base numbers. There are numerous examples of monoecious/dioecious species pairs in the family, with the dioecious species always displaying half the number of chromosomes than their monoecious counterpart. For Chara typically dioecious=14, monoecious=28 (or other multiples of 14). *C. braunii* is monoecious, but is unique in having the dioecious chromosome number of 14. There are no known dioecious sister taxa to *C. braunii*, perhaps due to the already reduced genome. Scale bar = 2 µm.

Figure S2, related to STAR methods: Assembly characteristics and decontamination

A) k-mer frequency analysis of the S276 paired end read data with k=25. Number of 25-mers at frequency 3 to 200 are shown with the solid line. Circles shows the points from 16 to 80 as what was recognized the major peak, presumably representing the single copy region in *C. braunii*. B) Scatter plot of mapped reads of two *C. braunii* strains on each scaffold. Blue and light blue points are scaffolds with GC content of at least 55% and less than 55%, respectively. C) Frequency distribution of scaffold wise GC content compared between putative *C. braunii* derived scaffolds (blue) and other scaffolds (green).

Figure S3, related to STAR methods: Ks-based analysis of *C. braunii* paralogs

Paranome-based WGD signature prediction. (A) Ks frequency plot highlighting mixture model components mean and standard-deviation (top: #component, bottom: mean Ks) based on raw Ks value classification. (B) Ks frequency plot highlighting mixture model components mean and standard-deviation (top: #component, bottom: mean Ks) based on log-transformed Ks value classification. (C) Ks group assignment for raw Ks classification. (D) Ks group assignment for log-transformed Ks classification. (E) Significant zero crossing (SiZer) plot. (F) Significant convexity (SiCon) plot. (G-J) Significant features of kernel density estimates using indicated bandwidths, highlighting significant gradient regions in blue and significant curvature regions in green using a significance level of 0.05. Red vertical lines represent Ks value of 0.1 and 2.0, dotted red vertical line represents Ks value of 0.235 corresponding to 12.5 Ma ago (these events might be no WGDs but only more or less recent local duplication events). For *C. braunii* no single predicted WGD signature was supported by three different bandwidth kernel densities (cf. STAR Methods).

Figure S4, related to Figure 6: Expression profiles during sexual reproduction.

Expression profile of trihelix TF genes based on RNA-seq evidence (Table S4) was visualized as A) a Venn diagram using venny (http://bioinfogp.cnb.csic.es/tools/venny/) and B) as a heatmap showing gene expression and DEGs from reproductive organs with RPKM > 1 in minimum two samples. C) Shows expression of differentially expressed TFs/TRs during sexual reproduction. D) Expression of DEGs associated with seeds during sexual reproduction. Transcripts per million (TPM) were transformed to log2 scale and clustered using the euclidean distance method and the complete clustering method (B, C, D).

Figure S5, related to Figure 5: Exon-intron structure comparison of MIKC^C-type, MIKC*-type and charophyte MIKC-type genes.

(A) Exon-intron structures of representatives of MIKC^C-type and MIKC*-type genes together with the charophyte MIKC-type genes *CbMADS1*, *CbMADS2* and *KnMADS1*. The exons encoding MADS-, I- , K- and C-domains are color coded in black, red, blue and green, respectively. Among the three Type II genes that were identified in the *C. braunii* genome only *CbMADS1* shows a canonical MIKC-type gene sequence. In contrast *CbMADS2* lacks most (but not all) introns and thus probably evolved via a retrotransposition and recombination event. *CbMADS3* lacks the conserved K-box that encodes for the protein-protein interacting K-domain (data not shown). (B and C) Analysis of exon-intron structures suggest that *CbMADS1* directly descends from an ancestral MIKC-type gene that was a common ancestor of MIKC^C- and MIKC*-type genes. (B) It was previously suggested that the N-terminal part of the K-domain of MIKC*-type proteins evolved through a duplication of two K-domain exons of an ancestral MIKC-type gene (Kwantes et al., 2012). The aligned amino acid sequences encoded by exon 2 of *CbMADS1*, and by the first K-domain exons of *KnMADS1*, *MpMADS1*, *PPM3*, *SmMADS4* and *AGL30* indeed strongly support this hypothesis. (C) In addition, striking similarities between the aligned amino acid sequences encoded by exon 5 of *CbMADS1*, exon 6 of *KnMADS1* and exons 5 and 6 of *MpMADS2*, *PPM1*, *SmMADS3* and *SEP3*, respectively, suggest that also the K-domain of MIKC^C-type proteins evolved through an exon duplication of an ancestral MIKC-type gene. This is especially intriguing considering the fact that, based on structural data, the last two K-domain exons of most if not all MIKC^C-type genes encode for a protein-protein interaction interface that facilitates tetramer formation of MIKC^C-type proteins (Puranik et al., 2014). It has already been suggested that the ability of MIKC^C-type proteins to tetramerize was an important precondition to evolve and diversify efficient developmental switches that facilitated the transition to land and the evolution of complex body plans of land plants (Theißen et al., 2016). Thus it is tempting to speculate that an exon duplication of an ancestral MIKC^C-type gene in the MRCA of extant land plants created the molecular prerequisites for this evolutionary novelty.

Figure S6, related to Figures 5/6: Transcriptome analyses of reproduction and early development.

GO enrichment word clouds (category biological process); genes down-regulated (A) or up-regulated (B) in oogonia as compared to antheridia, genes down-regulated (C) or up-regulated (D) in zygotes as compared to oogonia. Antheridia are strongly enriched with the GO category GO:0015074 “DNA integration” (A). 349 gene models expressed in antheridia were classified in this category; of these, 324 genes were found to be overlapping with a TE to at least 50 % (Table S4). Most of these genes were annotated as “integrase”, “ribonuclease H-like”, “reverse transcriptase”, and “aspartyl protease” by homology-based approach, terms typical of Ty3/Gypsy pol gene composition (Havecker et al., 2004). Ty3/Gypsy elements represent 20 % of the *C. braunii* genome. These results might indicate mobilization of retrotransposons and other mobile elements during male gametogenesis. This could be a consequence of genome rearrangement during male gamete formation. One could also imagine that mobilization and integration of retrotransposons might enhance genomic diversity during sexual reproduction.

Figure S7, related to Figure 6: Major reactive oxygen species scavenging pathway in plants.

Proteins associated with ROS scavenging are in bold. Number of genes found for *A. thaliana* and *C. braunii* (in green) are indicated in brackets. APx: Ascorbate peroxidase, Asn: ascorbate, DHA: Dehydroascorbate, DHAR: Dehydroascorbate reductase, GPx: Plant glutathione peroxidase, GR: Glutathione reductase, Grx: Glutaredoxins superfamily, GSH: reduced glutathione, GSSH: oxidized glutathione. Kat: Catalase, MDAR: Monodehydroascorbate reductase, PrxR: Peroxiredoxins family, RBOH: Respiratory burst oxidase homolog also called NADPH oxidase, SOD: Superoxide dismutase, Trx: Thioredoxins, MDA: Monodehydroascorbate, adapted from (Inupakutika et al., 2016).

STAR Methods

CONTACT FOR REAGENT AND RESOURCE SHARING

Further information and requests for resources and reagents should be directed to and will be fulfilled by the lead contact Stefan A. Rensing (stefan.rensing@biologie.uni-marburg.de).

EXPERIMENTAL MODEL AND SUBJECT DETAILS

Two strains of *C. braunii* (S276 and S277) were used. The strain S276 was isolated from the thallus, which germinated from the bottom soil of Lake Kasumigaura (Ibaraki, Japan) and was maintained at Kobe University. The unialgal isolation of this strain was achieved as follows. First, collected oospores were surface sterilized for 5 to 8 min in 20% (v/v) NaClO (aq) with 0.05% (v/v) Tween20. The sterilized oospores were then transferred into autoclaved soil-water medium for the Charales (SWC-3), containing distilled water and two layers of substrate: a mixture of black soil and river sand on top of a layer of leaf mould. In the present study, strain S277 was newly collected from a pond at Saijo (Ehime, Japan) on October 18, 2011. Newly collected specimens of *C. braunii* were identified based on their *rbc*L DNA sequences. The methods employed for field collection and DNA barcoding followed (Sakayama et al., 2009). The thalli were collected using a handmade anchor. Total DNA was extracted from field-collected samples using the Qiagen DNeasy Plant Mini Kit. Partial *rbc*L DNA sequences were amplified using the primers CHAR-RF-1 (5'-ATGTCACCACAGACAGAAACTAA-3') and CHAR-RR-4 (5'-GCTCCTGGAGCATTTCCCCAAG-3'). PCR conditions were 95 °C for 5min; 32 cycles at 95 °C for 40s, 55 °C for 40s, and 72 °C for 1.5min; and 72 °C for 7 min using Ex Taq (Takara Bio). PCR products were sequenced using the primers CHAR-RF-1, CHAR-RR-4, CHAR-RF-2 (5'-GAGCTGTATATGAATGTCTTCG-3') and CHAR-RR-3 (5'-GTTTCTGCTTGAGATTTATA-3'). The sequences obtained were aligned with published *rbc*L DNA sequences of the genus *Chara* downloaded from GenBank. Sequence alignment was performed using MUSCLE (Edgar, 2004) with default options. The aligned dataset of the *rbc*L DNA sequences was subjected to the Neighbour-Joining (NJ) method with Jukes-Cantor distances and 1,000 bootstrap replicates, using MEGA 6.0. Based on NJ trees, field-collected samples were identified at the species level. The unialgal culture of S277 was established following the same procedure as outlined for S276. The pressed specimens of S276 and S277 (TNS-AL 209137 and 209138) were deposited at the Herbarium, Department of Botany, National Science Museum (TNS), Tsukuba, Japan. Routine culture was essentially performed at 23 °C with a 16-h light: 8-h dark cycle with 24.5 μmol photons m^{-2} s^{-1} illumination provided by fluorescent lamps using soil-water medium for the Charales (SWC-3).

METHOD DETAILS

DNA extraction

Thalli of strain S276 were harvested in SWC-3 medium, washed with distilled water, frozen in liquid nitrogen, and stored at -80 °C until DNA extraction. High molecular weight DNA was prepared by the CTAB method followed by purification with Qiagen Genomic Tip. The frozen powder was weighed and poured on 6 volumes of 2X CTAB buffer (2%

hexadecyltrimethylammonium bromide [CTAB], 1.4M NaCl, 100 mM Tris-Cl pH 8, 20 mM EDTA, 1% Polyvinylpyrrolidone, 1% 2-mercaptoethanol) on a hotplate stirrer at 60 °C. After two rounds of Chloroform:IAA 25:1 extraction, the supernatant was mixed with 3 col of CTAB precipitation buffer (1% CTAB, 50 mM Tris-Cl pH 8, 10 mM EDTA). The precipitate was recovered by centrifugation and dissolved in NaCl solution (1 M NaCl, 10 mM Tris-Cl pH 8, 1 mM EDTA), then precipitated with 0.6 vol of 2-propanol. The precipitate was dissolved in TE and further purified with a Qiagen Genomic Tip according to the manufacturer's instruction. The integrity of the DNA was confirmed with pulsed field electrophoresis using CHEF DR-II (Bio-Rad). Alternatively, genomic DNA from harvested thalli was isolated by grinding the flash frozen material, adding 15 mL extraction buffer (100mM Tris, 50mM EDTA, 500mM NaCl, 10mM 2-mercaptoethanol; pH8) and 2 mL 10% SDS, and incubating for 10 min at 65 °C with mild agitation. Subsequently, 5.4 mL 5M potassium acetate were added and incubated 20 min on ice. After centrifugation at 13,000 g for 20 min at 4 °C the DNA is precipitated by adding 14 mL 2-propanol, incubation for 30 min at -20 °C and centrifugation at 13,000 g for 15 min at 4 °C. After the isopropanol precipitation the air dryed pellet was dissolved in 700 µl 1x TE buffer (pH 8), 1-3µl RNaseA (10mg/ml) was added and incubated for 10 min at 37 °C. To purify the DNA 600 µl phenol/chloroform 1:1 were added, mixed, centrifuged at 10,000 g for one minute and the aqueous phase extracted. To this phase 600 µl chloroform/isoamylalcohol 24:1 were added, mixed, centrifuged at 10,000 g for one minute and the aqueous phase extracted. To precipitate the DNA 70 µl 3M Na-acetate and 500 µl isopropanol were added, mixed and centrifuged at 10,000 g for ten minutes. The pellet was washed with one ml 70% ethanol, dried and afterwards was dissolved in deionized water. Quality was controlled using Nanodrop, Qubit measurement and agarose gel electrophoresis.

Chromosome observation

The thalli with young antheridia were collected within the first hour of the dark period and fixed in ethanol:acetic acid (3:1). Fixed material was stored at 4 °C until used. Chromosome preparations were made using the Feulgen squash method (Fig. S1). Fixed samples were rehydrated by passing through a graded series of ethanols and rinsed gently in distilled water. The samples were treated with 1N HCl for 5 min at room temperature, then treated with 1N HCl for 8 min in a water bath at 60 °C, and rinsed gently in distilled water. Afterwards, the samples were transferred into Schiff's reagent (Merck Millipore) for 60 min at room temperature. After rinsing the samples in distilled water, antheridia were removed from the thallus and dissected to remove the shield cells. The antheridial filaments were placed on a glass slide and covered with a glass cover-slip. Then, they were squashed to spread the cells and observed.

Genome sequencing and assembly

Genomic DNA of the uni-algal strain S276 isolated from Lake Kasumigaura (Ibaraki, Japan) was sequenced as the reference genome using Illumina technology and sequences were compared with those of the strain S277 that was isolated from the pond at Ehime (Japan). Approximately 0.25 Gbp of scaffolds were present in only one of the datasets and found to be of bacterial origin. After removal of these prokaryotic sequences, 1.75 Gbp of scaffold data (N50 size of 2.26 Mbp at #234) were obtained, of which 1.43 Gbp were assembled into contigs. This corresponds to ~74% of the *C. braunii* genome as measured by flow cytometry (1.89-1.96

Gbp) and to ~61% of the 2.35 Gbp estimated by k-mer analysis. The plastid and mitochondrial genome were assembled separately to recover 187,771 and 67,059 bp circular genomes, respectively.

Genome sequencing of *C. braunii* strain S276

A paired-end library with insert size of 250 bp was constructed using an S2 ultrasonicator (Covaris) and a TruSeq DNA PCR-Free LT Sample Prep Kit (Illumina) according to the manufacturer's protocols. The products were size-selected on an agarose gel and purified using the Qiagen MinElute Gel Extraction Kit. Nucleotide sequences were determined for 150 bp from both ends with an Illumina HiSeq 2500. Sixteen Mate-pair libraries were constructed using a Nextera Mate-pair library construction kit with standard and modified input DNA of 5.6, 8, and 20 μg in the reaction. The first set, four libraries were constructed using the standard protocol, a gel-free method starting with 1 μg DNA (one library), and gel-excision starting with 4 μg DNA (three libraries). In the Gel-free protocol tagmented DNA was purified with AMPure XP resulting in a broad size with a peak at 2.7 kbp. In the Gel (+) protocol, the size range was 3-5 kbp, 5-8 kbp, and larger, resulting in a peak of 4.5, 5.8, and 9 kbp, respectively, as measured with a Bioanalyzer after purification with a Zymoclean Large Fragment DNA Recovery Kit. After circularization, fragmentation with Covaris S2, end-repair, A-tailing and adapter ligation, gel-free and 4.5 kbp library were amplified for 10 cycles, whereas 5.8 kbp and 9 kbp libraries were amplified for 15 cycles. After purification and quantification, the libraries were further subjected to 8, 6, 6, and 8 cycles of PCR, for gel-free, 4.5, 5.8 and 9 kbp libraries, respectively (Table S1A).

In the second set, two libraries were constructed using 20 μg DNA instead of the standard 4 μg DNA to obtain larger fragment size distribution after tagmentation. In this sample, though the large molecules were not well separated on the agarose gel, three fractions, thick band at high molecular weight above all marker bands, below the band to 12 kbp, and a 8-12kbp fraction were recovered. The size of the recovered DNA could not be measured accurately using a Bioanalyzer, though the peak was around the 17kbp marker. The final amplification was done for 21 cycles and additional 8 cycles. The lowest 8-12 kbp fraction did not amplify well and was not used in further analysis.

In the third set, five libraries were constructed using 5.6 μg of starting DNA (1.4-fold of standard) and an additional five libraries using 8.0 μg of starting DNA (2-fold of standard); pulsed field electrophoresis on a CHEF-DRII (Bio-Rad) was used for the separation after the tagmentation. The electrophoretic conditions were 6 V/cm, 11 hours, switch time 1-6 s, on 1% agarose gel, in 0.5 X TBE buffer. The gel was stained with SYBR Gold and the gel slices were recovered in five fractions each. The lower limit of each slice was 5.0, 7.5, 10.0, 15.0, and 23.5 kbp. After purification, the DNA was immediately subjected to circularization without measuring its size. The final amplification was conducted for 15 cycles. Of these (Table S1A), 15 had good insert size distribution when mapped to a preliminary version of the assembly, but one (S276MP3 xk) had not and thus excluded for further analysis.

Another two mate pair libraries were constructed by GATC (3-4 kbp fragment size) and sequenced on an Illumina HiSeq 2000. One library was constructed using Crelox with an insert size of 3 kbp. DNA was fragmented using the Covaris S2 AFA instrument and sequencing was performed on an Illumina HiSeq 2000 at 2 x 100 bp.

K-mer frequency analysis

K-mer frequency with $k = 25$ in the paired end reads were counted with JELLYFISH (Marcais and Kingsford, 2011), applying the min-quality=20 option. A clear peak at 51 was observed with a valley at 16 (Fig. S2A). The peak at 51 was interpreted as the single copy genomic sequence and those less than 16 were mostly k-mers containing sequencing errors. The cumulative *k*-mer count from 16 upto 10,000 (which was the default upper limit of JELLYFISH) divided by 51 suggested the genome size be 2.355 Gbp. Note that this number includes *k*-mers derived from organellar and bacterial sequences and supposed to be overestimate for the nuclear genome size. With the peak at 51, the amount of paired-end reads are supposed to be sufficient for the assembly. The region from 16 to 80 as the putative single copy region comprised 0.95 Gbp.

Assembly

The raw sequences were assembled with ALLPATHS-LG (Gnerre et al., 2011). Initially the assembly started with R48517 on a machine having 768 GB of memory and 32 CPU cores. After running a month this process stopped at UnipathPatcher phase. Continuation was tried with the settings: PATCH_UNIPATHS=False FIX_LOCAL=False PATCH_SCAFFOLDS=False FIX_SOME_INDELS=False; unfortunately this failed again. The run directory was copied to a machine having 2 TB of memory and 80 cores and the assembly was continued with R48777 and completed after another twenty days (with 48 slots=threads), with reported peak memory usage of 1,756 GB. The assembly resulted in 28,091 scaffolds with a total length of 1.99 Gbp, comprised of 250,979 contigs with a total length of 1.65 Gbp. The library information is summarized in Table S1B.

Genome sequencing of *C. braunii* strain S277

Thalli of strain S277 were harvested in SWC-3 medium, washed with distilled water, frozen in liquid nitrogen, and stored at -80 °C until DNA extraction. Total DNA was extracted as described above. A paired end library was constructed using a TruSeq DNA PCR-free library preparation kit (Illumina) and sequenced with HiSEQ (DRA accession: DRR054048). 1.1 µg of DNA was fragmented with Covaris S2, using micro tube, duty cycle 10%, intensity 4, 200 cycles/burst and total time of 80 s. The fragments were size selected using a bead-based method following the 350-bp protocol.

PacBio sequencing of fosmid clones for quality control

C. braunii S276 genomic DNA was cloned into the pNGS fosmid vector using the aNxSeq 40 kbp Mate-Pair Cloning Kit (Lucigen). Six fosmid clones with verified end sequence and one 96 well plate of undetermined clones were pooled and shotgun sequenced on a PacBio SMRT cell (608 Mbp, 63,768 reads post-filtering). The resulting reads were assembled into contigs using HGAP (Chin et al., 2013) in smrtanalysis (PacificBiosciences). The contig sequences were further polished with two rounds of Quiver. Bacterial contamination was removed using MEGAN, and comparative mapping of S276 and S277 reads, resulting in 22 probable *C. braunii* contigs. All but one of those could be BLAST-mapped to the assembly. One clone appeared to be chimeric based on mapping Illumina mate-pair library data on the clone. Of the remaining 20, 14 were mapping to single scaffolds, the other 6 to 2-4 scaffolds. 10 of the 22 contigs were found to map with >=95% identity and >= 90% coverage to the assembly, the remaining 12 did not meet these parameters, probably due to assembly gaps. In summary, 45% of the assembled fosmid clones had high quality representations in the assembly, and 91% could be mapped, demonstrating the good quality of the assembly.

Distinction of bacterial sequences

Paired end sequences of S276 and S277 were mapped to the assembly with bwa mem (Burrows-Wheeler Aligner) (Li and Durbin, 2010) and the number of mapped sequences were counted on each scaffold (Fig. S2). Number of tags of both samples on each scaffold was plotted and we found two groups. The two groups were separated by a line in which S277 had 1/100 of S276 tags (Fig. S2B). The GC content of each scaffold was calculated and compared between the two groups. The group showing less tags in S277 had a higher GC content distribution (Fig. S2C). Thus, these scaffolds were presumed to be derived of different organisms, which were probably bacteria that survived autoclaving. In addition, scaffold_64 was found to be of bacterial origin in manual inspection during gene prediction. Further, the genomic scaffolds were split into 1 kbp fragments. Using tera-BLASTn 9.0.0 on DeCypher 9.0.0.25 (http://www.timelogic.com/catalog/757/tera-blast) each fragment was BLASTed against the NCBI nt database. The BLAST output was analysed by MEGAN 6 (Huson et al., 2016) and bacterial hits assigned to the 1 kbp fragments. All scaffolds containing more than 50 % of bacterial hit fragments were extracted. If no non-bacterial hits were contained on the scaffold and the bit score of the bacterial contamination exceeded 50 per hit the scaffold was removed as contamination. This affected 153 scaffolds with a total length of 312 kbp (Table S5), containing 120 gene models (marked in Table S4). Thus, 11,655 scaffolds totaling 1,751,225,565 bp, comprised of 234,221 contigs totaling 1,429,911,168 bp were recovered as representing the *C. braunii* nuclear genome. N50 scaffold size, and N50 contig size were 2,261,426 bp (at #234) and 10,124 bp (at #41,610), respectively.

Microbiome analysis

The diversity of microorganisms is expected to be low due to lab-culturing conditions and DNA sequence extraction protocols. To isolate the microorganisms remaining in the bulk of data, we mapped reads to the eukaryotic genome and only analyzed reads left unmapped. Given that S276 and S277 were reared at different geographical locations, analyzes were done on both sets separately. The two separate sets of remaining reads were assembled into contigs and analyzed from a meta-genomics point of view. Two separate assemblies have been generated using CLC-assembly cell using the larger word-size (kmer) of 50 nt to force more specificity (CLC bio, Aarhus, Denmark). These assemblies resulted in respectively 322685 contigs with a total size of 76.7 Mbp (N50 242 bp, max size 167358 bp, min size 100 bp) and 325720 contigs with a total size of 90.1 Mbp (N50 373 bp, max size 172440 bp, min size 100 bp). The obtained contigs represent a mixture of microorganisms that where clustered using CONCOCT (Alneberg et al., 2014) according to the manual, using BEDtools (Quinlan, 2014), Picard-tools and R, to create and format the needed input files. Several runs were done, aiming at providing the minimal number of differentiated clusters. In some cases large clusters were isolated and submitted again for a new round of clustering. The clusters (or bins) were calculated based on read coverage and sequence tetramer composition of the contigs following an iterative fitting of mixture-of-Gaussian models on the available data; each group is supposed to represent an organism that was further characterized to establish the species. Taxonomic assignment of the bins was performed using a similarity-based labeling of the fragments with MEGAN5. A first assessment of the quality and completeness of the bins was done by monitoring the presence of 36 COG single copy genes. 16S rRNA genes were isolated from the sequences using online RNAmmer 1.2 Server (Lagesen et al., 2007) and provided to SINA Alignment Service within Silva database for classification (Pruesse et al., 2012). Not all clusters could be identified up to species level, but for those for which we could find a reference genome, we show also a level of completeness by comparing to the respective reference genomes using nucmer from the MUMmer (Delcher et al., 1999) v3.23 package (Table S1T, S1U).

Transcriptome sequencing

Thalli of strain S276 were harvested in SWC-3 medium under controlled laboratory conditions at 23 °C with a 16-h light: 8-h dark cycle with 24.5 μmol photons m^{-2} s^{-1} illumination provided by fluorescent lamps. Two and seven different samples, for full-length cDNA and RNA-seq analyses, respectively, were collected, frozen in liquid nitrogen, and stored at −80 °C until further processing. Frozen samples were ground in liquid nitrogen. Total RNAs were then extracted with ISOGEN (Nippon Gene, Tokyo, Japan), and purified using the Qiagen RNeasy Plant Mini Kit. For the extraction of total RNA in oospores and rhizoids, Fruit-mate (Takara Bio, Shiga, Japan) was used prior to the extraction by ISOGEN. Full-length cDNA libraries were constructed using the oligo-capping method. Total RNA was treated with bacterial alkaline phosphatase (BAP; Takara) at 37°C for 40 min with RNasin (Promega). After extraction with phenol:chloroform (1:1) twice and ethanol precipitation, the RNA was treated with tobacco acid pyrophosphatase (TAP; in house purified) with RNasin at 37°C for 45 min. The BAP-TAP treated RNA were ligated with 5′-oligo (5′-AGC AUC GAG UCG GCC UUG UUG GCC UAC UGG-3′) using T4 RNA ligase (Takara).The first strand cDNAs were amplified using 5′ (5′-AGC ATC GAG TCG GCC TTG TTG-3′) and 3′ (5′-GCG GCT GAA GAC GGC CTA TGT-3′) PCR primers. The amplified cDNAs were digested with SfiI and cloned into DraIII-digested pME18S-FL3-3 (AB009864). Clones were picked and sequenced with ABI sequencers at National Institute of Genetics, Japan. After filtering for vector, synthetic oligonucleotides, and low-quality sequences 73,388 reads were left in total (Table S1D). RNA-seq libraries were constructed via the Illumina mRNA-Seq Sample Prep Kit using RNA extracted from various tissues (Table S1E). 76 or 101 bp paired end sequencing was performed on an Illumina HiSEQ 2000. Additionally, a late reproductive phase thalli (harvested 2-3 weeks after appearing of the gametangial primordia) library was constructed as RNA-ligation based stranded library using the combined method of mRNA-Seq Sample Prep Kit and Small RNA Sample Preparation Kit (Illumina), following the manufacturer's instructions. This library was sequenced by 76 bp single end sequencing performed on a GAIIx (Illumina).

Quantitative transcriptome comparison of antheridia, oogonia, and zygotes

Antheridia and oogonia were hand-dissected in Qiagen RNA*later* from *C. braunii* thalli (strain S276) grown under a 14:10 hours light:dark cycle at 22 °C. Zygotes were collected once detached from mother plants grown in identical conditions. Samples were flash frozen in liquid nitrogen then kept at -80 °C until further processing. Approximately 20 mg of starting material was ground in liquid nitrogen then total RNA was extracted using Ambion mirVana kit following manufacturer's recommendations. DNA was digested from RNA extracts using Promega RQ1 DNase and RNA was cleaned using a Qiagen RNeasy MinElute Cleanup Kit. RNA was then amplified using an Ovation RNA-Seq System V2 (NuGEN) amplification kit following manufacturer's protocol. Final amplified cDNAs were cleaned using the Qiagen PCR cleanup kit. Three biological replicates were obtained for antheridia, oogonia and zygotes. One sample containing vegetative and reproductive tissues was similarly prepared, except for the amplification step. 20 µg of RNA from each replicate was paired-end sequenced on an Illumina HiSeq 2000 platform at the Beijing Genomics Institute in China; at least 2 x 10 million reads were obtained per sample. Reads were processed to remove low quality sequences, PCR adapters, foreign sequences introduced by the amplification procedure and any detectable bias using Trimmomatic v0.36 (Bolger et al., 2014) and Perl scripts. Transcript were inferred from the reads pooled and aligned to the *C. braunii* genome sequence using Tophat v2.1.0 (Kim et al., 2013) and Cufflinks v2.0.2 (Trapnell et al., 2010). Both programs were given the *C. braunii* genomic structure as a guide. A custom Perl script was then used to clean Cufflinks predictions from spurious gene fusions and other detectable problems. Unaligned reads were further normalised, assembled and scaffolded into transcripts. Both reference guided and *de novo* assemblies were merged. Coding sequences were predicted, and sequence annotation and GO terms were obtained from transcripts using a pipeline based on BLAST v2.2.29 (Altschul et al., 1997) and TransDecoder v2.0.1 (Haas et al., 2013). A summary of assembly and read mapping statistics is presented in Table S1W. Read counts were obtained by mapping reads onto the inferred transcriptome with RSEM v1.2.11 (Li and Dewey, 2011). Differential expression was tested between zygotes and oogonia samples and between oogonia and antheridia samples and was conducted in R using DESeq2 v1.14.1 (Love et al., 2014). Genes were considered differentially expressed between two conditions with an adjusted p-value < 0.01 and a log2 fold-change (logFC) > 2. Differentially expressed genes are listed in Table S2. GO terms enrichment analysis was conducted in R using topGO v2.22.0. Enriched GO terms and associated genes are listed in Table S3. Heatmaps were generated using R and the package pheatmap v1.0.8. Visualization of the GO terms was implemented using word clouds via the http://www.wordle.net application. The weight of the given terms was defined as the -log10(q-values) and the color scheme used for the visualization was red for down-regulated GO terms and green for those up-regulated. See Table S2 for DEGs and Table S3 for GO analyses.

Identification of repeat sequences with RepeatModeler/RepeatMasker

A species-specific repeat model was constructed using RepeatModeler Version open-1.0.7 with ncbi engine. Repeats were identified using RepeatMasker version open-4.0.5 with Search Engine: NCBI/RMBLAST [2.2.27+] and RepeatMaskerLib.embl (Complete Database: 20140131), resulting in masking 46% of the genome. The breakdown is shown in Table S1F.

Gene prediction

High throughput cDNA sequencing (RNA-seq) was conducted on several libraries representing vegetative and reproductive stages, including thallus, gametangia and zygotes. These data were used together with full-length cDNA sequences to annotate the genome with AUGUSTUS. 35,445 putatively protein-coding genes were identified, of which 63% could be annotated using similarity-based approaches. A total of 13,331 gene models overlap to at least 50% with TE evidence and thus might not represent canonical protein-coding genes, bringing the number of protein-encoding genes down to 23,546. In total, the expression of 12,388 of those (53%) was supported by RNA-seq data (Table S4). Reciprocal best BLAST (Altschul et al., 1997) hit analysis of the *C. braunii* protein set revealed a high percentage presence of core gene sets: 96.43% of eukaryotic benchmarking universal single-copy orthologs (BUSCO, (Simao et al., 2015)), 98.65% CEGMA core eukaryotic genes (Parra et al., 2007), and 93.96% core gene families for green plants (Van Bel et al., 2012).

Gene prediction with Augustus (Keller et al., 2011) was performed following https://computationalbiologysite.wordpress.com/2013/07/25/incorporating-rnaseq-tophat-to-augustus/. Initial models were created based on the CEGMA output. RNA-seq data was mapped to the RepeatMasker masked *C. braunii* genome. Each accepted_hits.bam was sorted and processed with filterBam --uniq (--paired for paired data). Evidence of introns was extracted using bam2hints –intronsonly to obtain intron_hints.gff. The first round of Augustus was run with this as hints. An exon-exon junction database was constructed based on this output and bowtie was used to map the reads to the junctions. These mappings were further merged to the first intron hints and the second round of augustus was run. Gene prediction at this phase was manually investigated and confirmed genes on scaffold_0 and scaffold_2 were chosen and adjusted for the 5' and 3' ends of UTR based on RNA-seq mapping on Web Apollo (Lee et al., 2013). Thus, 120 manually inspected gene models were used to retrain Augustus. Construction of exon-part hints through wig file were performed according to http://augustus.gobics.de/binaries/readme.rnaseq.html. For the stranded RNA-seq data, forward and reverse mapped reads were separated with samtools and assigned the strand accordingly. Repeat hints were prepared by processing the gff file created by the RepeatMasker with "sed –e s/similarity/nonexonpart/ -e 's/Target.*/src=RM/'". Amino acid sequence of *A. thaliana* (TAIR10_pep_20110103_representative_gene_model_updated) and *P. patens* (P.patens.V6_filtered_cosmoss_proteins.fas) were mapped to the genome using exonerate and converted as hint data. The full-length EST sequences were mapped using blat (Kent, 2002) with -minIdentity=92 -extendThroughN parameters and converted to EST hints. All these hints were merged to a single hints file and the final run of Augustus was run with --gff3=on --UTR=on --alternatives-from-evidence=true --allow_hinted_splicesites=atac with a merged hints file. The output was collected and gene models predicted on the 11,808 scaffolds that were treated as *C. braunii* genome. Thus, we obtained 36,877 transcripts from 35,883 loci. For annotation see Table S4.

Assembly of organellar genomes

Organellar genomes were assembled using NOVOPlasty (Dierckxsens et al., 2017) v2.5.3. For chloroplast genome, two lanes of paired end data were processed using the *Chara vulgaris* chloroplast genome (NC_008097.1) as seed. This resulted in 4 possible reconstructions, two in 187 kbp and the remaining two in 200 kbp, i.e. contig arrangement 01+02+03+04+06, 01+04+05, 01+02+03+04+05, or 01+04+06. The differences are on whether 02 and 03 are inserted and whether the end is 05 or 06. 02 and 03 is contained in 01 and seems to represent an inverted repeat region and insertion of them would be excess. The 05 and 06 contain 27,447-bp common sequence, which is the small single copy region. Given there are about equal number of molecules that is flipped at the inverted repeat region, both reconstructions are equally valid and one is arbitrarily chosen. The mitochondrial genome was assembled using the *C. vulgaris* mitochondrial genome (NC_005255.1) as seed input and specifying the chloroplast genome obtained as above. This resulted in a single circularized assembly of 67,059 bp, which is very close to 67,737 of the *C. vulgaris* mitochondrial genome.

Repeat/TE annotation

Repetitive elements collectively contribute approximately 1.1 Gbp of the genome assembly. This estimate is probably low, given that highly similar repeats are challenging to assemble and that there is ~0.5 Gbp size difference between the ungapped (1.43 Gbp) assembly and C-value estimates (1.9 Gbp). Transposable elements (TEs) and unclassified repeats are abundant (61% and 37% of repeat annotation, respectively), with Gypsy-type LTR retrotransposons representing 24% (343 Mbp) of the ungapped assembly (Table S1G).

We have used the REPET package v2.4 to perform *de novo* identification, classification and annotation of repetitive elements in the *C. braunii* assembly as decribed in (Jouffroy et al., 2016). We first launched the TEdenovo pipeline on a sub-genome comprising contigs of size above 20 kb and representing a total of 362 Mb (12,655 contigs). We used default settings except that the minimum number of copies per group was set to 5 (minNbSeqPerGroup: 5), resulting in a library of 3,140 consensus sequences. This library was subsequently filtered by using the TEannot pipeline against the whole assembly and discarding consensus sequences without a single full length match, resulting in a library of 2,161 sequences. This filtered library was used to annotate the whole genome assembly using the TEannot pipeline. Threshold annotation scores were determined for each consensus as the 99th percentile of the scores obtained against a randomized sequence (whole genome reversed, not complemented and masked with TRF). Consensus sequences were then classified using the features detected with PASTEC followed by semi-manual curation. In addition to the HMM comparison against PFAM implemented in PASTEC, we have also used RPS-BLAST (-F T -e 1e-2) to search for more remote homologies against a library of CDD domains identified in the repbase library.

Several unclassified consensus sequences have been classified in putative retrotransposons because they contain at least one of the following domains: cd00024 Chromatin organization modifier, cd00303 Retropepsins, cd01650 RT nLTR, cd01651 RT G2 intron, cd05482 Retropepsins, cd06095 Retropepsin, cd06222 RNase H, pfam00385 Chromo, pfam00552 Integrase, pfam00665 Integrase, pfam02093 Gag P30, pfam03708 Avian retrovirus envelope protein, pfam03732 Retrotransposon gag protein, pfam07727 Reverse transcriptase, pfam10536 Plant mobile domain, pfam13966 zinc-binding in reverse transcriptase, pfam13975 gag-polyprotein putative aspartyl protease, pfam13976 GAG-pre-integrase domain, and smart00298 Chromatin organization modifier domain.

Based on the REPET results, percentage overlap of protein coding gene models with TEs was assessed and added to Table S4. Gene models overlapping to 100% with TE evidence are considered true TE genes, while those overlapping to at least 50% (but less than 100%) might be protein-coding genes present in TE regions, or might encode TE-based proteins. All genes were kept in the gene catalog so that individual evaluation (e.g. based on the homology-based annotation) is possible.

Screening for whole genome duplication events

To identify whole genome duplication (WGD) events we employed the KeyS software (Rensing et al., 2007) to obtain Ks (synonymous substitution) distributions of paralogous genes for *C. braunii.* In brief, paralogous genes were defined by a self-BLAST retaining only BLAST hits that showed at least 50% query and subject coverage and an alignment length according to the twilight zone *sensu* (Rost, 1999). Gene pairs with a BLAST identity of 98% or higher were further tested at the nucleic acid level to remove nearly identical sequences using optimal global alignments and a threshold of 98% identity. For nearly identical gene pairs only the longer sequence was kept and all gene pairs containing the shorter sequence were discarded (Rensing et al., 2007). The paralogous genes were further clustered using a minimal connectivity threshold of 50% (half linkage) and Ks values were calculated at the cluster nodes (representing duplication events rather than gene pairs) using the maximum likelihood method of CODEML implemented in PAML v4.7 (Yang, 2007).
The following procedure has been described recently (Lang et al., 2018), please see there for related citations. Briefly, we employed mixture modeling to find WGD signatures using the *mclust* v5.1 R package (Scrucca et al., 2016) to fit a mixture model of Gaussian distributions to the raw Ks and log-transformed Ks distributions. All Ks values ≤ 0.1 were excluded for analysis to avoid the incorporation of allelic and/or splice variants and to prevent the fitting of a component to infinity, while Ks values > 5.0 were removed because of Ks saturation. Further, only WGD signatures were evaluated between the Ks range of 0.235 (12.5 Ma ago) to account for recently duplicated gene pairs to Ks of 2.0 to account for misleading mixture modeling above this upper limit. Because model selection criteria used to identify the optimal number of components in the mixture model are prone to over fitting we also used SiZer and SiCon as implemented in the *feature* v1.2.13 R package (Duong et al., 2008) to distinguish components corresponding to WGD features at a bandwidth of 0.0188, 0.047, 0.094 and 0.188 (corresponding to 1 Ma, 2.5 Ma, 5 Ma and 10 Ma ago) and a significance level of 0.05.

Deconvolution of the overlapping distributions that can be derived from paranome-based Ks values without structural information shows that using mixture model estimation based on log-transformed Ks values mimics structure-based WGD predictions better than using raw Ks values, and can predict young WGD signatures and can pin point older WGD signatures (Lang et al., 2018). Since WGD signature prediction based on paranome-based Ks values can be misleading and is prone to over prediction we only considered Ks distribution peaks in a range of 0.235 to 2.0 as possible WGD signatures, thus excluding young paralogs potentially derived from tandem or segmental duplication and those for which accurate dating cannot be achieved due to high age (Fig. S3).

Genome comparison

C. braunii was compared with eight further Viridiplantae genomes. In addition to the genome length, GC content and the number of annotated genes, the mean intergenic and the mean intron length were calculated. The intergenic length was performed by extracting the genome regions not covered by the gff3 annotation file with bedtools complement (Quinlan, 2014) version 2.25.0. The intron length was calculated by extracting the distance between the annotated CDS regions. Both mean length and the corresponding standard deviation were calculated using awk (Table S1L). The gene density of the *C. braunii* genome is relatively sparse as compared to e.g. *A. thaliana*, *O. sativa* (rice) or two algae (*K. nitens* and *Chlamydomonas reinhardtii*), but similar to other Gbp-sized genomes like *Z. mays* or *H. vulgare* (Fig. 3 and Table S1L); the distance between genes is comparable to the approximately equal-sized *Z. mays* genome.

Comparative analysis of gene and transposons in selected plant and algae species

The genome sequences and annotations of *K. nitens*, *C. reinhardtii*, *A. thaliana*, *M. polymorpha*, *Oryza sativa*, *P. patens*, *C. braunii*, *Z. mays*, *H. vulgare* were downloaded and processed with GAG and the genome tools gff3 validator, to obtain consistent annotation files. For each annotated gene, intronic regions were inferred using the GenomeTools gff3 program. The *K. nitens* annotation file was manually curated for consistency with the other annotations and the GFF3 data standard.

Subsequently, intact full-length long terminal repeat transposon elements (LTREs) were predicted using the GenomeTools LTRharvest and LTRdigest software (Steinbiss et al., 2009) utilizing a set of TE-associated PFAM domains and a compilation of eukaryotic tRNAs. The pipeline was implemented as a BASH/PBS shell script (run_LTR_harvest_digest.sh). The resulting set of candidate LTREs was filtered to contain 2 LTRs, >=1 protein domain match and 2 target site duplications. These filtered elements were considered to represent intact full-length LTREs whose nucleotide sequences were extracted and searched against the genome using Vmatch requiring >=80% sequence identity and 100 bp alignment length. Depending on the repeat content and genome size, genomes where either split at gap boundaries into preferably 100 Mbp stretches using the UCSC toolkit faSplit (A: Snakemake workflow: split_approach), or directly processed as a whole FASTA file (B: Snakemake workflow: vmatch_mask) (Köster and Rahmann, 2012). Resulting putative LTRE fragments were merged into non-redundant, non-overlapping regions using the reduce function implemented in the R/Bioconductor package GenomicRanges (A) (Lawrence et al., 2013) or the bedtools merge program (B).

Helitrons were predicted using the HelitronScanner software using the parameters reported for element inference and copy number prediction in plant genomes reported in the initial manuscript (Xiong et al., 2014). Additional fragments were inferred by matching 50 bp from the 3' terminus of each full-length helitrons against the respective genome utilizing Vmatch (Abouelhoda et al., 2004) following the same approach as described for LTREs. Resulting matches and full-length helitrons were merged into non-redundant, non-overlapping regions using the bedtools merge program. The pipeline was implemented in the Snakemake workflow in folder helitrons/.

Gene-to-gene, gene-to-LTRE, LTRE-to-gene and LTRE-to-LTRE distances were inferred using an R script utilizing the distanceToNearest function from the R/Bioconductor GenomicRanges package (get_distances.R/get_distances.sh). Subsequent data analysis and plotting was carried out and documented in the R Jupyter Notebooks: folder analysis/: analyseWindows.ipynb, Distances.ipynb, Introns.ipynb, Lengths.ipynb. All described, generated materials and software needed to reproduce this analysis are available from the accompanying Mendeley Data repository (doi:10.17632/9hzzf9m4kh.1), arranged as an archive ("ComparativeTE_and_genes.Lang.tar.gz") that contains input, output and scripts.

In-depth analyses of specific gene families

Cell wall biosynthesis

Glycosyltransferases in the *C. braunii* genome assembly were initially identified via BLAST, using the Carbohydrate Acting enZYme database (CAZY) as of 2016-06-01 as query and a cut-off value of 10^{-25}. The sequences were manually verified by alignment with known cell wall biosynthetic glucosyltransferases and deposited in Table S1H. Phylogenetic trees were constructed using Phylogeny.fr with standard settings, starting with muscle alignment, curation of alignment by deletion of positions with gaps, and finally PhyML maximum likehood tree construction (Guindon et al., 2010). The phylogenetic trees (Data S1A, B) were statistically supported by approximate likelihood-ratio tests using default settings and values between 0 and 1 were obtained, as with bootstrap values. Approximate likelihood-ratio-test (aLRT) values were included when values were under 0.7 where *C. braunii* sequences are present.

Cell division

In order to compare the mode of cell division of algae and land plants we compiled a list of 221 *Arabidopsis* genes involved in cytokinesis (Table S1C), focusing on genes required for phragmoplast and PPB function. With these 221 *A. thaliana* proteins, a BLASTp (version 2.6.0+) search was performed against published plant and algal genomic/transcriptomic datasets (key resource table), including *C. braunii* and *K. nitens*. The e-value cutoff was set to 1E-4 and the number of database sequences to show alignment for was set to 3,000. The BLAST result was filtered according to (Rost, 1999) to keep homologous sequences only. Mutiple sequence alignments for phylogenetic trees of protein families were conducted using MAFFT (Katoh and Standley, 2013) in the automatic mode, and manually curated. The best fitting evolutionary model based was determined using ProtTest (Darriba et al., 2011) and applied in Bayesian phylogenetic inference using MrBayes (Ronquist et al., 2012) with two hot and two cold chains (Data S1Q-U) until the standard deviation of split frequencies dropped below 0.01 or for 6 mio generations (actin and cyclin).

Using the amplification score that shows potential gene expansion between *K. nitens* and *C. braunii* (Table S1C) we performed phylogenetic analyses as outlined above and found cyclin genes to be amplified in *C. braunii*, suggesting a more intricate regulation of the cell cycle as compared to *K. nitens*. While there is a single A1-type cyclin in both algae, the *C. braunii* genome encodes three B1-type cyclins (like *A. thaliana*), whereas *K. nitens* encodes only one (Table S1C, Data S1Q). We also found evidence that membrane trafficking is more elaborate; there are three genes coding for EXOCYST 70A in *A. thaliana*, two in *C. braunii* (and in the transcriptomes of several Zygnematophyceae), and a single gene in *K. nitens* (as in *Mesostigma viride* and Chlorophyta; Data S1R). With regard to the SNARE complex, we find that the *A. thaliana* NOVEL PLANT SNARE (NPSN) 11/12/13 clade contains two *C. braunii* (and two *Nitella mirabilis*) and a single *K. nitens* (and *M. viride*) protein (Data S1S).

Phytohormones: ETH

For the identification of putative homologs for ETH biosynthesis and signaling genes, BLASTp/tBLASTn searches were carried out against the *C. braunii* gene models and genome assembly using representative *A. thaliana* protein sequences as queries [ACS1 (AT3G61510), ACO1 (AT2G19590), ETR1 (AT1G66340), CTR1 (AT5G03730), EIN2 (AT5G03280), EIN3 (AT3G20770); Table S1J]. Translated sequences of putative ETH biosynthesis/signaling genes from *C. braunii* were then used as queries in reciprocal BLASTp searches to the *A. thaliana* protein database. Multiple ACO homologs were found in the *C. braunii* genome, however, the reciprocal BLASTp search suggests that these homologs are likely to be other oxidases. The other candidate *C. braunii* ETH biosynthesis/signaling protein sequences were manually verified and screened for essential protein domains [ACS (PR00753), ETR/ERS (ETH Binding Domain), CTR1 (PF14381 and CD13999), EIN3 (PF04873 and C-terminal Signaling Domain), EBF (IPR001810)]. An additional search with BLASTP 2.8.0+ using the representative *A. thaliana* proteins as queries and the putative homologs as the subjects was performed.

Phytohormones: ABA

For the identification of putative homologs for ABA biosynthesis and signaling genes, BLASTn/BLASTp searches were carried out against the *C. braunii* gene models and genome assembly using representative *A. thaliana* genomic/protein sequences as queries (Table S1J). An additional search with BLASTP 2.8.0+ using the representative *A. thaliana* proteins as queries and the putative homologs as the subjects was performed. The obtained *C. braunii* protein sequences were manually verified and screened for essential protein domains [PSY (PF00494), PDS (PF01593), GTG1 (PF12537), SnRK/CPK (PF00069)].

Phytohormones: SL

For the identification of putative homologs for SL biosynthesis and signaling genes, BLASTn/BLASTp searches were carried out against the *C. braunii* gene models and genome assembly using representative *A. thaliana* genomic/protein sequences as queries (Table S1J). An additional search with BLASTP 2.8.0+ using the representative *A. thaliana* proteins as queries and the putative homologs as the subjects was performed. The obtained *C. braunii* protein sequences were manually verified and screened for essential protein domains [CCD (PF03055)].

Phytohormones: Jasmonates (JA), Salicylates (SA), Gibberellins (GA), Brassinosteroids (BR)

For the identification of putative homologs for JA, SA, GA and BR biosynthesis and signaling genes, BLASTn/BLASTp searches were carried out against the *C. braunii* gene models and genome assembly using representative *A. thaliana* genomic/protein sequences as queries (Table S1J). Canonical (land-plant like) signaling pathways for JA, SA, GA and BR have been shown to have arisen in land plants [JA - (Han, 2017); SA - (Wang et al., 2015)], vascular plants [GA - (Gao et al., 2008; Wang et al., 2015)] and seed plants [BR - (Vriet et al., 2015)] respectively. Consistent with these findings, none of the genes encoding steps in the biosynthesis or signaling pathways for GA, JA, SA or BR appear to be present in the *C. braunii* genome (Table S1J). However, JA was found in *C. australis* (Beilby et al., 2015), JA and SA were detected in *K. nitens* (Hori et al., 2014), and GA was detected in *Chara tomentosa*, suggesting a different synthesis than known in land plants as in the case of AUX and ABA (Table 1, Fig. 4).

Phytohormones: AUX transport

For the identification of putative homologs for AUX transporter genes, tBLASTn/BLASTp searches were carried out against the *C. braunii* gene models and genome assembly using representative *A. thaliana* genomic/protein sequences as queries (Table S1J and S11).

Predicted coding sequences of PIN proteins were manually aligned with representative PIN sequences from previously published alignments, PIN sequences from charophyte algae were obtained from the NCBI database. The PIN sequence of *K. nitens* (GAQ81096.1) originated from the complete genome assembly, other algal sequences were obtained from the SRA database (Leinonen et al., 2011) of individual sequencing project by using the BLASTn algorithm, using the sequence from *K. nitens* as a query. The resulting hits were assembled with CAP3 (Huang and Madan, 1999) and repeatedly BLASTed against respective SRA databases to increase sequence length. Maximum-likelihood phylogenetic analysis was performed in MEGA 7.0 software using amino acid representation of highly conserved N- and C-terminal part of PIN sequence, LG+G+I substitution model and 500 bootstrap replicates (Data S1C, D).

Phytohormones: AUX signaling

For charophyte algae, mRNA sequences were downloaded and protein sequences were predicted with ESTScan v3.0.3 (Iseli et al., 1999) using the *A. thaliana* matrix [-M Arabidopsis_thaliana.smat]. Subsequently all proteins were screened with *hmmsearch* of the HMMer software suite (v3.1b2) for the abundance of the PFAM v30.0 domains: Auxin_resp (PF06507), AUX_IAA (PF02309), B3 (PF02362), F-box (PF00646) and F-box-like (PF12937) using either the gathering threshold [--cut_ga] option or an E-value of 0.1 for the complete sequence [-E 0.1] and an E-value of 0.1 for the domain [--domE 0.1] to account for possible sampling bias and cutoff bias of the curated PFAM model.

The obtained results were used to classify the proteins into possible AUX gene families: ARFs [mandatory domains: Auxin_resp + B3; optional: AUX_IAA], Aux/IAA [mandatory: AUX_IAA - Auxin_resp] and TIR1/AFB [mandatory: F-box or F-box-like]. For the AUX gene familiy TIR1/AFB an additional BLAST search with BLAST+ (v2.5.0) [-matrix BLOSUM45 -evalue 1e-5] using representative *A. thaliana* genes as queries [AT3G62980.1 (TIR1), AT4G03190.1 (AFB1), AT3G26810.1 (AFB2), AT1G12820.1 (AFB3), AT4G24390.2 (AFB4), AT5G49980.1 (AFB5)] and the domain containing proteins as the subjects was performed. Only BLAST hits with a query coverage (alignment length / query length) of at least 50% and a minimal protein identity according to formula (2) of (Rost, 1999) were retained as possible AUX gene family candidates. Maximum-likelihood phylogenetic analysis for each AUX gene family was performed on manual curated multiple sequence alignments obtained via MAFFT (v7.305b) and the E-INS-i algorithm. *IQ-TREE* (Nguyen et al., 2015) v1.5.3 was applied using the standard non-parametric bootstrap option with 1,000 replicates and the best model selected by *IQ-TREE* (Table S1K, Data S1E-G).

Phytohormones: AUX,* in silico *modeling of* C. braunii *LRR FBPs.

Leucine-RichRepeat (LRR)-containing F-Box Proteins (FBPs) from *C. braunii* with sequence similarity to land plant LRR FBPs were *in silico* modeled using “intensive” modeling mode in Protein Homology/analogY Recognition Engine V 2.0 (Phyre2) (Kelley et al., 2015). Various PDB molecule templates (coronatine-insensitive protein 1: Chain B (c3ogmB) and Chain D (c3oglD); transport inhibitor response 1: Chain E (c2p1nE); f-box/lrr-repeat max2 homolog: Chain A (c5hywA), skp2: Chain C (c1fs2C) and Chain K (c1fqvk); and protein toll: Chain A (c4lxrA)) were sele-cted to model *C. braunii* LRR FBPs based on heuristics to maximize confidence, percentage identity and alignment coverage. Structural prediction from regions modeled *ab initio* are highly unreliable. The final models (color-coded by the confidence of the match to the templates overall) were submitted to 3DLigandSite server (Wass et al., 2010) to predict potential binding sites (gray structures cartoon depiction); see Data S1P.

Phytohormones: CK

In order to identify putative CK receptors, BLAST searches were carried out against the *C. braunii* gene models and genome assembly, using PpCHK4 and AHK4 as queries. The detected sequences were run against the Interpro and PFAM databases to detect the domains (histidine kinase and response regulators) which are found in CK receptors. Two sequences were identified containing the domain architecture of CK receptors (CHBRA123g00790 and CHBRA19g00270). In order to identify putative histidine phosphor transfer protein (HPT), a search with the HPT domain (Interpro IPR008207) was conducted and retrieved one sequence (CbHPT1, CHBRA650g00040) (Table S1J). For identification of the response regulators (type-A and type-B) we used the PFAM domains Response_reg (PF00072) and Myb_DNA-binding (PF00249) in an hmmsearch and did not find any gene models. In order to make sure that this result is not due to a missing or fragmentary gene model we also screened the available transcriptome data (transcripts were translated in all possible frames). While two A-type response regulators (RRA) could be detected in the transcriptome (comp31700c0seq1num3, comp64895c0seq1/2 rc num2, Table S1J/S1K, Data S1H), no combination of the two domains and thus no B-type (RRB) could be detected. All sequences harboring Response_reg domains were aligned with the response regulator domains of the *Arabidopsis* response regulators ARR1 and ARR14 (RRB) as well as ARR4 and ARR9 (RRA) and ARR 22 (RRC – not known to be involved in CK signaling) using the muscle implementation of the MEGA 7.0 suite. Using the alignment, a maximum likelihood tree was calculated with the pairwise distances estimated by a JTT model and 100 bootstrap samples. Again, two sequences were determined as RRAs. Of the *Chara* sequences in the RRB clade, again none contained a MYB domain (Data S1H).

Photorespiration

In land plants, the canonical photorespiratory pathway employs 8 enzymes, namely 2PG-phosphatase (PGPase), glycolate oxidase (GOX), glutamate:glyoxylate aminotransferase (GGT), glycine decarboxylase (GDC), serine hydroxymethyltransferase (SHMT), serine/alanine:glyoxylate aminotransferase (SGT), hydroxypyruvate reductase (HPR) and glycerate 3-kinase (GLYK) (Bauwe et al., 2010). Particularly, the glycolate oxidation step, which is performed by GOX in the plant peroxisomes, is catalysed by glycolate dehydrogenase in the mitochondrium of the green algae *C. reinhardtii* (Nakamura et al., 2005) and in the cytosol of cyanobacteria. To analyze the photorespiration in the Charophyte algae *C. braunii*, the protein sequences of enzymes from *A. thaliana* were used to identify homologue proteins in *C. braunii* by a BLASTp similarity search against the Chbra.pep.20151207.orcae database (Table S1M). To verify, if *C. braunii* also possess genes to oxidize glycolate via a glycolate dehydrogenase like Chlorophytes and cyanobacteria do, the polyphyletic proteins from *C. reinhardtii* (ABG36932.1) and *Synechocystis sp.* PCC 6803 (Sll0404 and Slr0806) were used as templates in similarity searches. To verify, if a putative glycolate oxidase prefers the substrate glycolate over lactate, three amino acids in the active site that were shown to be responsible for the substrate preference (Hackenberg et al., 2011) were analyzed. To this end, the putative glycolate oxidase from *C. braunii* and verified glycolate oxidase proteins of the land plants *A.*

thaliana and *Spinacia oleracea*, the red alga *Cyanidioschyzon merolae* and characterized L-lactate oxidase proteins from the cyanobacterium *Nostoc* sp. PCC 7120 and the bacterium *Aerococcus viridans* were aligned and the corresponding amino acids in the active sites of the proteins compared.

Retrograde signaling and PAPs

Protein data from the genomes of *C. reinhardtii, K. nitens, C. braunii,* and *P. patens* was screened for orthologs of the flowering plant-type retrograde signaling pathway or PAPs *via* a reciprocal best BLASTp approach using *A. thaliana* sequenes as query. For GUN1, the BLASTp analyses were repeated using reciprocal pHMMER surveys. To further pinpoint the relation of *Cb*GUN1 to other PPRs, the high similarity *K. nitens* protein GAQ81958.1 was used as a query in BLASTP (2.2.26) search to a database comprising the NCBI nr dataset as of January 2015 supplemented with *K. nitens*, *Pinus taeda* 1.01, and *P. patens* v3.3 Ppav3.3 datasets and 912 hit sequences were retrieved through (http://moss.nibb.ac.jp/cgi-bin/blast-nr-Kfl). Two *C. braunii* proteins Cbr_g9159.t1 (GUN1) and Cbr_g31394.t1, and a *M. polymorpha* protein Mapoly0154s0039.1 were added to this set. From this set, top 500 hits with GAQ81958.1 were retrieved and aligned with mafft version 6.811b and converted to nexus format file through (http://moss.nibb.ac.jp/cgi-bin/selectNalign). The alignment was edited to retain 242 aa (others were excluded; further 47 proteins that showed low conservation in the retained regions were deleted). The nexus file was subjected to http://moss.nibb.ac.jp/cgi-bin/makenjtree to construct a NJ tree based on JTT distance with 1,000 bootstraps using PHYLIP 3.695. Sequences identical within the retained 242 aa sites were treated as a single OTUs and 381 OTUs remained in the final tree. The organism name the sequence originated was recovered using NCBI taxonomydb (ftp://ftp.ncbi.nih.gov/pub/taxonomy/accession2taxid/prot.accession2taxid.gz, ftp://ftp.ncbi.nih.gov/pub/taxonomy/taxdump.tar.gz). The subcellular localization of PAPs was predicted using three online tools (Table S1N).

Transcription factors and transcriptional regulators

Transcription associated proteins (TAPs) comprise transcription factors (TFs, acting in sequence-specific manner, typically by binding to *cis*-regulatory elements) and transcriptional regulators (TRs, acting on chromatin or via protein-protein interaction. We classified all *C. braunii* proteins into 122 families and sub families of TAPs by first screening the proteins for domains and then applying a domain-based rule set to distinguish the TAPs (Lang et al., 2010; Wilhelmsson et al., 2017). We compared this genome-wide classification with genomic protein sets from *Cyanidioschyzon merolae*, *C. reinhardtii*, *Cyanophora paradoxa*, *K. nitens* and several land plants, as well as with transcriptomic data of Charophyta (Timme et al., 2012), *M. polymorpha* and ferns (Table S1Q, S1Z). The phylogenetic tree for the trihelix family (Data S1J) was inferred as mentioned above for the cell division related families.

For the Homeodomain (HD) and basic Helix-Loop-Helix (bHLH) phylogenetic analyses (Table S1O, S1P), the *C. braunii* genome was searched using a BLASTp query that was assembled from the previously characterized bHLH and HD protein sequences (Catarino et al., 2016) in *At*, *A. thaliana*; *Os, O. sativa*; *Sm, Selaginella moellendorffi*; *Pp*, *P. patens*; *Mp*, *M. polymorpha; Kf, K. nitens; Cr, C. reinhardtii*; *Ot*, *Ostreococcus tauri*; *Vc, Volvox carteri; Cm*, *C. Merolae* with the addition of bHLH proteins sequences from *Cv, Coccomyxa subellipsoidea* (previously *Chlorella vulgaris*. The results of the BLASTp search were analyzed manually to ensure the presence of the HD or the bHLH conserved domain using SMART and PFAM. All protein sequences were aligned using MAFFT (Katoh and Standley, 2013) and further manually aligned independently for HD and bHLH. The Maximum likelihood analysis was carried out using PhyML (Guindon et al., 2010) 3.0, using the JTT amino acid substitution model and a predicted gamma distribution. Branch support was tested using a Shimodaira-Hasegawa-like approximate likelihood ratio test (SH-like aLRT). The generated unrooted trees were visualised using MEGA 6.0.

MADS box sequences were identified using the aforementioned domain-based rule set to distinguish the TAPs (Lang et al., 2010). Phylogenies were calculated with MrBayes (Huelsenbeck and Ronquist, 2001) applying mixed AA model for 50,000,000 generations based on an amino acid alignment of Type I and Type II MADS-domain proteins from a broad set of land plants together with MADS-domain proteins from charophytes. Sequences were aligned with MAFFT (Katoh and Standley, 2013) applying E-INS-i mode. Intron structure was determined by using the transcript sequence as query for BLAST searches against the genome scaffolds. Subsequently, the genomic region that harbors the gene was extracted and aligned to the transcript sequence.

Motor proteins

PFAM domains related to the three classes of motor proteins were retrieved from the whole predicted proteomes of *C. braunii*, *C. reinhardtii*, *P. patens*, and *A. thaliana* using Interproscan (Table S1S). These selected domain signatures not only include the true motors but also domains associated with the tasks the motors have to fulfill in a cell. Since motor proteins are comparably long gene prediction on draft genomes can lead to a slight overestimation of domain numbers. Thus, retrieved predicted gene structures were examined, whether they reside adjacent to another predicted gene encoding for a motor protein part. If the domain structures from known complete proteins conformed with a fusion of two or more adjacent gene models in *C. braunii*, we used this fused gene model for further analysis.

Action potential related ion channels and transport proteins

Ion channels, transporters and pumps predicted to be involved in electrical signaling in plants were identified in the *C. braunii* genome *via* a tBLASTn/BLASTp approach using *A. thaliana* sequences as bait as well as on the basis of PFAM domains. Subsequent BLASTp searches of retrieved sequences against TAIR10 (https://www.arabidopsis.org) and SWISSPROT were employed to identify closest homologs. Finally, sequences were were classified into respective transporter families according to TCDB (Saier et al., 2016) and ARAMEMNON (Schwacke et al., 2003) (Table S1R). When partially split models were found, they were manually annotated with reference to RNA-seq evidence through a genome browser at https://chara.asrc.kanazawa-u.ac.jp/Cbr1/jbrowse/.

LysM-RLKs

The *C. braunii* genome was screened for LysM-RLK genes via tBLASTn using Medicago NFP and Rice CERK1 as bait sequences (Table S1V). Hits with E-value < 10^{-30} were collected and deduplicated. These sequences were aligned using MAFFT (Katoh and Standley, 2013) with LysM-RLKs from embryophytes and *Nitella mirabilis*. Using MEGA 6.0 the best substitution model (JTT+G) was determined and a maximum likelihood tree was inferred using all sites and 100 bootstrap resamplings (Fig. 5C, Data S1L-N).

PPR proteins

Genomic protein sets were scanned for presence of the PFAM domain PPR (http://pfam.xfam.org/family/PF01535) using HMMscan. The number of proteins harboring two or more PPR domains were considered PPR proteins putatively involved in organellar RNA editing (Maier et al., 2008) and are shown in Table S1Y.

ROS-associated genes

21 families belonging to the well-known reactive oxygen species (ROS) gene network were searched using as a first screen the follwing PFAM. PF00141 for Class III Prx (CIII) and Ascorbate Prx (APx and APx-R), PF00199 and PF06628 for catalases (Kat), PF00255 for glutathione Prx (GPx), PF00578 and PF08534 for peroxiredoxin family, PF03098 for dioxygenase (DiOx), PF08022, PF01794, PF08030 and PF08414 for NADPH Oxidase (RBOH) and Ferric reduction oxidase (FRO), PF02777 and PF00080 for superoxide dismutase family (MnSOD, FeSOD, Cu/ZnSOD), PF00462 for Glutaredoxins superfamily, PF01786 for Alternative Oxidase (AOX and PTOX), PF02298 for Blue-copper-binding protein superfamily, PF00210 for ferritin (FER), PF13417 for dehydroascorbate reductase (DHAR), PF07992 and PF02852 for Monodehydroascorbate reductase (MDAR) and Glutathione reductase (GR), PF07992, PF02943 and PF00085 for thioredoxin superfamily and PF01070 Glycolate Oxidases (GOx). *Arabidopsis* sequences belonging to the "ROS gene network" have been used to confirm the *C. braunii* families affiliation.

Only alpha-DiOxygenase (DiOx) and APx-R were not detected in the *C. braunii* assembly. The 19 other families have been found in *C. braunii* with various conservation rates (Table S1X). Among these families, Class III peroxidases (Prx), described as secreted peroxidases, are usually members of a large family. The *C. braunii* genome contained 14 homologous sequences (Table S1X), which is much lower as compared with flowering plants (73 in *A. thaliana*) but higher than in *K. nitens* (3). All the 14 sequences are derived from a single gene in an ancestor of *C. braunii* as they form a presumably monophyletic clade (Data S1O). Before these duplication events only one or a few initial sequences may have existed, implied by the single sequence detected in *Chlorokybus atmophyticus* transcriptome data (Timme et al., 2012) and the low number of three sequences found in *K. nitens*. The CIII Prx protein sequences from *K. nitens* (3 sequences), *C. braunii* (14 sequences), *P. paten*s (57 sequences) and *A. thaliana* (73 sequences) were aligned using MAFFT and the tree constructed using Maximum Likelihood implemented in MEGA (Data S1O).

UBQ proteasome system (UPS)

Arabidopsis genes encoding components of the plant Ubiquitin proteasome system (UPS) were manually selected and used as query sequences in a tBLASTn analysis to identify respective orthologous genes in the *C. braunii* genome. Hits with E-values $< 10^{-10}$ were collected and annotated following a reciprocal best BLASTp approach using TAIR10 (Table S1I).

QUANTIFICATION AND STATISTICAL ANALYSES

All details of the applied statistics (*e.g.* for RNAseq-based differential gene expression analysis) are provided alongside the respective analysis in the Methods Details section. For the differential gene expression analysis between antheridia, oogonia, and zygotes, three true biological replicates were sequenced and used for the statistical analysis (computed using DESeq2). No sequencing points, i.e. samples, were removed during the analysis.

DATA AND SOFTWARE AVAILABILITY

Raw Illumina (DRA004353, DRA006568) and PacBio (DRA006569) genomic sequence data have been deposited in the DDBJ Sequence Read Archive (DRA) at the DNA Data Bank of Japan (DDBJ) under BioProject PRJDB3348. The main scaffolds are available as entries BFEA01000001-BFEA01011654, the accompanying organisms scaffolds as BFBZ01000001-BFBZ01016437. The chloroplast genome is available as AP018555, the mitochondrial as AP018556. Raw Illumina RNA-seq data used for annotation (DRA006080, DRA002641) have been deposited in the DRA at the DDBJ under BioProject PRJDB3228. Raw Illumina RNA-seq data of reproductive stages have been deposited to NCBI SRA (PRJNA445548). The genome and its annotation is available for human curation *via* the ORCAE interface at the URL: http://bioinformatics.psb.ugent.be/orcae/. The data is freely available for browsing as well as for bulk downloads and blast searches. Persons who would like to contribute and edit the data using the web interface will have to request an account by sending an email. Any change made to gene structures will be processed automatically by adding protein domains (running interpro) and best-blast hits. These changes will be shared with the community immediately. 69,969 ABI reads of a cDNA library (minimum length of 100 bp) have been deposited at the DDBJ under the accession numbers LU106825 to LU176793 (Table S1D). Alignments that are the basis for the phylogenetic trees as well as the genome comparison datasets resulting in Fig. 3 have been deposited as Mendeley Datasets (doi:10.17632/9hzzf9m4kh.1).

Supplemental Tables and Files

The supplemental/supporting information is arranged into:

- a PDF containing Figures S1-S7;
- a PDF containing phylogenetic trees and alignments Data S1A-U;
- five Excel spreadsheets containing Tables S1-5 (with indexing of sheets);
- alignments and supporting data for the genome comparisons (related to Fig. 3) in Mendeley (doi:10.17632/9hzzf9m4kh.1).

Supplemental Tables

Table S1, related to STAR methods: details of assembly, annotation and comparative analyses, with index in first sheet.

Table S1A: Genome libraries and accession numbers

Table S1B: Libraries used for assembly

Table S1C: Cell division

Table S1D: EST data deposited in DDBJ

Table S1E: RNA-seq used for annotation

Table S1F: Repeatmasker results

Table S1G: Repetitive elements

Table S1H: Cell wall biosynthesis

Table S1I: UBQ proteasome system

Table S1J: Phytohormones

Table S1K: Auxin signaling and transport

Table S1L: Genome comparison

Table S1M: Photorespiratory pathway

Table S1N: PAP localization prediction

Table S1O: bHLH and HD TFs comparison

Table S1P: bHLH and HD TFs *C. braunii*

Table S1Q: Transcription factors and transcriptional regulators

Table S1R: Ion channels

Table S1S: Motor proteins

Table S1T: Assembled bacterial genomes

Table S1U: Most abundant bacterial genera

Table S1V: LysM RLKs

Table S1W: Reproductive transcriptome

Table S1X: ROS network

Table S1Y: PPR proteins

Table S1Z: Transcription factors and transcriptional regulators gene Ids

Table S1AA: genome and transcriptome datasets used for comparative studies

Table S2, related to Fig. 5/6 and STAR methods: Differential gene expression analyses of rerproductive stages, with index in first sheet.

Table S2A: zygote versus oogonia

Table S2B: oogonia versus antheridia

Table S3, related to Fig. 5/6 and STAR methods: Gene Ontology analyses of the differential expression data in Table S2, with index in first sheet.

Table S3A: zygote versus oogonia up GO enrichment

Table S3B: zygote versus oogonia up genes

Table S3C: zygote versus oogonia down GO enrichment

Table S3D: zygote versus oogonia down genes

Table S3E: oogonia versus antheridia up GO enrichment

Table S3F: oogonia versus antheridia up genes

Table S3G: oogonia versus antheridia down GO enrichment

Table S3H: oogonia versus antheridia down genes

Table S4, related to Fig. 5/6 and STAR methods: *C. braunii* protein coding gene annotation (Gene Ontology, best blast hits, trihelix TFs, expression data, overlap with TE evidence, decontamination).

Table S5, related to STAR methods: Decontamination analyses.

S5A	summary
S5B	underlying data

Data S1, related to STAR methods: phylogenetic trees and alignments.

KEY RESOURCES TABLE

REAGENT or RESOURCE	SOURCE	IDENTIFIER
Critical Commercial Assays		
DNeasy Plant Mini Kit	Qiagen	Cat# 69106
Ex Taq	Takara Bio, Shiga, Japan	Cat# RR001A
BAP	Takara Bio, Shiga, Japan	Cat# 2120A
Fruit-mate for RNA Purification	Takara Bio, Shiga, Japan	Cat# 9192
T4 RNA ligase	Takara Bio, Shiga, Japan	Cat #2050A
Genomic Tip	Qiagen	Cat# 10243
ISOGEN	Nippon Gene, Tokyo, Japan	Cat# 311-02501
RNasin	Promega	Cat # N2111
MinElute Gel Extraction Kit	Qiagen	Cat# 28604
mirVana	Ambion	Cat# AM1560
mRNA-Seq Sample Prep Kit	Illumina	Cat# RS-100-0801
Nextera Mate-pair library construction kit	Illumina	Cat# FC-132-1001
NxSeq 40 kb Mate-Pair Cloning Kit	Lucigen	Cat# 42028-1
Ovation RNA-Seq System V2	NuGEN	Cat# 7102-32
RNeasy Plant Mini Kit	Qiagen	Cat# 74904
Schiff's reagent	Merck Millipore	Cat# 1.09033.0500
Small RNA Sample Preparation Kit	Illumina	Cat# FC-102-1009
TruSeq DNA PCR-Free LT Sample Prep Kit	Illumina	Cat# FC-121-3001
Zymoclean Large Fragment DNA Recovery Kit	Zymo Research	Cat# D4045
Deposited Data		
ARAMEMNON (plant membrane protein database)	Schwacke et al. 2003	http://aramemnon.uni-koeln.de
Carbohydrate-Active enZYmes Database (CAZy)	Lombard et al., 2014	http://www.cazy.org
Chara braunii ABI reads cDNA libraries	This study	DDBJ accessions LU106825 to LU176793
Chara braunii Illumina RNA-seq data of reproductive stages	This study	BioProject PRJNA445548
Chara braunii Illumina RNA-seq data used for annotation	This study	BioProject PRJDB3228
Chara braunii PacBio and Illumina genomic DNA sequencing data	This study	BioProject PRJDB3348
Genomic and transcriptomic data used for comparative analysis, see Table SAA	This study	n/a
Glycosyltransferase repertoire of *S. moellendorffii* and *P. patens*	PMID: 22567114	https://doi.org/10.1371/journal.pone.0035846.s017
Phylogenetic trees and alignments, data for Fig. 3	This study	Mendeley doi:10.17632/9hzzf9m4kh.1
Transporter Classification Database (TCDB)	Saier et al. 2016	http://tcdb.org

Experimental Models: Organisms/Strains		
Chara braunii S276	isolated from soil of Lake Kasumigaura (Ibaraki, Japan)	maintained at Kobe University; Herbarium press TNS-AL 209137 available at the National Science Museum (TNS), Tsukuba, Japan
Chara braunii S277	collected from a pond at Saijo (Ehime, Japan) for this study	maintained at Kobe University; Herbarium press TNS-AL 209138 available at the National Science Museum (TNS), Tsukuba, Japan
Software and Algorithms		
3DLigandSite	Wass et al., 2010	http://www.sbg.bio.ic.ac.uk/3dligandsite/
ALLPATHS-LG	Gnerre et al., 2011	http://software.broadinstitute.org/allpaths-lg/blog/?page_id=12
Augustus	Keller et al., 2011	http://bioinf.uni-greifswald.de/augustus/
BEDtools v2.25.0	Quinlan, 2014	http://bedtools.readthedocs.io/en/latest/
Bioconductor Package GenomicRanges	Lawrence et al., 2013	https://bioconductor.org/packages/release/bioc/html/GenomicRanges.html
Burrows-Wheeler Aligner (bwa mem v.0.7.8-r455)	Li and Durbin, 2009	https://sourceforge.net/projects/bio-bwa/files/
CEGMA	Parra et al., 2007	http://korflab.ucdavis.edu/datasets/cegma/#SCT8
CLC Assembly Cell	QIAGEN Bioinformatics	https://www.qiagenbioinformatics.com/products/clc-assembly-cell/
CONCOCT	Alneberg et al., 2014	https://github.com/BinPro/CONCOCT
Cufflinks v2.0.2	Trapnell et al., 2010	https://github.com/cole-trapnell-lab/cufflinks
DESeq2 v1.14.1	Love et al., 2014	https://bioconductor.org/packages/release/bioc/html/DESeq2.html
ESTScan	Iseli et al., 1999	http://estscan.sourceforge.net

feature v1.2.13	Duong et al., 2008	https://cran.r-project.org/web/packages/feature/index.html
GAG - Genome Annotation Generator V1.0	released under an MIT License (MIT), copyright © 2014 GAG Developers	http://genomeannotation.github.io/GAG/
GenomeTools [gff3/LTRdigest/LTRharvest] V1.5.9	Steinbiss et al., 2009	http://genometools.org/
HelitronScanner V1.0	Xiong et al., 2014	https://sourceforge.net/projects/helitronscanner/files/
HGAP & Quiver	Chin et al., 2013	https://www.pacb.com/support/software-downloads/
IQ-Tree v1.5.3	Nguyen et al., 2015	http://www.iqtree.org
JELLYFISH	Marçais and Kingsford, 2011	http://www.cbcb.umd.edu/software/jellyfish/
Jupyter Notebook and IRKernel	Thomas Kluyver, Philipp Angerer, Jan Schulz	http://jupyter.org/ https://github.com/IRkernel/IRkernel
KeyS	Rensing et al., 2007	http://plantco.de/research.html
MAFFT v6.811b / v7.305b	Katoh and Standley, 2013	https://mafft.cbrc.jp/alignment/software/
mclust v5.1	Scrucca et al., 2016	https://CRAN.R-project.org/package=mclust
MEGAN5 v5.11.3 / v6	Huson et al., 2016	http://ab.inf.uni-tuebingen.de/software/megan6/
MrBayes v3.2.6	Huelsenbeck and Ronquist, 2001	http://mrbayes.sourceforge.net/
MUMmer v3.23	Delcher et al., 1999	http://mummer.sourceforge.net
MUSCLE v3.8.31	Edgar et al., 2004	https://www.drive5.com/muscle/
NOVOPlasty ver 2.5.3	Dierckxsens et al., 2017	https://github.com/ndierckx/NOVOPlasty
PAML v4.7	Yang, 2007	http://abacus.gene.ucl.ac.uk/software/paml.html
PASTEC	Hoede et al., 2014	https://urgi.versailles.inra.fr/Tools/PASTEClassifier
pheatmap v1.0.8	Raivo Kolde	https://cran.r-project.org/web/packages/pheatmap/index.html
PHYLIP 3.695	Jerry Shurman, Mark Moehring, Joe Felsenstein	http://evolution.genetics.washington.edu/phylip.html

PhyML 3.0	Guindon et al., 2010	http://www.atgc-montpellier.fr/phyml/
Phyre2	Kelley et al., 2015	http://www.sbg.bio.ic.ac.uk/phyre2/html/page.cgi?id=index
Picard-tools 1.129	Broad Institute	http://broadinstitute.github.io/picard.
Prottest	Darriba et al. 2011	https://github.com/ddarriba/prottest3
RepeatMasker version open-4.0.5	Arian F.A. Smit, Robert Hubley & Phil Green	http://www.repeatmasker.org
RepeatModeler Version open-1.0.7	Arian F.A. Smit and Robert Hubley	http://www.repeatmasker.org/RepeatModeler/
REPET package v2.4	Flutre et al., 2011	https://urgi.versailles.inra.fr/Tools/REPET
RSEM v1.2.11	Li and Dewey, 2011	https://github.com/deweylab/RSEM
RNAmmer 1.2	Lagesen et al, 2007	http://www.cbs.dtu.dk/services/RNAmmer/
SINA Alignment Service (Silva database for classification)	Pruesse et al, 2012	https://www.arb-silva.de/aligner/
Smrtanalysis 2.0.1	PacificBiosciences	http://programs.pacificbiosciences.com/l/1652/2013-06-04/2t28z7
Snakemake v4.3.1	Köster and Rahmann, 2012	https://snakemake.readthedocs.io/en/stable/
Tandem Repeats Finder (TRF)	Benson, 1999	http://tandem.bu.edu/trf/trf.html
tera-BLASTn 9.0.0	Active Motif, Inc.	http://www.timelogic.com/catalog/757/tera-blast
topGO v2.22.0	Adrian Alexa and Jörg Rahnenführer	https://bioconductor.org/packages/release/bioc/html/topGO.html
Tophat v2.1.0	Kim et al., 2013	https://ccb.jhu.edu/software/tophat/index.shtml
TransDecoder v2.0.1	Haas et al, 2013	https://github.com/TransDecoder/TransDecoder
Trimmomatic v0.36	Bolger et al., 2014	http://www.usadellab.org/cms/?page=trimmomatic
Vmatch v2.3.0	Abouelhoda et al., 2004	http://www.vmatch.de/
Web Apollo	Lee et al., 2013	http://genomearchitect.github.io
Other		

Chara braunii genome interface for gene models open for human curation	This study	http://bioinformatics.psb.ugent.be/orcae/
DeCypher 9.0.0.25 (Biocomputing Platform)	TimeLogic	http://www.timelogic.com/catalog/752/biocomputing-platforms

Figure 1

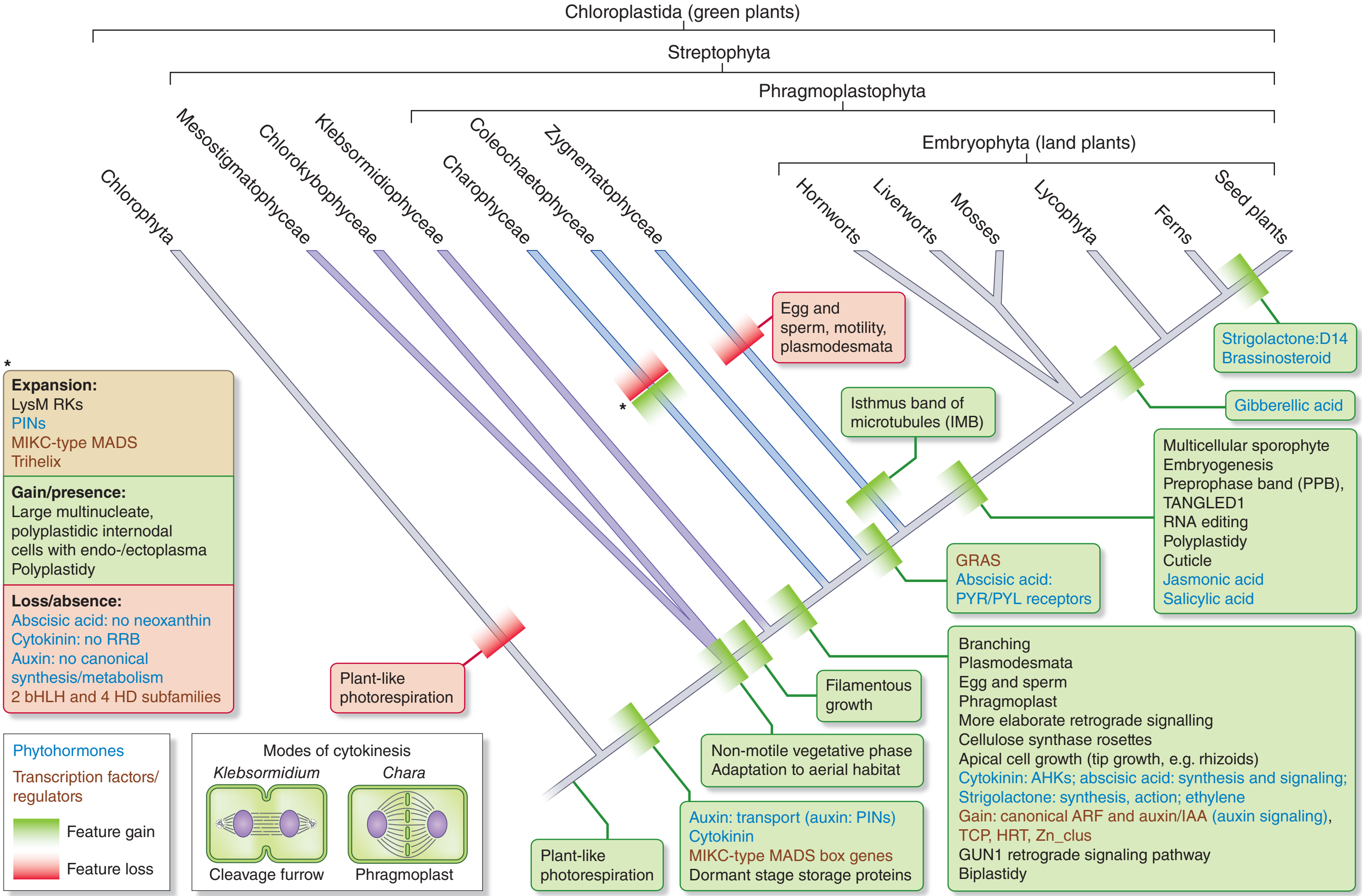
Chloroplastida (green plants)
Streptophyta
Phragmoplastophyta
Embryophyta (land plants)
Chlorophyta
Mesostigmatophyceae
Chlorokybophyceae
Klebsormidiophyceae
Charophyceae
Coleochaetophyceae
Zygnematophyceae
Hornworts
Liverworts
Mosses
Lycophyta
Ferns
Seed plants
Egg and sperm, motility, plasmodesmata
Strigolactone:D14
Brassinosteroid
Gibberellic acid
Isthmus band of microtubules (IMB)
Multicellular sporophyte
Embryogenesis
Preprophase band (PPB),
TANGLED1
RNA editing
Polyplastidy
Cuticle
Jasmonic acid
Salicylic acid
GRAS
Abscisic acid: PYR/PYL receptors
*
Expansion:
LysM RKs
PINs
MIKC-type MADS
Trihelix
Gain/presence:
Large multinucleate, polyplastidic internodal cells with endo-/ectoplasma
Polyplastidy
Loss/absence:
Abscisic acid: no neoxanthin
Cytokinin: no RRB
Auxin: no canonical synthesis/metabolism
2 bHLH and 4 HD subfamilies
*
Plant-like photorespiration
Filamentous growth
Branching
Plasmodesmata
Egg and sperm
Phragmoplast
More elaborate retrograde signalling
Cellulose synthase rosettes
Apical cell growth (tip growth, e.g. rhizoids)
Cytokinin: AHKs; abscisic acid: synthesis and signaling;
Strigolactone: synthesis, action; ethylene
Gain: canonical ARF and auxin/IAA (auxin signaling),
TCP, HRT, Zn_clus
GUN1 retrograde signaling pathway
Biplastidy
Non-motile vegetative phase
Adaptation to aerial habitat
Phytohormones
Transcription factors/ regulators
Feature gain
Feature loss
Modes of cytokinesis
Klebsormidium
Chara
Cleavage furrow
Phragmoplast
Plant-like photorespiration
Auxin: transport (auxin: PINs)
Cytokinin
MIKC-type MADS box genes
Dormant stage storage proteins

Figure 2

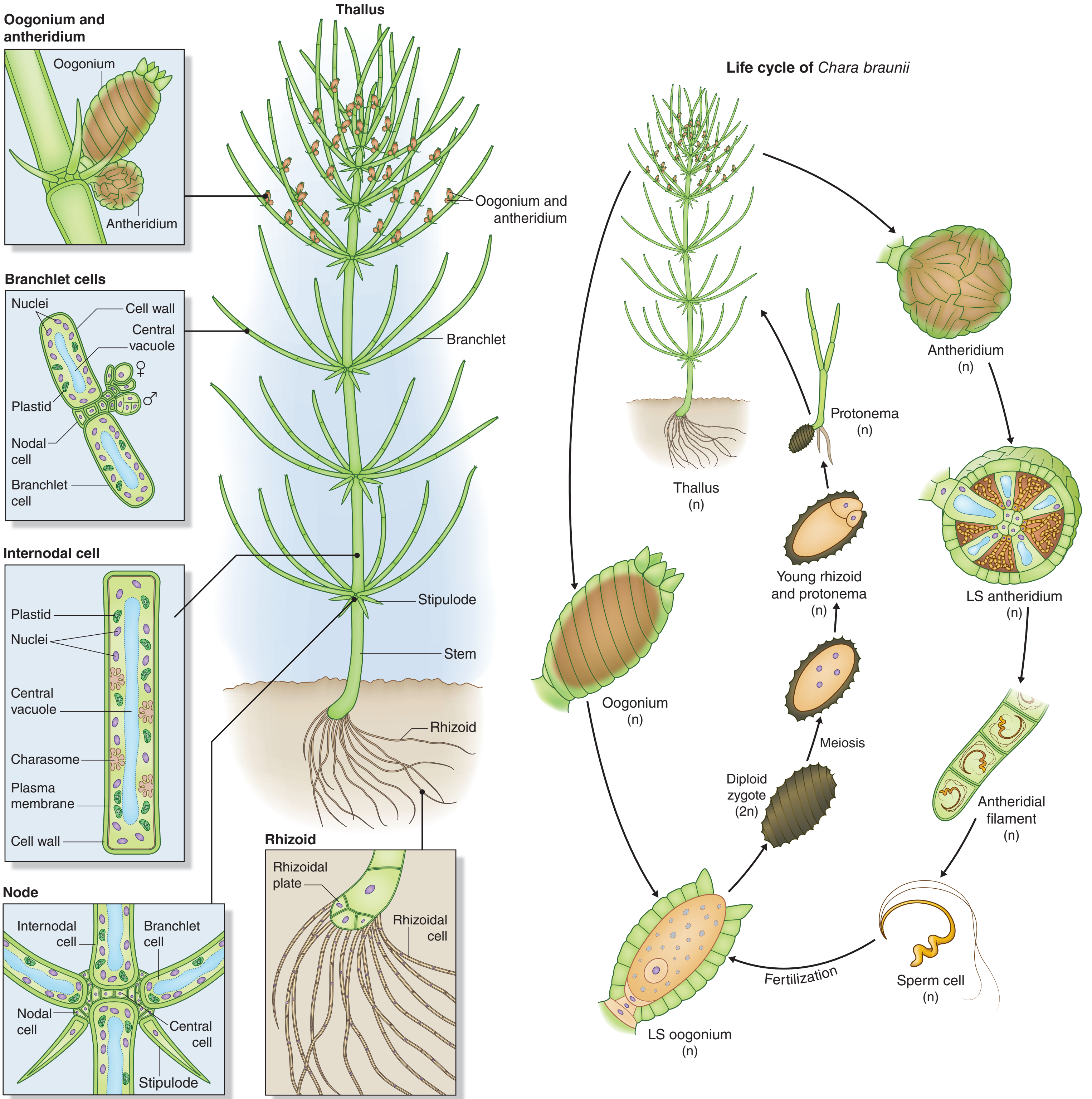
Oogonium and antheridium
Oogonium
Antheridium
Branchlet cells
Nuclei
Cell wall
Central vacuole
♀
♂
Plastid
Nodal cell
Branchlet cell
Internodal cell
Plastid
Nuclei
Central vacuole
Charasome
Plasma membrane
Cell wall
Node
Internodal cell
Branchlet cell
Nodal cell
Central cell
Stipulode
Thallus
Oogonium and antheridium
Branchlet
Stipulode
Stem
Rhizoid
Rhizoid
Rhizoidal plate
Rhizoidal cell
Life cycle of *Chara braunii*
Thallus (n)
Antheridium (n)
Protonema (n)
LS antheridium (n)
Young rhizoid and protonema (n)
Oogonium (n)
Meiosis
Diploid zygote (2n)
Antheridial filament (n)
Sperm cell (n)
Fertilization
LS oogonium (n)

Click here to download Figure Figure3.png

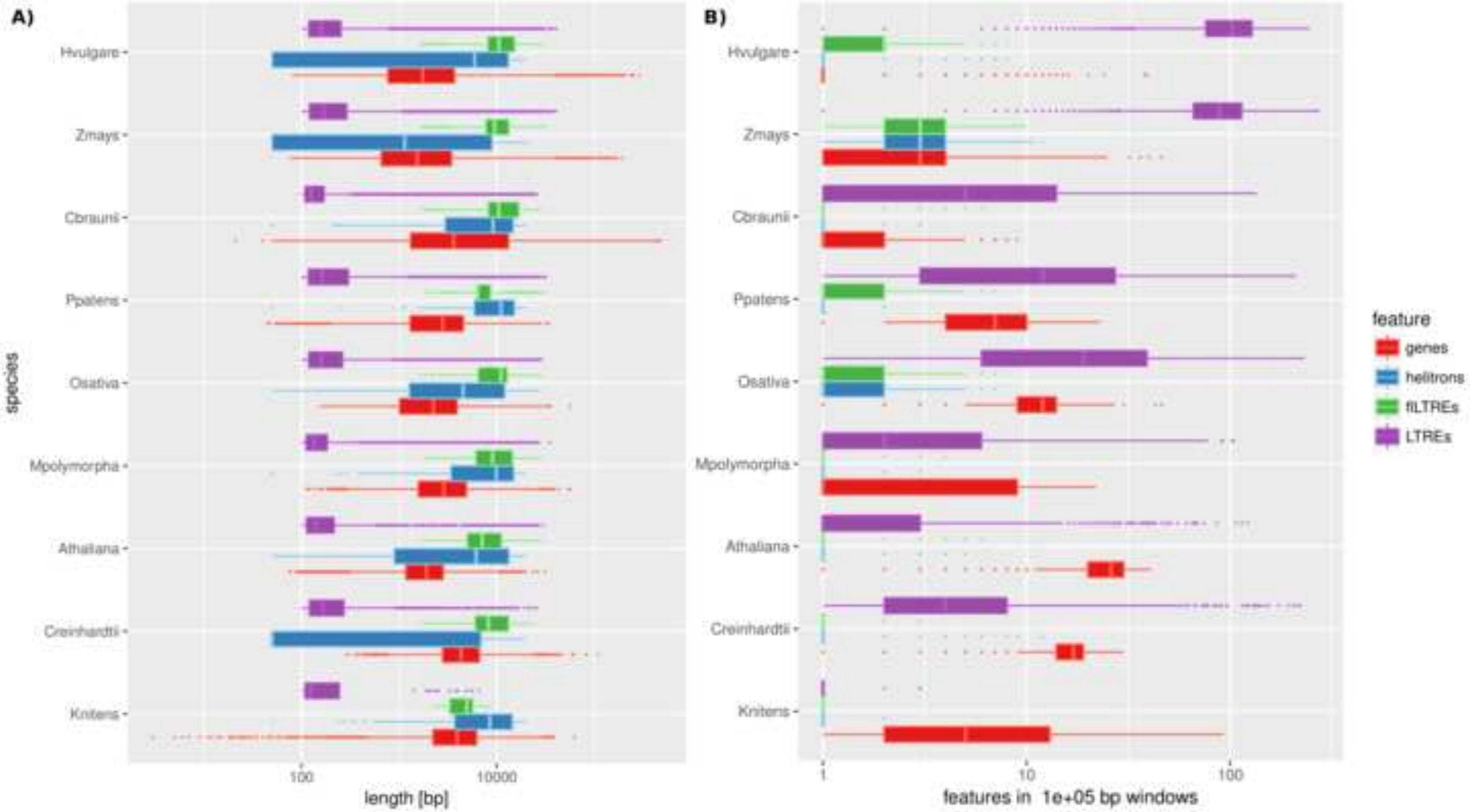

Figure 4

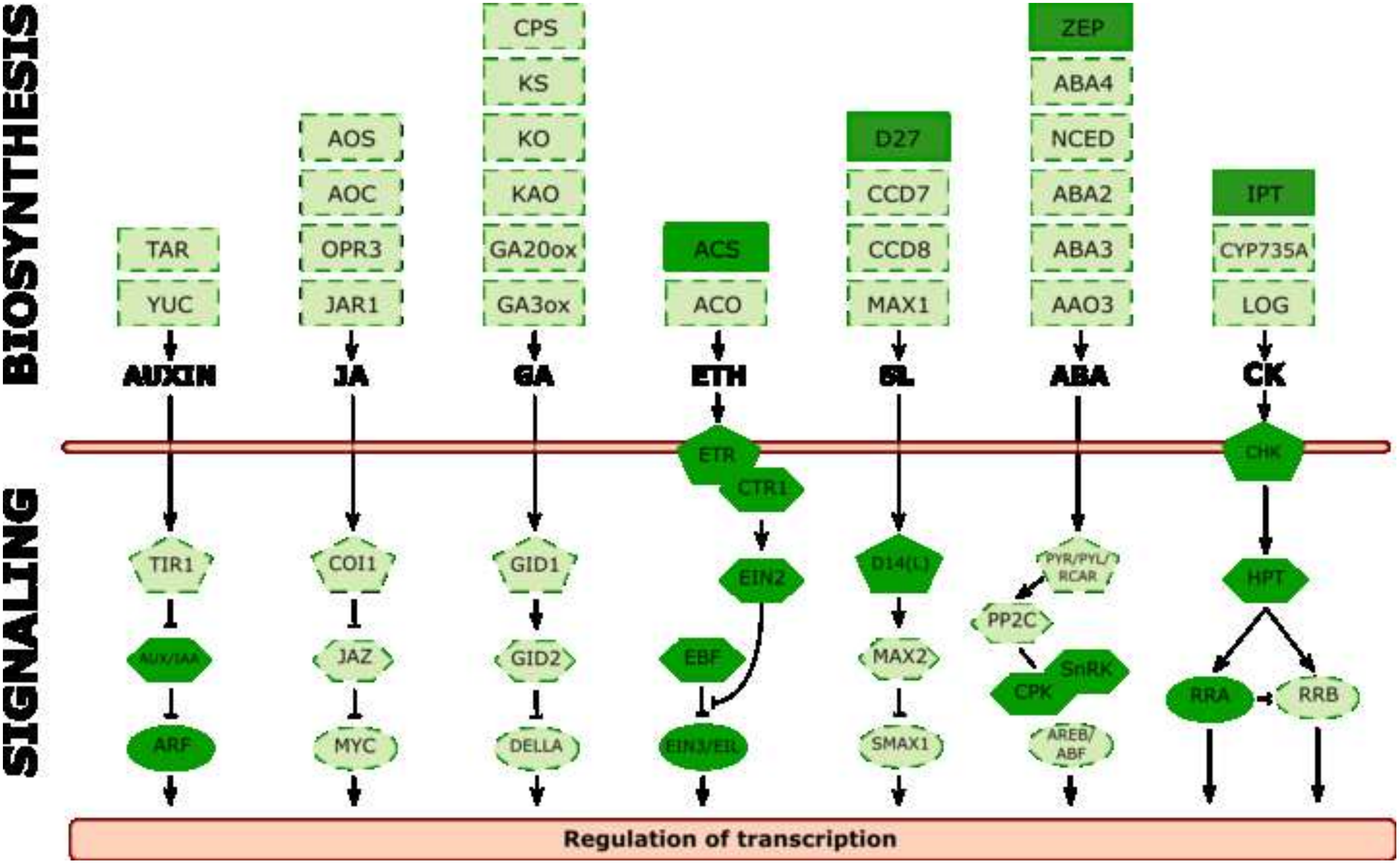
BIOSYNTHESIS
SIGNALING
TAR
YUC
AUXIN
TIR1
AUX/IAA
ARF
AOS
AOC
OPR3
JAR1
JA
COI1
JAZ
MYC
CPS
KS
KO
KAO
GA20ox
GA3ox
GA
GID1
GID2
DELLA
ACS
ACO
ETH
ETR
CTR1
EIN2
EBF
EIN3/EIL
D27
CCD7
CCD8
MAX1
SL
D14(L)
MAX2
SMAX1
ZEP
ABA4
NCED
ABA2
ABA3
AAO3
ABA
PYR/PYL/
RCAR
PP2C
SnRK
CPK
AREB/
ABF
IPT
CYP735A
LOG
CK
CHK
HPT
RRA
RRB
Regulation of transcription

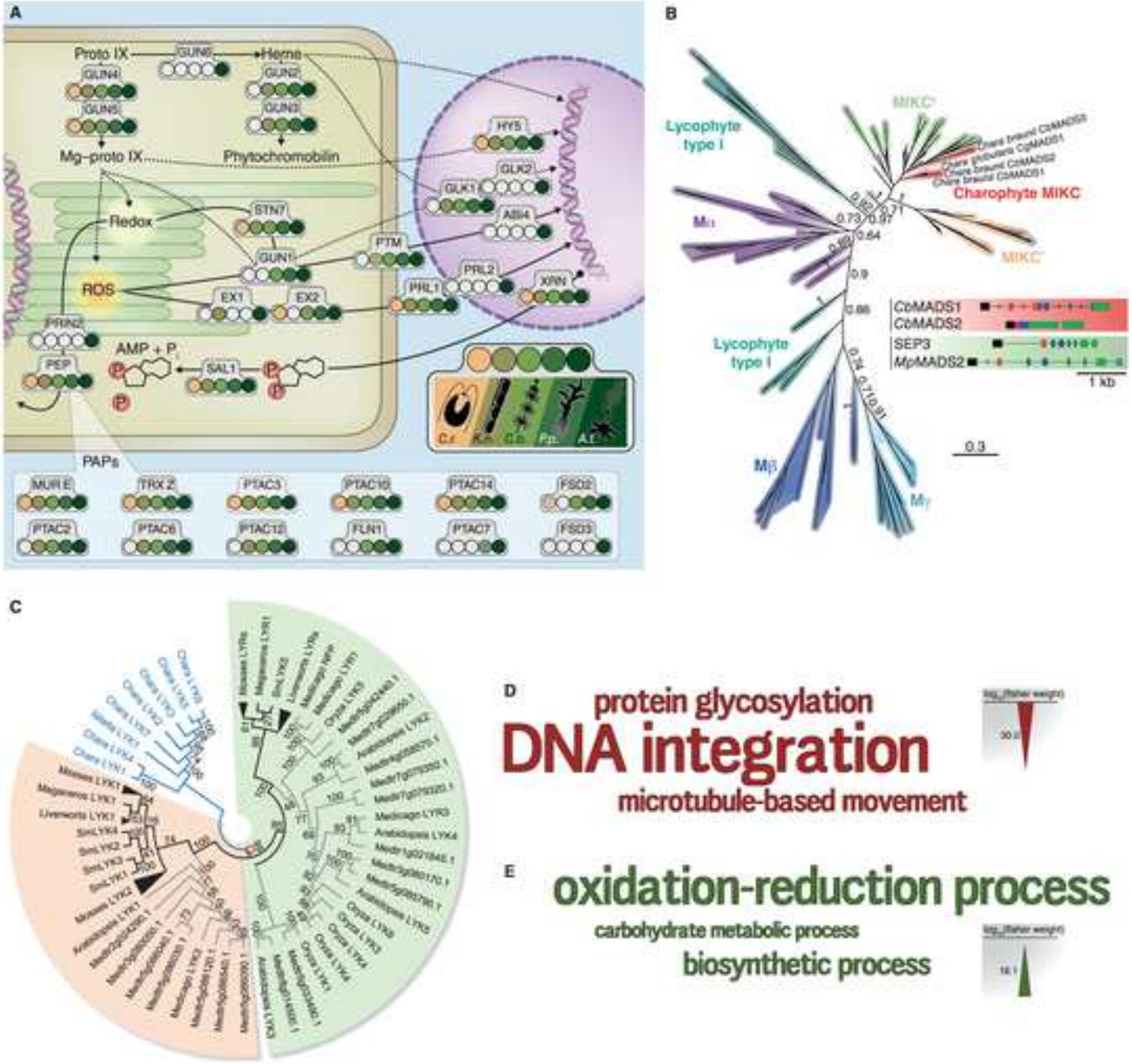
A
Proto IX
GUN6
Heme
GUN4
GUN5
GUN2
GUN3
Mg-proto IX
Phytochromobilin
Redox
STN7
GUN1
ROS
EX1
EX2
PTM
HY5
GLK2
GLK1
ABI4
PRL2
PRL1
XRN
PRIN2
PEP
AMP + P
SAL1
P
C.r.
K.n.
C.b.
P.p.
A.t.
PAPs
MUR E
TRX Z
PTAC3
PTAC10
PTAC14
FSD2
PTAC2
PTAC6
PTAC12
FLN1
PTAC7
FSD3
B
Lycophyte type I
MIKC*
Chara braunii CbMADS3
Chara globularis CgMADS1
Chara braunii CbMADS2
Chara braunii CbMADS1
Charophyte MIKC
Mα
MIKC^C
Mβ
Mγ
0.82
0.73
0.97
0.71
0.64
0.95
0.9
0.86
0.74
0.71
0.91
CbMADS1
CbMADS2
SEP3
MpMADS2
1 kb
0.3
C
Chara LYK1
Chara LYK4
Chara LYK7
Chara LYK2
Chara LYK3
Chara LYK5
Chara LYK6
Mosses LYK7
Magnoliids LYK7
Liverworts LYK7
SmLYK4
SmLYK2
SmLYK3
SmLYK1
Mosses LYK2
Arabidopsis LYK1
Medicago LYK3
Medicago LYR3
Arabidopsis LYK4
Arabidopsis LYK2
Arabidopsis LYK5
Oryza LYK1
Oryza LYK2
Oryza LYK3
Oryza LYK4
Oryza LYK5
Arabidopsis LYK3
Mosses LYR6
Magnoliids LYR1
SmLYR5
Liverworts LYR6
Medicago NFP
100
D
protein glycosylation
DNA integration
microtubule-based movement
log2(fisher weight)
30.0
E
oxidation-reduction process
carbohydrate metabolic process
biosynthetic process
log2(fisher weight)
16.1

Figure 6

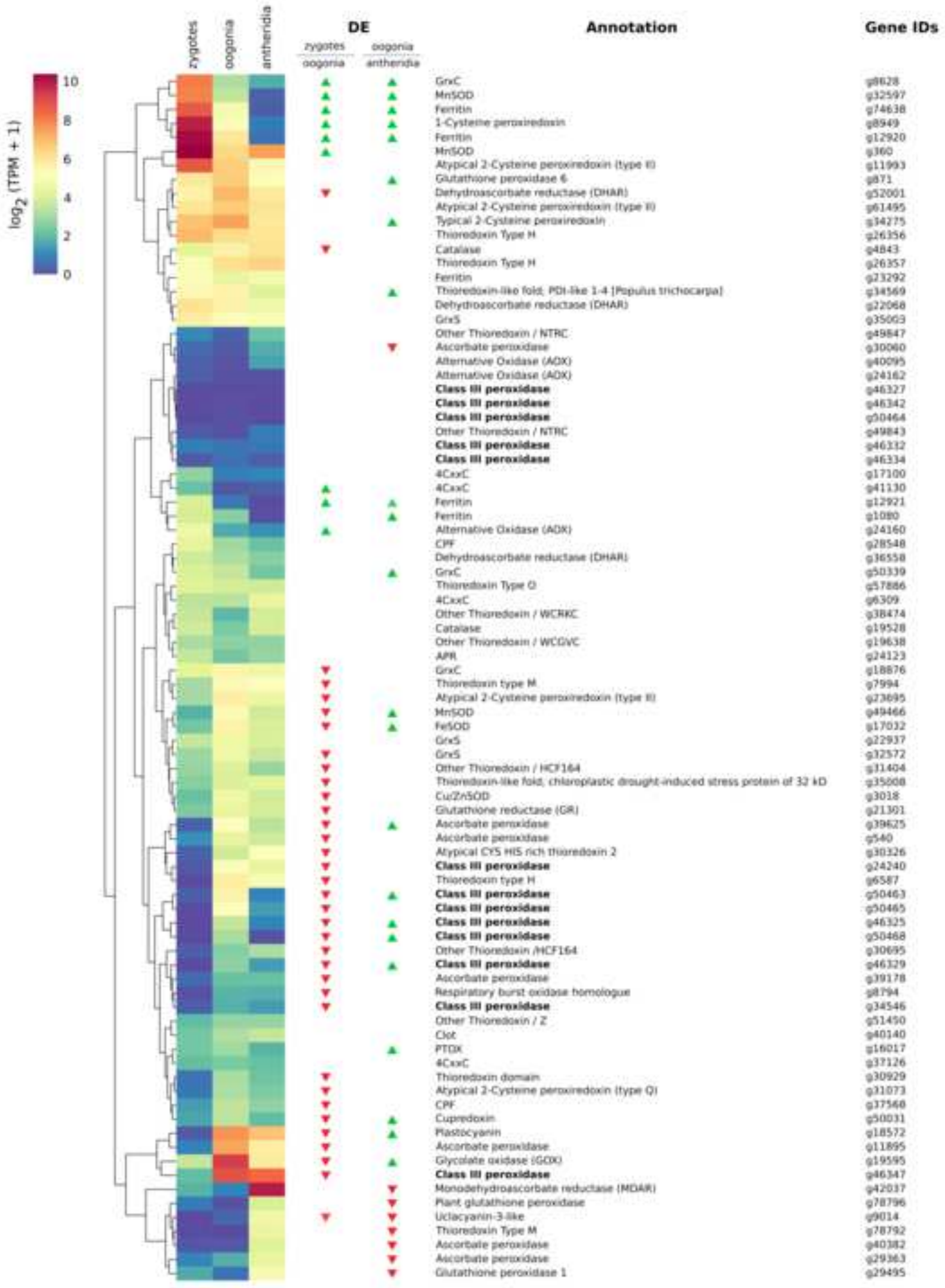
log2 (TPM + 1)
0
2
4
6
8
10
zygotes
oogonia
antheridia
DE
zygotes / oogonia
oogonia / antheridia
Annotation
Gene IDs
GrxC g8628
MnSOD g32597
Ferritin g74638
1-Cysteine peroxiredoxin g8949
Ferritin g12920
MnSOD g360
Atypical 2-Cysteine peroxiredoxin (type II) g11993
Glutathione peroxidase 6 g871
Dehydroascorbate reductase (DHAR) g52001
Atypical 2-Cysteine peroxiredoxin (type II) g61495
Typical 2-Cysteine peroxiredoxin g34275
Thioredoxin Type H g26356
Catalase g4843
Thioredoxin Type H g26357
Ferritin g23292
Thioredoxin-like fold; PDI-like 1-4 [Populus trichocarpa] g34569
Dehydroascorbate reductase (DHAR) g22068
GrxS g35063
Other Thioredoxin / NTRC g49847
Ascorbate peroxidase g30060
Alternative Oxidase (AOX) g40095
Alternative Oxidase (AOX) g24162
Class III peroxidase g46327
Class III peroxidase g46342
Class III peroxidase g50464
Other Thioredoxin / NTRC g49843
Class III peroxidase g46332
Class III peroxidase g46334
4CxxC g17100
4CxxC g41130
Ferritin g12921
Ferritin g1080
Alternative Oxidase (AOX) g24160
CPF g28548
Dehydroascorbate reductase (DHAR) g36558
GrxC g50339
Thioredoxin Type O g57886
4CxxC g6309
Other Thioredoxin / WCRKC g38474
Catalase g19528
Other Thioredoxin / WCGVC g19638
APR g24123
GrxC g18876
Thioredoxin type M g7994
Atypical 2-Cysteine peroxiredoxin (type II) g23695
MnSOD g49466
FeSOD g17032
GrxS g22937
GrxS g32572
Other Thioredoxin / HCF164 g31404
Thioredoxin-like fold; chloroplastic drought-induced stress protein of 32 kD g35008
Cu/ZnSOD g3018
Glutathione reductase (GR) g21301
Ascorbate peroxidase g39625
Ascorbate peroxidase g540
Atypical CYS HIS rich thioredoxin 2 g30326
Class III peroxidase g24240
Thioredoxin type H g6587
Class III peroxidase g50463
Class III peroxidase g50465
Class III peroxidase g46325
Class III peroxidase g50468
Other Thioredoxin /HCF164 g30695
Class III peroxidase g46329
Ascorbate peroxidase g39178
Respiratory burst oxidase homologue g8794
Class III peroxidase g34546
Other Thioredoxin / Z g51450
Clot g40140
PTOX g16017
4CxxC g37126
Thioredoxin domain g30929
Atypical 2-Cysteine peroxiredoxin (type Q) g31073
CPF g37568
Cupredoxin g50031
Plastocyanin g18572
Ascorbate peroxidase g11895
Glycolate oxidase (GOX) g19595
Class III peroxidase g46347
Monodehydroascorbate reductase (MDAR) g42037
Plant glutathione peroxidase g78796
Uclacyanin-3-like g9014
Thioredoxin Type M g78792
Ascorbate peroxidase g40382
Ascorbate peroxidase g29363
Glutathione peroxidase 1 g29495

Nishiyama et al.

The *Chara* genome: secondary complexity and implications for plant terrestrialization

Data S1: Phylogenetic trees and alignments

Throughout this document, *C. braunii* sequences/clades are marked green where suitable. Similarly, *K. nitens* (previously: *K. flaccidum*) is marked blue, *A. thaliana* / blast query sequences in red.

Figures are referenced by Data S1 and an alphabetic index here and when referred to in the manuscript. All alignments, showing the accession numbers of all sequences used, are available as fasta files from Mendeley (doi:10.17632/9hzzf9m4kh.1).

Methodological details of phylogenetic tree inference are in STAR methods.

Five letter codes abbreviating the species names are comprised of the first three letters of the genus followed by the first two letter of the species, e.g. ARATH = *Arabidopsis thaliana* and can be looked up in the key resource table. Transcriptomic datasets are marked by "tr" after the five letter species code.

Data S1A: Maximum Likelihood GT43 phylogeny.
Data S1B: Maximum Likelihood GT47 phylogeny.
Data S1C: PIN phylogeny.
Data S1D: PIN alignment.
Data S1E: Maximum likelihood phylogenetic reconstruction for the ARF auxin signaling gene family.
Data S1F: Maximum likelihood phylogenetic reconstruction for the AUX/IAA auxin signaling gene family.
Data S1G: Maximum likelihood phylogenetic reconstruction for the TIR1/AFB auxin signaling gene family.
Data S1H: Maximum likelihood tree of response regulators.
Data S1I: *Cb*GUN1 clusters with land plant GUN1 proteins.
Data S1J: Phylogenetic tree of trihelix transcription factors.
Data S1K: Phylogenetic tree of plant MADS-box genes.
Data S1L: Condensed Maximum likelihood tree of the LysM-RLK family.
Data S1M: Alignment of the Chara LysM-RLK with representative LYK and LYR from angiosperms.
Data S1N: Midpoint-rooted Maximum Likelihood tree of the LysM-RLK family.
Data S1O: Outgroup-rooted phylogenetic analysis of *C. braunii* class III peroxidases
Data S1P: *In silico* modeling of *C. braunii* LRR FBPs.
Data S1Q: Phylogenetic tree of cyclin proteins.
Data S1R: Phylogenetic tree of EXOCYST 70A proteins.
Data S1S: Phylogenetic tree of NPSN proteins.
Data S1T: Phylogenetic overview tree of canonical actin proteins.
Data S1U: Phylogenetic tree of canonical actin proteins.

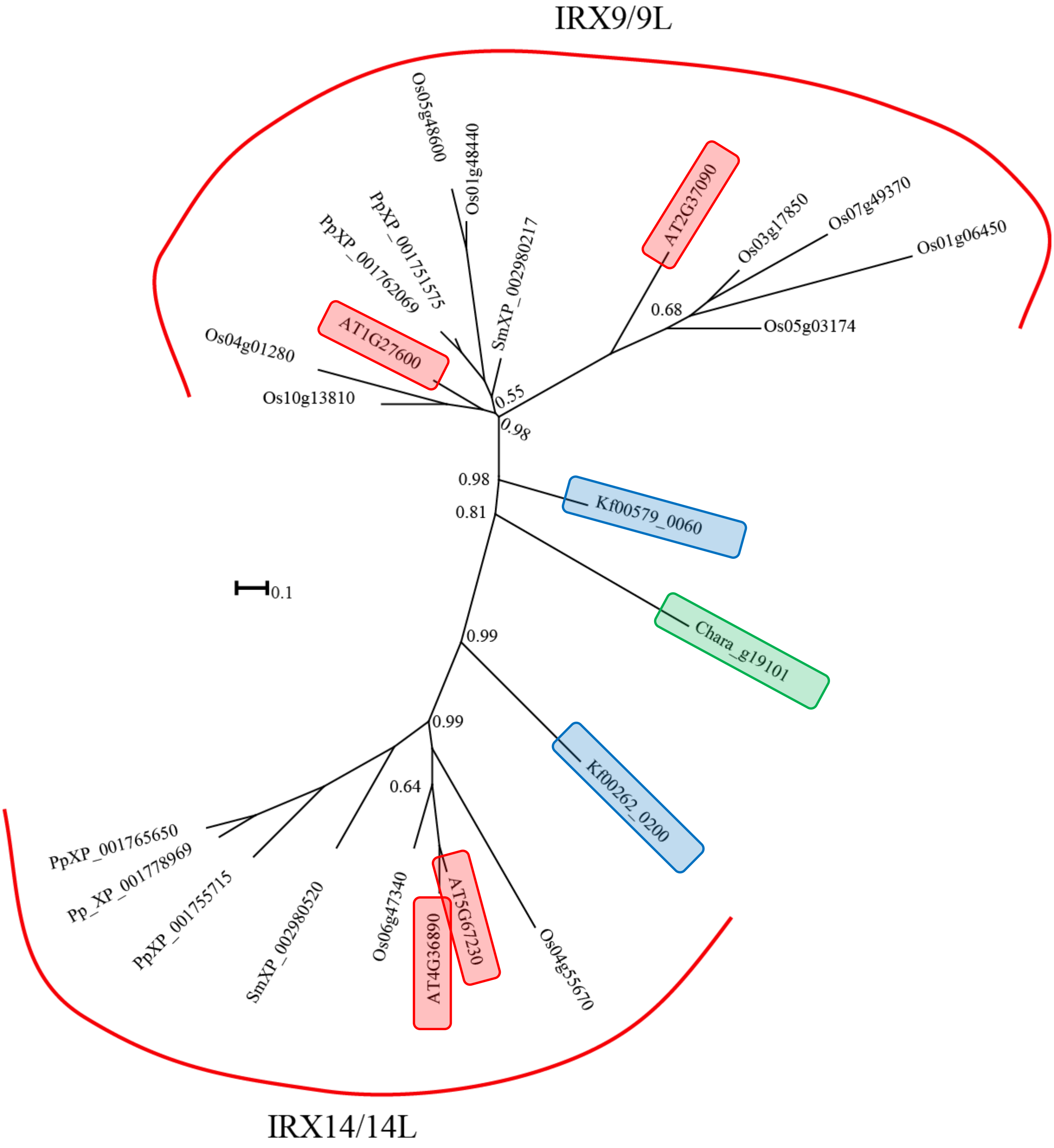

Data S1A: Maximum Likelihood GT43 phylogeny.

GT43 contain activities involved in xylan biosynthesis, in a so far unknown manner. Both clades are not, at least in higher plants, suggested to be direct xylan synthases. *C. braunii* has a single member (green) with an apparent ancestral location in neither of the defined clades of GT43. *A. thaliana* sequences are marked red, *K. nitens* sequences blue.

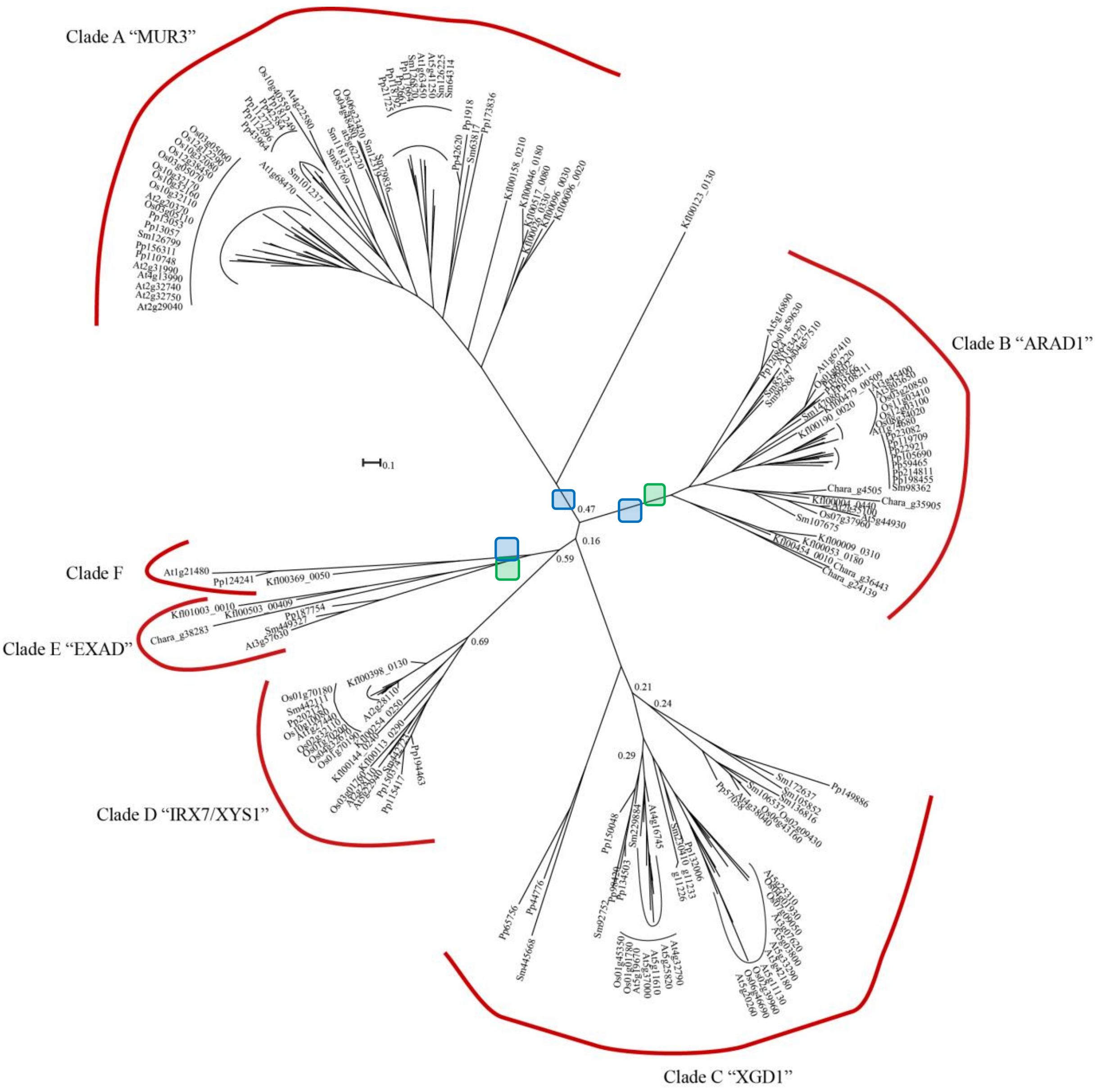

Data S1B: Maximum Likelihood GT47 phylogeny.

Phylogenetic tree of GT47 showing the identified *C. braunii* sequences in Clade B and Clade E, putative arabinosyltransferases involved in the biosynthesis of arabinan and extensin, respectively. Note the absence of *C. braunii* sequences from Clade A (xyloglucan galactosylation) and Clade D (xylan synthase). Presence of *C. braunii* and *K. nitens* sequences in clades is shown by a green or blue box on the branch of that clade.

#

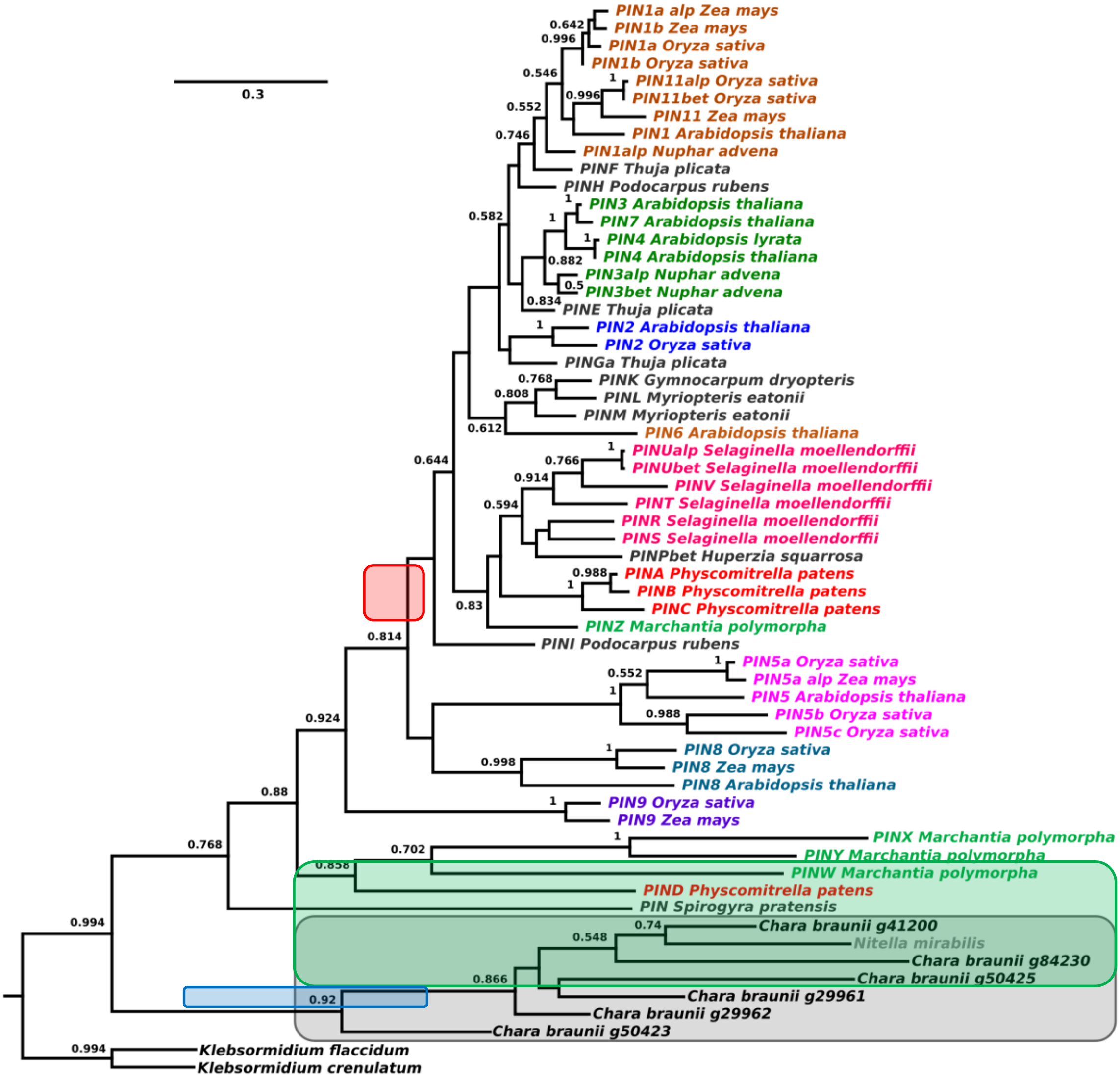

Data S1C: PIN phylogeny.

Maximum likelihood reconstruction of PIN protein family focused on algal species. 500 bootstrap replications, result (in %) indicated above branches. *C. braunii* sequences are marked by a green box, the *K. nitens* sequence by a blue box, and the clade harboring the *A. thaliana* sequences by a red box.

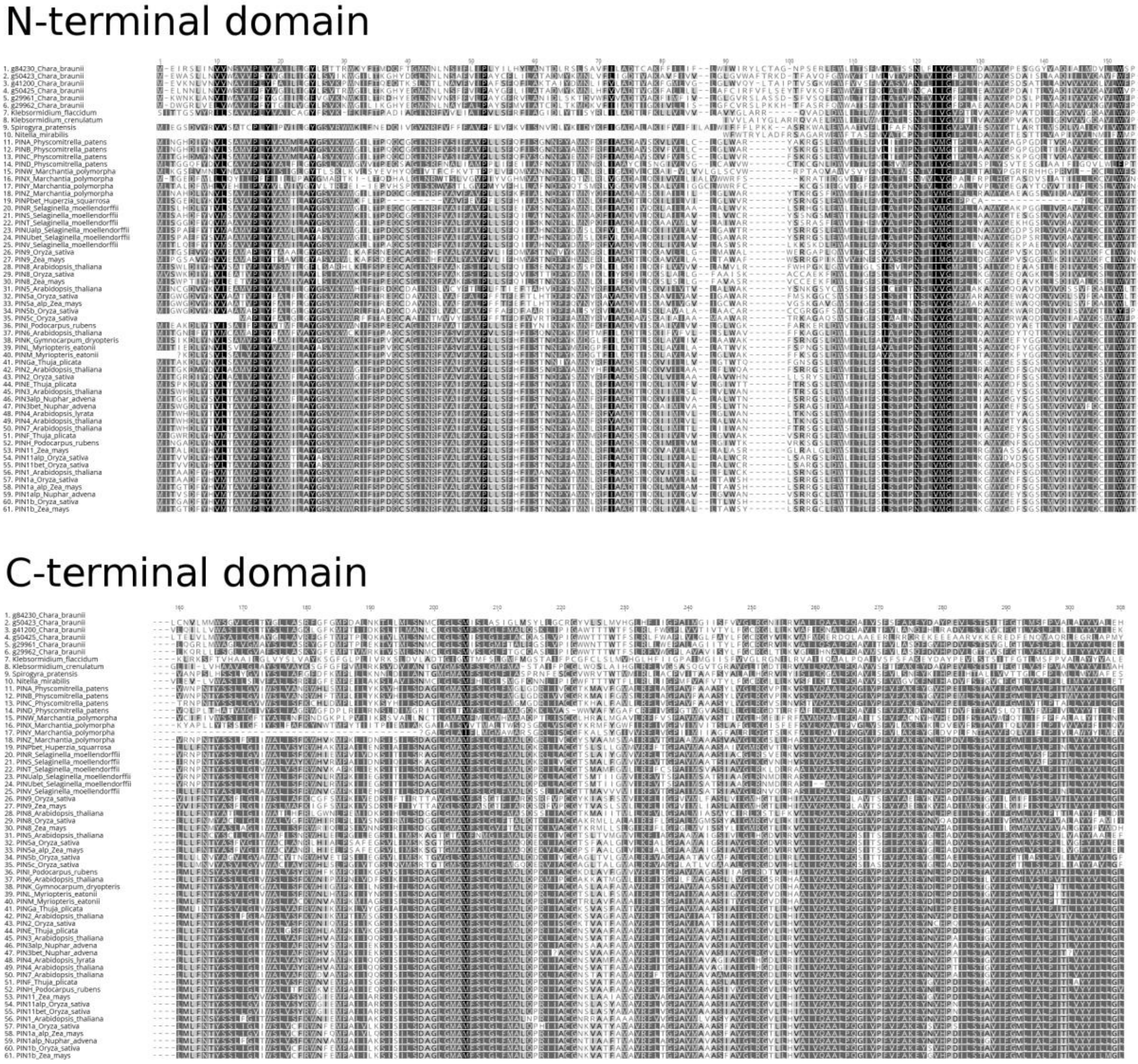
N-terminal domain
C-terminal domain
1. g84230_Chara_braunii
2. g50423_Chara_braunii
3. g41200_Chara_braunii
4. g50425_Chara_braunii
5. g29961_Chara_braunii
6. g29962_Chara_braunii
7. Klebsormidium_flaccidum
8. Klebsormidium_crenulatum
9. Spirogyra_pratensis
10. Nitella_mirabilis
11. PINA_Physcomitrella_patens
12. PINB_Physcomitrella_patens
13. PINC_Physcomitrella_patens
14. PIND_Physcomitrella_patens
15. PINW_Marchantia_polymorpha
16. PINX_Marchantia_polymorpha
17. PINY_Marchantia_polymorpha
18. PINZ_Marchantia_polymorpha
19. PINPbet_Huperzia_squarrosa
20. PINR_Selaginella_moellendorffii
21. PINS_Selaginella_moellendorffii
22. PINT_Selaginella_moellendorffii
23. PINUalp_Selaginella_moellendorffii
24. PINUbet_Selaginella_moellendorffii
25. PINV_Selaginella_moellendorffii
26. PIN9_Oryza_sativa
27. PIN9_Zea_mays
28. PIN8_Arabidopsis_thaliana
29. PIN8_Oryza_sativa
30. PIN8_Zea_mays
31. PIN5_Arabidopsis_thaliana
32. PIN5a_Oryza_sativa
33. PIN5a_alp_Zea_mays
34. PIN5b_Oryza_sativa
35. PIN5c_Oryza_sativa
36. PINI_Podocarpus_rubens
37. PIN6_Arabidopsis_thaliana
38. PINK_Gymnocarpum_dryopteris
39. PINL_Myriopteris_eatonii
40. PINM_Myriopteris_eatonii
41. PINGa_Thuja_plicata
42. PIN2_Arabidopsis_thaliana
43. PIN2_Oryza_sativa
44. PINE_Thuja_plicata
45. PIN3_Arabidopsis_thaliana
46. PIN3alp_Nuphar_advena
47. PIN3bet_Nuphar_advena
48. PIN4_Arabidopsis_lyrata
49. PIN4_Arabidopsis_thaliana
50. PIN7_Arabidopsis_thaliana
51. PINF_Thuja_plicata
52. PINH_Podocarpus_rubens
53. PIN11_Zea_mays
54. PIN11alp_Oryza_sativa
55. PIN11bet_Oryza_sativa
56. PIN1_Arabidopsis_thaliana
57. PIN1a_Oryza_sativa
58. PIN1a_alp_Zea_mays
59. PIN1alp_Nuphar_advena
60. PIN1b_Oryza_sativa
61. PIN1b_Zea_mays

Data S1D: PIN alignment.

C. braunii sequences are shown on top.

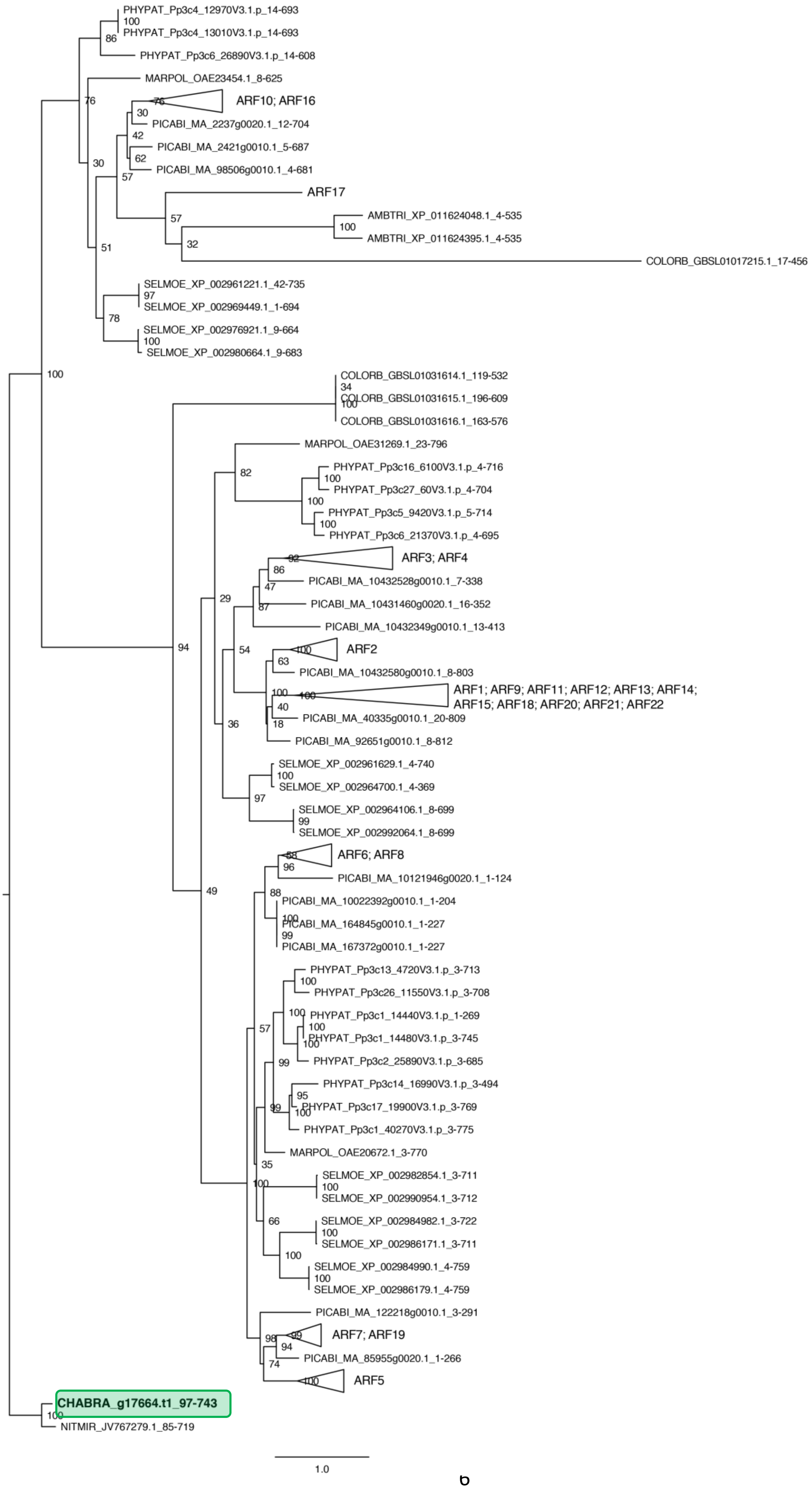
PHYPAT_Pp3c4_12970V3.1.p_14-693
100
PHYPAT_Pp3c4_13010V3.1.p_14-693
86
PHYPAT_Pp3c6_26890V3.1.p_14-608
MARPOL_OAE23454.1_8-625
76
75
ARF10; ARF16
30
PICABI_MA_2237g0020.1_12-704
42
PICABI_MA_2421g0010.1_5-687
62
30
PICABI_MA_98506g0010.1_4-681
57
ARF17
57
AMBTRI_XP_011624048.1_4-535
100
AMBTRI_XP_011624395.1_4-535
32
51
COLORB_GBSL01017215.1_17-456
SELMOE_XP_002961221.1_42-735
97
SELMOE_XP_002969449.1_1-694
78
SELMOE_XP_002976921.1_9-664
100
SELMOE_XP_002980664.1_9-683
100
COLORB_GBSL01031614.1_119-532
34
COLORB_GBSL01031615.1_196-609
100
COLORB_GBSL01031616.1_163-576
MARPOL_OAE31269.1_23-796
82
PHYPAT_Pp3c16_6100V3.1.p_4-716
100
PHYPAT_Pp3c27_60V3.1.p_4-704
100
PHYPAT_Pp3c5_9420V3.1.p_5-714
100
PHYPAT_Pp3c6_21370V3.1.p_4-695
92
ARF3; ARF4
86
47
PICABI_MA_10432528g0010.1_7-338
29
87
PICABI_MA_10431460g0020.1_16-352
PICABI_MA_10432349g0010.1_13-413
94
54
100
ARF2
63
PICABI_MA_10432580g0010.1_8-803
100
100
ARF1; ARF9; ARF11; ARF12; ARF13; ARF14;
ARF15; ARF18; ARF20; ARF21; ARF22
40
PICABI_MA_40335g0010.1_20-809
18
36
PICABI_MA_92651g0010.1_8-812
SELMOE_XP_002961629.1_4-740
100
SELMOE_XP_002964700.1_4-369
97
SELMOE_XP_002964106.1_8-699
99
SELMOE_XP_002992064.1_8-699
58
ARF6; ARF8
96
PICABI_MA_10121946g0020.1_1-124
49
88
PICABI_MA_10022392g0010.1_1-204
100
PICABI_MA_164845g0010.1_1-227
99
PICABI_MA_167372g0010.1_1-227
PHYPAT_Pp3c13_4720V3.1.p_3-713
100
PHYPAT_Pp3c26_11550V3.1.p_3-708
100
PHYPAT_Pp3c1_14440V3.1.p_1-269
100
57
PHYPAT_Pp3c1_14480V3.1.p_3-745
100
PHYPAT_Pp3c2_25890V3.1.p_3-685
99
PHYPAT_Pp3c14_16990V3.1.p_3-494
95
99
PHYPAT_Pp3c17_19900V3.1.p_3-769
100
PHYPAT_Pp3c1_40270V3.1.p_3-775
MARPOL_OAE20672.1_3-770
35
SELMOE_XP_002982854.1_3-711
100
100
SELMOE_XP_002990954.1_3-712
66
SELMOE_XP_002984982.1_3-722
100
SELMOE_XP_002986171.1_3-711
100
SELMOE_XP_002984990.1_4-759
100
SELMOE_XP_002986179.1_4-759
PICABI_MA_122218g0010.1_3-291
98
99
ARF7; ARF19
94
PICABI_MA_85955g0020.1_1-266
74
100
ARF5
CHABRA_g17664.t1_97-743
100
NITMIR_JV767279.1_85-719
1.0

Data S1E: Maximum likelihood phylogenetic reconstruction for the ARF auxin signaling gene family.

The *C. braunii* ARF candidate is highlighted in bold/green. Angiosperm ARF proteins are clustered and the corresponding *A. thaliana* members are given for the collapsed clades. The ML tree shown is rooted on the *C. braunii* sequence clade to visualize the relationship of the examined genes without suggesting any ancestry. The bootstrap values were assessed with the ultrafast bootstrap approximation using 1,000 replicates and the corresponding values are depicted next to the tree nodes on an amino acid alignment of a set of species as indicated in Table S11.

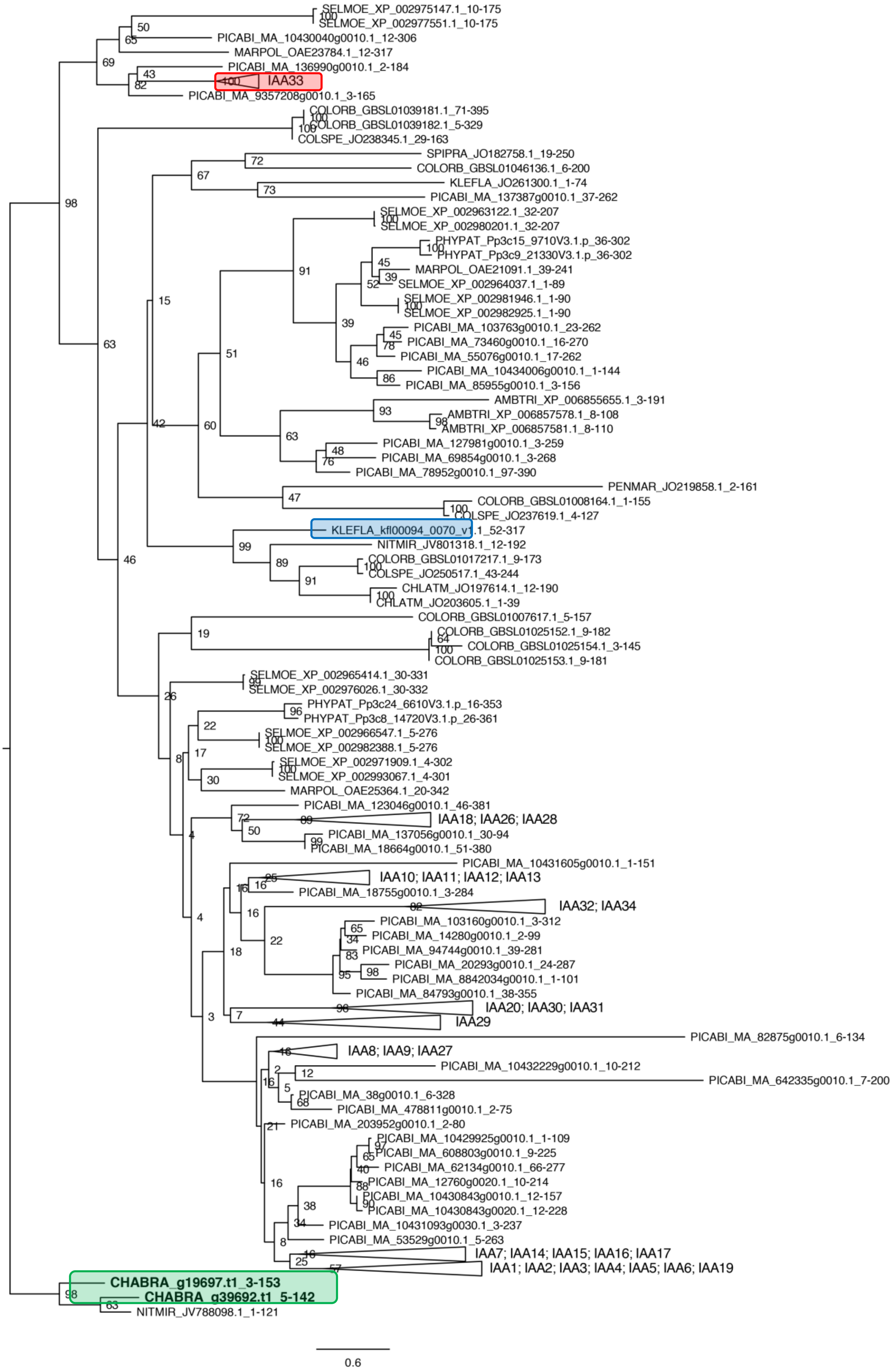
SELMOE_XP_002975147.1_10-175
100
SELMOE_XP_002977551.1_10-175
50
65
PICABI_MA_10430040g0010.1_12-306
69
MARPOL_OAE23784.1_12-317
PICABI_MA_136990g0010.1_2-184
43
100
IAA33
82
PICABI_MA_9357208g0010.1_3-165
COLORB_GBSL01039181.1_71-395
100
100
COLORB_GBSL01039182.1_5-329
COLSPE_JO238345.1_29-163
SPIPRA_JO182758.1_19-250
72
COLORB_GBSL01046136.1_6-200
67
KLEFLA_JO261300.1_1-74
73
PICABI_MA_137387g0010.1_37-262
98
SELMOE_XP_002963122.1_32-207
100
SELMOE_XP_002980201.1_32-207
PHYPAT_Pp3c15_9710V3.1.p_36-302
100
PHYPAT_Pp3c9_21330V3.1.p_36-302
45
91
MARPOL_OAE21091.1_39-241
39
52
SELMOE_XP_002964037.1_1-89
15
SELMOE_XP_002981946.1_1-90
100
SELMOE_XP_002982925.1_1-90
39
PICABI_MA_103763g0010.1_23-262
45
PICABI_MA_73460g0010.1_16-270
78
63
PICABI_MA_55076g0010.1_17-262
51
46
PICABI_MA_10434006g0010.1_1-144
86
PICABI_MA_85955g0010.1_3-156
AMBTRI_XP_006855655.1_3-191
93
98
AMBTRI_XP_006857578.1_8-108
42
60
AMBTRI_XP_006857581.1_8-110
63
PICABI_MA_127981g0010.1_3-259
48
PICABI_MA_69854g0010.1_3-268
76
PICABI_MA_78952g0010.1_97-390
PENMAR_JO219858.1_2-161
47
COLORB_GBSL01008164.1_1-155
100
COLSPE_JO237619.1_4-127
KLEFLA_kfl00094_0070_v1.1_52-317
NITMIR_JV801318.1_12-192
99
46
COLORB_GBSL01017217.1_9-173
89
100
COLSPE_JO250517.1_43-244
91
CHLATM_JO197614.1_12-190
100
CHLATM_JO203605.1_1-39
COLORB_GBSL01007617.1_5-157
COLORB_GBSL01025152.1_9-182
19
64
COLORB_GBSL01025154.1_3-145
100
COLORB_GBSL01025153.1_9-181
SELMOE_XP_002965414.1_30-331
99
SELMOE_XP_002976026.1_30-332
26
PHYPAT_Pp3c24_6610V3.1.p_16-353
96
PHYPAT_Pp3c8_14720V3.1.p_26-361
22
SELMOE_XP_002966547.1_5-276
100
17
SELMOE_XP_002982388.1_5-276
8
SELMOE_XP_002971909.1_4-302
100
30
SELMOE_XP_002993067.1_4-301
MARPOL_OAE25364.1_20-342
PICABI_MA_123046g0010.1_46-381
72
89
IAA18; IAA26; IAA28
4
50
PICABI_MA_137056g0010.1_30-94
99
PICABI_MA_18664g0010.1_51-380
PICABI_MA_10431605g0010.1_1-151
25
IAA10; IAA11; IAA12; IAA13
16
16
PICABI_MA_18755g0010.1_3-284
82
IAA32; IAA34
16
4
PICABI_MA_103160g0010.1_3-312
65
34
PICABI_MA_14280g0010.1_2-99
22
PICABI_MA_94744g0010.1_39-281
83
18
PICABI_MA_20293g0010.1_24-287
98
95
PICABI_MA_8842034g0010.1_1-101
PICABI_MA_84793g0010.1_38-355
96
IAA20; IAA30; IAA31
7
3
44
IAA29
PICABI_MA_82875g0010.1_6-134
46
IAA8; IAA9; IAA27
2
12
PICABI_MA_10432229g0010.1_10-212
16
PICABI_MA_642335g0010.1_7-200
5
PICABI_MA_38g0010.1_6-328
68
PICABI_MA_478811g0010.1_2-75
21
PICABI_MA_203952g0010.1_2-80
PICABI_MA_10429925g0010.1_1-109
97
65
PICABI_MA_608803g0010.1_9-225
40
PICABI_MA_62134g0010.1_66-277
16
88
PICABI_MA_12760g0020.1_10-214
38
PICABI_MA_10430843g0010.1_12-157
90
PICABI_MA_10430843g0020.1_12-228
34
PICABI_MA_10431093g0030.1_3-237
8
PICABI_MA_53529g0010.1_5-263
16
IAA7; IAA14; IAA15; IAA16; IAA17
25
57
IAA1; IAA2; IAA3; IAA4; IAA5; IAA6; IAA19
CHABRA_g19697.t1_3-153
98
CHABRA_g39692.t1_5-142
63
NITMIR_JV788098.1_1-121
0.6

Data S1F: Maximum likelihood phylogenetic reconstruction for the AUX/IAA auxin signaling gene family.

The *C. braunii* AUX/IAA candidates most similar to *A. thaliana* IAA33 (red) are highlighted in bold/green; the *K. nitens* sequence is shown in blue. Angiosperm AUX/IAA proteins are clustered and the corresponding *A. thaliana* members are given for the collapsed clades. The ML tree shown is rooted on the Charales sequences to visualize the relationship of the examined genes without suggesting any ancestry. The bootstrap values were assessed with the ultrafast bootstrap approximation using 1,000 replicates and the corresponding values are depicted next to the tree nodes on an amino acid alignment of a set of species as indicated in Table S11.

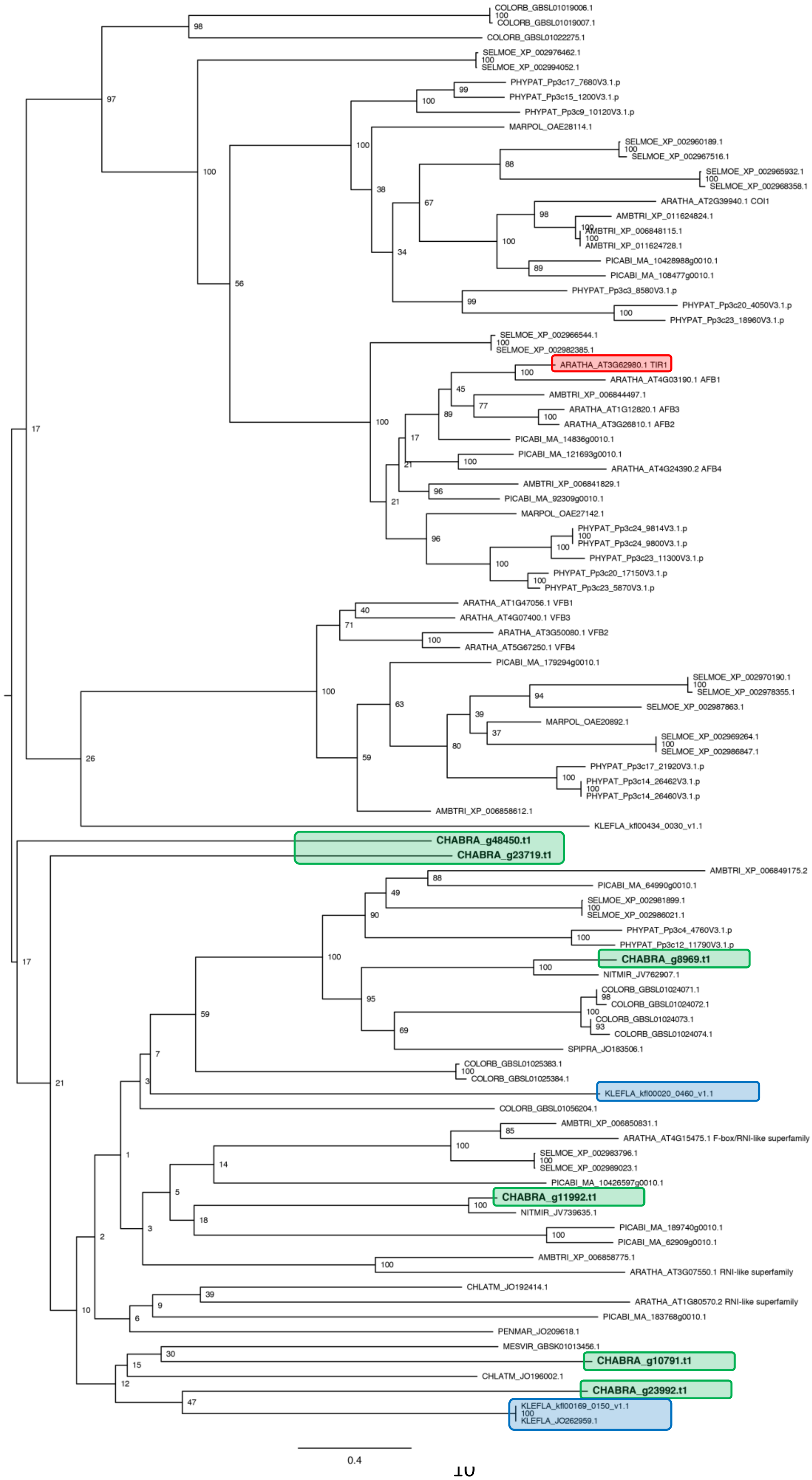
COLORB_GBSL01019006.1
100
COLORB_GBSL01019007.1
COLORB_GBSL01022275.1
SELMOE_XP_002976462.1
100
SELMOE_XP_002994052.1
PHYPAT_Pp3c17_7680V3.1.p
PHYPAT_Pp3c15_1200V3.1.p
PHYPAT_Pp3c9_10120V3.1.p
MARPOL_OAE28114.1
SELMOE_XP_002960189.1
100
SELMOE_XP_002967516.1
SELMOE_XP_002965932.1
100
SELMOE_XP_002968358.1
ARATHA_AT2G39940.1 COI1
AMBTRI_XP_011624824.1
AMBTRI_XP_006848115.1
100
AMBTRI_XP_011624728.1
PICABI_MA_10428988g0010.1
PICABI_MA_108477g0010.1
PHYPAT_Pp3c3_8580V3.1.p
PHYPAT_Pp3c20_4050V3.1.p
PHYPAT_Pp3c23_18960V3.1.p
SELMOE_XP_002966544.1
100
SELMOE_XP_002982385.1
ARATHA_AT3G62980.1 TIR1
ARATHA_AT4G03190.1 AFB1
AMBTRI_XP_006844497.1
ARATHA_AT1G12820.1 AFB3
ARATHA_AT3G26810.1 AFB2
PICABI_MA_14836g0010.1
PICABI_MA_121693g0010.1
ARATHA_AT4G24390.2 AFB4
AMBTRI_XP_006841829.1
PICABI_MA_92309g0010.1
MARPOL_OAE27142.1
PHYPAT_Pp3c24_9814V3.1.p
100
PHYPAT_Pp3c24_9800V3.1.p
PHYPAT_Pp3c23_11300V3.1.p
PHYPAT_Pp3c20_17150V3.1.p
PHYPAT_Pp3c23_5870V3.1.p
ARATHA_AT1G47056.1 VFB1
ARATHA_AT4G07400.1 VFB3
ARATHA_AT3G50080.1 VFB2
ARATHA_AT5G67250.1 VFB4
PICABI_MA_179294g0010.1
SELMOE_XP_002970190.1
100
SELMOE_XP_002978355.1
SELMOE_XP_002987863.1
MARPOL_OAE20892.1
SELMOE_XP_002969264.1
100
SELMOE_XP_002986847.1
PHYPAT_Pp3c17_21920V3.1.p
PHYPAT_Pp3c14_26462V3.1.p
100
PHYPAT_Pp3c14_26460V3.1.p
AMBTRI_XP_006858612.1
KLEFLA_kfl00434_0030_v1.1
CHABRA_g48450.t1
CHABRA_g23719.t1
AMBTRI_XP_006849175.2
PICABI_MA_64990g0010.1
SELMOE_XP_002981899.1
100
SELMOE_XP_002986021.1
PHYPAT_Pp3c4_4760V3.1.p
PHYPAT_Pp3c12_11790V3.1.p
CHABRA_g8969.t1
NITMIR_JV762907.1
COLORB_GBSL01024071.1
98
COLORB_GBSL01024072.1
100
COLORB_GBSL01024073.1
93
COLORB_GBSL01024074.1
SPIPRA_JO183506.1
COLORB_GBSL01025383.1
100
COLORB_GBSL01025384.1
KLEFLA_kfl00020_0460_v1.1
COLORB_GBSL01056204.1
AMBTRI_XP_006850831.1
ARATHA_AT4G15475.1 F-box/RNI-like superfamily
SELMOE_XP_002983796.1
100
SELMOE_XP_002989023.1
PICABI_MA_10426597g0010.1
CHABRA_g11992.t1
NITMIR_JV739635.1
PICABI_MA_189740g0010.1
PICABI_MA_62909g0010.1
AMBTRI_XP_006858775.1
ARATHA_AT3G07550.1 RNI-like superfamily
CHLATM_JO192414.1
ARATHA_AT1G80570.2 RNI-like superfamily
PICABI_MA_183768g0010.1
PENMAR_JO209618.1
MESVIR_GBSK01013456.1
CHABRA_g10791.t1
CHLATM_JO196002.1
CHABRA_g23992.t1
KLEFLA_kfl00169_0150_v1.1
100
KLEFLA_JO262959.1
0.4

Data S1G: Maximum likelihood phylogenetic reconstruction for the TIR1/AFB auxin signaling gene family.

Chara proteins containing F-box or F-box-like domains with considerable similarity to the TIR1/AFB proteins from *A. thaliana* are highlighted in bold/green. For proteins from *A. thaliana* the gene alias is given. The midpoint rooted ML tree shown should visualize the relationship of the examined genes without suggesting any ancestry. The bootstrap values were assessed with the ultrafast bootstrap approximation using 1,000 replicates and the corresponding values are depicted next to the tree nodes on an amino acid alignment of a set of species as indicated in Table S11. The *A. thaliana* TIR1 sequences is marked in red, the *K. nitens* sequences in blue.

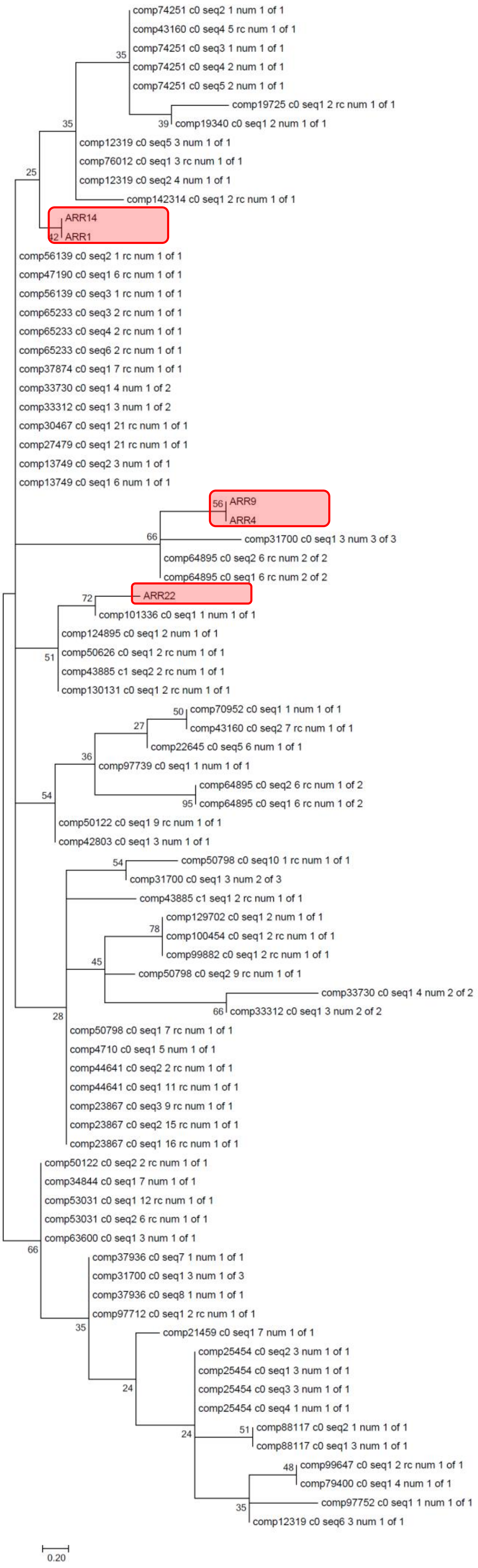
comp74251 c0 seq2 1 num 1 of 1
comp43160 c0 seq4 5 rc num 1 of 1
35
comp74251 c0 seq3 1 num 1 of 1
comp74251 c0 seq4 2 num 1 of 1
comp74251 c0 seq5 2 num 1 of 1
comp19725 c0 seq1 2 rc num 1 of 1
35
39
comp19340 c0 seq1 2 num 1 of 1
comp12319 c0 seq5 3 num 1 of 1
comp76012 c0 seq1 3 rc num 1 of 1
25
comp12319 c0 seq2 4 num 1 of 1
comp142314 c0 seq1 2 rc num 1 of 1
ARR14
42
ARR1
comp56139 c0 seq2 1 rc num 1 of 1
comp47190 c0 seq1 6 rc num 1 of 1
comp56139 c0 seq3 1 rc num 1 of 1
comp65233 c0 seq3 2 rc num 1 of 1
comp65233 c0 seq4 2 rc num 1 of 1
comp65233 c0 seq6 2 rc num 1 of 1
comp37874 c0 seq1 7 rc num 1 of 1
comp33730 c0 seq1 4 num 1 of 2
comp33312 c0 seq1 3 num 1 of 2
comp30467 c0 seq1 21 rc num 1 of 1
comp27479 c0 seq1 21 rc num 1 of 1
comp13749 c0 seq2 3 num 1 of 1
comp13749 c0 seq1 6 num 1 of 1
56
ARR9
ARR4
66
comp31700 c0 seq1 3 num 3 of 3
comp64895 c0 seq2 6 rc num 2 of 2
comp64895 c0 seq1 6 rc num 2 of 2
72
ARR22
comp101336 c0 seq1 1 num 1 of 1
comp124895 c0 seq1 2 num 1 of 1
51
comp50626 c0 seq1 2 rc num 1 of 1
comp43885 c1 seq2 2 rc num 1 of 1
comp130131 c0 seq1 2 rc num 1 of 1
50
comp70952 c0 seq1 1 num 1 of 1
27
comp43160 c0 seq2 7 rc num 1 of 1
comp22645 c0 seq5 6 num 1 of 1
36
comp97739 c0 seq1 1 num 1 of 1
comp64895 c0 seq2 6 rc num 1 of 2
54
95
comp64895 c0 seq1 6 rc num 1 of 2
comp50122 c0 seq1 9 rc num 1 of 1
comp42803 c0 seq1 3 num 1 of 1
54
comp50798 c0 seq10 1 rc num 1 of 1
comp31700 c0 seq1 3 num 2 of 3
comp43885 c1 seq1 2 rc num 1 of 1
comp129702 c0 seq1 2 num 1 of 1
78
comp100454 c0 seq1 2 rc num 1 of 1
comp99882 c0 seq1 2 rc num 1 of 1
45
comp50798 c0 seq2 9 rc num 1 of 1
comp33730 c0 seq1 4 num 2 of 2
66
comp33312 c0 seq1 3 num 2 of 2
28
comp50798 c0 seq1 7 rc num 1 of 1
comp4710 c0 seq1 5 num 1 of 1
comp44641 c0 seq2 2 rc num 1 of 1
comp44641 c0 seq1 11 rc num 1 of 1
comp23867 c0 seq3 9 rc num 1 of 1
comp23867 c0 seq2 15 rc num 1 of 1
comp23867 c0 seq1 16 rc num 1 of 1
comp50122 c0 seq2 2 rc num 1 of 1
comp34844 c0 seq1 7 num 1 of 1
comp53031 c0 seq1 12 rc num 1 of 1
comp53031 c0 seq2 6 rc num 1 of 1
comp63600 c0 seq1 3 num 1 of 1
66
comp37936 c0 seq7 1 num 1 of 1
comp31700 c0 seq1 3 num 1 of 3
comp37936 c0 seq8 1 num 1 of 1
comp97712 c0 seq1 2 rc num 1 of 1
35
comp21459 c0 seq1 7 num 1 of 1
comp25454 c0 seq2 3 num 1 of 1
comp25454 c0 seq1 3 num 1 of 1
24
comp25454 c0 seq3 3 num 1 of 1
comp25454 c0 seq4 1 num 1 of 1
51
comp88117 c0 seq2 1 num 1 of 1
24
comp88117 c0 seq1 3 num 1 of 1
48
comp99647 c0 seq1 2 rc num 1 of 1
comp79400 c0 seq1 4 num 1 of 1
comp97752 c0 seq1 1 num 1 of 1
35
comp12319 c0 seq6 3 num 1 of 1
0.20

Data S1H: Maximum likelihood tree of response regulators.

C. braunii transcripts (derived from the RNA-seq based transcriptome representation) clustering with *A. thaliana* (marked in red) response regulators ARR1 and ARR14 (RRB), ARR4 and ARR9 (RRA) and ARR 22 (RRC). No response regulators could be identified in the genome; in order to make sure that this result is not due to a missing or fragmentary gene model we screened the transcriptome. While two response regulator transcripts could be detected clustering with the A-type (ARR4 and ARR9, RRA), no RRB (ARR1 and ARR14) could be detected (*cf*. STAR Methods).

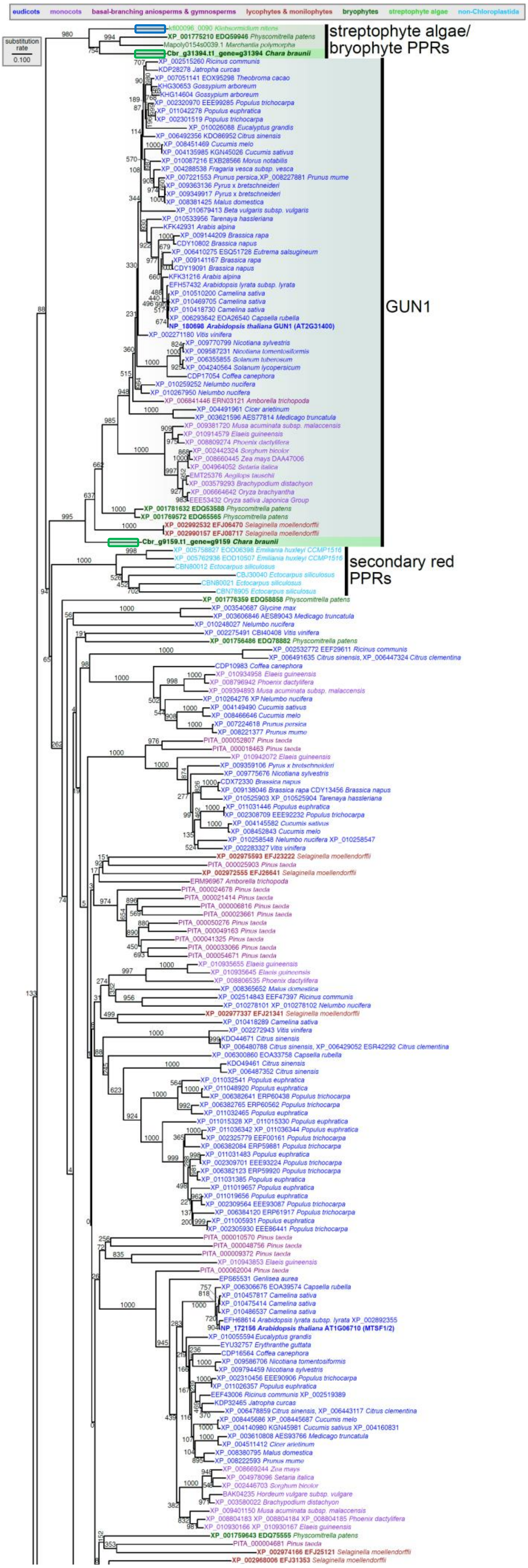
eudicots
monocots
basal-branching angiosperms & gymnosperms
lycophytes & monilophytes
bryophytes
streptophyte algae
non-Chloroplastida
substitution rate
0.100
streptophyte algae/ bryophyte PPRs
GUN1
secondary red PPRs
kfl00096_0090 Klebsormidium nitens
XP_001775210 EDQ59946 Physcomitrella patens
Mapoly0154s0039.1 Marchantia polymorpha
Cbr_g31394.t1_gene=g31394 Chara braunii
XP_002515260 Ricinus communis
KDP28278 Jatropha curcas
XP_007051141 EOX95298 Theobroma cacao
KHG30653 Gossypium arboreum
KHG14604 Gossypium arboreum
XP_002320970 EEE99285 Populus trichocarpa
XP_011042278 Populus euphratica
XP_002301519 Populus trichocarpa
XP_010026088 Eucalyptus grandis
XP_006492356 KDO86952 Citrus sinensis
XP_008451469 Cucumis melo
XP_004135985 KGN45026 Cucumis sativus
XP_010087216 EXB28566 Morus notabilis
XP_004288538 Fragaria vesca subsp. vesca
XP_007221553 Prunus persica,XP_008227881 Prunus mume
XP_009363136 Pyrus x bretschneideri
XP_009349917 Pyrus x bretschneideri
XP_008381425 Malus domestica
XP_010679413 Beta vulgaris subsp. vulgaris
XP_010533956 Tarenaya hassleriana
KFK42931 Arabis alpina
XP_009144209 Brassica rapa
CDY10802 Brassica napus
XP_006410275 ESQ51728 Eutrema salsugineum
XP_009141167 Brassica rapa
CDY19091 Brassica napus
KFK31216 Arabis alpina
EFH57432 Arabidopsis lyrata subsp. lyrata
XP_010510200 Camelina sativa
XP_010469705 Camelina sativa
XP_010418730 Camelina sativa
XP_006293642 EOA26540 Capsella rubella
NP_180698 Arabidopsis thaliana GUN1 (AT2G31400)
XP_002271180 Vitis vinifera
XP_009770799 Nicotiana sylvestris
XP_009587231 Nicotiana tomentosiformis
XP_006355855 Solanum tuberosum
XP_004240564 Solanum lycopersicum
CDP17054 Coffea canephora
XP_010259252 Nelumbo nucifera
XP_010267950 Nelumbo nucifera
XP_006841446 ERN03121 Amborella trichopoda
XP_004491961 Cicer arietinum
XP_003621596 AES77814 Medicago truncatula
XP_009381720 Musa acuminata subsp. malaccensis
XP_010914579 Elaeis guineensis
XP_008809274 Phoenix dactylifera
XP_002442324 Sorghum bicolor
XP_008660445 Zea mays DAA47006
XP_004964052 Setaria italica
EMT25376 Aegilops tauschii
XP_003579293 Brachypodium distachyon
XP_006664642 Oryza brachyantha
EEE53432 Oryza sativa Japonica Group
XP_001781632 EDQ53588 Physcomitrella patens
XP_001769572 EDQ65565 Physcomitrella patens
XP_002992532 EFJ06470 Selaginella moellendorffii
XP_002990157 EFJ08717 Selaginella moellendorffii
Cbr_g9159.t1_gene=g9159 Chara braunii
XP_005758827 EOD06398 Emiliania huxleyi CCMP1516
XP_005762936 EOD10507 Emiliania huxleyi CCMP1516
CBN80012 Ectocarpus siliculosus
CBJ30040 Ectocarpus siliculosus
CBN80021 Ectocarpus siliculosus
CBN78905 Ectocarpus siliculosus
XP_001778359 EDQ58858 Physcomitrella patens
XP_003540687 Glycine max
XP_003606846 AES89043 Medicago truncatula
XP_010248027 Nelumbo nucifera
XP_002275491 CBI40408 Vitis vinifera
XP_001756486 EDQ78882 Physcomitrella patens
XP_002532772 EEF29611 Ricinus communis
XP_006491635 Citrus sinensis, XP_006447324 Citrus clementina
CDP10983 Coffea canephora
XP_010934958 Elaeis guineensis
XP_008796942 Phoenix dactylifera
XP_009394893 Musa acuminata subsp. malaccensis
XP_010264276 XP Nelumbo nucifera
XP_004149490 Cucumis sativus
XP_008466646 Cucumis melo
XP_007224618 Prunus persica
XP_008221377 Prunus mume
PITA_000052807 Pinus taeda
PITA_000018463 Pinus taeda
XP_010942072 Elaeis guineensis
XP_009359106 Pyrus x bretschneideri
XP_009775676 Nicotiana sylvestris
CDX72330 Brassica napus
XP_009138046 Brassica rapa CDY13456 Brassica napus
XP_010525903 XP_010525904 Tarenaya hassleriana
XP_011031446 Populus euphratica
XP_002308709 EEE92232 Populus trichocarpa
XP_004145582 Cucumis sativus
XP_008452843 Cucumis melo
XP_010258548 Nelumbo nucifera XP_010258547
XP_002283327 Vitis vinifera
XP_002975593 EFJ23222 Selaginella moellendorffii
PITA_000025903 Pinus taeda
XP_002972555 EFJ26641 Selaginella moellendorffii
ERM96967 Amborella trichopoda
PITA_000024678 Pinus taeda
PITA_000021414 Pinus taeda
PITA_000006816 Pinus taeda
PITA_000023661 Pinus taeda
PITA_000050276 Pinus taeda
PITA_000049163 Pinus taeda
PITA_000041325 Pinus taeda
PITA_000033066 Pinus taeda
PITA_000054671 Pinus taeda
XP_010935655 Elaeis guineensis
XP_010935645 Elaeis guineensis
XP_008806535 Phoenix dactylifera
XP_008365652 Malus domestica
XP_002514843 EEF47397 Ricinus communis
XP_010278101 XP_010278102 Nelumbo nucifera
XP_002977337 EFJ21341 Selaginella moellendorffii
XP_010418289 Camelina sativa
XP_002272943 Vitis vinifera
KDO44671 Citrus sinensis
XP_006480788 Citrus sinensis, XP_006429052 ESR42292 Citrus clementina
XP_006300860 EOA33758 Capsella rubella
KDO49461 Citrus sinensis
XP_006487352 Citrus sinensis
XP_011032541 Populus euphratica
XP_011048920 Populus euphratica
XP_006382641 ERP60438 Populus trichocarpa
XP_006382765 ERP60562 Populus trichocarpa
XP_011032465 Populus euphratica
XP_011015328 XP_011015330 Populus euphratica
XP_011036342 XP_011036344 Populus euphratica
XP_002325779 EEF00161 Populus trichocarpa
XP_006382084 ERP59881 Populus trichocarpa
XP_011031483 Populus euphratica
XP_002309701 EEE93224 Populus trichocarpa
XP_006382123 ERP59920 Populus trichocarpa
XP_011031385 Populus euphratica
XP_011019657 Populus euphratica
XP_011019656 Populus euphratica
XP_002309564 EEE93087 Populus trichocarpa
XP_006384120 ERP61917 Populus trichocarpa
XP_011005931 Populus euphratica
XP_002305930 EEE86441 Populus trichocarpa
PITA_000010570 Pinus taeda
PITA_000048756 Pinus taeda
PITA_000009372 Pinus taeda
XP_010943853 Elaeis guineensis
PITA_000062004 Pinus taeda
EPS65531 Genlisea aurea
XP_006306676 EOA39574 Capsella rubella
XP_010457817 Camelina sativa
XP_010475414 Camelina sativa
XP_010486537 Camelina sativa
EFH68614 Arabidopsis lyrata subsp. lyrata XP_002892355
NP_172156 Arabidopsis thaliana AT1G06710 (MTSF1/2)
XP_010055594 Eucalyptus grandis
EYU32757 Erythranthe guttata
CDP16564 Coffea canephora
XP_009586706 Nicotiana tomentosiformis
XP_009794459 Nicotiana sylvestris
XP_002310456 EEE90906 Populus trichocarpa
XP_011026357 Populus euphratica
EEF43006 Ricinus communis XP_002519389
KDP32465 Jatropha curcas
XP_006478859 Citrus sinensis, XP_006443117 Citrus clementina
XP_008445686 XP_008445687 Cucumis melo
XP_004140980 KGN45981 Cucumis sativus XP_004160831
XP_003610808 AES93766 Medicago truncatula
XP_004511412 Cicer arietinum
XP_008380795 Malus domestica
XP_008222593 Prunus mume
XP_008669244 Zea mays
XP_004978096 Setaria italica
XP_002446703 Sorghum bicolor
BAK04235 Hordeum vulgare subsp. vulgare
XP_003580022 Brachypodium distachyon
XP_009401150 Musa acuminata subsp. malaccensis
XP_008804183 XP_008804184 XP_008804185 Phoenix dactylifera
XP_010930166 XP_010930167 Elaeis guineensis
XP_001759643 EDQ75555 Physcomitrella patens
PITA_000004681 Pinus taeda
XP_002974166 EFJ25121 Selaginella moellendorffii
XP_002968006 EFJ31353 Selaginella moellendorffii

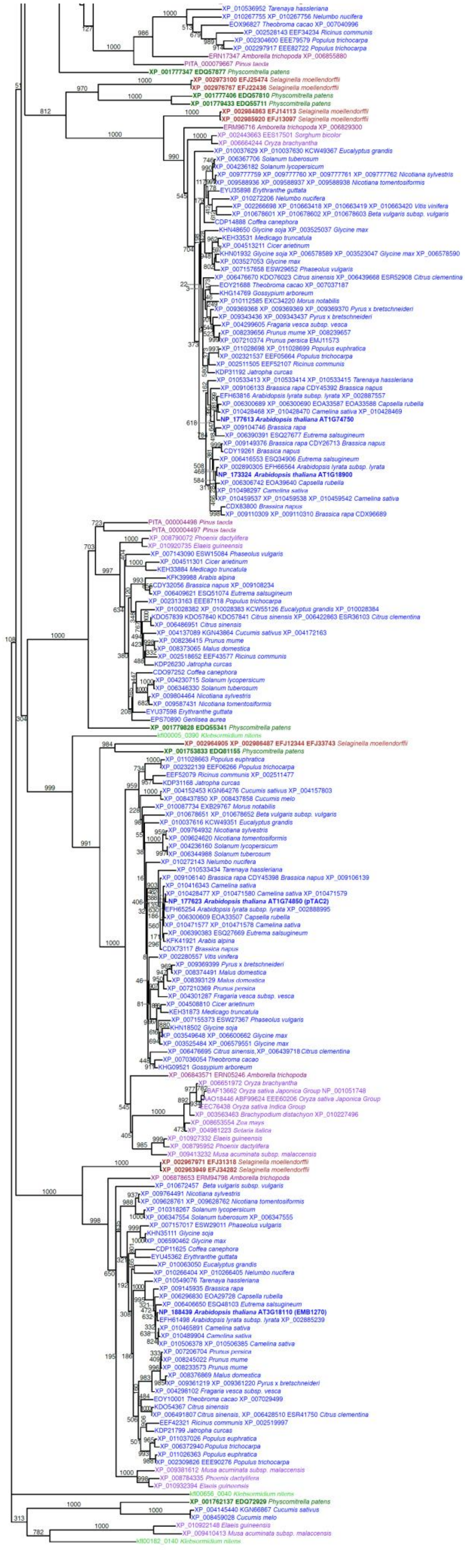

XP_010536952 Tarenaya hassleriana
XP_010267755 XP_010267756 Nelumbo nucifera
EOX96827 Theobroma cacao XP_007040996
XP_002528143 EEF34234 Ricinus communis
XP_002304600 EEE79579 Populus trichocarpa
XP_002297917 EEE82722 Populus trichocarpa
ERN17347 Amborella trichopoda XP_006855880
PITA_000079667 Pinus taeda
XP_001777347 EDQ57877 Physcomitrella patens
XP_002973100 EFJ25474 Selaginella moellendorffii
XP_002976767 EFJ22436 Selaginella moellendorffii
XP_001777406 EDQ57810 Physcomitrella patens
XP_001779433 EDQ55711 Physcomitrella patens
XP_002984863 EFJ14113 Selaginella moellendorffii
XP_002985920 EFJ13097 Selaginella moellendorffii
ERM96716 Amborella trichopoda XP_006829300
XP_002443663 EES17501 Sorghum bicolor
XP_006664244 Oryza brachyantha
XP_010037629 XP_010037630 KCW49367 Eucalyptus grandis
XP_006367706 Solanum tuberosum
XP_004236182 Solanum lycopersicum
XP_009777759 XP_009777760 XP_009777761 XP_009777762 Nicotiana sylvestris
XP_009588936 XP_009588937 XP_009588938 Nicotiana tomentosiformis
EYU35898 Erythranthe guttata
XP_010272206 Nelumbo nucifera
XP_002266698 XP_010663418 XP_010663419 XP_010663420 Vitis vinifera
XP_010678601 XP_010678602 XP_010678603 Beta vulgaris subsp. vulgaris
CDP14888 Coffea canephora
KHN48650 Glycine soja XP_003525037 Glycine max
KEH33531 Medicago truncatula
XP_004513211 Cicer arietinum
KHN01932 Glycine soja XP_006578589 XP_003523047 Glycine max XP_006578590
XP_003527053 Glycine max
XP_007157658 ESW29652 Phaseolus vulgaris
XP_006476670 KDO76023 Citrus sinensis XP_006439668 ESR52908 Citrus clementina
EOY21688 Theobroma cacao XP_007037187
KHG14769 Gossypium arboreum
XP_010112585 EXC34220 Morus notabilis
XP_009369368 XP_009369369 XP_009369370 Pyrus x bretschneideri
XP_009343436 XP_009343437 Pyrus x bretschneideri
XP_004299605 Fragaria vesca subsp. vesca
XP_008239656 Prunus mume XP_008239657
XP_007210374 Prunus persica EMJ11573
XP_011028698 XP_011028699 Populus euphratica
XP_002321537 EEF05664 Populus trichocarpa
XP_002511505 EEF52107 Ricinus communis
KDP31192 Jatropha curcas
XP_010533413 XP_010533414 XP_010533415 Tarenaya hassleriana
XP_009106133 Brassica rapa CDY45392 Brassica napus
EFH63816 Arabidopsis lyrata subsp. lyrata XP_002887557
XP_006300689 XP_006300690 EOA33587 EOA33588 Capsella rubella
XP_010428468 XP_010428470 Camelina sativa XP_010428469
NP_177613 Arabidopsis thaliana AT1G74750
XP_009104746 Brassica rapa
XP_006390391 ESQ27677 Eutrema salsugineum
XP_009149376 Brassica rapa CDY26713 Brassica napus
CDY19261 Brassica napus
XP_006416553 ESQ34906 Eutrema salsugineum
XP_002890305 EFH66564 Arabidopsis lyrata subsp. lyrata
NP_173324 Arabidopsis thaliana AT1G18900
XP_006306742 EOA39640 Capsella rubella
XP_010498297 Camelina sativa
XP_010459537 XP_010459538 XP_010459542 Camelina sativa
CDX83800 Brassica napus
XP_009110309 XP_009110310 Brassica rapa CDX96689
PITA_000004498 Pinus taeda
PITA_000004497 Pinus taeda
XP_008790072 Phoenix dactylifera
XP_010920735 Elaeis guineensis
XP_007143090 ESW15084 Phaseolus vulgaris
XP_004511301 Cicer arietinum
KEH33884 Medicago truncatula
KFK39988 Arabis alpina
CDY32056 Brassica napus XP_009108234
XP_006409621 ESQ51074 Eutrema salsugineum
XP_002313163 EEE87118 Populus trichocarpa
XP_010028382 XP_010028383 KCW55126 Eucalyptus grandis XP_010028384
KDO57839 KDO57840 KDO57841 Citrus sinensis XP_006422863 ESR36103 Citrus clementina
XP_006486951 Citrus sinensis
XP_004137089 KGN43864 Cucumis sativus XP_004172163
XP_008236415 Prunus mume
XP_008373065 Malus domestica
XP_002518652 EEF43577 Ricinus communis
KDP26230 Jatropha curcas
CDO97252 Coffea canephora
XP_004230715 Solanum lycopersicum
XP_006346330 Solanum tuberosum
XP_009804464 Nicotiana sylvestris
XP_009587431 Nicotiana tomentosiformis
EYU37598 Erythranthe guttata
EPS70890 Genlisea aurea
XP_001779828 EDQ55341 Physcomitrella patens
kfl00005_0390 Klebsormidium nitens
XP_002964905 XP_002986487 EFJ12344 EFJ33743 Selaginella moellendorffii
XP_001753833 EDQ81155 Physcomitrella patens
XP_011028663 Populus euphratica
XP_002322139 EEF06266 Populus trichocarpa
EEF52079 Ricinus communis XP_002511477
KDP31168 Jatropha curcas
XP_004152453 KGN64276 Cucumis sativus XP_004157803
XP_008437850 XP_008437858 Cucumis melo
XP_010087734 EXB29767 Morus notabilis
XP_010678651 XP_010678652 Beta vulgaris subsp. vulgaris
XP_010037616 KCW49351 Eucalyptus grandis
XP_009764932 Nicotiana sylvestris
XP_009624620 Nicotiana tomentosiformis
XP_004236160 Solanum lycopersicum
XP_006344988 Solanum tuberosum
XP_010272143 Nelumbo nucifera
XP_010533434 Tarenaya hassleriana
XP_009106140 Brassica rapa CDY45398 Brassica napus XP_009106139
XP_010416343 Camelina sativa
XP_010428477 XP_010471580 Camelina sativa XP_010471579
NP_177623 Arabidopsis thaliana AT1G74850 (pTAC2)
EFH65254 Arabidopsis lyrata subsp. lyrata XP_002888995
XP_006300609 EOA33507 Capsella rubella
XP_010471577 XP_010471578 Camelina sativa
XP_006390383 ESQ27669 Eutrema salsugineum
KFK41921 Arabis alpina
CDX73117 Brassica napus
XP_002280557 Vitis vinifera
XP_009369399 Pyrus x bretschneideri
XP_008374491 Malus domestica
XP_008393129 Malus domestica
XP_007210369 Prunus persica
XP_004301287 Fragaria vesca subsp. vesca
XP_004508810 Cicer arietinum
KEH31873 Medicago truncatula
XP_007155373 ESW27367 Phaseolus vulgaris
KHN18502 Glycine soja
XP_003549648 XP_006600662 Glycine max
XP_003525484 XP_006579551 Glycine max
XP_006476695 Citrus sinensis, XP_006439718 Citrus clementina
XP_007036054 Theobroma cacao
KHG09521 Gossypium arboreum
XP_006843571 ERN05246 Amborella trichopoda
XP_006651972 Oryza brachyantha
BAF13662 Oryza sativa Japonica Group NP_001051748
AAO18446 ABF99624 EEE60206 Oryza sativa Japonica Group
EEC76438 Oryza sativa Indica Group
XP_003563463 Brachypodium distachyon XP_010227496
XP_008653554 Zea mays
XP_004981223 Setaria italica
XP_010927332 Elaeis guineensis
XP_008795952 Phoenix dactylifera
XP_009413232 Musa acuminata subsp. malaccensis
XP_002967971 EFJ31318 Selaginella moellendorffii
XP_002963949 EFJ34282 Selaginella moellendorffii
XP_006878653 ERM94798 Amborella trichopoda
XP_010672457 Beta vulgaris subsp. vulgaris
XP_009764491 Nicotiana sylvestris
XP_009628761 XP_009628762 Nicotiana tomentosiformis
XP_010318267 Solanum lycopersicum
XP_006347554 Solanum tuberosum XP_006347555
XP_007157017 ESW29011 Phaseolus vulgaris
KHN35111 Glycine soja
XP_006590462 Glycine max
CDP11625 Coffea canephora
EYU45362 Erythranthe guttata
XP_010063050 Eucalyptus grandis
XP_010266404 XP_010266405 Nelumbo nucifera
XP_010549076 Tarenaya hassleriana
XP_009145935 Brassica rapa
XP_006296830 EOA29728 Capsella rubella
XP_006406650 ESQ48103 Eutrema salsugineum
NP_188439 Arabidopsis thaliana AT3G18110 (EMB1270)
EFH61498 Arabidopsis lyrata subsp. lyrata XP_002885239
XP_010465891 Camelina sativa
XP_010489904 Camelina sativa
XP_010506378 XP_010506385 Camelina sativa
XP_007206704 Prunus persica
XP_008245022 Prunus mume
XP_008233573 Prunus mume
XP_008376869 Malus domestica
XP_009361219 XP_009361220 Pyrus x bretschneideri
XP_004298102 Fragaria vesca subsp. vesca
EOY10001 Theobroma cacao XP_007029499
KDO54367 Citrus sinensis
XP_006491807 Citrus sinensis, XP_006428510 ESR41750 Citrus clementina
EEF42321 Ricinus communis XP_002519997
KDP21799 Jatropha curcas
XP_011037026 Populus euphratica
XP_006372940 Populus trichocarpa
XP_011026363 Populus euphratica
XP_002309826 EEE90276 Populus trichocarpa
XP_009381612 Musa acuminata subsp. malaccensis
XP_008784335 Phoenix dactylifera
XP_010932394 Elaeis guineensis
kfl00656_0040 Klebsormidium nitens
XP_001762137 EDQ72929 Physcomitrella patens
XP_004145440 KGN66867 Cucumis sativus
XP_008459028 Cucumis melo
XP_010922148 Elaeis guineensis
XP_009410413 Musa acuminata subsp. malaccensis
kfl00182_0140 Klebsormidium nitens

Data S1I: *Cb*GUN1 clusters with land plant GUN1 proteins.

Neighbour-joining phylogeny of 381 tetratricopeptide (TPR) and pentatricopeptide repeat (PPR) proteins from a broad range of photosynthetic eukaryotes (see color code at the top). Note the well-supported clades of (i) GUN1 proteins, including *Cb*GUN1 (g9159, green frame), and (ii) the streptophyte algae- and bryophyte- specific PPRs, including the *K. nitens* protein kfl00096_0090 (blue frame) and the *C. braunii* protein g31394 (green frame).Values from 1,000 bootstrap replicates are shown at the nodes.

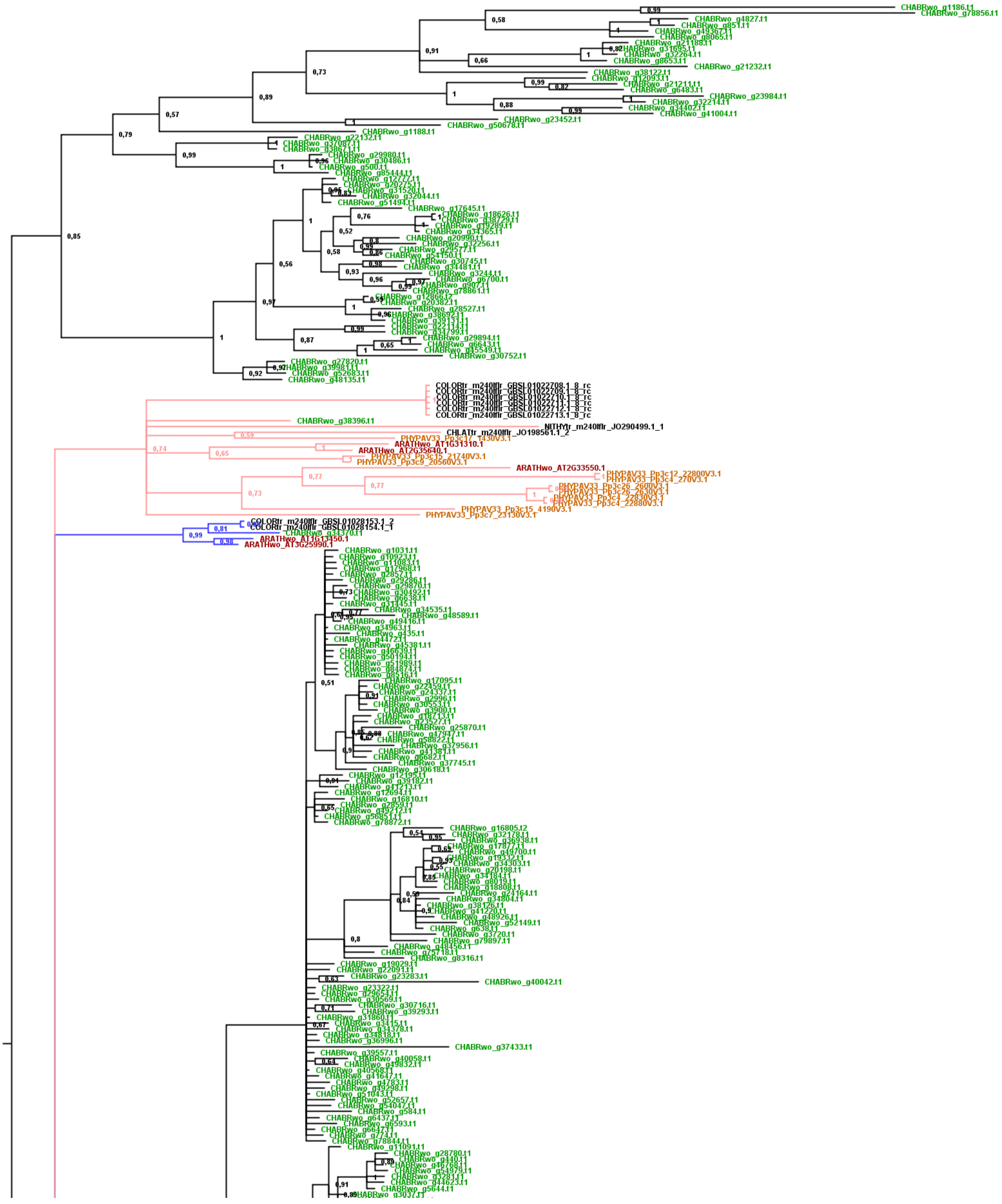
0,99
CHABRwo_g1186.t1
CHABRwo_g78856.t1
0,58
CHABRwo_g4827.t1
1
CHABRwo_g851.t1
1
CHABRwo_g49367.t1
CHABRwo_g8065.t1
CHABRwo_g21188.t1
0,91
0,82
CHABRwo_g31695.t1
1
CHABRwo_g32264.t1
0,66
CHABRwo_g8653.t1
CHABRwo_g21232.t1
0,73
CHABRwo_g38122.t1
CHABRwo_g12093.t1
0,99
CHABRwo_g21211.t1
0,82
CHABRwo_g6483.t1
1
CHABRwo_g23984.t1
0,89
1
CHABRwo_g32214.t1
0,88
CHABRwo_g34402.t1
0,99
CHABRwo_g41004.t1
0,57
CHABRwo_g23452.t1
1
CHABRwo_g50678.t1
0,79
CHABRwo_g1188.t1
CHABRwo_g22132.t1
1
CHABRwo_g37087.t1
CHABRwo_g38671.t1
0,99
CHABRwo_g29980.t1
0,96
CHABRwo_g30486.t1
1
CHABRwo_g500.t1
CHABRwo_g85444.t1
CHABRwo_g12777.t1
CHABRwo_g20275.t1
0,95
CHABRwo_g31520.t1
0,83
CHABRwo_g32044.t1
CHABRwo_g51494.t1
CHABRwo_g17645.t1
0,85
1
0,76
1
CHABRwo_g18626.t1
CHABRwo_g38729.t1
1
CHABRwo_g19289.t1
CHABRwo_g34365.t1
0,52
0,8
CHABRwo_g20990.t1
0,99
CHABRwo_g32256.t1
0,58
CHABRwo_g29577.t1
0,86
CHABRwo_g54150.t1
0,56
0,98
CHABRwo_g30745.t1
CHABRwo_g34481.t1
0,93
CHABRwo_g3244.t1
0,96
0,97
CHABRwo_g6700.t1
0,99
CHABRwo_g907.t1
CHABRwo_g78861.t1
0,59
CHABRwo_g12866.t2
0,97
CHABRwo_g20382.t1
1
CHABRwo_g28527.t1
0,96
CHABRwo_g38692.t1
CHABRwo_g39131.t1
0,99
CHABRwo_g22114.t1
CHABRwo_g34799.t1
1
CHABRwo_g29894.t1
0,87
1
0,65
CHABRwo_g6643.t1
CHABRwo_g45549.t1
CHABRwo_g30752.t1
CHABRwo_g27820.t1
0,97
CHABRwo_g39981.t1
0,92
CHABRwo_g52683.t1
CHABRwo_g48135.t1
COLORtr_m240lflr_GBSL01022708.1_8_rc
COLORtr_m240lflr_GBSL01022709.1_8_rc
1
COLORtr_m240lflr_GBSL01022710.1_8_rc
COLORtr_m240lflr_GBSL01022711.1_8_rc
COLORtr_m240lflr_GBSL01022712.1_8_rc
COLORtr_m240lflr_GBSL01022713.1_8_rc
CHABRwo_g38396.t1
NITHYtr_m240lflr_JO290499.1_1
0,59
CHLATtr_m240lflr_JO198561.1_2
PHYPAV33_Pp3c17_1430V3.1
0,74
1
ARATHwo_AT1G31310.1
0,65
ARATHwo_AT2G35640.1
1
PHYPAV33_Pp3c15_21740V3.1
PHYPAV33_Pp3c9_20560V3.1
ARATHwo_AT2G33550.1
0,77
1
PHYPAV33_Pp3c12_22800V3.1
PHYPAV33_Pp3c4_270V3.1
0,77
PHYPAV33_Pp3c26_2600V3.1
0,73
1
PHYPAV33_Pp3c26_2630V3.1
PHYPAV33_Pp3c4_22830V3.1
PHYPAV33_Pp3c4_22880V3.1
PHYPAV33_Pp3c15_4190V3.1
PHYPAV33_Pp3c7_23130V3.1
0,98
COLORtr_m240lflr_GBSL01028153.1_2
0,81
COLORtr_m240lflr_GBSL01028154.1_1
0,99
CHABRwo_g34370.t1
0,98
ARATHwo_AT1G13450.1
ARATHwo_AT3G25990.1
CHABRwo_g1031.t1
CHABRwo_g10923.t1
CHABRwo_g11083.t1
CHABRwo_g17968.t1
CHABRwo_g2857.t1
CHABRwo_g29286.t1
CHABRwo_g29870.t1
0,73
CHABRwo_g30492.t1
CHABRwo_g6638.t1
CHABRwo_g31445.t1
0,77
CHABRwo_g34535.t1
0,61
CHABRwo_g48589.t1
0,95
CHABRwo_g49416.t1
CHABRwo_g34963.t1
CHABRwo_g435.t1
CHABRwo_g4472.t1
CHABRwo_g45381.t1
CHABRwo_g46639.t1
CHABRwo_g50194.t1
CHABRwo_g51989.t1
CHABRwo_g84874.t1
CHABRwo_g8516.t1
0,51
CHABRwo_g17095.t1
CHABRwo_g22459.t1
0,91
CHABRwo_g24337.t1
CHABRwo_g2996.t1
CHABRwo_g30553.t1
CHABRwo_g3900.t1
CHABRwo_g18713.t1
CHABRwo_g23527.t1
CHABRwo_g25870.t1
0,85
0,88
CHABRwo_g47947.t1
0,62
CHABRwo_g58822.t1
CHABRwo_g37956.t1
0,9
CHABRwo_g41381.t1
CHABRwo_g6682.t1
CHABRwo_g37745.t1
CHABRwo_g30618.t1
CHABRwo_g12195.t1
0,94
CHABRwo_g39182.t1
CHABRwo_g41213.t1
CHABRwo_g12694.t1
CHABRwo_g16810.t1
0,65
CHABRwo_g2859.t1
CHABRwo_g49212.t1
CHABRwo_g56851.t1
CHABRwo_g78872.t1
CHABRwo_g16805.t2
0,54
CHABRwo_g32178.t1
0,95
CHABRwo_g36938.t1
CHABRwo_g17877.t1
0,69
CHABRwo_g49700.t1
CHABRwo_g19332.t1
0,93
CHABRwo_g34303.t1
0,55
CHABRwo_g20198.t1
0,85
CHABRwo_g34184.t1
CHABRwo_g8019.t1
CHABRwo_g18808.t1
0,59
CHABRwo_g24164.t1
0,84
CHABRwo_g34804.t1
CHABRwo_g38126.t1
0,9
CHABRwo_g41220.t1
CHABRwo_g48926.t1
CHABRwo_g52149.t1
CHABRwo_g638.t1
CHABRwo_g3720.t1
0,8
CHABRwo_g79897.t1
CHABRwo_g48456.t1
CHABRwo_g75718.t1
CHABRwo_g8316.t1
CHABRwo_g19029.t1
CHABRwo_g22091.t1
0,63
CHABRwo_g23283.t1
CHABRwo_g40042.t1
CHABRwo_g23322.t1
CHABRwo_g29654.t1
CHABRwo_g30569.t1
0,71
CHABRwo_g30716.t1
CHABRwo_g39293.t1
CHABRwo_g31860.t1
0,67
CHABRwo_g3415.t1
CHABRwo_g34378.t1
CHABRwo_g34818.t1
CHABRwo_g36996.t1
CHABRwo_g37433.t1
CHABRwo_g39557.t1
0,64
CHABRwo_g40058.t1
CHABRwo_g49832.t1
CHABRwo_g40568.t1
CHABRwo_g41647.t1
CHABRwo_g4783.t1
CHABRwo_g49298.t1
CHABRwo_g51043.t1
CHABRwo_g52657.t1
CHABRwo_g54047.t1
CHABRwo_g584.t1
CHABRwo_g6437.t1
CHABRwo_g6593.t1
CHABRwo_g6647.t1
CHABRwo_g774.t1
CHABRwo_g78844.t1
CHABRwo_g11091.t1
CHABRwo_g28780.t1
CHABRwo_g440.t1
0,89
CHABRwo_g46768.t1
CHABRwo_g54979.t1
1
CHABRwo_g3281.t1
0,91
CHABRwo_g44623.t1
CHABRwo_g5644.t1
0,89
CHABRwo_g3037.t1

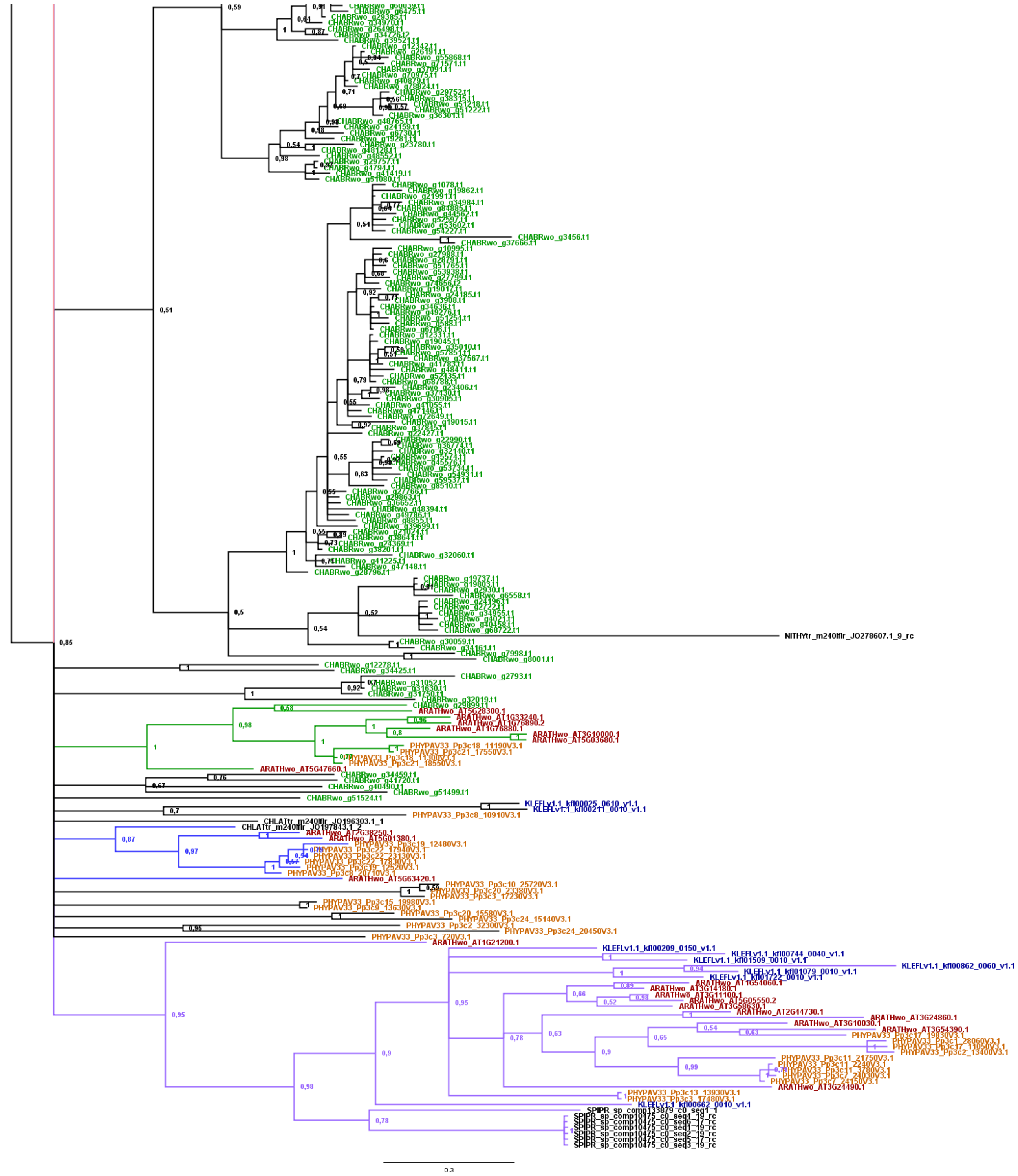

Data S1J: Phylogenetic tree of trihelix transcription factors.

Phylogenetic analysis based on the trihelix domain shows that most of the trihelix paralogs were probably secondarily gained in the *Chara* lineage; Bayesian inference based on the trihelix domain, midpoint-rooted, numbers at the nodes represent posterior probabilities. Land plant sequences (*A. thaliana* and *P. patens*) are shown in red, *C. braunii* sequences in green, *K. nitens* sequences in blue. Sequences of other charophytes are shown in black. Colored branches correspond to trihelix sub families according to Kaplan-Levy et al., 2012: GT-1 blue, GT-2 green, SIP1 lavender and SH4 beige. Three *Chara* trihelix proteins group within previously defined clades, namely g38396 in SH4, g34370 in GT-1 and g29899 in GT-2. All three are expressed in vegetative tissue (supplemental file 3).

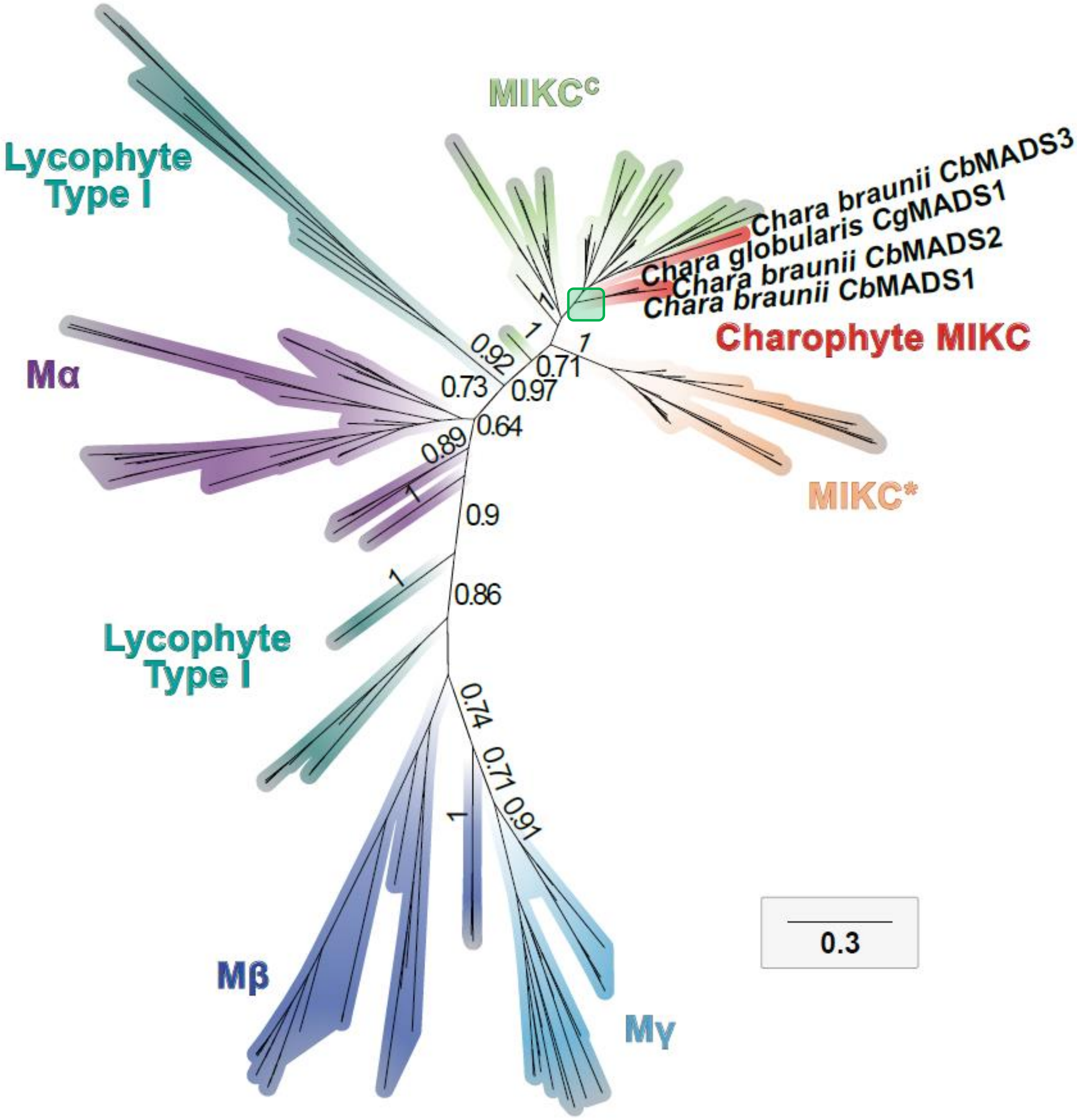

Data S1K: Phylogenetic tree of plant MADS-box genes.

The three previously described groups of Type I MADS-box genes in angiosperms Mα, Mβ and Mγ as well as lycophyte Type I genes are highlighted in purple, dark blue, light blue and cyan, respectively. The two groups of MIKC^{C}- and MIKC*-type genes found in land plants and the charophyte MIKC-type genes are highlighted in green, orange and red, respectively. The posterior probabilities of main branches are depicted next to the tree. The unrooted tree shown here only visualizes the relationship of the examined genes without suggesting any ancestry. *C. braunii* branches are marked by a green box.

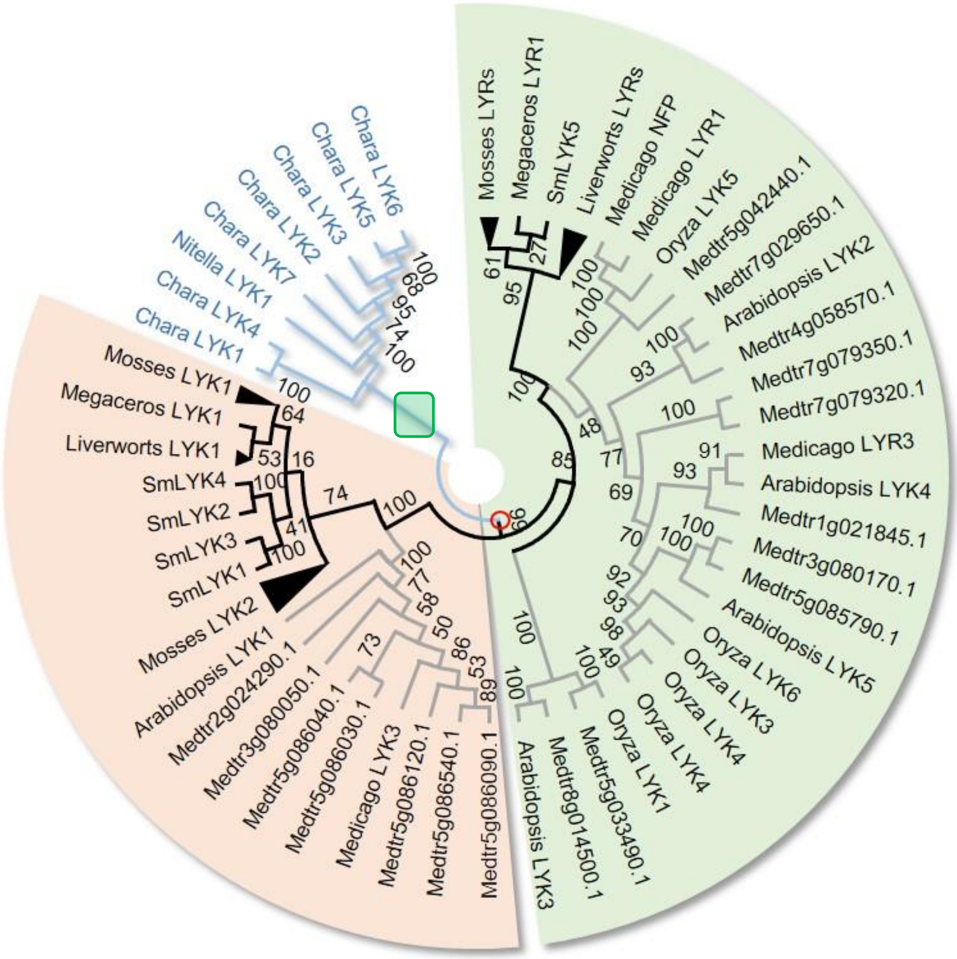

Data S1L: Condensed Maximum likelihood tree of the LysM-RLK family.

The charophyte sequences form a single cluster (green box), presumably a clade (blue branches) encompassing seven *C. braunii* sequences. Assuming these charophyte sequence serve as outgroup to land plant LysM-RLK genes, the duplication (red circle) leading to the LYK (orange) and LYR (green) subclades occurred before the divergence of extant embryophytes. The mosses, liverworts, hornworts and *Selaginella* genes form a clade which is a sister group to a clade of angiosperm genes in each of LYK and LYR subclass.

```
                                     10        20        30        40        50        60
                            ....|....|....|....|....|....|....|....|....|....|....|....|
OsCERK1                     ------------------------------------------------------------
MtLYK3_-_Medtr5g086130.1    ------------------------------------------------------------
g49675                      MWHGEEWCNVVSAAVCAHTIDLSMDLPLWFAGTNIEDRPEDDNMAVYQESTVICIAHAFR
g50598                      ------------------------------------------------------------
g44510                      MAGACYIHVLLMLLRFLATIVLFAVRPFSAAVMSFAVRPFAA------------------
g91196                      ------------------------------------------------------------
g30047                      ------------------------------------------------------------
g8984                       MSQRHHDTVLWSAVRRNASLPAPVFAADFVHLLWAEGWIAVHLRDGLWFGVVVAFKTTKL
g8619                       ------------------------------------------------------------
MtNFP_-_Medtr5g019040.1     ------------------------------------------------------------

                                     70        80        90       100       110       120
                            ....|....|....|....|....|....|....|....|....|....|....|....|
OsCERK1                     ------------------------------------------------------------
MtLYK3_-_Medtr5g086130.1    ------------------------------------------------------------
g49675                      RAVQMGAHIDGDFISYDRLCRVADCFRLLFAACMWIMRMAGDDPRSHYKAFYLANLLAKP
g50598                      ------------------------------------------------------------
g44510                      ------------------------------------------------------------
g91196                      ------------------------------------------------------------
g30047                      ------------------------------------------------------------
g8984                       TCEQVCQQHRAEQSRAEQNRADPD------------------------------------
g8619                       ------------------------------------------------------------
MtNFP_-_Medtr5g019040.1     ------------------------------------------------------------

                                    130       140       150       160       170       180
                            ....|....|....|....|....|....|....|....|....|....|....|....|
OsCERK1                     ------------------------------------------------------------
MtLYK3_-_Medtr5g086130.1    ------------------------------------------------------------
g49675                      TLVASMHRPFDHRRSVVRAAKVVTERLGKVNATFGEYPDYIPEWEPYGIGFRHDMSITGP
g50598                      ------------------------------------------------------------
g44510                      ------------------------------------------------------------
g91196                      ------------------------------------------------------------
g30047                      ------------------------------------------------------------
g8984                       ------------------------------------------------------------
g8619                       ------------------------------------------------------------
MtNFP_-_Medtr5g019040.1     ------------------------------------------------------------

                                    190       200       210       220       230       240
                            ....|....|....|....|....|....|....|....|....|....|....|....|
OsCERK1                     ------------------------------------------------------------
MtLYK3_-_Medtr5g086130.1    ------------------------------------------------------------
g49675                      EYAKKLDWQEEKAGELYVAAMGEERADKSFIEKDSKKTTVSRGGIVERILLCPLSSSCPL
g50598                      ------------------------------------------------------------
g44510                      ------------------------------------------------------------
g91196                      ------------------------------------------------------------
g30047                      ------------------------------------------------------------
g8984                       -------------------------------------------------------RSSSM
g8619                       ------------------------------------------------------------
MtNFP_-_Medtr5g019040.1     ------------------------------------------------------------

                                    250       260       270       280       290       300
                            ....|....|....|....|....|....|....|....|....|....|....|....|
OsCERK1                     ------------------------------------------------------------
MtLYK3_-_Medtr5g086130.1    ------------------------------------------------------------
g49675                      PPLSSYPRSTSEHCAGMASPPQQQQPNRCAGMASPPPQQQQPKRCAGMASPPQQQPNRCA
g50598                      ------------------------------------------------------------
g44510                      ------------------------------------------------------------
g91196                      ------------------------------------------------------------
g30047                      ------------------------------------------------------------
g8984                       MESDVRRAATAVECVDCHHRNNGVAAKPSLSQASGTSTSSSACVPPAYWGLFLAFVQALL
g8619                       ------------------------------------------------------------
MtNFP_-_Medtr5g019040.1     ------------------------------------------------------------

                                    310       320       330       340       350       360
                            ....|....|....|....|....|....|....|....|....|....|....|....|
OsCERK1                     -------------------------------MFSLPALLIGACAFAAAAVAASGDGCRAG
MtLYK3_-_Medtr5g086130.1    ----------------------------MNLKNGLLLFILFLDCVFFKVESKCVKGCDVA
g49675                      GKGSLRRQPDRCAGKASLQPHTPSPLHVPLLSFSQIVLLCSLFLTPPYIPIASGLRCQVD
g50598                      ---------MAFYHGYPRVTPFYCPRVDSPLVNAICTHVLTLLIILARVSCALAVPCSAV
g44510                      ---------VVRSFAVRMLPFAVAVRSFVVRPFVAVVLSTAVTLMCATLPSALAISCSAA
g91196                      ----------------------------------MVFAATALMSMSAILSSAVGIPCSVA
g30047                      -----------------------------------------------MIPLACGVTCRSS
g8984                       AGRTGKIGGGVAGSRGPTTPVLMMRCRPTAALGWLVLLWLCSGHQSLCIPAACAFACSTE
g8619                       -----------MGCGTRRLHHHCRGWNGPAVLHWLLMSLLCGSHFSVLFLPCSGYPCRPA
MtNFP_-_Medtr5g019040.1     ------------------MSAFFLPSSSHALFLVLMLFFLTNISAQPLYISETNFTCPVD

                                    370       380       390       400       410       420
                            ....|....|....|....|....|....|....|....|....|....|....|....|
OsCERK1                     -----CSLAIAAYYFSEGS--NLTFIATIFAIGGGGYQA---LLPYNPA-ITNPDYVVTG
MtLYK3_-_Medtr5g086130.1    ---------LASYYIIPSI--QLRNISNFMQSKIVLTNSFDVIMSYNRDVVFDKSGLISY
g49675                      --DQQSCTAFVVYRIQVGD--SMRDICDRFRQYEGVVLV---INNM-----TEATRLTVN
g50598                      --DQQQCTAYVAYRLQVGD--MEADIASRFGLGR----------------DPDLMSSIGS
g44510                      MGDDMNCTAFVVYRPQRGD--TFDDVVRRFAQDPVVNRY---PFRNDSGPDNDL------
g91196                      MGDDKNCTAFVAYRPRRAD--TWHDLAIRFAQDPVINPY---PILIHGGSDNDLLTL---
g30047                      --DQATCTSYVVYTWQEGE--RVADVAKRFGLNLANDSA---RITI----DPDHI-----
g8984                       ---DSSCQAYAVYVVSVGD--RLEDICSRFQVTFADISA---VNPV------CNFTLHPG
```

```
g8619                     --HDTSCQAYAVYDVRPGD--RVQDISKLFDDDYRDVAS---VNKL----DLGNLTLLPD
MtNFP_-_Medtr5g019040.1   --SPPSCETYVAYRAQSPNFLSLSNISDIFNLSPLRIAK---ASNI----EAEDKKLIPD

                                 430       440       450       460       470       480
                          ....|....|....|....|....|....|....|....|....|....|....|....|
OsCERK1                   DRVLVPFPCSCLGLPAAPAST--FLAGAIPYPLPLPRGGGD-------------------
MtLYK3_-_Medtr5g086130.1  TRINVPFPCECIGGE--------FLGHVFEYTT---K-EGD-------------------
g49675                    RELIIPVSCSC-----NQSRSAQVYWARPTYPV---Q-VDD-------------------
g50598                    GLQIIPVFCSCTNRSSSQSASG-FETARLTYTV---Q-SGD-------------------
g44510                    -LLLFPVACSC-----NESRR--QYETDLFYTV---Q-SGD-------------------
g91196                    -LSLFPVPCSC-----NESRR--QFETDIFYTV---E-TGD-------------------
g30047                    -ELIFPVTCSC-----NRTRQA-FRTDRISYVV---EAEGGAAGGGGGGEGGEGGGGGGR
g8984                     QNLLIPLSCLC-----NDEG---FFQASIQHVV---R-DDQ-------------------
g8619                     QQLYIPLTCHC-----DERNA--VFYATVNHVI---AFDGE-------------------
MtNFP_-_Medtr5g019040.1   QLLLVPVTCGC-----TKN----HSFANITYSI---K-QGD-------------------

                                 490       500       510       520       530       540
                          ....|....|....|....|....|....|....|....|....|....|....|....|
OsCERK1                   --TYDAVAAN-YADLTTAAWLEATNAYP--PGRIPGGDGRVNVTINCSCG-DERVSPRYG
MtLYK3_-_Medtr5g086130.1  --DYDLIANTYYASLTTVELLKKFNSY---DPNHIPVKAKINVTVICSCG-NSQISKDYG
g49675                    --TLEKIQNDLYQNLTAISDIVEVNRLG--GQDYLMAGWTLRIPIPCACN--TSDGGSFS
g50598                    --TVDKIATSKYQSLTSTTEIGAATGLQ--NVDVINPGDVLRIPIPCACNRTSAKASQSR
g44510                    --TLSRIADREYDSLISISDMVKVNGIS--VEDFIDVAWRLKIAIRCACN-SSSAGREFE
g91196                    --SLSGIAYLKYESLLSVADMVQANGVS--DPDYVRVGWRLKIAIRCACNSSSSAGRDFD
g30047                    SVSVLKIASSRYQSLTSAEDIMDANGIEDVNENSVAAGQTLKIPIRCACN--VSEGEQFQ
g8984                     --TLHEVASTSFHNLTTAEDIADASRIN--TLQSVHAGQSLRIPISCGCNASSLSWLRAP
g8619                     --TIESIASVLFQNLSHAQEIVNASGLT--HGVAVQPGQTVSVPIRCGCNSTALLSVRTP
MtNFP_-_Medtr5g019040.1   --NFFILSITSYQNLTNYLEFKNFNPNL--SPTLLPLDTKVSVPLFCKCPSKNQLNKGIK

                                 550       560       570       580       590       600
                          ....|....|....|....|....|....|....|....|....|....|....|....|
OsCERK1                   LFLTY-PLWDGETLESVAAQYGFSSPAEMELIRRYNPGMGGVSGK----------GIVFI
MtLYK3_-_Medtr5g086130.1  LFVTY-PLRSDDTLAKIATKAGL----DEGLIQNFNQDANFSIGS----------GIVFI
g49675                    SFVTYVPGSTGETADAIAAKFQT----TVGNIRRASMIAEEEGVVDVY-------RPLIV
g50598                    SYLTYGPASGSEKYATIAQTFNS----TARAILDLNGVVGDPVTVSSTVNPSQRPQPLII
g44510                    SYLTISSKSTSDTPSGVAQRFNT----TVDAIQRVNGLFGSDFVDFE--------GPLIV
g91196                    SYITYCPNSTFETPADVAQRFNT----TVAAIRTVNGIVGPRFDLFDRDN-----RPLVI
g30047                    SYVTYRPRDTSDTPASVAKKFSS----TVEAMQRVNGYVGAVVFRANQ-------EPIIV
g8984                     SYLTY-VLQQGDTIDSVANTFGS----DNQTIQKSNGGAGGVLQLRPG-------IKLII
g8619                     SFLTY-VVGNDTDVRSIAQTFRS----SERLILEANAGAQADLPLDPG-------TRLVI
MtNFP_-_Medtr5g019040.1   YLITY-VWQDNDNVTLVSSKFGAS---QVEMLAENNHNFTASTN-----------RSVLI

                                 610       620       630       640       650       660
                          ....|....|....|....|....|....|....|....|....|....|....|....|
OsCERK1                   PVKDPNGSYHPLKSGGMGNSLS--------------------------------------
MtLYK3_-_Medtr5g086130.1  PGRDQNGHFFPLYSRTGIAKGS--------------------------------------
g49675                    PTNS-VYSLFSGSGGGDWGRWS---------SGDGAAGGRPSSSSDYMTRHGSESAAYQS
g50598                    PTNN-SYPRLPGGDTSSPPPLN---------GGGATNGGSPPVSGGGGTNGGSPP----V
g44510                    PTHR-IFHREPSAPDSLVSSSSIPIPMTPCVPTTVLPSLPTPVSPVWPSAVTSPPPSLTI
g91196                    PTHR-IFQRPSAPP-------------------------PVDATPVMPSVATPPAPS--V
g30047                    PTNTWRTLRFSSSSSQDQDQIF---------RGGGGGGPRED------------------
g8984                     PSNW-TLPNVRSQDRPPMVPRN---------KAEGSESPPLEPASKPGSGNPSETAHTSL
g8619                     PAYL-SFPTRSDEGSRARARSS-------GGDPSLSIATEPPAYPRNGVRGGASGAEDTT
MtNFP_-_Medtr5g019040.1   PVTSLPKLDQPSSNGRKSSSQN--------------------------------------

                                 670       680       690       700       710       720
                          ....|....|....|....|....|....|....|....|....|....|....|....|
OsCERK1                   ------------------------------GGAIAGIVIACIAIFIVAIWLIIMFYRWQK
MtLYK3_-_Medtr5g086130.1  ---------------------------------AVGIAMAGIFGLLLFVIYIYAKYFQKK
g49675                    ATSSSSSSSSSPSSTRKNSRGEVG-----TLGLWIWVIVGVGILAVLAGASALTVRILRE
g50598                    SGGGTNNNGSIPTDGGG------------NQALSIWGIAIAIVIVVGGMAMLIVFFVIW
g44510                    SMSRSQSRPSASTSR--------------IVPAWLWGLIAVPVVMFVAICALIVYIVRQF
g91196                    SGPRSRSSFAVSSSQ-----------------IALSVLSALVVVIFGVICALIVCFVRQL
g30047                    -----------------------------THQVHEGVPPWQVILLASTLFVLIPIFIALF
g8984                     MGGSGVNAGSDPNPKSSHSDGNQF-----PIAMVVGVLAGAAVVFLIAAVAAVICLAQRA
g8619                     STQANGTTNTASVPMDTPGKGKTGHDPAIPFELIIGILAGTTVVLMLAIICAMIYIARRV
MtNFP_-_Medtr5g019040.1   ------------------------------LALIIGISLGSAFFILVLTLSLVYVYCLKM

                                 730       740       750       760       770       780
                          ....|....|....|....|....|....|....|....|....|....|....|....|
OsCERK1                   FRKATSRPSPEETSHLDDASQA--------------------------------------
MtLYK3_-_Medtr5g086130.1  EEEKTKLPQTSRAFSTQDASGSAEYETSGSSG----------------------------
g49675                    QRPPSPPLPPSWCKDVSGSGPWAF-----------------GRTLDLSVISRSRSLSFLG
g50598                    RRRRP------TPGPGQVVETSRFWHWLSKAGLLRH-----SSSLGAMRYSKSGRL----
g44510                    PRELS------CRTCGPAFGLSQQCQHQGPAYGIDDR----DKVKGL-KAAKRPRQHY--
g91196                    RLARS---------TGARFGLCLRLRPSAPR-GIGDR----EVD----KATRRPRQCYPL
g30047                    RRYGWPTCSRSDDGGHSLSFSCRFLHNSSESCGCALS----HKPLYSTRGKQEGDSSN--
g8984                     GKPGG-----DNWTDVDKWGWADWREWSRGSGRWGRF----SRGSGNSRGSFGGRGWR--
g8619                     AKGTS------VRTAAADWERREWAEWSTESAARWQLSVIGSRALPVTRASATLPVPQ--
MtNFP_-_Medtr5g019040.1   KRLNR-------------------------------------------------------

                                 790       800       810       820       830       840
                          ....|....|....|....|....|....|....|....|....|....|....|....|
OsCERK1                   ------------------------------------------------------------
MtLYK3_-_Medtr5g086130.1  ------------------------------------------------------------
g49675                    CHVAGSDYSSGVEDSKYISYGFDSQLDRLRGGGVGGGGPGAELSGSGVDVSSGGGGAGGG
g50598                    ------------------------------------PGGEATTTAAGGGGGGGGGGGGGG
g44510                    ---TPDKRWRGVKNMDDQACRRKE------------ASGCAFVNGCGG----GGGKKLGK
```

```
g91196                    PPPPPPPPQRVKRGRDEEVILHKFDCGEAAAGRAVAEVGCCEANDVGRAGAEGGGRRGGM
g30047                    -----------------------DSRLWRSSGHHNVHDLNTDSSDVDWGGGEGGGGGGGG
g8984                     --------------------------------GTSIPGTAVRQQASSGVMRSSGSTLGGV
g8619                     -------------------------LMNTFRRRDIIHTSISNTSSLEGFSSHGGNCAKFI
MtNFP_-_Medtr5g019040.1   ------------------------------------------------------------

                                 850       860       870       880       890       900
                          ....|....|....|....|....|....|....|....|....|....|....|....|
OsCERK1                   ------------------------------------------------------------
MtLYK3_-_Medtr5g086130.1  ------------------------------------------------------------
g49675                    GTADRVAIVSLDSARGKAVDNRH-------------------AFSVDDNRRGKVIPIELY
g50598                    GGDN--------------------------------------------------------
g44510                    GGGKRGRQG------------------------------------------------VRR
g91196                    GGGGGGGVR---------------------------------------RDHIKRHKCETD
g30047                    GGRGGHAKGGGDARGEVREGGGEEEERRGKEEKAGGVGCWPIPITVEDTTKQKQKQKQKE
g8984                     PASLRTSGTAPDLLGLRGMD-----------------------------DVNRLGGSQLD
g8619                     PGVDNGSGGNV----------------------------------------------GRT
MtNFP_-_Medtr5g019040.1   ---------------------------------------------------------STS

                                 910       920       930       940       950       960
                          ....|....|....|....|....|....|....|....|....|....|....|....|
OsCERK1                   -----------EGIKVERSIEFSYEEIFNATQGFSMEHKIGQGGFGSVYYAELRGEKTAI
MtLYK3_-_Medtr5g086130.1  --HATGSAAGLTGIMVAKSTEFTYQELAKATNNFSLDNKIGQGGFGAVYYAELRGEKTAI
g49675                    SEKIPPTGGVGGVGGGGGIGTFSYHELAHATNGFSPANQIGKGLSGPVFYAKLRGREVAI
g50598                    -------WVSLDDEEEDRRVVFSLRELEESTDGFNEANLIGRGGSCEVFYANLRGREVAI
g44510                    EIKWQSGKHKTLEEDGRKFVIFSLKELEEATDGFSSDSKIGRGSSCEVFYAQLRGREVAI
g91196                    NKVINNLDLSELEKEGRKFIVFSREELEQASNGFSSDNQIGRGSSCRVFYAQLRDREVAI
g30047                    KEREKEREVVQLKEEATGVSVFSLPELEDATDGFSNANQIGIGASCQVFYGVLRGREVAI
g8984                     RQPGRGSLSAFGVEDPARLIVFPYKELLKATGRFNEVNKIGEGAYGSVYYARVRGRDAAV
g8619                     VEASASPHKSAAAMVSPSLSVFTYKDLMKATDHFSELKKIAEGSYGSTYRGLLEGRDVTV
MtNFP_-_Medtr5g019040.1   SSETADKLLSGVSGYVSKPTMYEIDAIMEGTTNLSDNCKIGE----SVYKANIDGRVLAV

                                 970       980       990      1000      1010      1020
                          ....|....|....|....|....|....|....|....|....|....|....|....|
OsCERK1                   KKMGMQA-TQEFLAELKVLTHVHHLNLVRLIGYCVEN--CLFLVYEFIDNGNLSQHLQRT
MtLYK3_-_Medtr5g086130.1  KKMDVQA-SSEFLCELKVLTHVHHLNLVRLIGYCVEG--SLFLVYEHIDNGNLGQYLHGI
g49675                    KRLKVSWGPKELRKEMKVLRKVHHKHLVELIGFCADS--SLFLVFEYCHHGSLSGSLHSP
g50598                    KKMRFDY-SREFKKELKILSKVHHRHLVQLIGFCTDR--NLFLVYEYCHQGTLSSHLHEP
g44510                    KRMRLAW-RREFQKELKILSQVHHRHLVELIGFCTHG--YLLLVYEYCHQGTLSSHLHSP
g91196                    KRMRLVW-RRQFQKELRILSQVHHRHLVELIGFCTEQ--YLFLVYEYCHQGTLSSHLHSP
g30047                    KRLKFNY-TREFQKELKVLSRVHHRCLVGLIGYCIER--SMFLVYEYCHQGTLSSHLHSS
g8984                     KRLKSVK-EKEFQSELEMMCRVHHRHLLELLGYCTEH--CLILVHEYAEGGALKKHLHSP
g8619                     KKLKKSK-AEQFQSEMEVMSRVHHCHVLALVGYCVDR--CLMLVHEFAEKGSLNRHLHSP
MtNFP_-_Medtr5g019040.1   KKIKKDA-----SEELKILQKVNHGNLVKLMGVSSDNDGNCFLVYEYAENGSLEEWLFSE

                                1030      1040      1050      1060      1070      1080
                          ....|....|....|....|....|....|....|....|....|....|....|....|
OsCERK1                   GYA--------------PLSWATRVQIALDSARGLEYLHEHVVPVYVHRDIKSANILLDK
MtLYK3_-_Medtr5g086130.1  GTE--------------PLPWSSRVQIALDSARGLEYIHEHTVPVYIHRDVKSANILIDK
g49675                    AVHG-------------VLDWPTRAQVALDAAQALLYIHDRVHPSYVHGDVRSANILLDR
g50598                    ATHG-------------ALEWPARVQIALDAAEGLQYIHEHAKPSYVHCDIKSVNILLDQ
g44510                    DACGG------------PLDWRTRVQIALDAAQALLYIHDQVCPAYIHCDIKSVNILLDR
g91196                    DTCGG------------PLDWRTRVQIALDAAQALLYIHDRVHPAYVHCDIKSLNILLDR
g30047                    SSSSSSSSSSSSITPPLPLDWPTRVQIAIDAAKALLYIHDQVQPSYVHCDIKSVNILLDL
g8984                     TTNGFS-----------PLPWRSRVQIAVDVASALEYLHEHTRPSYVHRDIKSSNILLDK
g8619                     SRNGFL-----------PLAWSVRVQIAVDISSALEYLHERSWPGFIHHSISSRNIFLDK
MtNFP_-_Medtr5g019040.1   SSKTSNSVV--------SLTWSQRITIAMDVAIGLQYMHEHTYPRIIHRDITTSNILLGS

                                1090      1100      1110      1120      1130      1140
                          ....|....|....|....|....|....|....|....|....|....|....|....|
OsCERK1                   DFRAKIADFGLAKLTEV-------------------------GSMSQSLSTRVAGTFGYM
MtLYK3_-_Medtr5g086130.1  NLRGKVADFGLTKLIEV---------------------------GNSTLHTRLVGTFGYM
g49675                    NLRGKVGDFGLNKLTTKDDLQRGRS-----------------SHTAGQLRTLSGRNLAYM
g50598                    ELRGKVADFGVIKLTPAANSGGDGGSLAMTGSVAITTTAM--VVQDHTVSTKFAGTMGYM
g44510                    DLRGKVADFGVTKLIRPEGESGGSAISGDPRKP---------RKKKDTVSTKVAGTWGYM
g91196                    DLRGKVADFGVIKLIMPEGESLAAAGLRHS------------RKKNGTLSTKFAGTWGYM
g30047                    QLRGKVADFGVMKLMRKEGETVTPEMATRTTGVQSWHATWTSMWRSTSASTRFAGTMGYM
g8984                     DMRAKVADFGLIRLMGCE------------------------EGKGSMVSTGLVGTVGYM
g8619                     NMRAKTANFGLSKRIDWKDDS---------------------TLSLAVNTAELPDVVGYM
MtNFP_-_Medtr5g019040.1   NFKAKIANFGMARTSTN-------------------------------------------

                                1150      1160      1170      1180      1190      1200
                          ....|....|....|....|....|....|....|....|....|....|....|....|
OsCERK1                   PPE-ARYGEVSPKVDVYAFGVVLYELLSAKQAIVRSSESVSES-----------------
MtLYK3_-_Medtr5g086130.1  PPEYAQYGDVSPKIDVYAFGVVLYELITAKNAVLKTGESVAES-----------------
g49675                    APEYLQEGHVSTSVDVYSLGVVLLELLTGRNAAAFTVEQGSSGMTL--------------
g50598                    APEYMIYGRVSPMCDVYSFGVVLLELLTGQKAILPSEPRV--------------------
g44510                    APEYMIYGEVTPSSDVYSFGVVLLELIAGQRAIL------PRERVA--------------
g91196                    APEYMIYGEVTPSCDVYSFGVVLLELITGQRAIL------PRERLA--------------
g30047                    APEYMIYGHVSASCDVYSFGVVLLELITGRKAVLSPAEEREREKVV--------------
g8984                     APEYLKWGHVSTKADVYSFGVVLLELISGQEALSSTIDSHSSTVQIIGGGGWRHHRQSDH
g8619                     APECLKLGQVSTKADVYSFGVVLLELLSGQEAVSCA----AGSHIVQLSGGLHCESWALD
MtNFP_-_Medtr5g019040.1   --------SMMPKIDVFAFGVVLIELLTGKKAMTTK----ENGEVV--------------

                                1210      1220      1230      1240      1250      1260
                          ....|....|....|....|....|....|....|....|....|....|....|....|
OsCERK1                   ------------------------------------------------------------
MtLYK3_-_Medtr5g086130.1  ------------------------------------------------------------
```

```
g49675                        ------------------------------------------------------------
g50598                        ------------------------------------------------------------
g44510                        ------------------------------------------------------------
g91196                        ------------------------------------------------------------
g30047                        ------------------------------------------------------------
g8984                         IGGSGSMVVSETSGSFLESSGGGSESQSVSESFANVLVKRKLEKGKPEREREPPSASGAV
g8619                         YNGSSSTVVAETSGSFAESDFGSTPPDSSSELRAKRPV---IQKRVLDVEIRPYKTAKTR
MtNFP_-_Medtr5g019040.1       ------------------------------------------------------------

                                       1270      1280      1290      1300      1310      1320
                              ....|....|....|....|....|....|....|....|....|....|....|....|
OsCERK1                       ------------------------------------------------------------
MtLYK3_-_Medtr5g086130.1      ------------------------------------------------------------
g49675                        ------------------------------------------------------------
g50598                        ------------------------------------------------------------
g44510                        ------------------------------------------------------------
g91196                        ------------------------------------------------------------
g30047                        ------------------------------------------------------------
g8984                         VAAQPTTPFENDPRNVAQHESPSGAASRWGNSDGSLGSPSDGTGAVANAVPSCRSDSSPN
g8619                         LNRMGKRQGEGTKQHPPGNEGCENSNRYLENTTNSGGKKEDA------------------
MtNFP_-_Medtr5g019040.1       ------------------------------------------------------------

                                       1330      1340      1350      1360      1370      1380
                              ....|....|....|....|....|....|....|....|....|....|....|....|
OsCERK1                       ------------------------------------------------------------
MtLYK3_-_Medtr5g086130.1      ------------------------------------------------------------
g49675                        --------------------------IESSCTSSDCSYSTFSYSQGADFASL--------
g50598                        --------------------------QSPNLDLGPDAVPRPAYRERAPFR----------
g44510                        --------------------------AAAASELAPQPPSIP-------------------
g91196                        --------------------------AAENSELATHVTQPPTLP----------------
g30047                        --------------------------SSPSSAPPPPPPPPPPPPPTTPSPPPPPPTPPAP
g8984                         PTGKILSVNGKMLRLHGLMVEIVPEGDTFACKPVRVQQQQPVTSVTGCGEPDPVDDDPST
g8619                         -CGKILSVNGSKLRLRGLTVEVLADLSGPSSCKPVLSSSVENSASAIPTQEEPANSTTGS
MtNFP_-_Medtr5g019040.1       ------------------------------------------------------------

                                       1390      1400      1410      1420      1430      1440
                              ....|....|....|....|....|....|....|....|....|....|....|....|
OsCERK1                       ------------------------------------------------------------
MtLYK3_-_Medtr5g086130.1      ------------------------------------------------------------
g49675                        ------------------------------------------------------------
g50598                        ------------------------------------------------------------
g44510                        ------------------------------------------------------------
g91196                        ------------------------------------------------------------
g30047                        TATPTPPAAPFNAGLPLPAR----------------------------------------
g8984                         TTPLMPEGSPSSDSKSGSTSRRTRKGGFLMGDKGVGKGSSSQGSGKGREKAGNVEVQGEN
g8619                         MIAVSVPSSDP---------------------LPPCPHSVQASANDGCAVPTKGKAKSVA
MtNFP_-_Medtr5g019040.1       ------------------------------------------------------------

                                       1450      1460      1470      1480      1490      1500
                              ....|....|....|....|....|....|....|....|....|....|....|....|
OsCERK1                       ------------------------------------------------------------
MtLYK3_-_Medtr5g086130.1      ------------------------------------------------------------
g49675                        ------------------------------------------------------------
g50598                        ------------------------------------------------------------
g44510                        ------------------------------------------------------------
g91196                        ------------------------------------------------------------
g30047                        ------------------------------------------------------------
g8984                         SDAAAGGEARGEIQEEKSSKLSKSNSSRSKRTARGSTSQSAHSKSKGGLRKTRGRHGKQE
g8619                         AFSKHGKEVKIGIGKPRKADIAAGSNKKPVHALAMTSSHRKGPRSRKVAGKKYENKRRGD
MtNFP_-_Medtr5g019040.1       ------------------------------------------------------------

                                       1510      1520      1530      1540      1550      1560
                              ....|....|....|....|....|....|....|....|....|....|....|....|
OsCERK1                       --------------------------KGLVFLFEEALSAPNPTEALDELIDPSL-QGDYP
MtLYK3_-_Medtr5g086130.1      --------------------------KGLVQLFEEALHRMDPLEGLRKLVDPRL-KENYP
g49675                        --------------------------PSLPAALVLLIKQMKSPKDVKAIADPRLSESGYP
g50598                        --------------------------PFLTEVMVPRIKDMKAPAQVCPIVDPQL-GSDYP
g44510                        --------------------------KTLASSVAPLIKQMTSAEEVSVIVDPQL-GIAYP
g91196                        --------------------------ATLASSVAPLIKQMTAAEDVSAIVDPRL-DIAYP
g30047                        --------------------------PFLTEVMCPLINEMTCPGHVAAIIDRQL-GNGYP
g8984                         KAVDFSSSLDVGASVGRSWPRGVVQRKSLAEWIVPAFKCLGSPIDIVNLVDPDL-RDQYP
g8619                         GVKLLGAATEGTSPILRNSAVQRMLRCSLVSWIVPAIRSLGSPADVVCLVDPDM-RGQYP
MtNFP_-_Medtr5g019040.1       --------------------------ILWKDFWKIFDLEGNREERLRKWMDPKL-ESFYP

                                       1570      1580      1590      1600      1610      1620
                              ....|....|....|....|....|....|....|....|....|....|....|....|
OsCERK1                       VDSALKIASLAKSCTHEEPGMRPTMRSVVVALMALTANTDLRDMDYHPF-----------
MtLYK3_-_Medtr5g086130.1      IDSVLKMAQLGRACTRDNPLLRPSMRSIVVALMTLSSPTEDCDDDSSYENQSLINLLSTR
g49675                        KEAALQLARLAVECVSDKPQKRPQMKRVVYVMEDILAMSRPRHQPSADT---------AD
g50598                        QDLALQIGRLAMQCVQHEPELRPQMRRVVYLLDEILADTRRRTHQPSSA-------PSSD
g44510                        RDLTFELARVAAQCVELEPEDRPNMRRIVYVLDETLETYLMRSLHADYE-------ISID
g91196                        TDLTLQLARLAAQCVELEPDDRPEMKRVVYVLDETLSLAISRVCSSNTDDKMLAVRIAQD
g30047                        QESALQVAKLAVQCVATDPDQRPKMKQVVYVLELVRNRSAASGR----------------
g8984                         IEGVIKMAEVAVRCVQENPEARPDMKRVAYELDELMLLTQRWESAGRTT-----------
g8619                         PEVVAKMADLAVRCVQENPQARPNMSRVAYELDEILLLTRRWEALQCKAQPENHSRVVVR
MtNFP_-_Medtr5g019040.1       IDNALSLASLAVNCTADKSLSRPTIAEIVLCLSLLNQPSSEPMLERSLT-------SGLD

                                       1630      1640      1650      1660
```

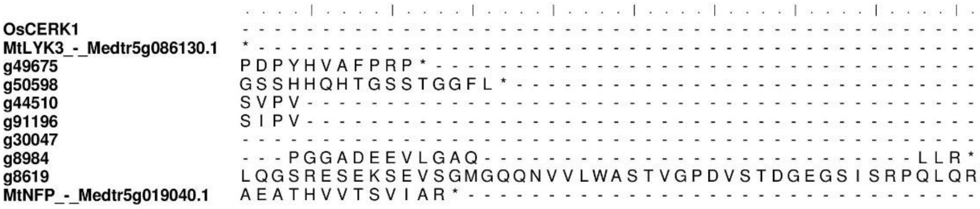

```
                          ....|....|....|....|....|....|....|....|....|.
OsCERK1                   ----------------------------------------------
MtLYK3_-_Medtr5g086130.1  *---------------------------------------------
g49675                    PDPYHVAFPRP*----------------------------------
g50598                    GSSHHQHTGSSTGGFL*-----------------------------
g44510                    SVPV------------------------------------------
g91196                    SIPV------------------------------------------
g30047                    ----------------------------------------------
g8984                     ---PGGADEEVLGAQ---------------------------LLR*
g8619                     LQGSRESEKSEVSGMGQQNVVLWASTVGPDVSTDGEGSISRPQLQR
MtNFP_-_Medtr5g019040.1   AEATHVVTSVIAR*--------------------------------
```

Data S1M: Alignment of the Chara LysM-RLK with representative LYK and LYR from angiosperms.

CXnC motif representative of the LysM domain are present in the predicted extracellular domain of the Chara LysM-RLK (Positions: 357/367; 429/431 and 527/529). The activation loop missing in LYR proteins such as Medicago NFP is present in the *C. braunii* sequences (Position 1123 – 1149).

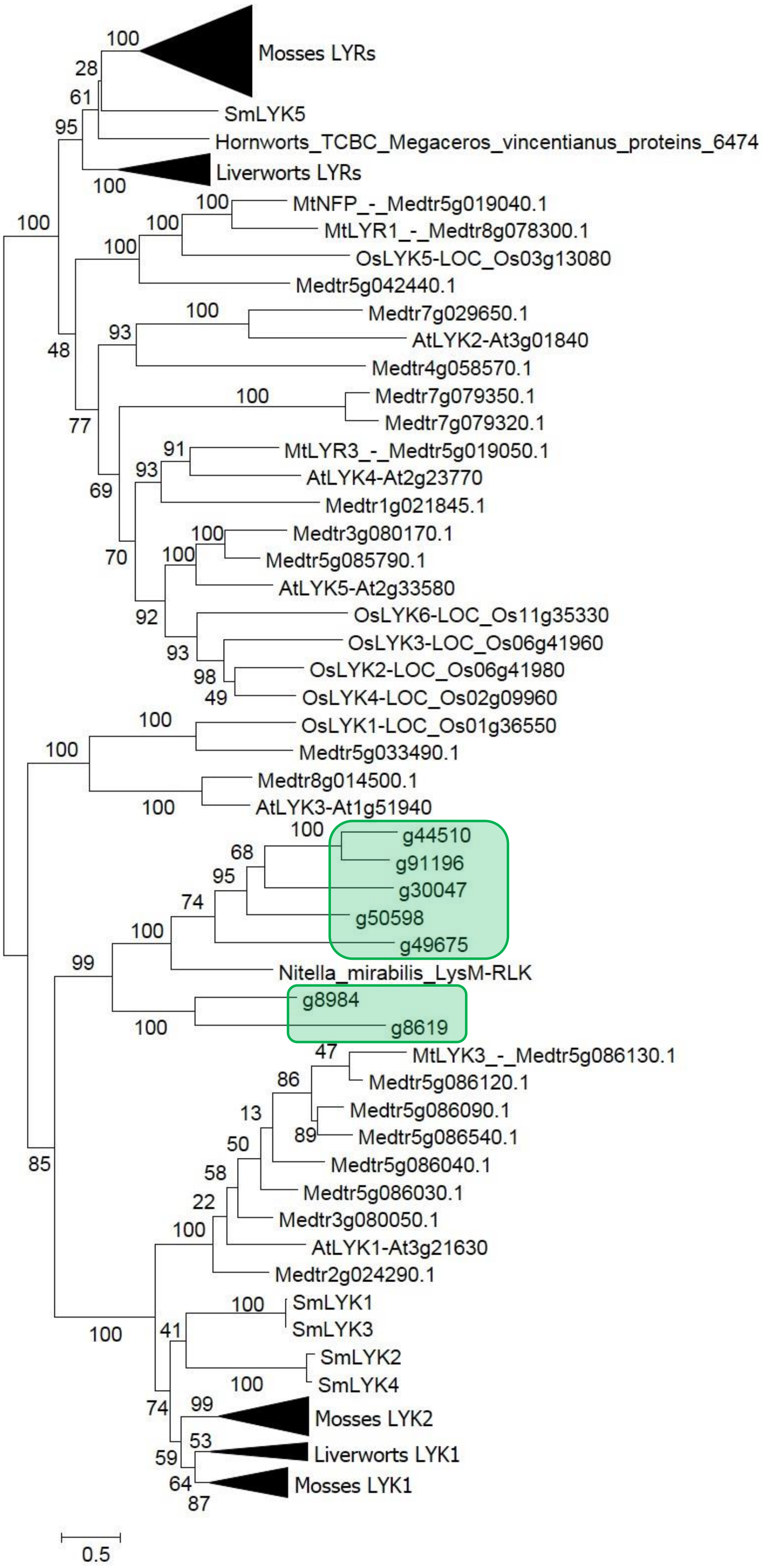

Data S1N: Midpoint-rooted Maximum Likelihood tree of the LysM-RLK family.

The Charales sequences form a single cluster, encompassing seven *C. braunii* sequences (green). For putative relationship to land plant genes see text and Fig. M13.

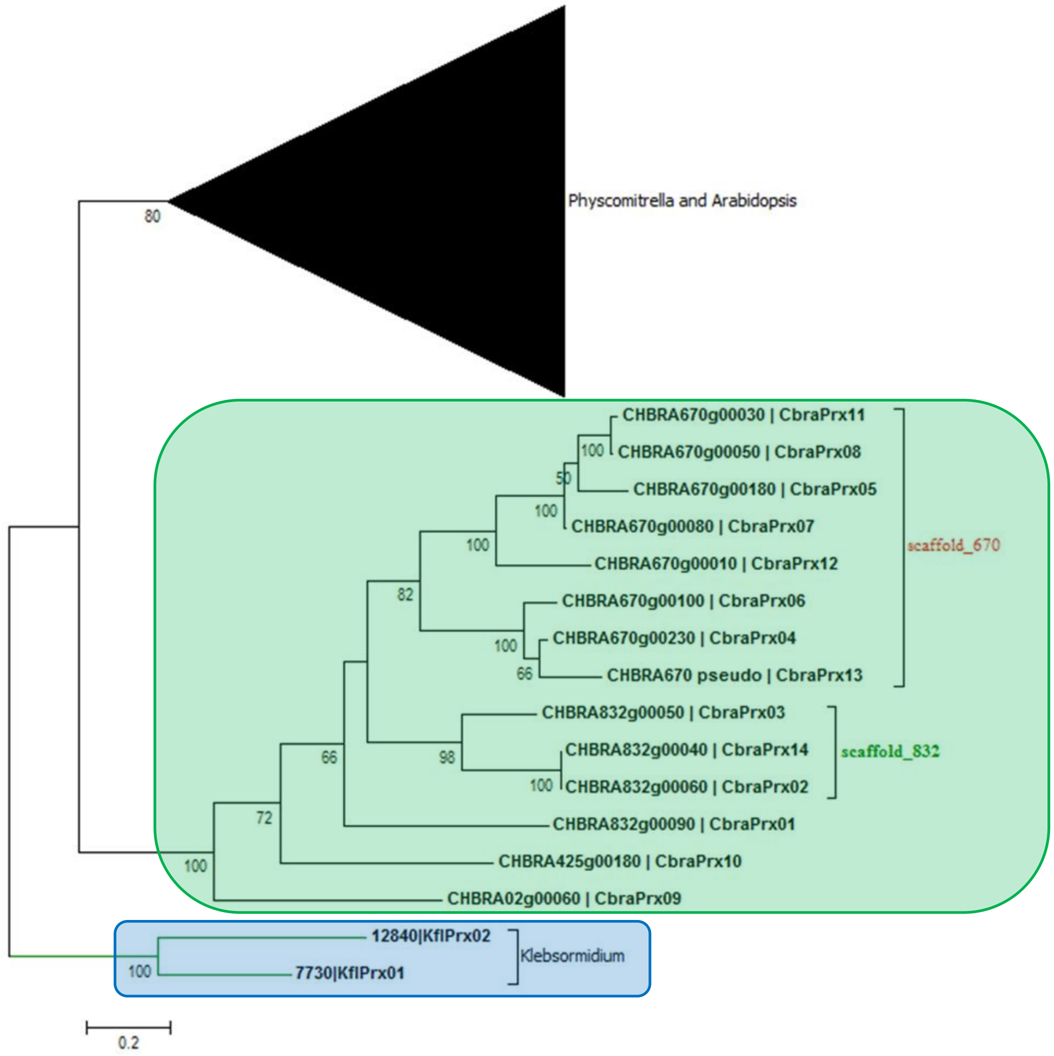
Physcomitrella and Arabidopsis
80
CHBRA670g00030 | CbraPrx11
100
CHBRA670g00050 | CbraPrx08
50
CHBRA670g00180 | CbraPrx05
100
CHBRA670g00080 | CbraPrx07
100
CHBRA670g00010 | CbraPrx12
scaffold_670
82
CHBRA670g00100 | CbraPrx06
100
CHBRA670g00230 | CbraPrx04
66
CHBRA670 pseudo | CbraPrx13
CHBRA832g00050 | CbraPrx03
66
98
CHBRA832g00040 | CbraPrx14
scaffold_832
100
CHBRA832g00060 | CbraPrx02
CHBRA832g00090 | CbraPrx01
72
CHBRA425g00180 | CbraPrx10
100
CHBRA02g00060 | CbraPrx09
12840|KflPrx02
Klebsormidium
100
7730|KflPrx01
0.2

Data S1O: Outgroup-rooted phylogenetic analysis of *C. braunii* class III peroxidases

The CIII Prx protein sequences from *K. nitens* (3 sequences), *C. braunii* (14 sequences), *P. patens* (57 sequences) and *A. thaliana* (73 sequences) as well as 2 APx sequences from *C. braunii* and *A. thaliana* (outgroup) were aligned using MAFFT and the tree constructed using Maximum Likelihood. Evolutionary analyses were conducted in MEGA7. All protein sequences are available using the CHBRA# or the CbraPrx# (http://peroxibase.toulouse.inra.fr). The collapsed triangle contains all *P. patens* and *A. thaliana* sequences, as well as one of the three *K. nitens* sequences. The other two *K. nitens* sequences are marked by a blue box, the *C. braunii* sequences by a green box.

LRR FBP	Modeled (%)	Confidence (%)	Multi-template and ab initio modeling		
			ab initio (# a.a.)	templates	i.d. (%)
CHABRA g10791_t1	87	>90	88	c3ogmB	17
				c2p1nE	18
				c3oglD	17
				c5hywA	18
CHABRA g11992_t1	79	>90	140	c3ogmB	21
				c2p1nE	21
				c3oglD	21
CHABRA g23992_t1	97	>90	253	c3ogmB	22
				c2p1nE	20
				c3oglD	22
				c5hywA	19
				c4lxrA	11
CHABRA g23719_t1	57	>90	528	c2p1nE	25
				c3ogmB	19
				c3oglD	19
				c5hywA	21

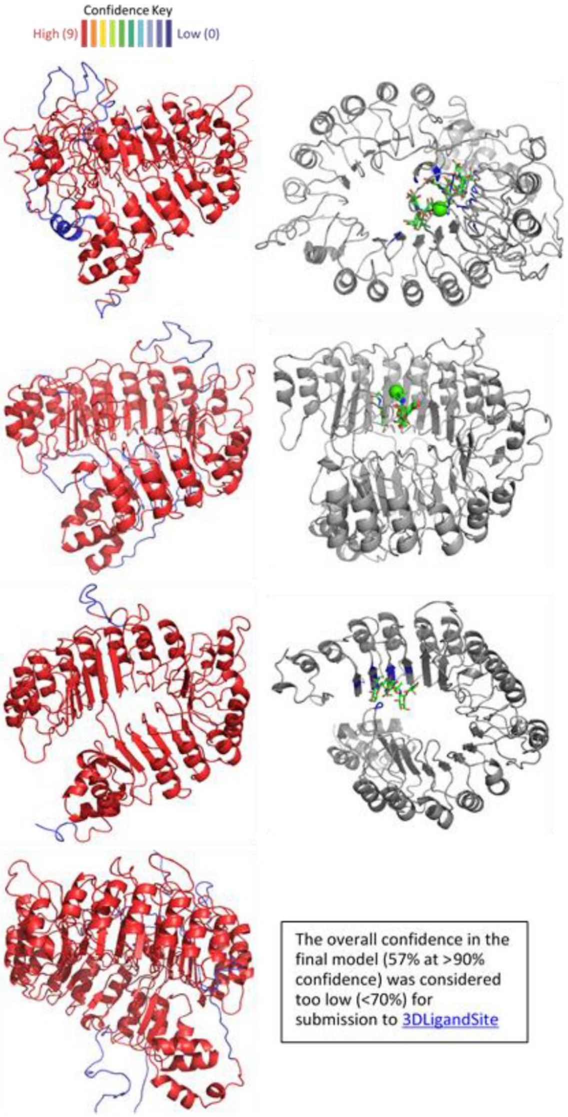

The overall confidence in the final model (57% at >90% confidence) was considered too low (<70%) for submission to 3DLigandSite

Data S1P: ***In silico*** **modeling of** ***C. braunii*** **LRR FBPs.**

Leucine-Rich-Repeat (LRR)-containing F-Box Proteins (FBPs) of *C. braunii* with sequence similarity to land plant LRR FBPs were *in silico* modeled using “intensive” modeling mode in Protein Homology/analogY Recognition Engine V 2.0 (Phyre2). The final models (color-coded by the confidence of the match to the templates overall) were submitted to 3DLigandSite server to predict potential binding sites (gray structures cartoon depiction). % i.d. percentage identity. See STAR Methods for details.

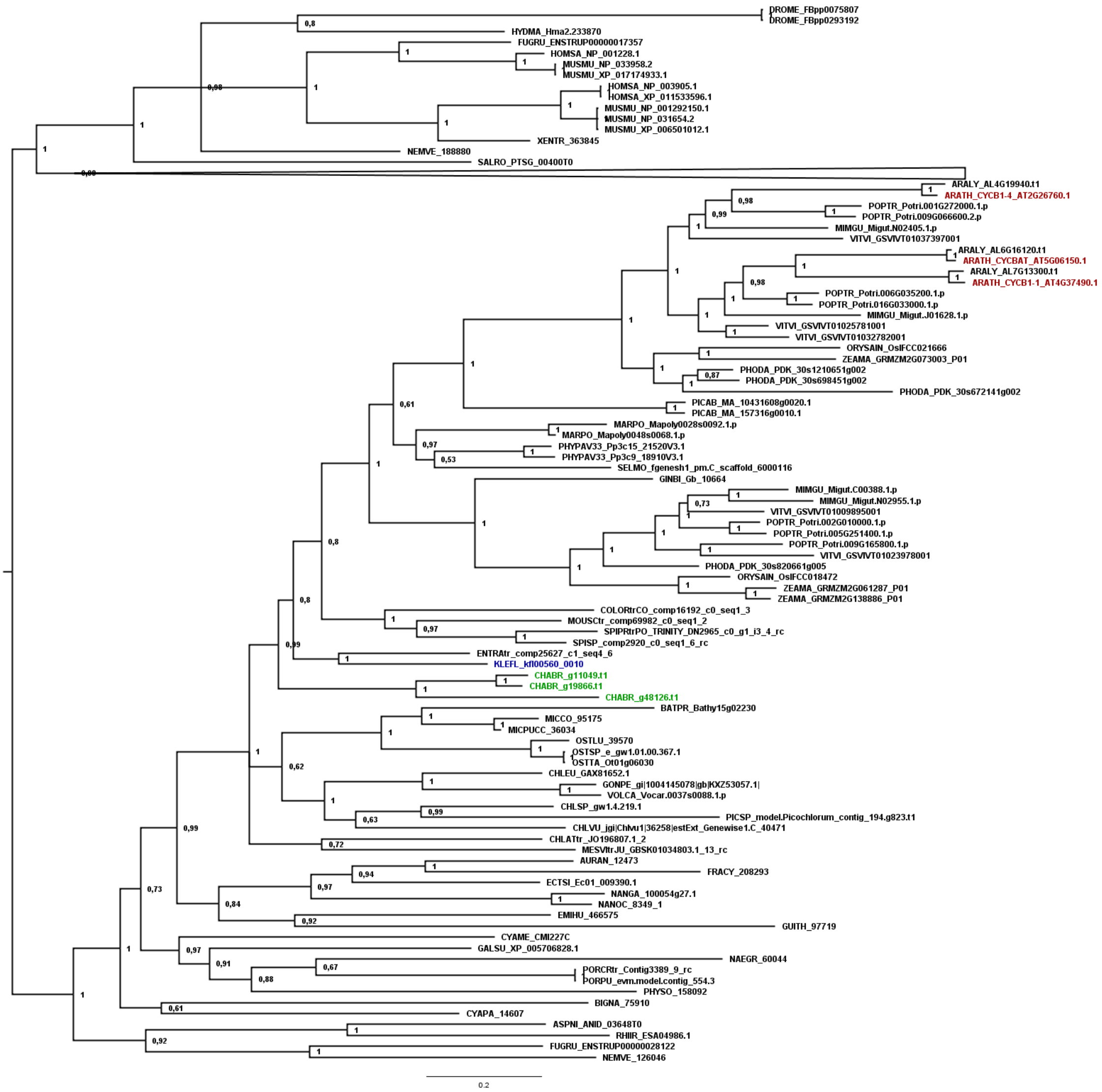

Data S1Q: Phylogenetic tree of cyclin proteins.

Midpoint-rooted Bayesian inference phylogenetic tree, numbers at the nodes are posterior probabilities. The *A. thaliana* CYCB sequences are shown in red, the *C. braunii* sequences belonging to that cluster in green, and the *K. nitens* sequence in blue. The clade containing the Archaeplastida CYCA sequences (one each of *C. braunii* and *K. nitens*) is collapsed.

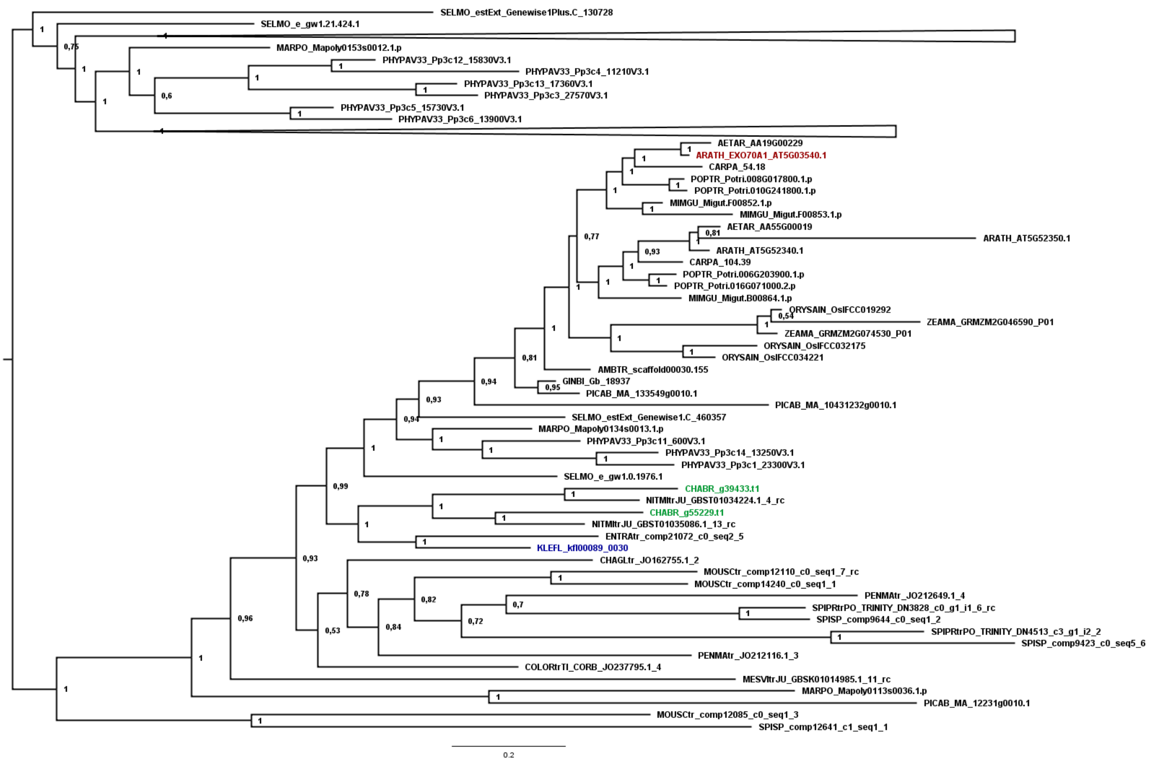

Data S1R: Phylogenetic tree of EXOCYST 70A proteins.

Midpoint-rooted Bayesian inference phylogenetic tree, numbers at the nodes are posterior probabilities. Two clades containing exclusively seed plant species are collapsed. The *A. thaliana* EXO70A sequence is shown in red, the *C. braunii* sequences belonging to that cluster in green, and the *K. nitens* sequence in blue.

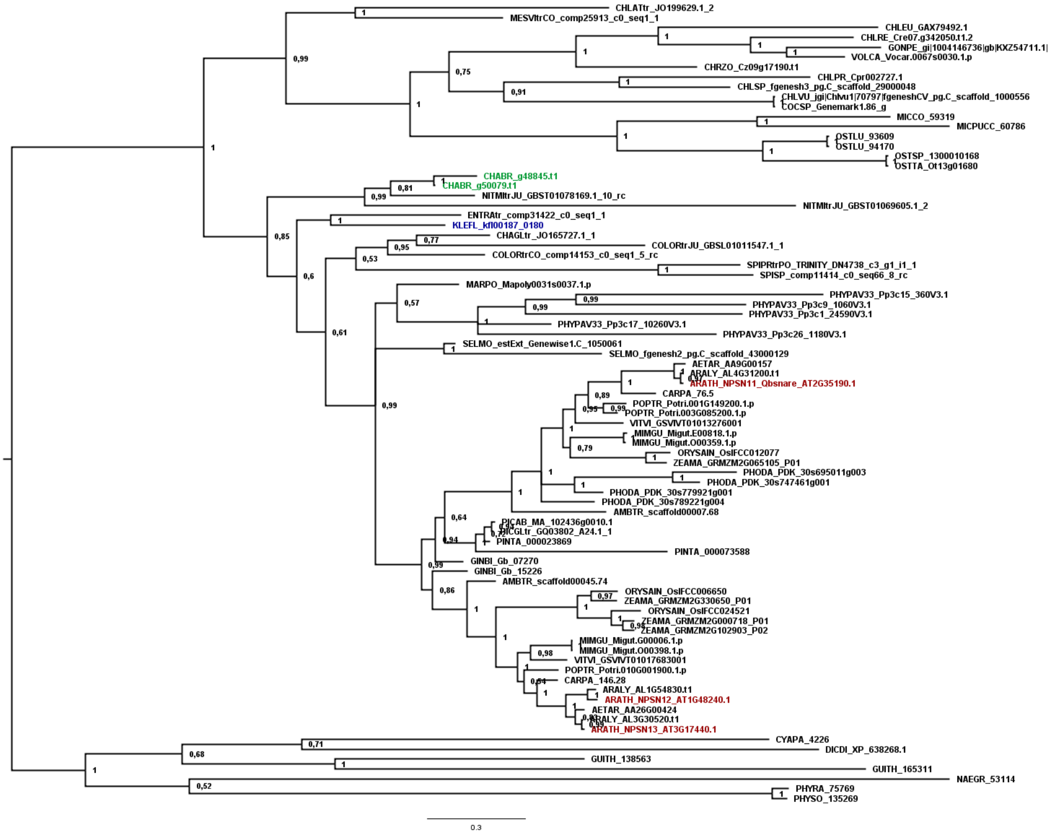

Data S1S: Phylogenetic tree of NPSN proteins.
Midpoint-rooted Bayesian inference phylogenetic tree, numbers at the nodes are posterior probabilities. The *A. thaliana* NPSN12/12/13 sequences are shown in red, the *C. braunii* sequences belonging to that cluster in green, and the *K. nitens* sequence in blue.

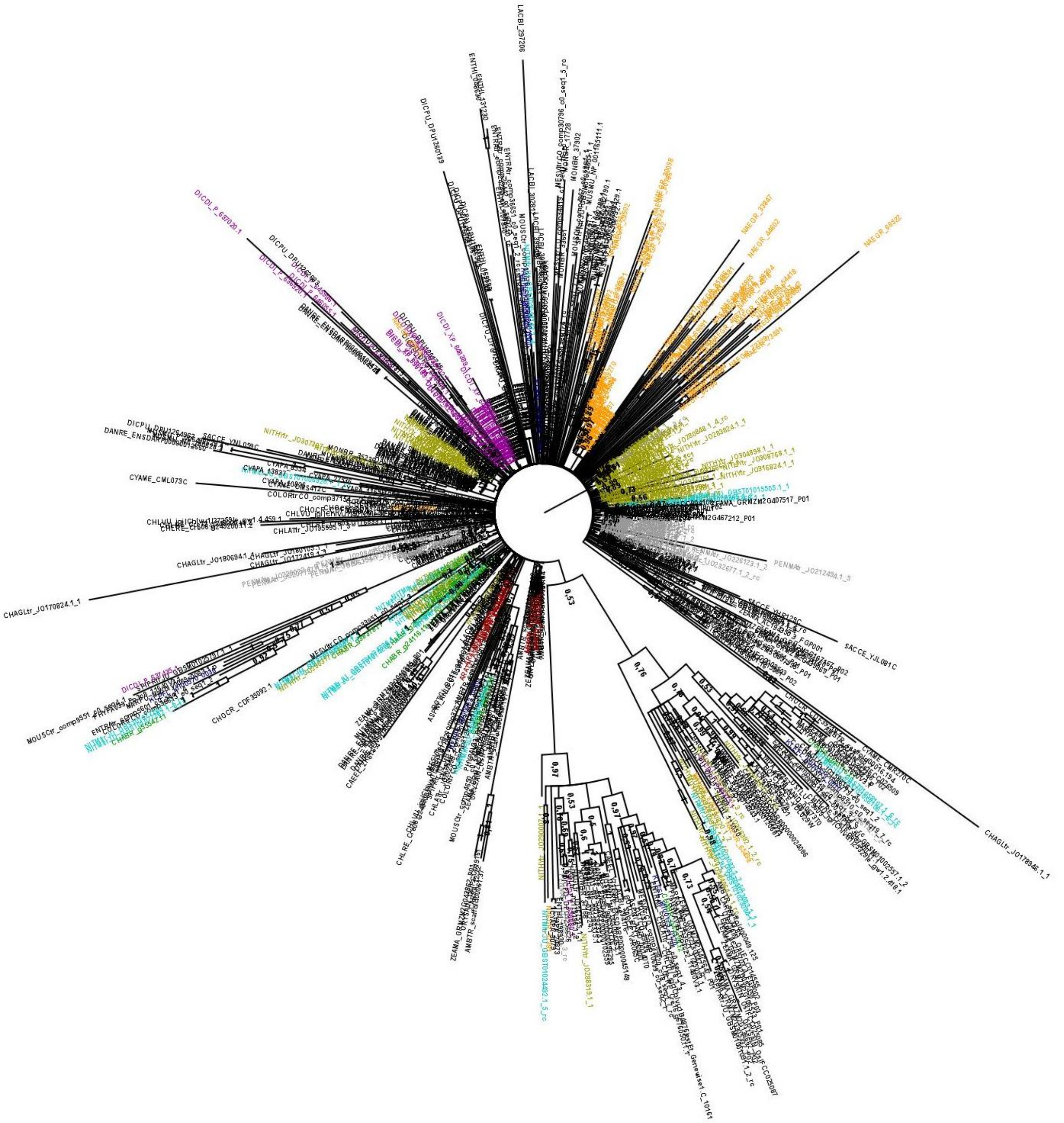

Data S1T: Phylogenetic overview tree of canonical actin proteins.

Midpoint-rooted Bayesian inference phylogenetic tree, numbers at the nodes are posterior probabilities. The *A. thaliana* actin sequences are shown in red, the *C. braunii* sequences in green, and the *K. nitens* sequences in blue. The sequences of *Naegleria gruberi* are shown in orange, those of *Dictyostelium discoideum* in purple. The transcriptomic sequences of *Nitella mirabilis* (cyan), *Nitella hyalina* (yellow) and *Penium margaritaceum* (grey) are also color-coded. See text for numbers of genes. See M21 for expanded tree.

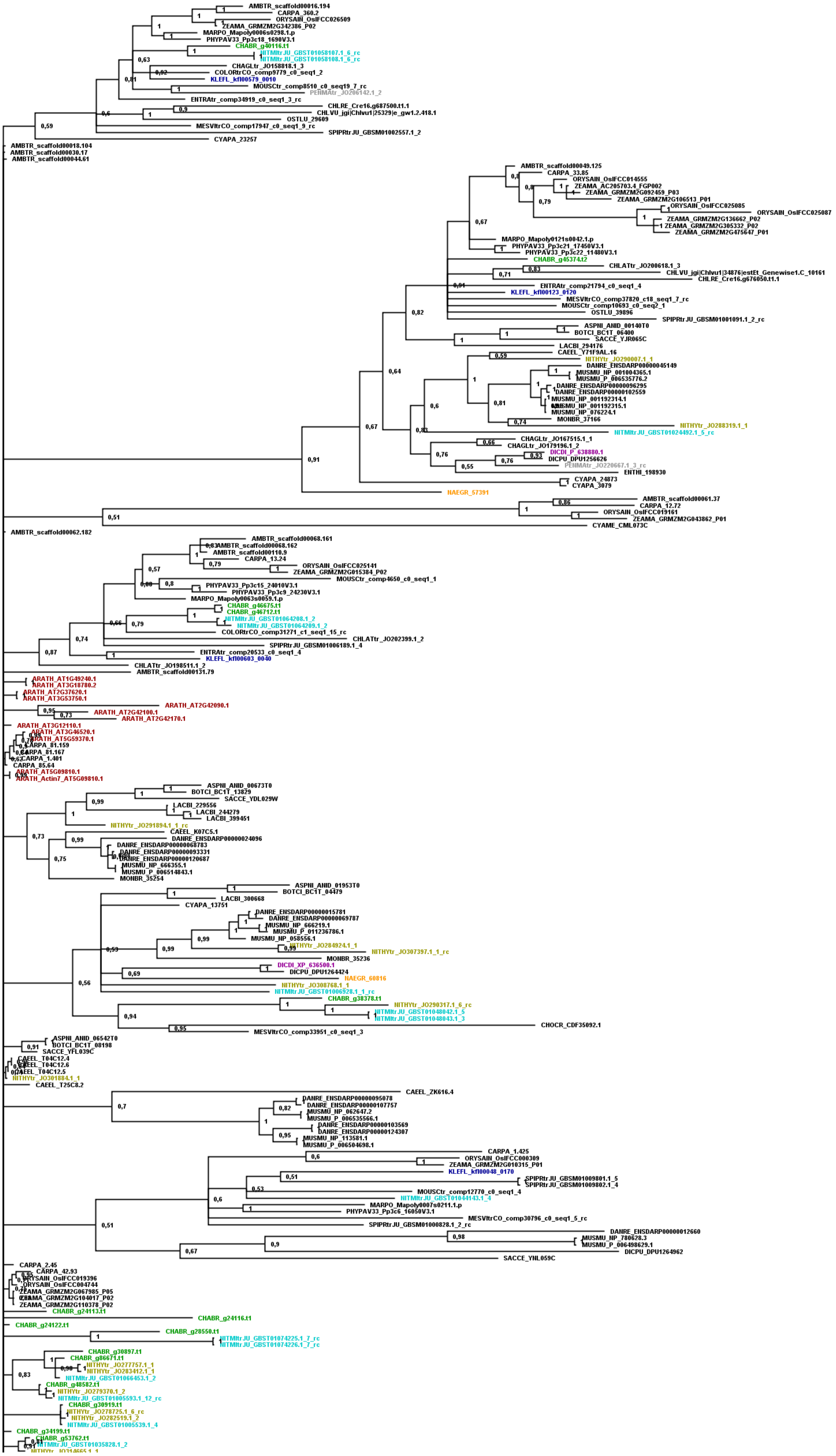

AMBTR_scaffold00016.194
CARPA_360.2
ORYSAIN_OsIFCC026509
ZEAMA_GRMZM2G342386_P02
MARPO_Mapoly0006s0298.1.p
PHYPAV33_Pp3c18_1690V3.1
CHABR_g40116.t1
NITMItrJU_GBST01058107.1_6_rc
NITMItrJU_GBST01058108.1_6_rc
CHAGLtr_JO158818.1_3
COLORtrCO_comp9779_c0_seq1_2
KLEFL_kfl00579_0010
MOUSCtr_comp8510_c0_seq19_7_rc
PENMAtr_JO206142.1_2
ENTRAtr_comp34919_c0_seq1_3_rc
CHLRE_Cre16.g687500.t1.1
CHLVU_jgi|Chlvu1|25329|e_gw1.2.418.1
OSTLU_29609
MESVItrCO_comp17947_c0_seq1_9_rc
SPIPRtrJU_GBSM01002557.1_2
CYAPA_23257
AMBTR_scaffold00018.104
AMBTR_scaffold00030.17
AMBTR_scaffold00044.61
AMBTR_scaffold00049.125
CARPA_33.85
ORYSAIN_OsIFCC014555
ZEAMA_AC205703.4_FGP002
ZEAMA_GRMZM2G092459_P03
ZEAMA_GRMZM2G106513_P01
ORYSAIN_OsIFCC025085
ORYSAIN_OsIFCC025087
ZEAMA_GRMZM2G136662_P02
ZEAMA_GRMZM2G305332_P02
ZEAMA_GRMZM2G475647_P01
MARPO_Mapoly0121s0042.1.p
PHYPAV33_Pp3c21_17450V3.1
PHYPAV33_Pp3c22_11480V3.1
CHABR_g45374.t2
CHLATtr_JO200618.1_3
CHLVU_jgi|Chlvu1|34876|estExt_Genewise1.C_10161
CHLRE_Cre16.g676050.t1.1
ENTRAtr_comp21794_c0_seq1_4
KLEFL_kfl00123_0120
MESVItrCO_comp37820_c18_seq1_7_rc
MOUSCtr_comp10693_c0_seq2_1
OSTLU_39896
SPIPRtrJU_GBSM01001091.1_2_rc
ASPNI_AND_00140T0
BOTCI_BC1T_06400
SACCE_YJR065C
LACBI_294176
CAEEL_Y71F9AL.16
NITHYtr_JO290007.1_1
DANRE_ENSDARP00000045149
MUSMU_NP_001004365.1
MUSMU_P_006535776.2
DANRE_ENSDARP00000096295
DANRE_ENSDARP00000102559
MUSMU_NP_001192314.1
MUSMU_NP_001192315.1
MUSMU_NP_076224.1
MONBR_37166
NITHYtr_JO288319.1_1
NITMItrJU_GBST01024492.1_5_rc
CHAGLtr_JO167515.1_1
CHAGLtr_JO179196.1_2
DICDI_P_638880.1
DICPU_DPU1256626
PENMAtr_JO220667.1_3_rc
ENTHI_198930
CYAPA_24873
CYAPA_3079
NAEGR_57391
AMBTR_scaffold00061.37
CARPA_12.72
ORYSAIN_OsIFCC019161
ZEAMA_GRMZM2G043862_P01
CYAME_CML073C
AMBTR_scaffold00062.182
AMBTR_scaffold00068.161
AMBTR_scaffold00068.162
AMBTR_scaffold00110.9
CARPA_13.24
ORYSAIN_OsIFCC025141
ZEAMA_GRMZM2G015384_P02
MOUSCtr_comp4650_c0_seq1_1
PHYPAV33_Pp3c15_24010V3.1
PHYPAV33_Pp3c9_24230V3.1
MARPO_Mapoly0063s0059.1.p
CHABR_g46675.t1
CHABR_g46712.t1
NITMItrJU_GBST01064208.1_2
NITMItrJU_GBST01064209.1_2
COLORtrCO_comp31271_c1_seq1_15_rc
CHLATtr_JO202399.1_2
SPIPRtrJU_GBSM01006189.1_4
ENTRAtr_comp20533_c0_seq1_4
KLEFL_kfl00603_0040
CHLATtr_JO198511.1_2
AMBTR_scaffold00131.79
ARATH_AT1G49240.1
ARATH_AT3G18780.2
ARATH_AT2G37620.1
ARATH_AT3G53750.1
ARATH_AT2G42090.1
ARATH_AT2G42100.1
ARATH_AT2G42170.1
ARATH_AT3G12110.1
ARATH_AT3G46520.1
ARATH_AT5G59370.1
CARPA_81.159
CARPA_81.167
CARPA_1.401
CARPA_85.64
ARATH_AT5G09810.1
ARATH_Actin7_AT5G09810.1
ASPNI_AND_00673T0
BOTCI_BC1T_13829
SACCE_YDL029W
LACBI_229556
LACBI_244279
LACBI_399451
NITHYtr_JO291894.1_1_rc
CAEEL_K07C5.1
DANRE_ENSDARP00000024096
DANRE_ENSDARP00000068783
DANRE_ENSDARP00000093331
DANRE_ENSDARP00000120687
MUSMU_NP_666355.1
MUSMU_P_006514843.1
MONBR_35254
ASPNI_AND_01953T0
BOTCI_BC1T_04479
LACBI_300668
CYAPA_13751
DANRE_ENSDARP00000015781
DANRE_ENSDARP00000069787
MUSMU_NP_666219.1
MUSMU_P_011236786.1
MUSMU_NP_058556.1
NITHYtr_JO284924.1_1
NITHYtr_JO307397.1_1_rc
MONBR_35236
DICDI_XP_636500.1
DICPU_DPU1264424
NAEGR_60816
NITHYtr_JO308768.1_1
NITMItrJU_GBST01006928.1_1_rc
CHABR_g38378.t1
NITHYtr_JO290317.1_6_rc
NITMItrJU_GBST01048042.1_5
NITMItrJU_GBST01048043.1_3
CHOCR_CDF35092.1
MESVItrCO_comp33951_c0_seq1_3
ASPNI_AND_06542T0
BOTCI_BC1T_08198
SACCE_YFL039C
CAEEL_T04C12.4
CAEEL_T04C12.6
CAEEL_T04C12.5
NITHYtr_JO301884.1_1
CAEEL_T25C8.2
CAEEL_ZK616.4
DANRE_ENSDARP00000095078
DANRE_ENSDARP00000107757
MUSMU_NP_062647.2
MUSMU_P_006535566.1
DANRE_ENSDARP00000103569
DANRE_ENSDARP00000124307
MUSMU_NP_113581.1
MUSMU_P_006504698.1
CARPA_1.425
ORYSAIN_OsIFCC000309
ZEAMA_GRMZM2G010315_P01
KLEFL_kfl00048_0170
SPIPRtrJU_GBSM01009801.1_5
SPIPRtrJU_GBSM01009802.1_4
MOUSCtr_comp12770_c0_seq1_4
NITMItrJU_GBST01044143.1_4
MARPO_Mapoly0007s0211.1.p
PHYPAV33_Pp3c6_16050V3.1
MESVItrCO_comp30796_c0_seq1_5_rc
SPIPRtrJU_GBSM01000828.1_2_rc
DANRE_ENSDARP00000012660
MUSMU_NP_780628.3
MUSMU_P_006498629.1
DICPU_DPU1264962
SACCE_YNL059C
CARPA_2.45
CARPA_42.93
ORYSAIN_OsIFCC019396
ORYSAIN_OsIFCC004744
ZEAMA_GRMZM2G067985_P05
ZEAMA_GRMZM2G104017_P02
ZEAMA_GRMZM2G110378_P02
CHABR_g24113.t1
CHABR_g24116.t1
CHABR_g24122.t1
CHABR_g28550.t1
NITMItrJU_GBST01074225.1_7_rc
NITMItrJU_GBST01074226.1_7_rc
CHABR_g30897.t1
CHABR_g86671.t1
NITHYtr_JO277757.1_1
NITHYtr_JO283412.1_1
NITMItrJU_GBST01066453.1_2
CHABR_g48582.t1
NITHYtr_JO279370.1_2
NITMItrJU_GBST01005593.1_12_rc
CHABR_g30919.t1
NITHYtr_JO278725.1_6_rc
NITHYtr_JO282519.1_2
NITMItrJU_GBST01005539.1_4
CHABR_g34199.t1
CHABR_g53762.t1
NITMItrJU_GBST01035828.1_2
NITHYtr_JO314665.1_1

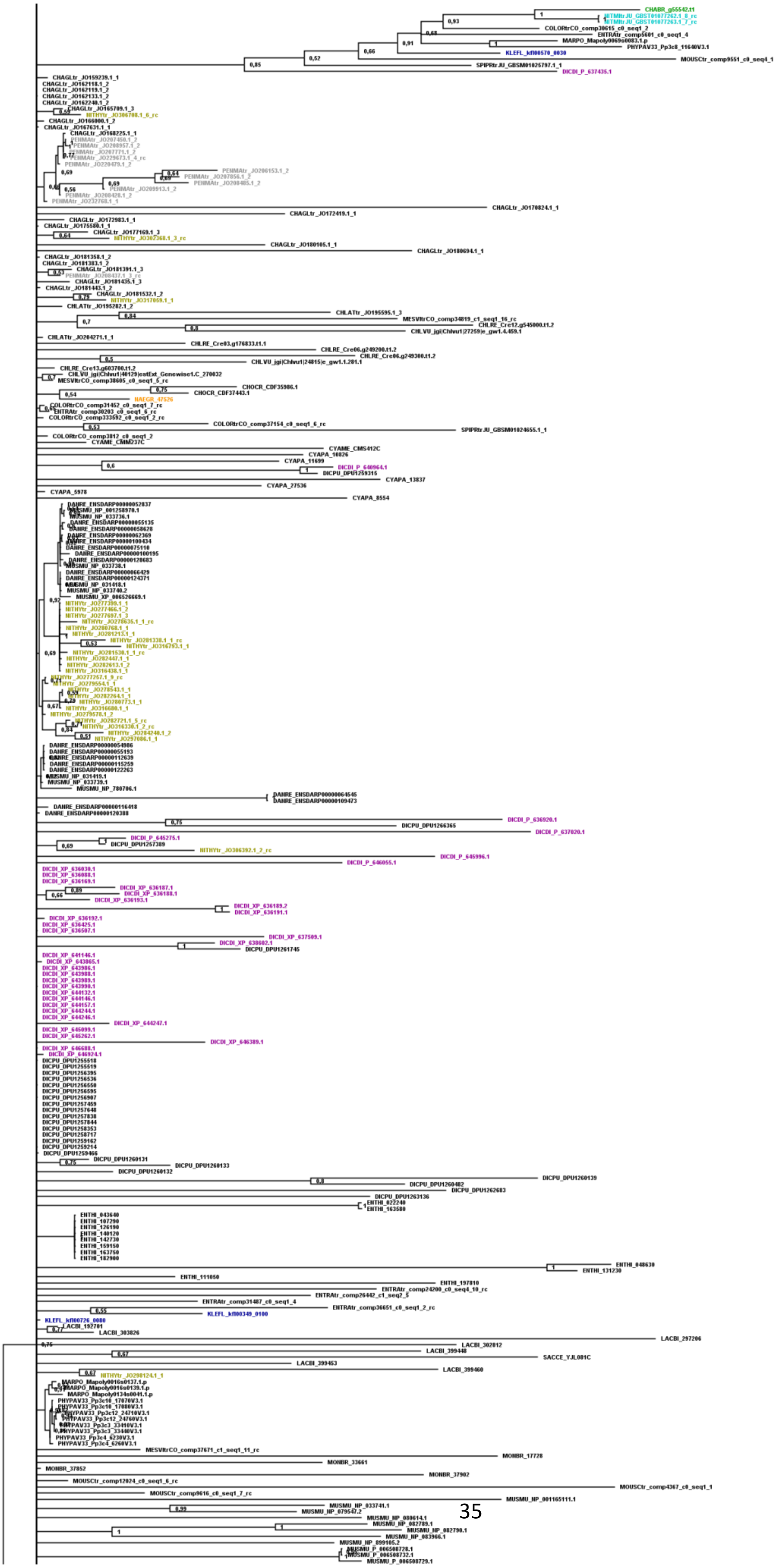
CHABR_g55542.t1
NITMltr.JU_GBST01077262.1_8_rc
NITMltr.JU_GBST01077263.1_7_rc
COLORtrCO_comp38615_c0_seq1_2
ENTRAtr_comp5601_c0_seq1_4
MARPO_Mapoly0069s0083.1.p
PHYPAV33_Pp3c8_11640V3.1
KLEFL_kfl00570_0030
MOUSCtr_comp9551_c0_seq4_1
SPIPRtr.JU_GBSM01025797.1_1
DICDI_P_637435.1
0,93
0,68
0,91
0,66
0,52
0,85
1
CHAGLtr_JO159239.1_1
CHAGLtr_JO162118.1_2
CHAGLtr_JO162119.1_2
CHAGLtr_JO162133.1_2
CHAGLtr_JO162240.1_2
CHAGLtr_JO165709.1_3
NITHYtr_JO306708.1_6_rc
CHAGLtr_JO166008.1_2
CHAGLtr_JO167631.1_1
CHAGLtr_JO168225.1_1
PENMAtr_JO207458.1_2
PENMAtr_JO208957.1_2
PENMAtr_JO207771.1_2
PENMAtr_JO229673.1_4_rc
PENMAtr_JO220479.1_2
PENMAtr_JO206153.1_2
PENMAtr_JO207856.1_2
PENMAtr_JO208485.1_2
PENMAtr_JO209913.1_2
PENMAtr_JO208428.1_2
PENMAtr_JO232768.1_1
0,64
0,69
0,56
0,69
CHAGLtr_JO170824.1_1
CHAGLtr_JO172419.1_1
CHAGLtr_JO172983.1_1
CHAGLtr_JO175580.1_1
CHAGLtr_JO177169.1_3
NITHYtr_JO302368.1_3_rc
0,64
CHAGLtr_JO180185.1_1
CHAGLtr_JO180694.1_1
CHAGLtr_JO181358.1_2
CHAGLtr_JO181383.1_2
CHAGLtr_JO181391.1_3
PENMAtr_JO208437.1_3_rc
0,53
CHAGLtr_JO181435.1_3
CHAGLtr_JO181443.1_2
CHAGLtr_JO181532.1_2
NITHYtr_JO317059.1_1
0,79
CHLATtr_JO195282.1_2
CHLATtr_JO195595.1_3
MESVItrCO_comp34819_c1_seq1_16_rc
CHLRE_Cre12.g545000.t1.2
CHLVU_jgi|Chlvu1|27259|e_gw1.4.459.1
0,84
0,7
0,8
CHLATtr_JO204271.1_1
CHLRE_Cre03.g176833.t1.1
CHLRE_Cre06.g249200.t1.2
CHLRE_Cre06.g249300.t1.2
CHLVU_jgi|Chlvu1|24815|e_gw1.1.281.1
0,5
CHLRE_Cre13.g603700.t1.2
CHLVU_jgi|Chlvu1|40129|estExt_Genewise1C_270032
MESVItrCO_comp38605_c0_seq1_5_rc
0,7
CHOCR_CDF35986.1
CHOCR_CDF37443.1
0,75
0,54
NAEGR_47526
COLORtrCO_comp31452_c0_seq1_7_rc
ENTRAtr_comp30203_c0_seq1_6_rc
COLORtrCO_comp333592_c0_seq1_2_rc
COLORtrCO_comp37154_c0_seq1_6_rc
0,53
SPIPRtr.JU_GBSM01024655.1_1
COLORtrCO_comp3812_c0_seq1_2
CYAME_CMM237C
CYAME_CMS412C
CYAPA_10826
CYAPA_11699
DICDI_P_640964.1
DICPU_DPU1259315
0,6
1
CYAPA_13837
CYAPA_27536
CYAPA_5978
CYAPA_8554
DANRE_ENSDARP00000052837
MUSMU_NP_001258970.1
MUSMU_NP_033736.1
DANRE_ENSDARP00000055135
DANRE_ENSDARP00000058628
DANRE_ENSDARP00000062369
DANRE_ENSDARP00000100434
DANRE_ENSDARP00000075110
DANRE_ENSDARP00000100195
DANRE_ENSDARP00000128683
MUSMU_NP_033738.1
DANRE_ENSDARP00000066429
DANRE_ENSDARP00000124371
MUSMU_NP_031418.1
MUSMU_NP_033740.2
MUSMU_XP_006526669.1
0,92
NITHYtr_JO277399.1_1
NITHYtr_JO277466.1_2
NITHYtr_JO277697.1_3
NITHYtr_JO278635.1_1_rc
NITHYtr_JO280768.1_1
NITHYtr_JO281213.1_1
NITHYtr_JO281338.1_1_rc
NITHYtr_JO316793.1_1
0,53
NITHYtr_JO281530.1_1_rc
NITHYtr_JO282447.1_1
NITHYtr_JO282613.1_2
NITHYtr_JO316438.1_1
0,69
NITHYtr_JO277257.1_9_rc
NITHYtr_JO279554.1_1
NITHYtr_JO278543.1_1
NITHYtr_JO282264.1_1
NITHYtr_JO280773.1_1
NITHYtr_JO316680.1_1
0,67
NITHYtr_JO279578.1_2
NITHYtr_JO282721.1_5_rc
NITHYtr_JO316330.1_2_rc
NITHYtr_JO284240.1_2
NITHYtr_JO297086.1_1
0,84
0,51
DANRE_ENSDARP00000054986
DANRE_ENSDARP00000055193
DANRE_ENSDARP00000112639
DANRE_ENSDARP00000115259
DANRE_ENSDARP00000122263
MUSMU_NP_031419.1
MUSMU_NP_033739.1
MUSMU_NP_780706.1
DANRE_ENSDARP00000064545
DANRE_ENSDARP00000109473
1
DANRE_ENSDARP00000116418
DANRE_ENSDARP00000120388
DICDI_P_636920.1
DICPU_DPU1266365
0,75
DICDI_P_637020.1
DICDI_P_645275.1
DICPU_DPU1257389
0,69
NITHYtr_JO306392.1_2_rc
DICDI_P_645996.1
DICDI_P_646055.1
DICDI_XP_636030.1
DICDI_XP_636088.1
DICDI_XP_636169.1
DICDI_XP_636187.1
DICDI_XP_636188.1
0,89
0,66
DICDI_XP_636193.1
DICDI_XP_636189.2
DICDI_XP_636191.1
1
DICDI_XP_636192.1
DICDI_XP_636425.1
DICDI_XP_636507.1
DICDI_XP_637509.1
DICDI_XP_638602.1
DICPU_DPU1261745
1
DICDI_XP_641146.1
DICDI_XP_643865.1
DICDI_XP_643986.1
DICDI_XP_643988.1
DICDI_XP_643989.1
DICDI_XP_643990.1
DICDI_XP_644132.1
DICDI_XP_644146.1
DICDI_XP_644157.1
DICDI_XP_644244.1
DICDI_XP_644246.1
DICDI_XP_644247.1
DICDI_XP_645099.1
DICDI_XP_645262.1
DICDI_XP_646389.1
DICDI_XP_646688.1
DICDI_XP_646924.1
DICPU_DPU1255518
DICPU_DPU1255519
DICPU_DPU1256395
DICPU_DPU1256536
DICPU_DPU1256550
DICPU_DPU1256595
DICPU_DPU1256907
DICPU_DPU1257459
DICPU_DPU1257648
DICPU_DPU1257838
DICPU_DPU1257844
DICPU_DPU1258353
DICPU_DPU1258717
DICPU_DPU1259162
DICPU_DPU1259214
DICPU_DPU1259466
DICPU_DPU1260131
DICPU_DPU1260133
0,75
DICPU_DPU1260132
DICPU_DPU1260139
DICPU_DPU1260482
DICPU_DPU1262683
0,8
DICPU_DPU1263136
ENTHI_022240
ENTHI_163580
1
ENTHI_043640
ENTHI_107290
ENTHI_126190
ENTHI_140120
ENTHI_142730
ENTHI_159150
ENTHI_163750
ENTHI_182900
ENTHI_048630
ENTHI_131230
1
ENTHI_111050
ENTHI_197810
ENTRAtr_comp24200_c0_seq4_10_rc
ENTRAtr_comp26442_c1_seq2_5
ENTRAtr_comp31487_c0_seq1_4
ENTRAtr_comp36651_c0_seq1_2_rc
0,55
KLEFL_kfl00349_0100
KLEFL_kfl00726_0080
LACBI_192701
LACBI_303826
0,7
LACBI_297206
0,75
LACBI_302812
LACBI_399448
0,67
SACCE_YJL081C
LACBI_399453
LACBI_399460
0,67
NITHYtr_JO298124.1_1
MARPO_Mapoly0016s0137.1.p
MARPO_Mapoly0016s0139.1.p
MARPO_Mapoly0134s0041.1.p
PHYPAV33_Pp3c10_17070V3.1
PHYPAV33_Pp3c10_17080V3.1
PHYPAV33_Pp3c12_24710V3.1
PHYPAV33_Pp3c12_24760V3.1
PHYPAV33_Pp3c3_33410V3.1
PHYPAV33_Pp3c3_33440V3.1
PHYPAV33_Pp3c4_6230V3.1
PHYPAV33_Pp3c4_6260V3.1
MESVItrCO_comp37671_c1_seq1_11_rc
MONBR_17728
MONBR_33661
MONBR_37852
MONBR_37902
MOUSCtr_comp12024_c0_seq1_6_rc
MOUSCtr_comp4367_c0_seq1_1
MOUSCtr_comp9616_c0_seq1_7_rc
MUSMU_NP_001165111.1
MUSMU_NP_033741.1
MUSMU_NP_079547.2
0,99
MUSMU_NP_080614.1
MUSMU_NP_082789.1
MUSMU_NP_082790.1
MUSMU_NP_083966.1
1
1
MUSMU_NP_899105.2
MUSMU_P_006508728.1
MUSMU_P_006508732.1
MUSMU_P_006508729.1

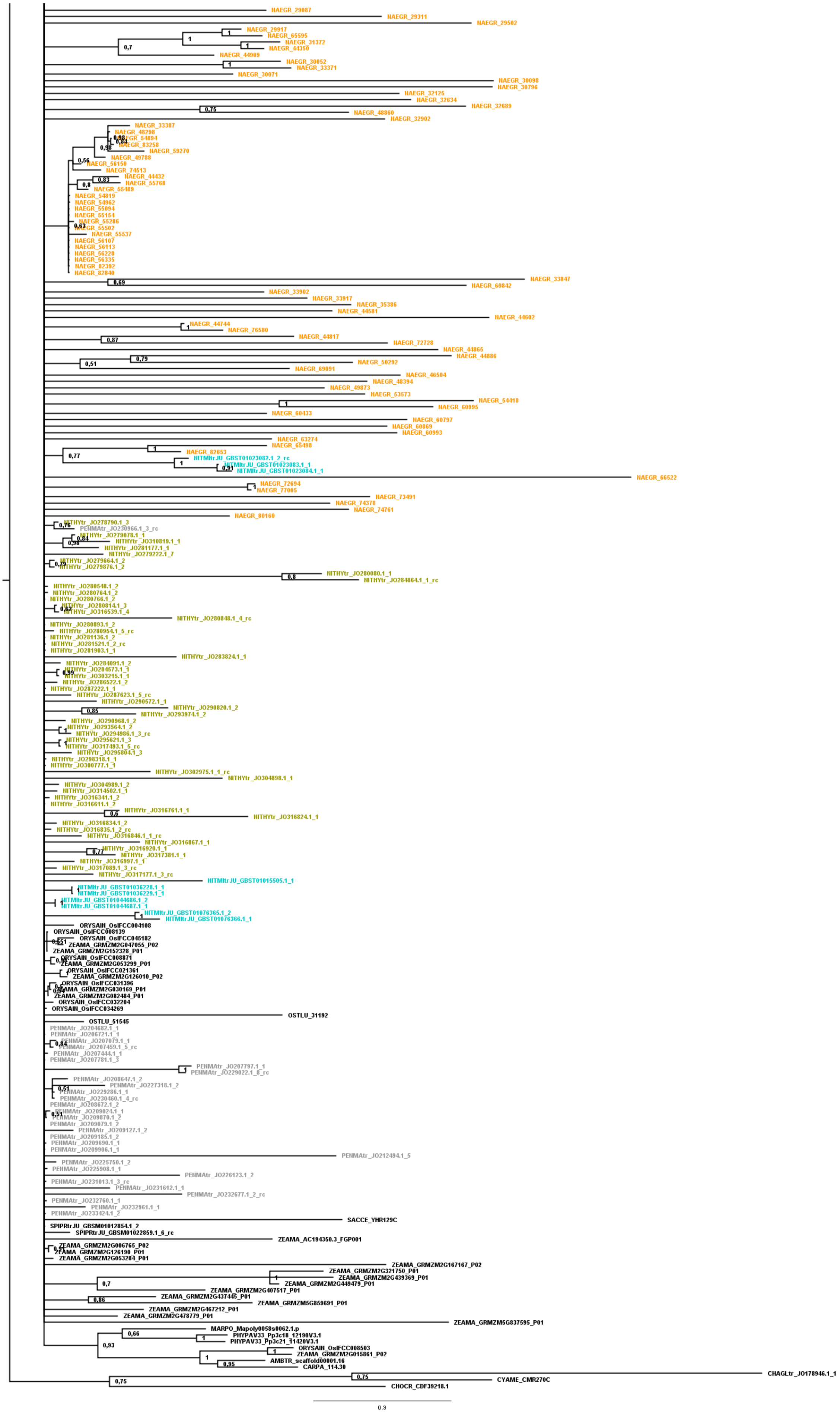
NAEGR_29087
NAEGR_29311
NAEGR_29502
NAEGR_29917
1
NAEGR_65595
1
NAEGR_31372
1
NAEGR_44350
0,7
NAEGR_44909
NAEGR_30052
1
NAEGR_33371
NAEGR_30071
NAEGR_30098
NAEGR_30796
NAEGR_32125
NAEGR_32634
NAEGR_32689
0,75
NAEGR_48860
NAEGR_32902
NAEGR_33387
NAEGR_48298
0,98
NAEGR_54894
0,84
NAEGR_83258
0,98
NAEGR_59270
NAEGR_49788
0,56
NAEGR_56150
NAEGR_74513
NAEGR_44432
0,83
NAEGR_55768
0,8
NAEGR_55489
NAEGR_54819
NAEGR_54962
NAEGR_55094
NAEGR_55154
NAEGR_55286
0,63
NAEGR_55502
NAEGR_55537
NAEGR_56107
NAEGR_56113
NAEGR_56228
NAEGR_56335
NAEGR_82392
NAEGR_82840
NAEGR_33847
0,69
NAEGR_60842
NAEGR_33902
NAEGR_33917
NAEGR_35386
NAEGR_44581
NAEGR_44602
NAEGR_44744
1
NAEGR_76580
NAEGR_44817
0,87
NAEGR_72728
NAEGR_44865
NAEGR_44886
0,79
NAEGR_50292
0,51
NAEGR_69091
NAEGR_46504
NAEGR_48394
NAEGR_49873
NAEGR_53573
NAEGR_54418
1
NAEGR_60995
NAEGR_60433
NAEGR_60797
NAEGR_60869
NAEGR_60993
NAEGR_63274
NAEGR_65498
1
NAEGR_82653
0,77
NITMItrJU_GBST01023082.1_2_rc
1
NITMItrJU_GBST01023083.1_1
0,91
NITMItrJU_GBST01023084.1_1
NAEGR_66522
NAEGR_72694
1
NAEGR_77005
NAEGR_73491
NAEGR_74378
NAEGR_74761
NAEGR_80160
NITHYtr_JO278790.1_3
0,76
PENMAtr_JO230966.1_3_rc
NITHYtr_JO279078.1_1
0,84
NITHYtr_JO310819.1_1
0,98
NITHYtr_JO281177.1_1
NITHYtr_JO279222.1_7
NITHYtr_JO279664.1_2
0,79
NITHYtr_JO279876.1_2
NITHYtr_JO280080.1_1
0,8
NITHYtr_JO284864.1_1_rc
NITHYtr_JO280548.1_2
NITHYtr_JO280764.1_2
NITHYtr_JO280766.1_2
NITHYtr_JO280814.1_3
0,62
NITHYtr_JO316539.1_4
NITHYtr_JO280848.1_4_rc
NITHYtr_JO280893.1_2
NITHYtr_JO280954.1_5_rc
NITHYtr_JO281136.1_2
NITHYtr_JO281521.1_2_rc
NITHYtr_JO281903.1_1
NITHYtr_JO283824.1_1
NITHYtr_JO284091.1_2
NITHYtr_JO284573.1_1
0,99
NITHYtr_JO303215.1_1
NITHYtr_JO286522.1_2
NITHYtr_JO287222.1_1
NITHYtr_JO287623.1_5_rc
NITHYtr_JO290572.1_1
NITHYtr_JO290820.1_2
0,85
NITHYtr_JO293974.1_2
NITHYtr_JO290968.1_2
NITHYtr_JO293564.1_2
1
NITHYtr_JO294986.1_3_rc
NITHYtr_JO295621.1_3
1
NITHYtr_JO317493.1_5_rc
NITHYtr_JO295804.1_3
NITHYtr_JO298318.1_1
NITHYtr_JO300777.1_1
NITHYtr_JO302975.1_1_rc
NITHYtr_JO304898.1_1
NITHYtr_JO304989.1_2
NITHYtr_JO314502.1_1
NITHYtr_JO316341.1_2
NITHYtr_JO316611.1_2
NITHYtr_JO316761.1_1
0,6
NITHYtr_JO316824.1_1
NITHYtr_JO316834.1_2
NITHYtr_JO316835.1_2_rc
NITHYtr_JO316846.1_1_rc
NITHYtr_JO316867.1_1
NITHYtr_JO316920.1_1
0,77
NITHYtr_JO317381.1_1
NITHYtr_JO316997.1_1
NITHYtr_JO317089.1_3_rc
NITHYtr_JO317177.1_3_rc
NITMItrJU_GBST01015505.1_1
NITMItrJU_GBST01036228.1_1
1
NITMItrJU_GBST01036229.1_1
NITMItrJU_GBST01044686.1_2
1
NITMItrJU_GBST01044687.1_1
NITMItrJU_GBST01076365.1_2
1
NITMItrJU_GBST01076366.1_1
ORYSAIN_OsIFCC004108
ORYSAIN_OsIFCC008139
ORYSAIN_OsIFCC045182
0,551
ZEAMA_GRMZM2G047055_P02
ZEAMA_GRMZM2G152328_P01
ORYSAIN_OsIFCC008871
0,98
ZEAMA_GRMZM2G053299_P01
ORYSAIN_OsIFCC021361
1
ZEAMA_GRMZM2G126010_P02
ORYSAIN_OsIFCC031396
0,5
0,54
ZEAMA_GRMZM2G030169_P01
ZEAMA_GRMZM2G082484_P01
ORYSAIN_OsIFCC032204
ORYSAIN_OsIFCC034269
OSTLU_31192
OSTLU_51545
PENMAtr_JO204682.1_1
PENMAtr_JO206721.1_1
PENMAtr_JO207079.1_1
0,84
PENMAtr_JO207459.1_5_rc
PENMAtr_JO207444.1_1
PENMAtr_JO207781.1_3
PENMAtr_JO207797.1_1
1
PENMAtr_JO229022.1_8_rc
PENMAtr_JO208647.1_2
PENMAtr_JO227318.1_2
0,51
PENMAtr_JO229286.1_1
PENMAtr_JO230460.1_4_rc
PENMAtr_JO208672.1_2
PENMAtr_JO209024.1_1
0,51
PENMAtr_JO209870.1_2
PENMAtr_JO209079.1_2
PENMAtr_JO209127.1_2
PENMAtr_JO209185.1_2
PENMAtr_JO209690.1_1
PENMAtr_JO209906.1_1
PENMAtr_JO212494.1_5
PENMAtr_JO225750.1_2
PENMAtr_JO225908.1_1
PENMAtr_JO226123.1_2
PENMAtr_JO231013.1_3_rc
PENMAtr_JO231612.1_1
PENMAtr_JO232677.1_2_rc
PENMAtr_JO232760.1_1
PENMAtr_JO232961.1_1
PENMAtr_JO233424.1_2
SACCE_YHR129C
SPIPRtrJU_GBSM01012854.1_2
SPIPRtrJU_GBSM01022859.1_6_rc
ZEAMA_AC194350.3_FGP001
ZEAMA_GRMZM2G006765_P02
0,91
ZEAMA_GRMZM2G126190_P01
ZEAMA_GRMZM2G053284_P01
ZEAMA_GRMZM2G167167_P02
ZEAMA_GRMZM2G321750_P01
1
ZEAMA_GRMZM2G439369_P01
0,7
ZEAMA_GRMZM2G449479_P01
ZEAMA_GRMZM2G407517_P01
ZEAMA_GRMZM2G437445_P01
0,86
ZEAMA_GRMZM5G859691_P01
ZEAMA_GRMZM2G467212_P01
ZEAMA_GRMZM2G478779_P01
ZEAMA_GRMZM5G837595_P01
MARPO_Mapoly0058s0062.1.p
0,66
PHYPAV33_Pp3c18_12190V3.1
1
PHYPAV33_Pp3c21_11420V3.1
0,93
ORYSAIN_OsIFCC008503
1
ZEAMA_GRMZM2G015861_P02
1
AMBTR_scaffold00001.16
0,95
CARPA_114.30
CHAGLtr_JO178946.1_1
0,75
CYAME_CMR270C
0,75
CHOCR_CDF39218.1
0.3

Data S1U: Phylogenetic tree of canonical actin proteins.

Midpoint-rooted Bayesian inference phylogenetic tree, numbers at the nodes are posterior probabilities. The *A. thaliana* actin sequences are shown in red, the *C. braunii* sequences in green, and the *K. nitens* sequences in blue. The sequences of *Naegleria gruberi* are shown in orange, those of *Dictyostelium discoideum* in purple. The transcriptomic sequences of *Nitella mirabilis* (cyan), *Nitella hyalina* (yellow) and *Penium margaritaceum* (grey) are also color-coded. See text for numbers of genes. In the case of *A. thaliana*, the usage of the ACTIN7 query for the blast approach (*cf*. STAR Methods) resulted in recovery of all canonical actins according to TAIR, namely ACTIN 1, 2, 3, 4, 7, 8, 9, 11 and 12, and of only two additional, actin-like, proteins.

Supplementary Figures S1-S7 for Nishiyama et al.

The *Chara* genome: secondary complexity and implications for plant terrestrialization

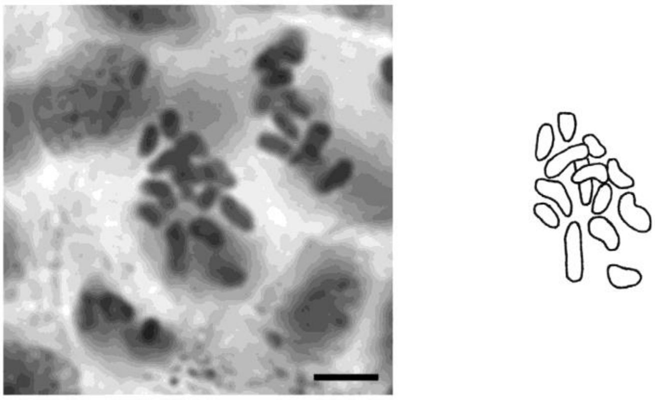

Figure S1, related to STAR methods: Chromosomes in an antheridial filament of *C. braunii* (n=14, strain S276).

The chromosomes during cell division in young antheridial filaments of strain S276 were observed after Feulgen staining. The chromosome number n=14 was confirmed by counts made on chromosomes during metaphase or anaphase. Most *Chara* species have either n=14 or n=28 chromosomes, Nitella and the other genera have different base numbers. There are numerous examples of monoicous/dioicous species pairs in the family, with the dioicous species always displaying half the number of chromosomes than their monoicous counterpart. For Chara typically dioicous=14, monoicous=28 (or other multiples of 14). *C. braunii* is monoicous, but is unique in having the dioicous chromosome number of 14. There are no known dioicous sister taxa to *C. braunii*, perhaps due to the already reduced genome. Scale bar = 2 µm.

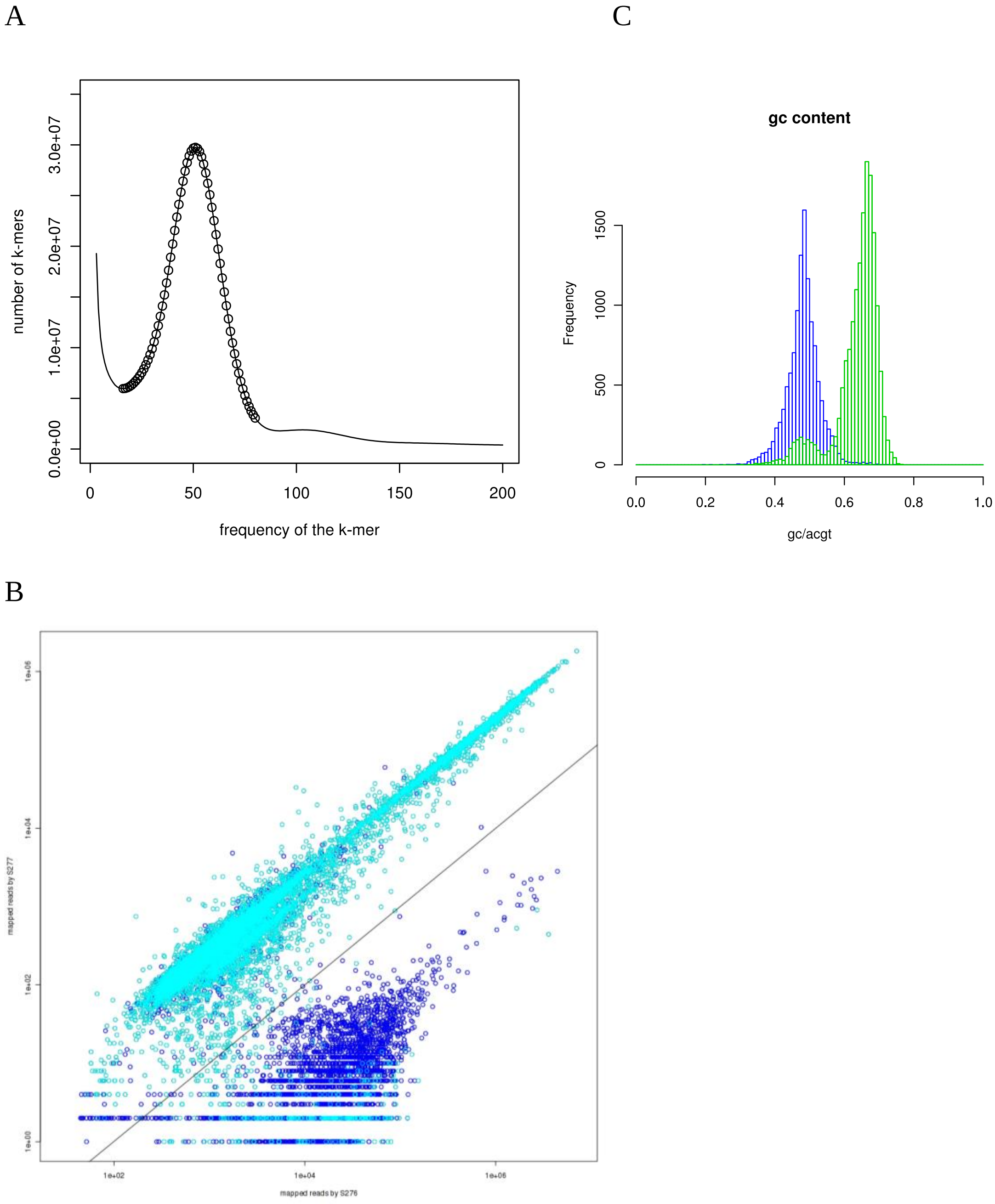

Figure S2, related to STAR methods: Assembly characteristics and decontamination

A) k-mer frequency analysis of the S276 paired end read data with k=25. Number of 25-mers at frequency 3 to 200 are shown with the solid line. Circles shows the points from 16 to 80 as what was recognized the major peak, presumably representing the single copy region in *C. braunii*.

B) Scatter plot of mapped reads of two *C. braunii* strains on each scaffold. Blue and light blue points are scaffolds with GC content of at least 55% and less than 55%, respectively.

C) Frequency distribution of scaffold wise GC content compared between putative *C. braunii* derived scaffolds (blue) and other scaffolds (green).

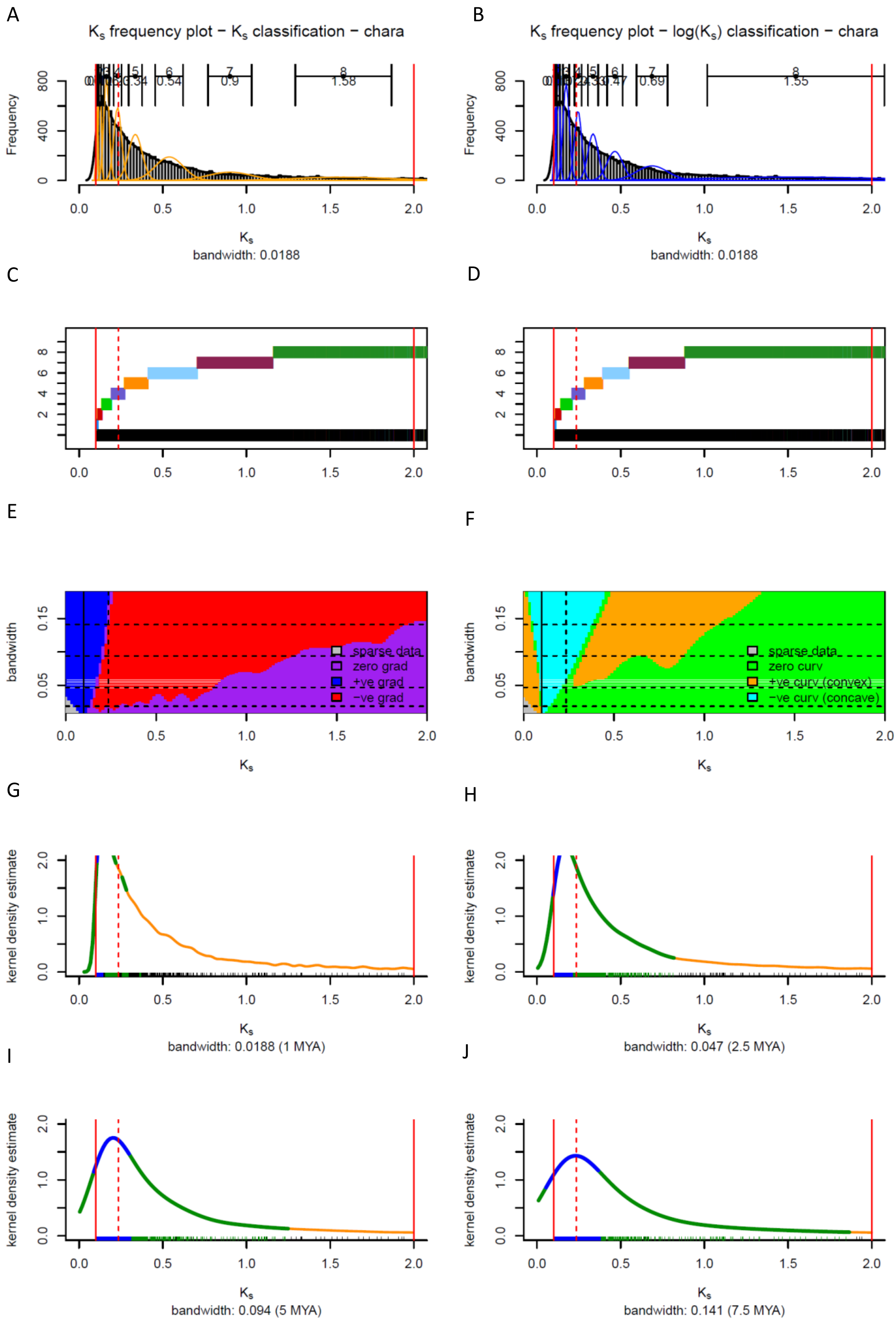

Figure S3, related to STAR methods: Ks-based analysis of *C. braunii* paralogs

Paranome-based WGD signature prediction. (A) Ks frequency plot highlighting mixture model components mean and standard-deviation (top: #component, bottom: mean Ks) based on raw Ks value classification. (B) Ks frequency plot highlighting mixture model components mean and standard-deviation (top: #component, bottom: mean Ks) based on log-transformed Ks value classification. (C) Ks group assignment for raw Ks classification. (D) Ks group assignment for log-transformed Ks classification. (E) Significant zero crossing (SiZer) plot. (F) Significant convexity (SiCon) plot. (G-J) Significant features of kernel density estimates using indicated bandwidths, highlighting significant gradient regions in blue and significant curvature regions in green using a significance level of 0.05. Red vertical lines represent Ks value of 0.1 and 2.0, dotted red vertical line represents Ks value of 0.235 corresponding to 12.5 Ma ago (these events might be no WGDs but only more or less recent local duplication events). For *C. braunii* no single predicted WGD signature was supported by three different bandwidth kernel densities (cf. STAR Methods).

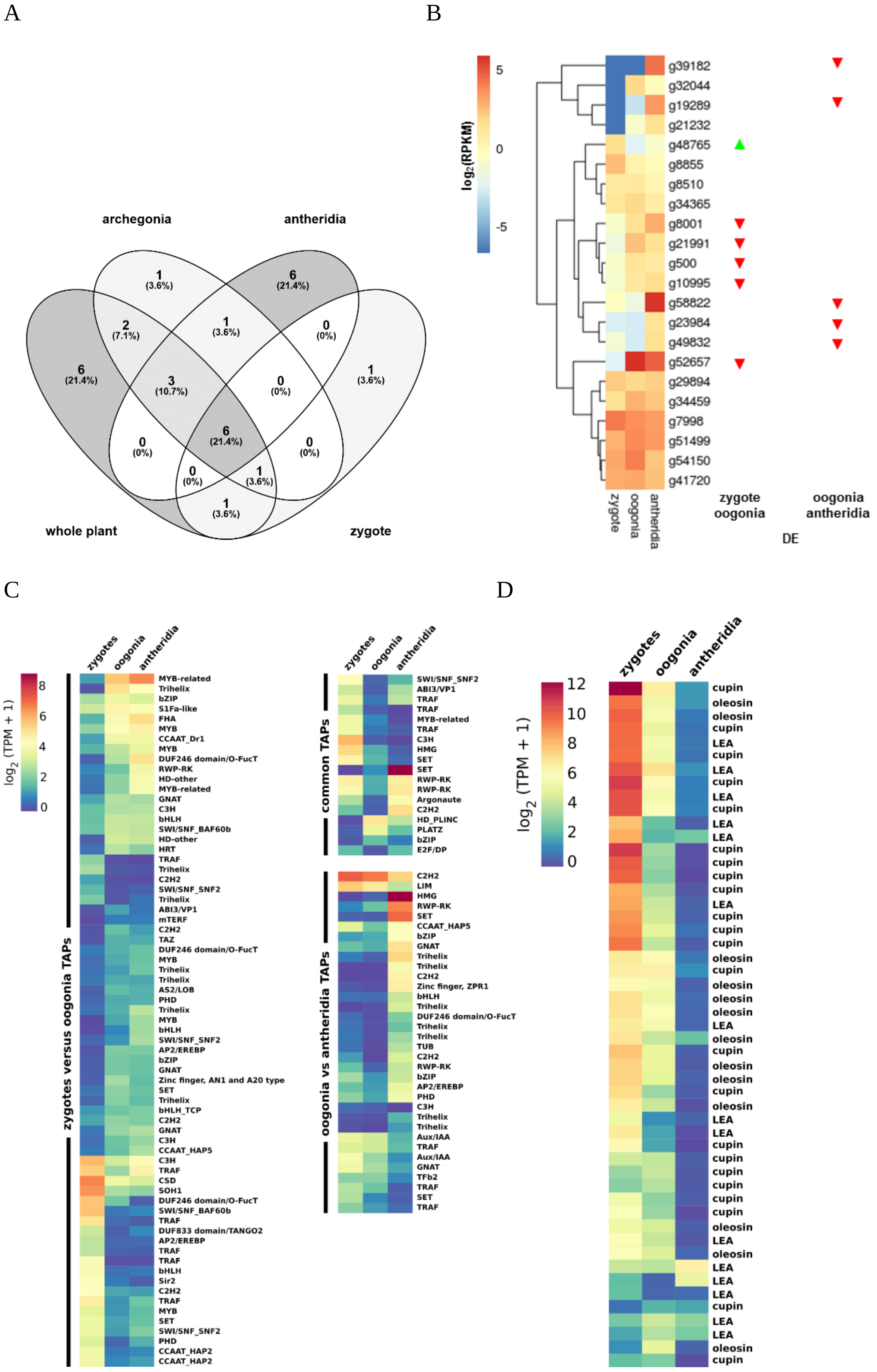
A
archegonia
antheridia
whole plant
zygote
1 (3.6%)
6 (21.4%)
2 (7.1%)
1 (3.6%)
0 (0%)
6 (21.4%)
3 (10.7%)
0 (0%)
1 (3.6%)
0 (0%)
6 (21.4%)
0 (0%)
0 (0%)
1 (3.6%)
1 (3.6%)
B
log2(RPKM)
5
0
-5
g39182
g32044
g19289
g21232
g48765
g8855
g8510
g34365
g8001
g21991
g500
g10995
g58822
g23984
g49832
g52657
g29894
g34459
g7998
g51499
g54150
g41720
zygote
oogonia
antheridia
zygote
oogonia
oogonia
antheridia
DE
C
log2 (TPM + 1)
8
6
4
2
0
zygotes
oogonia
antheridia
zygotes versus oogonia TAPs
MYB-related
Trihelix
bZIP
S1Fa-like
FHA
MYB
CCAAT_Dr1
MYB
DUF246 domain/O-FucT
RWP-RK
HD-other
MYB-related
GNAT
C3H
bHLH
SWI/SNF_BAF60b
HD-other
HRT
TRAF
Trihelix
C2H2
SWI/SNF_SNF2
Trihelix
ABI3/VP1
mTERF
C2H2
TAZ
DUF246 domain/O-FucT
MYB
Trihelix
Trihelix
AS2/LOB
PHD
Trihelix
MYB
bHLH
SWI/SNF_SNF2
AP2/EREBP
bZIP
GNAT
Zinc finger, AN1 and A20 type
SET
Trihelix
bHLH_TCP
C2H2
GNAT
C3H
CCAAT_HAP5
C3H
TRAF
CSD
SOH1
DUF246 domain/O-FucT
SWI/SNF_BAF60b
TRAF
DUF833 domain/TANGO2
AP2/EREBP
TRAF
TRAF
bHLH
Sir2
C2H2
TRAF
MYB
SET
SWI/SNF_SNF2
PHD
CCAAT_HAP2
CCAAT_HAP2
zygotes
oogonia
antheridia
common TAPs
SWI/SNF_SNF2
ABI3/VP1
TRAF
TRAF
MYB-related
TRAF
C3H
HMG
SET
SET
RWP-RK
RWP-RK
Argonaute
C2H2
HD_PLINC
PLATZ
bZIP
E2F/DP
oogonia vs antheridia TAPs
C2H2
LIM
HMG
RWP-RK
SET
CCAAT_HAP5
bZIP
GNAT
Trihelix
Trihelix
C2H2
Zinc finger, ZPR1
bHLH
Trihelix
DUF246 domain/O-FucT
Trihelix
Trihelix
TUB
C2H2
RWP-RK
bZIP
AP2/EREBP
PHD
C3H
Trihelix
Trihelix
Aux/IAA
TRAF
Aux/IAA
GNAT
TFb2
TRAF
SET
TRAF
D
log2 (TPM + 1)
12
10
8
6
4
2
0
zygotes
oogonia
antheridia
cupin
oleosin
oleosin
cupin
LEA
cupin
LEA
cupin
LEA
cupin
LEA
LEA
cupin
cupin
cupin
cupin
LEA
cupin
cupin
cupin
oleosin
cupin
oleosin
oleosin
oleosin
LEA
oleosin
cupin
oleosin
oleosin
cupin
oleosin
LEA
LEA
cupin
cupin
cupin
cupin
cupin
cupin
oleosin
LEA
oleosin
LEA
LEA
LEA
cupin
LEA
LEA
oleosin
cupin

Figure S4, related to Figure 6: Expression profiles during sexual reproduction.

Expression profile of trihelix TF genes based on RNA-seq evidence (supplemental file 3) was visualized as A) a Venn diagram using venny (http://bioinfogp.cnb.csic.es/tools/venny/) and B) as a heatmap showing gene expression and DEGs from reproductive organs with RPKM > 1 in minimum two samples. C) Shows expression of differentially expressed TFs/TRs during sexual reproduction. D) Expression of DEGs associated with seeds during sexual reproduction. Transcripts per million (TPM) were transformed to log2 scale and clustered using the euclidean distance method and the complete clustering method (B, C, D).

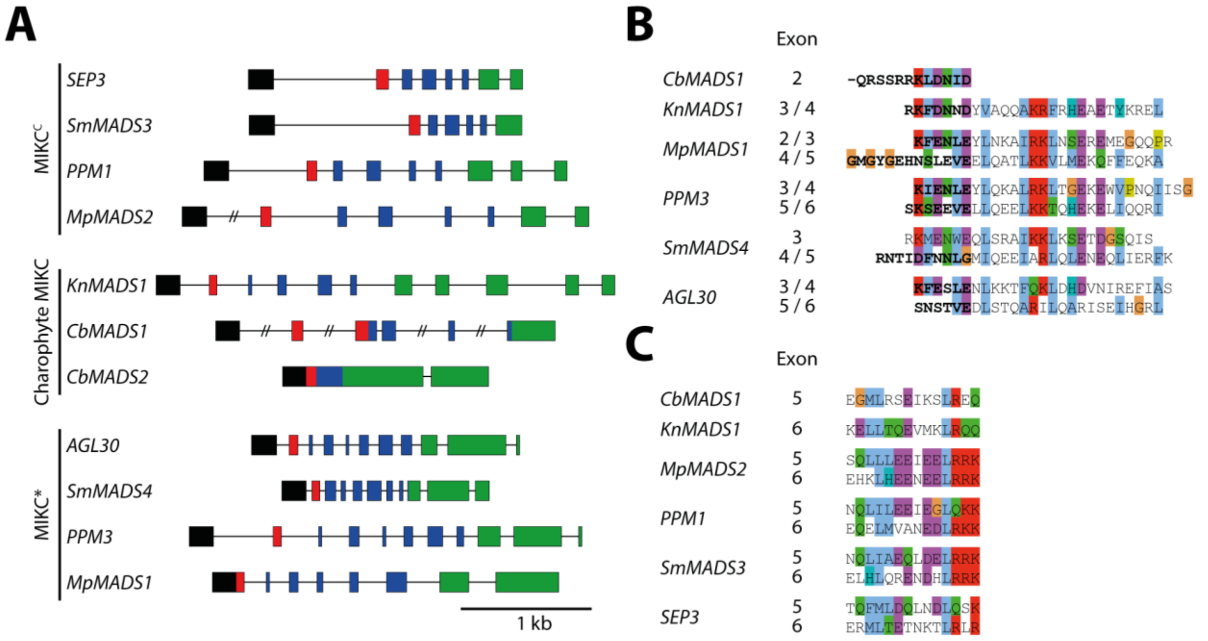
A
MIKC^C
SEP3
SmMADS3
PPM1
MpMADS2
Charophyte MIKC
KnMADS1
CbMADS1
CbMADS2
MIKC*
AGL30
SmMADS4
PPM3
MpMADS1
1 kb
B
Exon
CbMADS1 2 -QRSSRRKLDNID
KnMADS1 3 / 4 RKFDNNDYVAQQAKRFRHEAETYKREL
MpMADS1 2 / 3 KFENLEYLNKAIRKLNSEREMEGQQPR
4 / 5 GMGYGEHNSLEVEELQATLKKVLMEKQFFEQKA
PPM3 3 / 4 KIENLEYLQKALRKLTGEKEWVPNQIISG
5 / 6 SKSEEVELLQEELKKTQHEKELIQQRI
SmMADS4 3 RKMENWEQLSRAIKKLKSETDGSQIS
4 / 5 RNTIDFNNLGMIQEEIARLQLENEQLIERFK
AGL30 3 / 4 KFESLENLKKTFQKLDHDVNIREFIAS
5 / 6 SNSTVEDLSTQARILQARISEIHGRL
C
Exon
CbMADS1 5 EGMLRSEIKSLREQ
KnMADS1 6 KELLTQEVMKLRQQ
MpMADS2 5 SQLLLEEIEELRRK
6 EHKLHEENEELRRK
PPM1 5 NQLILEEIEGLQKK
6 EQELMVANEDLRKK
SmMADS3 5 NQLIAEQLDELRRK
6 ELHLQRENDHLRRK
SEP3 5 TQFMLDQLNDLQSK
6 ERMLTETNKTLRLR

Figure S5, related to Figure 5: Exon-intron structure comparison of MIKC^{C}-type, MIKC*-type and charophyte MIKC-type genes.

(A) Exon-intron structures of representatives of MIKC^{C}-type and MIKC*-type genes together with the charophyte MIKC-type genes *CbMADS1*, *CbMADS2* and *KnMADS1*. The exons encoding MADS-, I- , K- and C-domains are color coded in black, red, blue and green, respectively. Among the three Type II genes that were identified in the *C. braunii* genome only *CbMADS1* shows a canonical MIKC-type gene sequence. In contrast *CbMADS2* lacks most (but not all) introns and thus probably evolved via a retrotransposition and recombination event. *CbMADS3* lacks the conserved K-box that encodes for the protein-protein interacting K-domain (data not shown). (B and C) Analysis of exon-intron structures suggest that *CbMADS1* directly descends from an ancestral MIKC-type gene that was a common ancestor of MIKC^{C}- and MIKC*-type genes. (B) It was previously suggested that the N-terminal part of the K-domain of MIKC*-type proteins evolved through a duplication of two K-domain exons of an ancestral MIKC-type gene (Kwantes et al., 2011). The aligned amino acid sequences encoded by exon 2 of *CbMADS1*, and by the first K-domain exons of *KnMADS1*, *MpMADS1*, *PPM3*, *SmMADS4* and *AGL30* indeed strongly support this hypothesis. (C) In addition, striking similarities between the aligned amino acid sequences encoded by exon 5 of *CbMADS1*, exon 6 of *KnMADS1* and exons 5 and 6 of *MpMADS2*, *PPM1*, *SmMADS3* and *SEP3*, respectively, suggest that also the K-domain of MIKC^{C}-type proteins evolved through an exon duplication of an ancestral MIKC-type gene. This is especially intriguing considering the fact that the last two K-domain exons of most if not all MIKC^{C}-type genes encode for a protein-protein interaction interface that facilitates tetramer formation of MIKC^{C}-type proteins (Theißen et al., 2016). It has already been suggested that the ability of MIKC^{C}-type proteins to tetramerize was an important precondition to evolve and diversify efficient developmental switches that facilitated the transition to land and the evolution of complex body plans of land plants (Theißen et al., 2016). Thus it is tempting to speculate that an exon duplication of an ancestral MIKC^{C}-type gene in the MRCA of extant land plants created the molecular prerequisites for this evolutionary novelty.

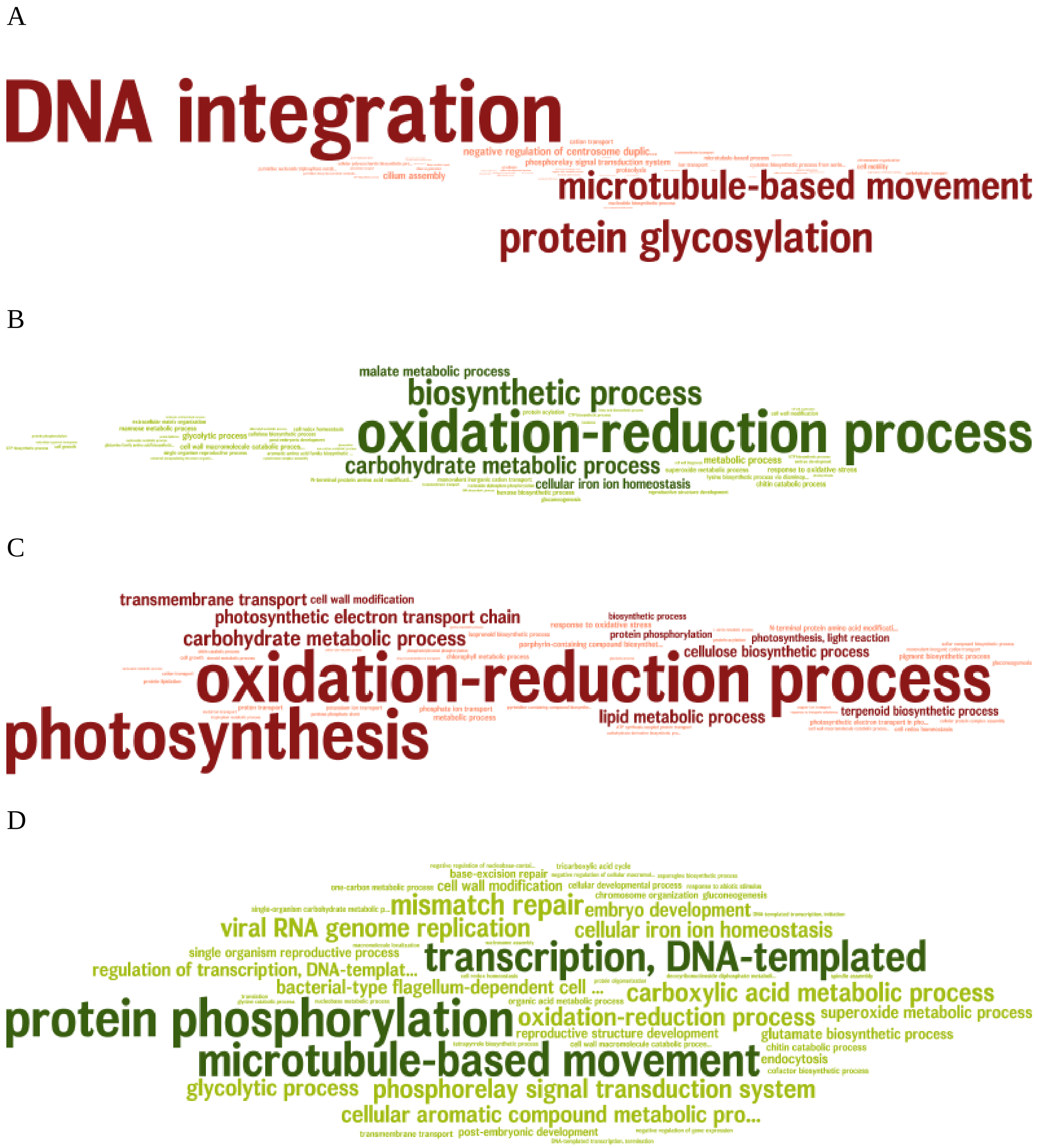

Figure S6, related to Figures 5/6: Transcriptome analyses of reproduction and early development. GO enrichment word clouds (category biological process); genes down-regulated (A) or up-regulated (B) in oogonia as compared to antheridia, genes down-regulated (C) or up-regulated (D) in zygotes as compared to oogonia. Antheridia are strongly enriched with the GO category GO:0015074 “DNA integration” (A). 349 gene models expressed in antheridia were classified in this category; of these, 324 genes were found to be overlapping with a TE to at least 50 % (supplemental file 3). Most of these genes were annotated as “integrase”, “ribonuclease H-like”, “reverse transcriptase”, and “aspartyl protease” by homology-based approach, terms typical of Ty3/Gypsy pol gene composition (Havecker et al., 2004). Ty3/Gypsy elements represent 20 % of the *C. braunii* genome. These results might indicate mobilization of retrotransposons and other mobile elements during male gametogenesis. This could be a consequence of genome rearrangement during male gamete formation. One could also imagine that mobilization and integration of retrotransposons might enhance genomic diversity during sexual reproduction.

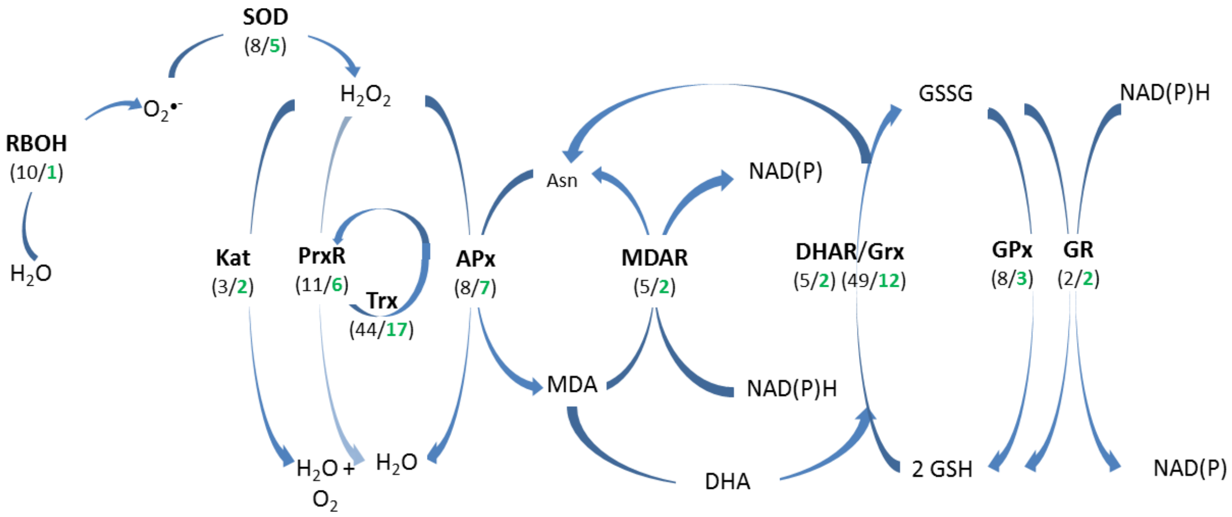

Figure S7, related to Figure 6: Major reactive oxygen species scavenging pathway in plants. Proteins associated with ROS scavenging are in bold. Number of genes found for *A. thaliana* and *C. braunii* (in green) are indicated in brackets. APx: Ascorbate peroxidase, Asn: ascorbate, DHA: Dehydroascorbate, DHAR: Dehydroascorbate reductase, GPx: Plant glutathione peroxidase, GR: Glutathione reductase, Grx: Glutaredoxins superfamily, GSH: reduced glutathione, GSSH: oxidized glutathione. Kat: Catalase, MDAR: Monodehydroascorbate reductase, PrxR: Peroxiredoxins family, RBOH: Respiratory burst oxidase homolog also called NADPH oxidase, SOD: Superoxide dismutase, Trx: Thioredoxins, MDA: Monodehydroascorbate, adapted from (Inupakutika et al., 2016).